

Investigation of microbial-derived metabolites as risk factors and key mediators of the microbiota-gut-brain axis in early cognitive decline and dementia.

Emily Connell, BSc

This thesis is submitted in accordance with the requirements for the degree of Doctor of Philosophy (PhD) to the University of East Anglia, Norwich.

University of East Anglia

Faculty of Medicine and Health Sciences

2025



This copy of the thesis has been supplied on condition that anyone who consults it is understood to recognise that its copyright rests with the author and that use of any information derived there-from must be in accordance with current UK Copyright Law. In addition, any quotation or extract must include full attribution.

Abstract

Emerging evidence suggests that the microbiota-gut-brain axis, a bidirectional communication system between the gut, its microbiota, and the central nervous system (CNS), may influence cognitive health and disease. Microbial-derived metabolites are key mediators of this communication, triggering physiological responses directly and indirectly influencing CNS function. Dysregulation of this system can promote cytotoxic metabolite production, neuroinflammation and cognitive decline. However, the exact mechanisms remain undefined. Here, we investigate the role of microbial-derived metabolites as potential risk factors and modulators of early cognitive decline. Using a targeted metabolomics approach, we identified six circulatory metabolites as composite predictors of prodromal Alzheimer's disease (AD), significantly distinguishing healthy individuals from patients with subjective or mild cognitive impairment. Multi-omics approaches further assessed the influence of dietary patterns on metabolite-mediated communication. Mice consuming a refined low-fat diet (rLFD), low in fibre and high in sucrose and processed carbohydrates, displayed significant gut microbial dysbiosis and colonic and neuronal bile acid dysmetabolism. Neuronal TCA concentrations inversely correlated with neuroinflammatory gene expression (*NFκB1*), suggesting a rLFD may promote detrimental neuronal processes. Conversely, we evaluated the protective benefits of a (poly)phenol-rich extract (Memophenol™) in a mouse model of chronic low-grade inflammation. Memophenol™ prevented LPS-induced increases in uremic toxins, indoxyl sulfate and TMAO, which coincided with shifts in *Romboutsia* and *Desulfovibrio*, respectively, and the expression of neuronal tight junction protein ZO-1, indicating a novel protective role. Finally, we assessed the efficacy of Neurosyn240, a Mediterranean diet-inspired supplement, as an early intervention against prodromal AD progression in 5xFAD mice. Neurosyn240 increased peripheral serotonin concentrations, which positively correlated with *Bifidobacterium* abundance, and negatively with hippocampal Iba-1+ microglia density. Neurosyn240 decreased LCA concentrations, which inversely correlated with *Parvibacter*, and was associated with reduced hippocampal amyloid deposits, highlighting novel microbiota-gut-brain axis connections. These results support a significant role for microbial-derived metabolites in early AD progression.

Access Condition and Agreement

Each deposit in UEA Digital Repository is protected by copyright and other intellectual property rights, and duplication or sale of all or part of any of the Data Collections is not permitted, except that material may be duplicated by you for your research use or for educational purposes in electronic or print form. You must obtain permission from the copyright holder, usually the author, for any other use. Exceptions only apply where a deposit may be explicitly provided under a stated licence, such as a Creative Commons licence or Open Government licence.

Electronic or print copies may not be offered, whether for sale or otherwise to anyone, unless explicitly stated under a Creative Commons or Open Government license. Unauthorised reproduction, editing or reformatting for resale purposes is explicitly prohibited (except where approved by the copyright holder themselves) and UEA reserves the right to take immediate 'take down' action on behalf of the copyright and/or rights holder if this Access condition of the UEA Digital Repository is breached. Any material in this database has been supplied on the understanding that it is copyright material and that no quotation from the material may be published without proper acknowledgement.

Contents

Abstract.....	2
List of Figures.....	5
List of Tables	6
Statement of publication.....	8
Chapter 1: General Introduction.....	9
1.1 Alzheimer's disease is a global health burden.....	9
1.2 Healthy Ageing and Age-Related Cognitive Decline	12
1.3.1 The Microbiota-Gut-Brain Axis.....	13
1.3.2 The Microbiota-Gut-Brain Axis in the context of Ageing and Cognitive Decline	16
1.4 Microbial-Derived Metabolites and Cognitive Decline	17
1.4.1 Bile acids.....	17
1.4.2 TMAO.....	25
1.4.2 Tryptophan.....	28
1.4.4 <i>p</i> -Cresol.....	32
1.4.5 Other Emerging Microbial-Derived Metabolites	33
1.5 Using Dietary Approaches to Modulate the Microbiota-Gut-Brain Axis	34
1.6 Dietary Components	37
1.7 Literature review conclusions and research gaps.....	40
1.8 Aims and outline of the thesis.....	42
Chapter 2: Circulatory dietary and gut-derived metabolites as risk factors of prodromal Alzheimer's disease	44
2.1 Introduction.....	44
2.2 Materials and Methods.....	45
2.3 Results.....	50
2.4 Discussion.....	60
Chapter 3: Refined diet consumption increases neuroinflammatory signalling through bile acid dysmetabolism.....	65
3.1. Introduction.....	65
3.2. Materials and Methods.....	66
3.3. Results.....	69
3.4. Discussion	77
Chapter 4: (Poly)phenol-rich grape and blueberry extract prevents LPS-induced disruption of the blood-brain barrier through the modulation of the gut microbiota-derived uremic toxins ..	81
4.1 Introduction.....	81
4.2. Materials and Methods.....	82
4.3. Results.....	86
4.4. Discussion.....	96

Chapter 5: Neuroprotective Effects of a Mediterranean Diet-Inspired Supplement through the Microbiota-Gut-Brain Axis in 5xFAD Mice: Insights into Alzheimer's Disease Pathology	100
5.1 Introduction.....	100
5.2 Material and Methods.....	101
5.3 Results.....	106
5.4 Discussion.....	117
Chapter 6: General discussion.....	121
6.1 Microbial-derived metabolites are associated with prodromal AD progression and form a novel composite risk factor for the early detection of AD.....	121
6.2 Refined dietary intake can detrimentally alter metabolite-mediated pathways of the microbiota-gut-brain axis	123
6.3 Dietary supplements can provide metabolite-mediated protective effects in a model of chronic low-grade inflammation and early AD neuropathology	125
6.4 Discussion of the experimental models and methodology.....	129
6.5 Future Directions	133
6.6 Overall Conclusion	136
List of Communications	137
References.....	139
Appendix.....	190

List of Figures

Figure 1.1: Microbial metabolites can directly and indirectly modulate the CNS through immune, neuronal and direct metabolite-mediated pathways within the microbiota-gut-brain axis.

Figure 1.2: Bile acids, TMAO and tryptophan metabolic pathways and their links to the brain.

Figure 1.3: Lifestyle factors associated with healthy and pathological ageing.

Figure 1.4: Components of a Mediterranean diet pattern and potential mechanisms underlying their cognitive benefits.

Figure 1.5: Key potential pathways through which microbial-derived metabolites influence cognitive function.

Figure 2.1: Microbiome beta diversity is significantly altered in early cognitive decline.

Figure 2.2: Metabolic shift occurs in early cognitive decline.

Figure 2.3: Serum metabolites and microbiome composition are significantly linked.

Figure 2.4: Six circulatory metabolites can distinguish stages of prodromal AD.

Figure 2.5: Cytotoxic bile acids (BA) are increased in early cognitive decline.

Figure 3.1. Composition of chow and rLFD.

Figure 3.2. rLFD significantly modulates the gut microbiome diversity and composition in male C57BL/6J mice.

Figure 3.3. rLFD altered the metabolomic profile in male C57BL/6J mice.

Figure 3.4. The gut microbiome and the metabolome profile of chow and rLFD male C57BL/6J mice are significantly related.

Figure 3.5. Bile acid profiles in both the colon and brain are modulated by a rLFD of C57BL/6J male mice

Figure 3.6. rLFD significantly modulates gene expression in the hippocampus and cortex of male mice.

Figure 4.1: Administration of LPS (0.5 mg per kg bw per week) and LPS + Memophenol™ supplementation does not significantly impact body weight.

Figure 4.2: Administration of LPS and LPS + Memophenol™ altered beta, but not alpha diversity of the gut microbiome in male C57BL/6J mice.

Figure 4.3: Microbial-derived uremic toxins were significantly modulated between groups and associated with changes in the gut microbiome composition in male C57BL/6J mice.

Figure 4.4: Procrustes analysis comparing to congruence of the gut microbiome and metabolome profile in male C57BL/6J mice.

Figure 4.5: Memophenol™ recovers LPS-induced decreases in ZO-1 in the hippocampus of male C57BL/6J mice.

Figure 4.6: Memophenol™ alters the transcriptional profile in the hippocampus of male C57BL/6J mice.

Figure 5.1: Supplementation of the Neurosyn240 diet for 12 weeks showed no significant difference in body weight to the control diet in both males and females.

Figure 5.2: Neurosyn240 did not significantly alter hippocampal-dependent cognitive function in male and female 5xFAD mice.

Figure 5.3: Neurosyn240 diet altered beta, but not alpha diversity of the gut microbiome in 5xFAD mice.

Figure 5.4: Neurosyn240 significantly modulated the circulatory metabolome profile in male and female 5xFAD mice which correlated with changes in the gut microbiome composition.

Figure 5.5: Procrustes analysis of the congruence of serum metabolite and microbiome profiles.

Figure 5.6: Male and female 5xFAD mice consuming a Neurosyn240 diet have reduced amyloid deposits in the hippocampus.

Figure 5.7: Male and female 5xFAD mice consuming a Neurosyn240 diet have reduced Iba-1 positive microglia in the hippocampus.

Figure 5.8: Neurosyn240 significantly modulated gene expression within the hippocampus of male and female 5xFAD mice.

Figure 5.9: Correlation analysis between Lrp2 expression and LCA in both control and Neurosyn240 males and females.

Figure 6.1: Summary of dietary modulation of metabolite-mediated pathways within the microbiota-gut-brain axis.

List of Tables

Table 1.1: Bile acids and their impact on cognition and AD.

Table 2.1: Baseline characteristics of the participants.

Table 2.2: Multiple linear regression model (adjusted for age, BMI, liver function (AST/ALT ratio), kidney function (creatinine) and diet) showing metabolites significantly associated with early cognitive decline.

Table 2.3: Comparison of area under the receiver operator curve (AUC)

Table 5.1: Sex-specific amyloid-associated genes with expression modulated by Neurosyn240 in comparison to control.

Acknowledgements

This PhD would not have been possible without the support, guidance, and encouragement of many people to whom I owe my deepest gratitude.

First and foremost, I would like to express my sincere thanks to my supervisors, Dr David Vauzour and Prof. Michael Müller, who invested a huge amount of time and effort in myself and the project. I feel fortunate to have had such personable supervisors who have helped me grow so much over the last few years as a scientist. A further special thanks to the excellent supervisors and mentors I had the pleasure of working with throughout my PhD, including Dr Gwen Le Gall, Dr Saber Sami and Dr Matthew Pontifex, each with vast experience and knowledge of their subject areas. It has been a privilege to work alongside you, and I would not be where I am today without your support and guidance.

I would also like to thank Dr Simon McArthur who helped me immensely with the immunohistochemistry analysis whilst hosting me at Queen Mary University London during the summer of 2023.

On a personal note, I am sincerely grateful for the many people who have supported me through the last few years. Tom, I could not have done this without your love, support and (above all) patience. I cannot thank you enough for your consistent encouragement and for sharing the difficulties that come with completing a PhD.

To my family and friends from home, thank you for your continued love and belief in me, and for listening to me endlessly discuss my PhD research for the last few years.

To my lab friends and colleagues at UEA: Erica Li, Bernie Breeze, Leonie Lang, Thomas Hunt, Alicia Nicklin, and Marrium Liaquat, thank you for your invaluable advice and incredible moral support throughout my PhD. From completing long sacrifice days together in the DMU, to many lunchtime chats or food trips in Norwich, I couldn't have done this without the fantastic support network you provided.

Statement of publication

My thesis integrates five manuscripts of which I am the primary author:

- Published: Chapters 1, 3 & 4.
- Submitted to journals for publication: Chapters 2 & 5.

These are combined with a discussion chapter (Chapter 6).

Chapter 1: General Introduction

A large proportion of my introduction presented below has been published in *Molecular Neurodegeneration* as a literature review article in 2022. (Connell E, Le Gall G, Pontifex MG, et al (2022) Microbial-derived metabolites as a risk factor of age-related cognitive decline and dementia. *Molecular Neurodegeneration* 17:43. <https://doi.org/10.1186/s13024-022-00548-6>). It has been updated and expanded with literature published in the last two years.

1.1 Alzheimer's disease is a global health burden

Age is among the most predominant risk factors for cognitive decline. Whilst some decline in cognition is considered an inevitable part of healthy ageing, deleterious changes in cognition, including mild cognitive impairment (MCI) and age-related dementias (e.g., Alzheimer's disease, AD), are estimated to impact approximately 15% and 11% of the population over 65 years respectively (Eshkoo et al. 2015; Alzheimer's Association 2019). By 2050, the global elderly population is expected to increase to 22% (World Health Organisation 2022), increasing incidences of cognitive decline also. Cognitive decline exacerbates broad social and economic issues, including depression, social withdrawal, difficulties performing everyday tasks, drastic reductions in quality of life and greater reliance on others (social care) (Tiwari et al. 2019). Understanding how to promote healthy ageing whilst resisting aberrant changes in cognition is therefore becoming a greater priority.

Numerous pathological changes have been identified in the postmortem brains of AD patients, including brain atrophy, synaptic and neuronal loss, oxidative damage, activated inflammatory cells, amyloid plaques mainly composed of the β -amyloid peptide ($A\beta$), and neurofibrillary tangles (NFTs) comprised of hyperphosphorylated aggregates of the microtubule-associated protein tau (Grundke-Iqbal et al. 1986; Walsh and Selkoe 2004; Medeiros et al. 2010). The latter two being key pathological hallmarks of AD (DeTure and Dickson 2019).

Amyloid plaques are formed by the extracellular nonvascular aggregation of $A\beta_{40}$ and $A\beta_{42}$ peptides resulting from the aberrant processing of amyloid precursor protein (APP) by β - and γ -secretases (Duyckaerts and Dickson 2011). $A\beta_{42}$ is more toxic to neurons both in cell culture and animal models and is the major form of $A\beta$ in amyloid plaques (Suzuki et al. 1994; Yan and Wang 2006; Marshall et al. 2016; Vadukul et al. 2017; De et al. 2019; Phillips 2019). Tau, a microtubule-associated protein, regulates the assembly and maintenance of the structural integrity of microtubules under physiological conditions. However, in the AD brain, tau is abnormally hyperphosphorylated and is polymerised into paired helical filaments (PHF) admixed with straight filaments (SF) forming NFTs within neurons (Medeiros et al. 2010; Barbier et al. 2019). These neuropathological aggregates lead to the loss of synapses and neurons in vulnerable regions, with the hippocampus and entorhinal cortex being among

the earliest areas affected, contributing to initial symptoms such as memory impairment (Subramanian et al. 2020). Neuroinflammation also plays a prominent role in AD. Activated microglia promote the transformation of resting astrocytes into reactive astrocytes, contributing to neurodegeneration, while excessive release of pro-inflammatory cytokines and glial cell polarisation further drive neuroinflammatory changes and exacerbate disease pathology (Martini-Stoica et al. 2018; Deng et al. 2024). As the disease progresses, neurodegeneration extends to the temporal, parietal, and frontal lobes, leading to more widespread cognitive decline, difficulties with problem-solving, social dependence, and eventually motor abnormalities (Duyckaerts and Dickson 2011).

Addressing modifiable risk factors can delay the onset, or even ameliorate cognitive decline (Kivipelto et al. 2001), whilst assisting with the identification of asymptomatic individuals with an increased chance of developing the condition in the future (Balagopal et al. 2011). Currently, hypertension (Reitz et al. 2007), diabetes mellitus (Profenno et al. 2010; Moheet et al. 2015), arteriosclerosis (Knopman et al. 2001), obesity (Dye et al. 2017) and hypercholesterolemia (Goldstein et al. 2008) are the most significant risk factors associated with age-related cognitive decline among others (Livingston et al. 2024). Given the connection between cognition and these metabolic diseases, it is perhaps unsurprising that dietary factors can elicit a substantial influence on cognitive function (Nutaitis et al. 2019) through the modulation of a microbiota-gut-brain axis (Gareau 2014). The microbiota-gut-brain axis is a complex communication system bridging the gut and central nervous system (CNS) that is modulated by the microbiome, a collection of 10^{14} microorganisms with an extensive functional gene repertoire (Berg et al. 2020). These microorganisms predominantly reside in the gut, metabolising dietary compounds into a vast range of metabolites. Although host-derived metabolites dominate the metabolome, with over two hundred thousand identified in humans compared to fewer than two thousand microbial-specific metabolites (Chakraborty 2024), microbial-derived metabolites, such as bile acids, trimethylamine-N-oxide (TMAO), tryptophan, *p*-cresol, and their derivatives, are increasingly recognised for their notable influence on cognitive decline and neurodegenerative diseases (Xu and Wang 2016). Metabolites can cross the intestinal epithelial barrier; a structure connected by tight junction proteins, lamina propria and reinforced by mucosal secretions (Chelakkot et al. 2018), primarily via active transport, and enter systemic circulation. From here, metabolites can directly initiate physiological responses by crossing the blood-brain barrier (BBB) and influencing the CNS (Mayer et al. 2014), or indirectly via immune regulation or *vagus* nerve stimulation (Figure 1.1) (Bonaz et al.

2018).

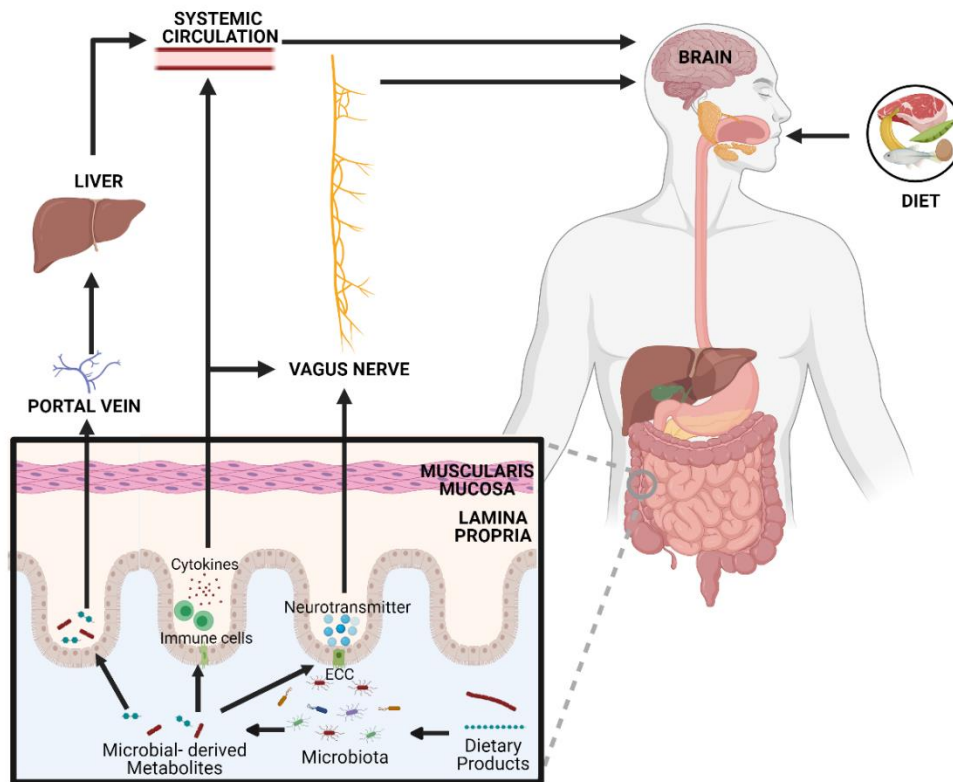


Figure 1.1: Microbial metabolites can directly and indirectly modulate the CNS through immune, neuronal and direct metabolite-mediated pathways within the microbiota-gut-brain axis. In the gut lumen, dietary products can be metabolised by the microbiota into neuroactive compounds, including neurotransmitters, (e.g. serotonin, dopamine), amino acids (e.g. tryptophan, tryptamine) and other microbial-derived metabolites (e.g. short-chain fatty acids, trimethylamine (TMA)). These compounds subsequently communicate with the central nervous system either directly, travelling through the portal vein, liver and crossing the blood-brain barrier, or indirectly via the production of neurotransmitters by enterochromaffin cells (ECC) or immune pathways (stimulated immune cells produce cytokines that can enter the blood or stimulate the vagus nerve).

The capability of microbial-derived bioactive metabolites to influence the CNS provides a novel mechanistic pathway for cognitive decline, warranting further exploration. Within the gastrointestinal (GI) tract, microbiota populations are in part reflective of their local physiological conditions. The small intestine, due to its proximity to the stomach, contains high concentrations of acids, oxygen and antimicrobials, thereby restricting bacterial growth to predominantly fast-growing anaerobes that can adhere to epithelia or mucus (Donaldson et al. 2016). Conversely, colonic regions promote much denser bacterial communities, dominated by anaerobes such as *Prevotellaceae* and *Lachnospiraceae*, that can digest complex carbohydrates (Donaldson et al. 2016).

In healthy adults, 80% of the identified faecal microbiota can be classified into three dominant phyla: Bacteroidetes, Firmicutes and Actinobacteria (Lay et al. 2005). However, on a more refined level, the microbiota is a highly complex and diverse bacterial ecosystem comprised of a hierarchy of dominant anaerobic bacteria, including *Bacteroides*, *Eubacterium*, *Bifidobacterium*, *Peptostreptococcus*, *Ruminococcus*, *Clostridium* and *Propionibacterium*, and sub-dominant bacteria of the Enterobacteriaceae family, including *Escherichia coli*, and the genera *Streptococcus*, *Enterococcus*, *Lactobacillus*, *Fusobacterium*, *Desulfovibrio* and *Methanobrevibacter* (Harmsen et al. 2002). At the genus level, key beneficial bacteria, such as *Lactobacillus* and *Bifidobacterium*, are known for their roles in maintaining gut barrier integrity, producing short-chain fatty acids (SCFAs), and modulating the immune response (Ouweland et al. 2002; Ríos-Covián et al. 2016). Conversely, certain members of the genera *Escherichia* (e.g., *E. coli*), *Enterococcus*, *Desulfovibrio* and *Clostridium* (specifically toxin-producing strains) are considered pathobionts as these microbes can drive inflammation under dysbiosis (Lupp et al. 2007; Buttó and Haller 2016). Elevated levels of Proteobacteria, particularly *Enterobacteriaceae*, are often associated with inflammatory states, such as inflammatory bowel disease (IBD) (Shin et al. 2015). Beneficial microbes, such as *Faecalibacterium prausnitzii* and *Akkermansia muciniphila*, are also crucial for anti-inflammatory effects and mucosal health, respectively (Miquel et al. 2013; Derrien et al. 2017).

Numerous intrinsic factors (e.g. genetics, immune response, metabolites) and extrinsic factors (e.g. diet, lifestyle) also impact gut microbial composition, making it an attractive therapeutic intervention target (Rothschild et al. 2018). The composition of these microbial communities determines the concentration of neurotransmitters or neuromodulators (including microbial-derived metabolites) released into circulation. Broad deviations in these microbial compositions, often referred to as “dysbiosis”, condition distinctly different metabolic profiles that may contribute to cognitive decline (Ling et al. 2021; Liu et al. 2020). Gut microbial composition is known to be significantly altered in patients with MCI, a transitional stage preceding AD, suggesting microbial changes may occur in the early stages of cognitive decline and influence its progression (Liu et al. 2019; Li et al. 2019; Saji et al. 2019; Nagpal et al. 2020; Zhang et al. 2021a).

Intestinal microbiota possess the capacity to produce hundreds of metabolites (Bostanciklioğlu 2019; Visconti et al. 2019), yet the influence of these compounds on cognitive health has not been uncovered. This chapter details the roles of newly emerging microbial-derived metabolites that are less explored in the context of cognitive health, including TMAO, bile acids, tryptophan, *p*-cresol and their derivatives.

1.2 Healthy Ageing and Age-Related Cognitive Decline

As we age, some of our cognitive abilities decline. Cognitive capabilities such as verbal skills, remain largely unaffected by brain ageing and can even improve over time (Murman 2015). Other essential

capabilities, including mental reasoning, memory (in particular episodic, working and recognition memory) and processing speed, steadily deteriorate with age (Murman 2015). During ageing, the brain undergoes various structural and functional changes. The most apparent is a gradual shrinkage of the brain, alongside an increase in ventricular space and cerebrospinal fluid (CSF) (Mortamet et al. 2005; Blinkouskaya et al. 2021). Brain atrophy increases in the elderly in an anterior-posterior gradient, with the most severe consequences taking place in the prefrontal regions (Raz and Rodrigue 2006; Blinkouskaya and Weickenmeier 2021). A reduction in white matter (the nerve fibres connecting different brain regions) integrity has been observed in normal cognitive aging, impairing the transfer of information between cortical regions (Sullivan and Pfefferbaum 2006), an essential process for higher cognitive functioning (Bolanzadeh et al. 2012).

Structural neuroimaging highlights differing trends in the neurobiology of pathological ageing and detrimental cognitive decline. Here, individuals are more likely to experience reductions in gray matter in the dorsolateral and medial prefrontal, parietal, and lateral temporal regions (Alexander et al. 2012; Irwin et al. 2018), alongside a loss of white matter integrity in the cingulum, corpus callosum, and superior longitudinal fasciculus (Adluru et al. 2014; Persson et al. 2006; Heise et al. 2011). This is instead of a decline in the frontal regions that typically occurs in healthy ageing.

AD is also associated with volume loss in the medial temporal lobe, a brain region highly associated with memory functions. Reduction typically starts in the anterolateral entorhinal cortex and advances medially across the remaining entorhinal cortex to the hippocampus (Thompson et al. 2004; Miller et al. 2015), with atrophy occurring at rates of 4.9-8.2%. In healthy ageing, atrophy in these regions occurs at a lower rate, diverging from pathological ageing, at 0.2-3.8% (Thompson et al. 2004). More recently, using longitudinal MRI and PET data, a similar divergence in volume loss has been noted in the locus coeruleus (Jacobs et al. 2021).

Finally, the default mode network (DMN), a resting-state network associated with cognitive processes of oneself (e.g., autobiographical memory), demonstrates connectivity patterns that distinguish healthy ageing from AD. Results from a task free-fMRI suggest AD patients have an accelerated ageing pattern of connectivity (Jones et al. 2011) and decreased resting-state activity in the posterior cingulate and hippocampus when compared with age-matched controls (Greicius et al. 2004). However, the biological mechanisms behind the heterogeneity of age-related cognitive decline are complex and not well understood.

1.3.1 The Microbiota-Gut-Brain Axis

The human gut microbiome represents a complex community of microbes that live in a mutualistic relationship with their host. Initially, these microorganisms were considered to be solely responsible for intestinal processes (fermentation of carbohydrates, synthesis of vitamins and xenobiotic metabolism)

(Rowland et al. 2018). However, over the last 20 years, this notion has been revised, owing to increasing evidence of a bidirectional communication system between the CNS and the GI tract, more commonly referred to as the ‘gut-brain axis’.

The gut-brain axis encompasses the CNS, the autonomic and enteric nervous system (ENS), and peripheral nerves and is vital for maintaining homeostasis. Signals from the brain control the secretory and sensory function of the gut, whilst the brain and gut communicate via physiological channels including the neuroendocrine, autonomic nervous system, neuroimmune pathways and molecules synthesised from gut microbes (Carabotti et al. 2015).

The ENS, consisting of neurons and glial cells in the intestinal submucosa and muscularis propria, facilitates bidirectional communication between the gut and the brain. Consisting of approximately 200-600 million neurons embedded in the gastrointestinal tract, the ENS regulates gut motility, secretion, and sensory functions independently of the CNS (Joly et al. 2021). Afferent neurons in the ENS can be activated by chemicals released by gut microorganisms and cells, leading to modifications in electrical activity in its related brain regions through the *vagus* nerve. The *vagus* nerve serves as a bridge between the ENS and the CNS, comprising 80% afferent and 20% efferent fibres (Agostoni et al. 1957). Afferent fibres connect to all four layers of the digestive tract, encompassing the mucosa, submucosa, muscular layer and serous layer, but do not cross the epithelial layer and therefore are not in direct contact with gut microbiota. As a result, the microbiota activates these fibres indirectly via the release of metabolites or bacterial products. Enteroendocrine cells (ECCs) make up approximately 1% of intestinal epithelial cells and can detect signals from the microbiota through toll-like receptors (TLRs), capable of identifying bacterial compounds such as lipopolysaccharides (LPS) (Abreu et al. 2005), or through receptors activated by microbiota-derived metabolites such as short-chain fatty acids (SCFAs) (Samuel et al. 2008). ECCs can subsequently interact with vagal afferent fibres through the release of serotonin or gut hormones (Li et al. 2000; Strader and Woods 2005). This indirect signalling between the gut microbiota and the brain via the *vagus* nerve can modulate certain cognitive functions. For example, rodents fed with the probiotic *Lactobacillus rhamnosus* for 28 days had a decrease in anxiety-related behaviour, whilst inducing region-dependent alterations in the γ -aminobutyric acid (GABA) receptor (Bravo et al. 2011). Importantly, this result only occurred with an intact *vagus* nerve, as mice undergoing a vagotomy did not display these behavioural and neurochemical changes. Similarly, in a colitis model, the normalisation of anxiety-like behaviours by the probiotic *Bifidobacterium longum* NCC3001 was found to be vagally dependent (Bercik et al. 2011b). However, the total effects of the microbiome are not solely dependent on the *vagus* nerve stimulation, as mice orally receiving a mixed antimicrobial treatment had altered exploratory behaviour and hippocampal BDNF, independently of vagal integrity (Bercik et al. 2011a). As such, whilst the *vagus* nerve provides a crucial bridge allowing communication between the gut, its microbiome and brain.

In addition to direct neural communication, the gut influences the brain through endocrine pathways, in which microbial-derived metabolites and gut hormones enter the bloodstream and interact with the central nervous system to regulate mood, cognition, and stress responses. ECCs play a key role in this process, secreting hormones such as glucagon-like peptide-1 (GLP-1), peptide YY (PYY), and cholecystokinin (CCK), which regulate appetite, metabolism, and emotional responses (Cryan et al. 2019). Disruptions in gut microbial composition can alter gut hormone release, affecting cognition and the hypothalamic-pituitary-adrenal (HPA) axis, a key regulator of stress responses. Dysbiosis has been associated with HPA axis overactivation, increased cortisol levels, and heightened stress susceptibility, which may contribute to mood disorders such as anxiety and depression (Keller et al. 2017). Probiotic interventions have been shown to normalise cortisol secretion and reduce stress-related behaviours (Tian et al. 2021). In 3xTg-AD mice, probiotic treatment increased plasma concentrations of gut hormones such as ghrelin, leptin, GLP-1 and gastric inhibitory polypeptide, which was associated with improved cognitive function (Bonfili et al. 2017).

Gut microbiota can also shape immune responses by modulating the activity of macrophages, dendritic cells, and T cells, which in turn influence neuroimmune interactions (Kowalski and Mulak 2019). Studies in germ-free (GF) mice have revealed that the absence of gut microbiota leads to immature gut-associated lymphoid tissue (GALT), reduced intestinal lymphocytes, decreased Immunoglobulin A production, and impaired antimicrobial peptide secretion, emphasising the role of microbes in immune system development (Mazmanian et al. 2005; Smith et al. 2007).

Microbial dysbiosis is associated with systemic inflammation. Gut microbiota can stimulate immune cells to release cytokines, including interleukin-6 (IL-6), tumour necrosis factor- α (TNF- α), and interleukin-1 β (IL-1 β). These inflammatory compounds can cross the blood-brain barrier (BBB) and contribute to neuroinflammation (Haase et al. 2020). Constipation-induced gut dysbiosis in mice resulted in increased intestinal and BBB permeability, which induced a Treg/Th17 and Treg17/Teff17 imbalance, cytokines disturbance and autoimmune encephalomyelitis (Lin et al. 2021). Bacterial components such as lipopolysaccharides (LPS) can also activate microglia, the brain's resident immune cells, further exacerbating neuroinflammatory pathways (Yu et al. 2023). On the other hand, beneficial gut bacteria produce anti-inflammatory metabolites such as butyrate, which help maintain intestinal barrier integrity and protect against systemic inflammation, reducing the risk of cognitive decline and neuropsychiatric disorders (Geng et al. 2020; Wang et al. 2020b; Travier et al. 2021).

Many gut bacteria also produce bioactive metabolites, such as short-chain fatty acids (SCFAs), kynurenines, melatonin, histamine, bile acids, and neurotransmitters, which are released into the blood and can directly or indirectly influence the brain (Wikoff et al. 2009; Org et al. 2017). Gut bacteria can produce neurotransmitters, such as γ -aminobutyric acid (GABA), dopamine, and serotonin, which influence brain function and behaviour (Roth et al. 2021). Microbial metabolites such as 4-ethylphenyl

sulfate (4EPS) have been identified as modulators of neurodevelopment, as 4EPS can cross the BBB and impair oligodendrocyte maturation, leading to anxiety-like behaviours in mice (Needham et al. 2022).

Since the gut microbiota is integral to the modulation of this communication at different levels (from the gut lumen to the CNS) and chronologically as we age, many have broadened the term to ‘microbiota-gut-brain axis’ (Cryan et al. 2019). Indeed, the existence of the microbiota-gut-brain axis is supported by substantial preclinical and human evidence, highlighting its effect on different cognitive domains. Firstly, GF mice show that the brain is markedly affected by the absence of microbiota, exhibiting deficiencies in learning, memory recognition and emotional behaviours (Heijtz et al. 2011; Gareau et al. 2011; Luczynski et al. 2016; Foster et al. 2017). These behavioural changes were accompanied by decreased brain-derived neurotrophic factor (BDNF) expression in the hippocampus (Diaz Heijtz et al. 2011; Gareau et al. 2011; Bercik et al. 2011a), a molecule that plays a critical role in promoting synaptic plasticity and supporting cognitive function (Neufeld et al. 2011; Baj et al. 2013; Lu et al. 2014), and significant microbiota-associated reduction in the quantity of dopamine and activation of serotonin synthesis pathways (Matsumoto et al. 2013; Clarke et al. 2013; Lukić et al. 2019; Lyte et al. 2020), suggesting an important role of microbiota in memory, brain health and behaviour. Secondly, chronic antibiotic depletion of microbiota populations alters tryptophan metabolism and the expression of key cognitive signalling molecules in the brain, including decreased BDNF, N-methyl-d-aspartate receptor subunit 2B (NR2B), neuropeptide Y system, oxytocin and vasopressin (Desbonnet et al. 2015; Fröhlich et al. 2016). These changes are associated with long-lasting effects on cognition and increases in anxiety-related behaviours (Verdu et al. 2008; Desbonnet et al. 2015). Finally, administering specific prebiotics/probiotics modulates behaviour in both rodents and humans, including reducing symptoms of depression, anxiety and stress (Bercik et al. 2011a; Liu et al. 2015; Azpiroz et al. 2017; Pinto-Sanchez et al. 2017; Burokas et al. 2017; Marx et al. 2020), alongside suppression of the inflammatory response, enhancement of hippocampal synaptic efficacy and alterations in tryptophan metabolism (Jia et al. 2016; Farhangi et al. 2018).

1.3.2 The Microbiota-Gut-Brain Axis in the context of Ageing and Cognitive Decline

As we age, microbiota composition and function changes (Odamaki et al. 2016). In humans, this has been associated with a decrease in species diversity, a reduction in Clostridiales and *Bifidobacterium* and a rise in Proteobacteria and pathobionts such as Enterobacteriaceae (O’Toole and Jeffery 2015; Odamaki et al. 2016; Wilmanski et al. 2021; Ghosh et al. 2022). However, abnormal alterations in intestinal microbiota composition, as seen in early cognitive decline and AD (Vogt et al. 2017; Li et al. 2019), are associated with local and systemic inflammation, and dysregulation of the microbiota-gut-brain axis (Sochocka et al. 2019). However, much of this relationship remains unexplained. Advances

in sequencing technologies have enabled us to investigate the association between cognitive decline and gut dysbiosis. These studies have highlighted differences in taxonomic levels of *Firmicutes*, *Enterobacteria*, *Bacteroides*, *Actinobacteria*, *Ruminococcus*, *Lachnospiraceae*, and *Selenomonadales* between AD patients in comparison to controls (Cattaneo et al. 2017; Vogt et al. 2017; Zhuang et al. 2018; Haran et al. 2019; Li et al. 2019; Varesi et al. 2022). Such dysregulation can increase inflammatory markers, cytokines and the permeability of the gut epithelial barrier ('leaky gut'), resulting in excessive leakage of bioactivated molecules, such as short-chain fatty acids (SCFAs), kynurenines, melatonin, histamine, bile acids, and neurotransmitters, into the blood. The resulting increase in neuroactive products can no longer efficiently be removed by the body's next barrier; the liver, and therefore can cause a variety of physiological changes directly and indirectly affecting the CNS, including a further decrease in BBB function (Obrenovich 2018). In the elderly population, this dysregulation becomes particularly relevant, as the BBB becomes more permeable with age (Verheggen et al. 2020). A more permeable BBB allows an increased influx of harmful blood components, including microbial metabolites, into the brain; a feature seen in AD patients (reviewed by (Sweeney et al. 2018)). This process promotes neuroinflammation and macrophage dysfunction, leading to neural injury and ultimately a reduction in cognitive function (Ticinesi et al. 2018; Wu et al. 2021).

1.4 Microbial-Derived Metabolites and Cognitive Decline

Emerging research has increasingly underscored the critical role of gut microbiota in influencing brain health through the production of microbial-derived metabolites. These bioactive compounds, generated from the metabolic activities of gut bacteria, can travel through the circulatory system to the CNS and impact neuronal function. Specific metabolites, such as bile acids, TMAO, tryptophan, *p*-cresol and derivatives, have garnered attention for their potential links to cognitive decline and neurodegenerative diseases. Disruptions in the balance of these metabolites promotes neuroinflammation, oxidative stress, and pathological changes within the brain (Haase et al. 2020; Brunt et al. 2020; Heylen et al. 2023). However, the role of specific metabolites in brain health and AD remains unclear.

1.4.1 Bile acids

Humans produce large, hydrophilic pools of primary bile acids (BA) from cholesterol in the liver that are secreted into bile (Figure 1.2). BAs are largely synthesised via two biosynthetic pathways: the classical pathway and the alternative pathway (Chiang 2013). The classic pathway produces the majority of BAs in humans (~90%) and is initiated by the cholesterol 7 α -hydroxylase (CYP7A1) enzyme to synthesise the primary BAs cholic acid (CA) and chenodeoxycholic acid (CDCA) (Šarenac and Mikov 2018). The alternative pathway contributes less than 10% of BA synthesis (with more minor pathways contributing the remainder) and is initiated by sterol 27-hydroxylase (CYP27A1) (Spichak et

al. 2021). After synthesis in the liver, CA and CDCA can be conjugated with hydrophilic taurine or glycine residues before they are secreted from hepatocytes into the bile canaliculi. Recent findings have shown that BAs can also conjugate with other amino acids such as glutamine, leucine, tyrosine, and phenylalanine, expanding the diversity of bile acid conjugates and suggesting additional roles in metabolic regulation (Quinn et al. 2020). BAs are stored in the gallbladder ready to be distributed into the small intestine following a meal to expedite digestion and emulsify dietary lipids and fat-soluble vitamins. Once secreted into the small intestine, more hydrophobic secondary BAs are formed by gut bacteria and are subsequently excreted or reabsorbed in the ileum to enter the enterohepatic circulation and recycle back to the liver (Guzior and Quinn 2021). This efficient process ensures BAs are recycled between 4 to 12 times a day (Chiang 2013).

In the brain, cholesterol can be metabolised by a final pathway known as the neural cholesterol pathway. As the brain is one of the more sensitive organs to hypercholesterolemia, this cholesterol breakdown is essential to maintaining brain health (Baloni et al. 2020). Excess cholesterol becomes oxidised into 24- and 25-hydroxycholesterol by cholesterol 24-hydroxylase (CYP46A1), an enzyme primarily expressed in the brain (McMillin and DeMorrow 2016). Once 24(S)-hydroxycholesterol is formed, it can pass through the BBB and enter circulation. From here, 24(S)-hydroxycholesterol travels back to the liver to be metabolised by CYP39A1 and continue in BA synthesis (McMillin and DeMorrow 2016). In mice with mutated CYP46A1 function, 24(S)-hydroxycholesterol is not formed and is associated with impairments in spatial, associative and motor learning, highlighting the importance of this pathway for maintaining cognitive function (Kotti et al. 2006).

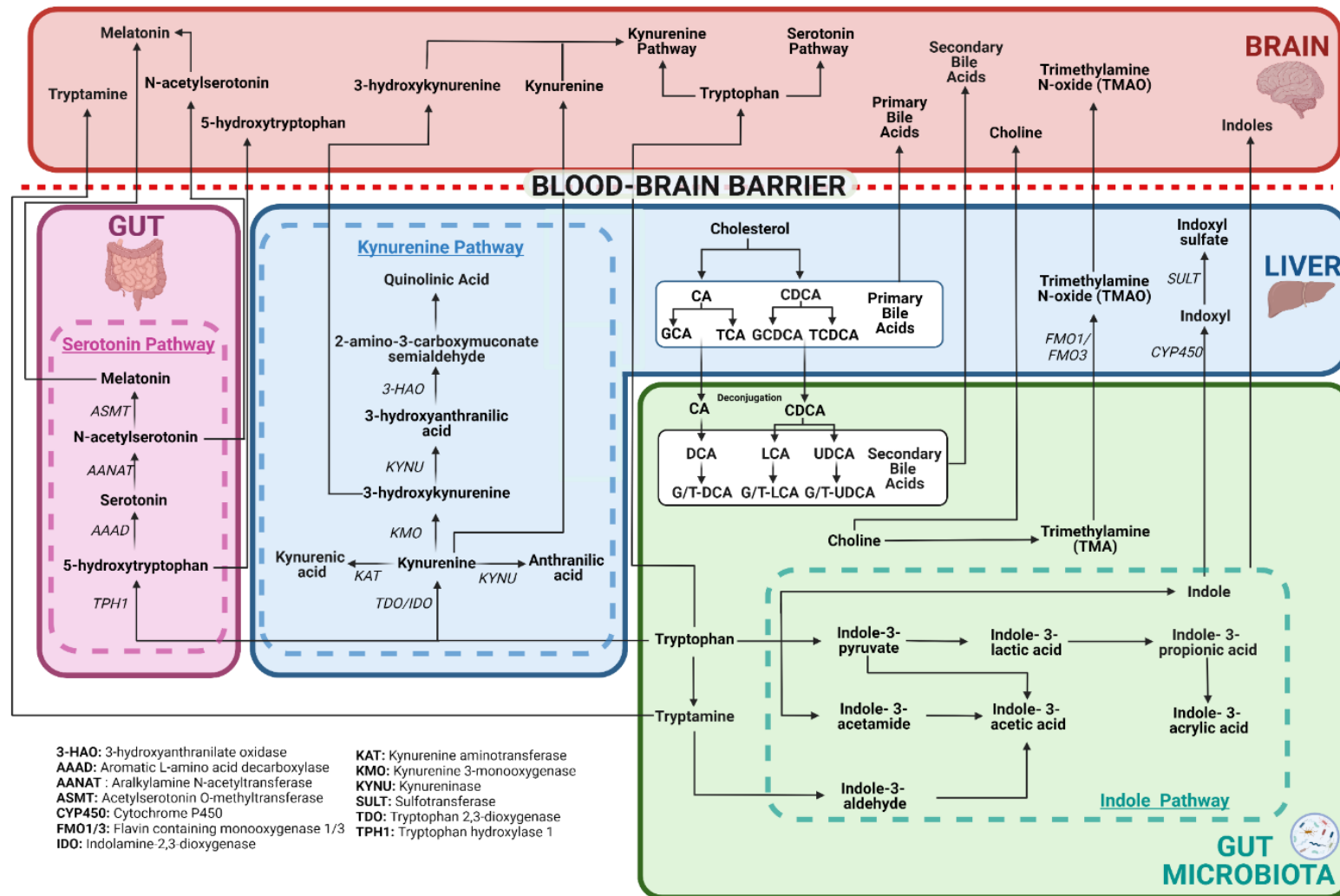


Figure 1.2: Bile acids, TMAO and tryptophan metabolic pathways and their links to the brain. Primary bile acids are produced from cholesterol breakdown in the liver. They can be conjugated with taurine or glycine residues before travelling to the gut, where they are deconjugated and converted to secondary bile

acids via microbial action. Bile acids have been found in the brain of humans and rodents suggesting they can cross the blood-brain barrier via either diffusion (unconjugated) or active transport (conjugated) and influence the central nervous system. TMAO is produced via a two-stage process. TMA is first formed from the microbial conversion of choline in the gut. TMA then travels to the liver, where the FMO1/3 enzyme converts it to TMAO. Recent evidence found TMAO in human brains, indicating it can cross the blood-brain barrier. Tryptophan can be metabolised via three key pathways. Firstly, via gut microbial action, tryptophan can be converted via the indole pathway into numerous indole derivatives, or the amino acid, tryptamine. Indoles and tryptamine are known to cross the BBB. Secondly, around 3% of dietary tryptophan is metabolised into serotonin and melatonin via numerous enzymes in the serotonin pathway. Notably, serotonin produced in the gut cannot cross the blood-brain barrier. However, the serotonin precursor, 5-hydroxytryptophan, and serotonin derivatives, N-acetylserotonin and melatonin, can cross the blood-brain barrier and influence the central nervous system. Finally, the majority of tryptophan (~90-95%) is metabolised via the kynurenine pathway, of which 90% occurs in the liver. This pathway is initiated by the TDO enzyme in the liver and the IDO enzyme in the brain. Only kynurenine, 3-hydroxykynurenine and tryptophan itself can cross the blood-brain barrier. However, once in the brain, tryptophan can be metabolised via both the kynurenine and serotonin pathways to form the pathway's intermediates.

Bile Acids in the Brain

Over 20 conjugated and unconjugated BAs and their receptors have been reported in both human and rodent brains (Baloni et al. 2020; Higashi et al. 2017; Mano et al. 2004; Pan et al. 2017), suggesting BAs can not only cross the BBB but also bind to nuclear receptors and initiate physiological responses (Quinn et al. 2014; Pan et al. 2017). However, the mechanism by which BAs cross the BBB is still uncertain. Unconjugated BAs may diffuse across the BBB as CA, CDCA and deoxycholic acid (DCA) are known to diffuse across phospholipid bilayers (Kamp et al. 1993) and concentrations in the brain correlate with serum levels (Higashi et al. 2017). On the other hand, conjugated bile salts must cross the BBB via active transport due to their hydrophilic anionic structure at physiological pH (Bron et al. 1977; Benedetti et al. 1997). Indeed, members of the solute carrier (SLC) family, such as the organic anion transporting polypeptides (OATP1A4 and 1C1) (Cheng et al. 2005) and the apical sodium-dependent bile acid transporter (ASBT or SLC10A2) (Nizamutdinov et al. 2017), and members of the ATP-binding cassette transporters (ABC) family such as ABCC2 and ABCC4 (Soontornmalai et al. 2006; Roberts et al. 2008) have been identified in the brain. Conversely, Baloni and colleagues through a large-scale transcriptomics analysis of 2,114 post-mortem brains identified only three BA transporters (ABCC1, ABCC4 and SLC51A/SLC51B) in the brain (Baloni et al. 2020). The primary role of these transporters is to reduce the concentration of cytotoxic molecules by transporting them into the bloodstream (Abbott et al. 2010). Yet, since these transporters occur on both the basolateral (blood-facing) and apical (brain-facing) side (Mertens et al. 2017), they may also transport molecules into the CNS from systemic circulation, indicating a potential endogenous signalling role of BAs in the brain. However, there is still a lack of direct evidence of *in vivo* transport of BA over the BBB (Mertens et al. 2017).

Bile Acids and Cognitive Function

While BA function in the GI tract is well-characterised, significantly fewer studies investigated their effect on the brain, limiting our knowledge (McMillin and DeMorrow 2016). Accumulating evidence suggests that cognition can be influenced by the dysregulation of BA synthesis and metabolism. Indeed, BAs profiles are reportedly altered in cases of MCI and AD, with an increase in cytotoxic secondary BAs and a decrease in primary BAs, suggesting a role of the gut microbiome in the disease progression (MahmoudianDehkordi et al. 2019). Recently, conjugated primary bile acids have been found to drive synaptic loss and cognitive decline in rodents (Ren et al. 2024). Increased serum concentrations of the secondary BA, DCA, have been observed in AD patients (Olazarán et al. 2015) and can modulate mitochondrial pathways causing apoptosis in a variety of tissues and cell types in BCS-TC2 human colon adenocarcinoma cells (Ignacio Barrasa et al. 2011). BA dysbiosis, resulting from either liver or microbiota dysfunction, has been subsequently associated with increased gut permeability, possibly through FXR and TGR5 receptor signalling, and inflammation, promoting further bacterial dysbiosis in

the gut (Tran et al. 2015). Inflammation is also a known trigger of microglial activation and reduced neuroplasticity (Jena et al. 2018), possibly through the production of reactive oxygen species (ROS) (Bernstein et al. 2009), highly reactive chemical molecules that can contribute to cognitive decline and AD progression (Dröge and Schipper 2007; Moreira et al. 2010). Although, some have proposed an important physiological role of ROS in brain metabolic signalling (Leloup et al. 2006).

Alternatively, some BAs have been reported to have neuroprotective effects on the brain (Table 1.1). The primary BA, CA, has been identified as an LXR ligand, which in turn promoted midbrain neural development and neurogenesis in zebrafish (Theofilopoulos et al. 2013). Tauroursodeoxycholic acid (TUDCA), a secondary conjugated BA, can suppress amyloid- β ($A\beta$)-induced apoptosis in neuronal cell cultures and rodent neurons through the inhibition of the E2F-1/p53/BAX pathway (Rodrigues et al. 2002; Ramalho et al. 2004). Similarly, in APP/PS1 double-transgenic mice, providing a TUDCA-enriched diet for 6 months reduced $A\beta$ aggregates, neuronal apoptosis, memory deficits and phosphorylation of TAU (Solá et al. 2006; Nunes et al. 2012; Dionísio et al. 2015). TUDCA has also been shown to induce anti-inflammatory effects in a mouse model of acute neuroinflammation through its binding and activation of G protein-coupled bile acid receptor 1/Takeda G protein-coupled receptor 5 (GPBAR1/TGR5), a receptor expressed on microglia (Yanguas-Casás et al. 2017). Finally, in adult rats, TUDCA also enhanced neural stem cell proliferation and early neurogenesis (Soares et al. 2018), processes that are significantly diminished in AD (Cosacak et al. 2019), with some research suggesting increasing neurogenesis may counteract AD pathological outcomes. Together these findings provide convincing evidence that cognition can be influenced by BAs. Yet further research is required to determine the involvement of specific BA transporters and receptors, as well as the subsequent mechanisms in their neuroprotective and detrimental effects.

Table 1.1: Bile acids and their impact on cognition and AD.

<i>Bile Acid</i>	<i>In Vitro/ In Vivo (species)</i>	<i>Model</i>	<i>Findings</i>	<i>Reference</i>
CA (Primary Bile Acid)	<i>In Vivo</i> (Male Sprague-Drawly rats)	Ibotenic Acid-Induced Dementia Model	A combination of administering baicalin, jasminoidin and cholic acid improved cognitive performance through the promotion of pathways related to neuroprotection and neurogenesis	(Zhang et al. 2013)
	<i>In Vivo</i> (Zebrafish)	Zebrafish embryos exposed to a cholic acid-treated medium	Cholic acid was identified as a LXR ligand, which in turn promoted neural development and neurogenesis in the midbrain of zebrafish.	(Theofilopoulos et al. 2013)
CDCA (Primary Bile Acid)	<i>In Vivo</i> (Adult male Wistar rats)	AlCl ₃ induced AD	CDCA treatment reduces neurotoxicity and cognitive decline via increased insulin signalling	(Bazzari et al. 2019)
	<i>In Vitro</i>	Primary dissociated cultures of the posterior hypothalamus	CDCA is an antagonist for NMDA and GABA _A receptors and can significantly reduce neuronal firing	(Schubring et al. 2012)
TCA (Primary Conjugated Bile Acid)	<i>In Vivo</i> (human)	Human brain tissue with AD pathology vs age-matched healthy controls	TCA was significantly lower (p=0.01) in AD patients than in age-matched controls	(Pan et al. 2017)
DCA (Secondary Bile Acid)	<i>In Vitro</i>	BCS-TC2 human colon adenocarcinoma cells	DCA modulates mitochondrial pathways causing apoptosis	(Ignacio Barrasa et al. 2011)
	<i>In Vivo</i> (human)	Serum samples from AD patients, amnesic MCI patients and healthy controls	DCA was increased in amnesic MCI and AD in comparison to healthy controls and correlated with cognitive symptoms	(Olazarán et al. 2015)

LCA (Secondary Bile Acid)	<i>In Vivo</i> (human)	Plasma samples from patients with AD, MCI and healthy controls	LCA was significantly higher in AD patients (p= 0.004) compared to healthy controls.	(Markstein et al. 2017)
UDCA (Secondary Bile Acid)	<i>In Vitro</i>	BV-2 microglial cell line	UDCA can initiate an anti-inflammatory effect by inhibiting NF-κB activation	(Joo et al. 2004)
TUDCA (Secondary Conjugated Bile Acid)	<i>In Vitro</i>	Neuron cell cultures and primary rat neurons	Inhibition of the E2F-1/p53/Bax pathway, leading to suppression of Aβ-induced apoptosis	(Ramalho et al. 2004)
	<i>In Vitro</i>	Primary cultures of rat cortical and hippocampal neurons	Reduction in synaptic deficits induced by Aβ through inhibiting the downregulation of postsynaptic density protein-95, leading to a reduction in neuronal death.	(Ramalho et al. 2013)
	<i>In Vivo</i> (mouse)	AD model: APP/PS1 double transgenic mice	Dietary TUDCA provided for 6 months decreased Aβ aggregation and enhanced memory retention.	(Nunes et al. 2012)
	<i>In Vivo</i> (mouse)	AD model: APP/PS1 double transgenic mice	Dietary TUDCA provided for 6 months decreased hippocampal and prefrontal amyloid deposition and inhibited spatial, recognition and contextual memory deficiencies.	(Lo et al. 2013)
	<i>In Vivo</i> (mouse)	AD model: APP/PS1 double transgenic mice	Intraperitoneal injections of TUDCA decreased Aβ deposition, glycogen synthase kinase 3β activity, phosphorylation of τ, and neuroinflammation.	(Dionísio et al. 2015)
	<i>In Vitro</i>	Aβ-treated primary rat cortical neurons	TUDCA prevented Aβ induced cytochrome c release and neuronal death through the PI3K signalling pathway	(Solá et al. 2003)
				(Solá et al. 2006)

	<i>In Vitro</i>	A β -treated primary rat cortical neurons	TUDCA reduced A β induced apoptosis through the binding to mineralocorticoid receptors	
--	-----------------	---	--	--

Bile Acids as a Risk Factor of Cognitive Decline

The association between BAs and cognitive decline, in particular with known AD pathologies (Nho et al. 2019), has raised speculations that BA profiles could be used as a risk factor of cognitive decline. Currently, there is limited research into the topic. However, Olazarán and colleagues investigated a large cohort of patients with MCI and AD and identified DCA as being independently associated with the presence of cognitive symptoms (Olazarán et al. 2015). Mapstone et al. identified seven blood-based markers which included glycoconjugated deoxycholic acid (GUDCA) and could predict the onset of AD or amnesic MCI within 2-3 years with an accuracy of over 90% (Mapstone et al. 2014). Similarly, Marksteiner and colleagues were able to differentiate between healthy controls and AD patients from the concentration of lithocholic acid (LCA) in plasma (Marksteiner et al. 2017). However, it should be noted this study utilised a relatively small sample size (n=80) and did not control for the effects of varied diets between individuals, warranting further investigation into the use of BAs as risk factors of cognitive decline.

1.4.2 TMAO

Trimethylamine N-oxide (TMAO) is a microbial-dependent metabolite generated by the breakdown of dietary fish, meat and fat (Mitchell et al. 2002; Vogt et al. 2018). Trimethylamine (TMA), the precursor to TMAO, is produced from the metabolism of choline, L-carnitine and phosphatidylcholine by anaerobic microbes in the gut, predominantly located in the small intestine (Figure 1.2) (Craciun and Balskus 2012; Stremmel et al. 2017). TMA subsequently travels through the portal vein to the liver where it is oxidised by flavin-containing monooxygenase 1 and 3 (FMO1 and FMO3) to form TMAO (Wang et al. 2020a). Once formed, TMAO can enter the systemic circulation, hence TMAO plasma levels (typically 3 $\mu\text{mol/L}$ in healthy individuals (Ufnal et al. 2015)) have been found to correlate with the gut microbial composition (Org et al. 2017).

TMAO and the Brain

In vivo studies have identified TMAO in the CSF of both mice and humans, implying that circulating TMAO can influence the CNS (Del Rio et al. 2017; Vogt et al. 2018). The high concentrations of TMAO detected in the human CSF suggest liver-derived TMAO can cross the BBB, however, the penetration mechanism is unclear (Vermetti et al. 2017). It is also possible a portion of TMAO found in the brain

may be synthesised *de novo*, as FMO3, the enzyme required to convert TMA to TMAO, has been detected in the adult brain (Zhang and Cashman 2006).

TMAO and Cognitive Decline

Over the last decade, TMAO has received increased attention in medical studies due to its links with cardiovascular diseases (Tang et al. 2014), obesity, diabetes (Gao et al. 2014), chronic kidney disease (Missailidis et al. 2016), metabolic syndrome (Barrea et al. 2018), brain ageing and cognitive impairment (Li et al. 2018a) and neurodegenerative disorders such as AD (Vogt et al. 2018). However, the influence of TMAO on cognition is unclear. In fact, there is much controversy as to whether TMAO promotes a positive or detrimental effect on the brain.

Both experimental (Li et al. 2018a; Gao et al. 2019; Govindarajulu et al. 2020) and clinical (Zhu et al. 2020; Brunt et al. 2020; He et al. 2020) studies suggest high levels of TMAO may be causally associated with cognitive decline. Vogt and colleagues discovered an increase in CSF TMAO in AD patients in comparison to controls, suggesting the metabolite may contribute to decreasing neurological function (Vogt et al. 2018). However, a recent Mendelian randomisation study disputes this relationship (Zhuang et al. 2020).

The mechanisms by which TMAO may contribute to cognitive decline remain broad and unclear. TMAO reportedly modulates lipid and hormonal homeostasis (Vogt et al. 2018), encourages platelet hyperreactivity via the enhancement of stimulus-dependent release of calcium ions (Zhu et al. 2016), modifies cholesterol and sterol breakdown, reduces reverse cholesterol transport (Koeth et al. 2013), and increases endothelial dysfunction through the induction of the NLRP3 inflammasome (Chen et al. 2017). Rodents fed supraphysiological doses of TMAO also suggest the metabolite promotes neuronal senescence, oxidative stress, mitochondrial dysfunction and prevents mTOR signalling (Li et al. 2018a). Furthermore, TMAO is known to upregulate macrophage scavenger receptors and induce CD68 expression (Koeth et al. 2013; Seldin et al. 2016), a marker known to correlate with cognitive impairment in rodents (Farso et al. 2013).

High circulating TMAO may also promote neuroinflammation, a recognised mediator of cognitive ageing and neurological function (Ownby 2010; Simen et al. 2011), by increasing brain NF- κ B and proinflammatory cytokines, thereby promoting proinflammatory signalling pathways (Brunt et al. 2020). Brunt and colleagues suggested that elevated TMAO in plasma and the brain can stimulate astrocytes, neuroinflammation and reduce cognitive function, especially in the subdomain of memory (Brunt et al. 2020). High circulating concentrations of TMAO also downregulated the antioxidant enzyme methionine sulfoxide reductase A (MSRA) in the hippocampus of aged rats with induced cognitive impairment by sevoflurane exposure (Zhao et al. 2019). This downregulation is suggested to

sensitise the hippocampus to oxidative stress, promoting microglial-mediated neuroinflammation and cognitive impairment. Collectively, studies indicate a detrimental effect of TMAO when modulated above physiologically relevant concentrations.

In line with this, reducing TMAO has been shown to alleviate cognitive impairment. 3,3-Dimethyl-1-butanol, an inhibitor of microbial TMA formation, reduced cognitive decline, long-term potentiation and pathological deterioration in AD transgenic mice (Gao et al. 2019). Similarly, the probiotic *Lactobacillus plantarum* decreased circulating TMAO levels, alleviating cognitive impairments and pathological deterioration, exhibiting the potential modulation of the gut microbiome for therapeutic benefit (Wang et al. 2020a).

In contrast to the evidence supporting a detrimental effect of TMAO upon the brain, several studies suggest TMAO may exert a neuroprotective effect when within normal physiological ranges (plasma levels ~0.5–5 μM). Hoyles and colleagues, using a mixed *in vitro* endothelial cell culture and *in vivo* rodent model approach, discovered that TMAO can enhance and protect BBB integrity through modulation of the actin cytoskeleton and tight junctions (Hoyles et al. 2021). Here, administering TMAO reduced paracellular permeability, likely due to an increase in annexin A1 expression. TMAO, therefore, may promote BBB function and help protect the brain from an influx of cytotoxic molecules. Interestingly, TMA, the precursor to TMAO, was found to have a deleterious effect on endothelial barrier integrity in rodents, inducing actin stress fibre formation and leading to increased presence in the CNS (McArthur et al. 2018).

TMAO is a naturally occurring osmolyte and as such has been found to stimulate TAU-induced tubulin assembly *in vitro* (Tseng and Graves 1998). TMAO, therefore, can promote and enhance microtubule assembly in hyperphosphorylated and most mutant TAU proteins, decreasing microtubule disassembly and neuronal death; two hallmark features of AD (Smith et al. 2000). TMAO overcomes functional deficits caused by phosphorylation by lowering the critical concentration of tubulin required for assembly (Tseng et al. 1999), with assembly occurring at a faster rate than wild-type TAU (Smith et al. 2000). Therefore, as an osmolyte, and with its ability to favourably hydrate partially denatured proteins, TMAO has been suggested as a potential therapeutic approach in AD and other protein misfolding conditions (Bose and Cho 2017).

Collectively, it seems plausible that TMAO affects the brain in a dose-dependent manner, as within a physiologically relevant range, TMAO may possess neuroprotective potential. However, interpreting the relationship between systemic TMAO and cognition is further complicated by studies indicating wide inter and intra-individual variations in circulating TMAO levels (Velasquez et al. 2016). TMAO concentrations vary with age (Wang et al. 2014), diet (Koeth et al. 2013) and cholic acid levels (a BA known to induce FMO3 expression via FXR activation (Janeiro et al. 2018)). In fact, plasma TMAO concentrations have been found to mirror an individual's intake of whole grains, fish and vegetables

(Costabile et al. 2021). TMAO levels are also influenced by renal clearance, as glomerular filtration rate is inversely related to plasma TMAO concentrations (Missailidis et al. 2016). As a result, changes in plasma TMAO may be a consequence of an accumulation of factors unrelated to cognitive decline (DiNicolantonio et al. 2019).

TMAO as a Risk Factor of Cognitive Decline

Due to TMAO's high association with atherosclerosis and cardiovascular disease, TMAO has been considered a risk factor of vascular dementia (Li et al. 2018b). However, a data-driven, hypothesis-free computational analysis into microbial metabolites and AD identified TMAO as one of the top potential biomarkers of neurodegeneration, successfully predicting changes in memory and fluid cognition in ageing individuals (Xu and Wang 2016). These results show promising potential for the use of TMAO as a risk factor of cognitive decline. However, the current contrasting evidence surrounding the relationship necessitates further *in vivo* investigation.

1.4.2 Tryptophan

Tryptophan is an essential aromatic amino acid that cannot be synthesised by animal cells (Agus et al. 2018). Humans, therefore, need to attain tryptophan through dietary sources such as fish, milk and chicken or, if vegetarian, seeds, soybeans and peas (Richard et al. 2009; Clarke et al. 2020). Tryptophan is a biosynthetic precursor to numerous microbial and host metabolites, making it essential to human health (Agus et al. 2018). Approximately 4-6% of tryptophan reaches the colon where gut microbiota metabolise it into a wide variety of molecules (Figure 1.2), thereby limiting the availability of tryptophan for the host (Gao et al. 2018). Evidence for the involvement of microbiota in tryptophan metabolism comes from GF mice, who display increased plasma tryptophan levels which are normalised after conventionalisation (Wikoff et al. 2009; Clarke et al. 2013).

Previous experimental reports implicate tryptophan and its derivatives in modulating human health and neurological function (Roager and Licht 2018). Gut microbiota can directly and indirectly modulate two major tryptophan metabolism pathways, the serotonin pathway and the kynurenine pathway (KP), affecting the concentration of various cognitively relevant metabolites and neurotransmitters (Stone and Darlington 2013; Jenkins et al. 2016; Savitz 2020). Conversely, the two pathways can negatively influence microbial proliferation and diversity (Dehhaghi et al. 2019). Gut microbiota can also directly metabolise tryptophan into indole and its derivatives (Agus et al. 2021), which has also been associated with cognitive function (Clarke et al. 2020).

The Kynurenine Pathway and Cognitive Decline

Around 90-95% of dietary tryptophan is metabolised by the KP, mainly taking place in the liver, forming the intermediates kynurenic acid, quinolinic acid, picolinic acid, 3-hydroxykynurenine (3-HK) and nicotinamide adenine dinucleotide, known as kynurenines (Badawy 2017). Only tryptophan, 3-HK and kynurenine are known to readily cross the BBB. However, fluctuations in the systemic concentrations of these metabolites directly impact KP metabolism in the CNS, including the synthesis of kynurenic acid and quinolinic acid in the brain (Schwarcz et al. 2012). Quinolinic acid, an endogenous neurotoxin, is known to activate N-methyl-D-aspartate (NMDA) receptors, increase neuronal activity, elevate intracellular calcium concentrations and modulate BBB integrity (Lugo-Huitrón et al. 2013). Quinolinic acid can also increase neuronal glutamate release whilst inhibiting its reuptake by astrocytes and inhibiting glutamate synthetase (an enzyme playing a crucial role in the glutamate metabolism in astrocytes) to produce a cytotoxic response (Ting et al. 2009; Fujigaki et al. 2017). Kynurenic acid, on the other hand, plays a neuroprotective role against quinolinic acid's toxicity, acting as an antagonist on both glycine and glutamate modulatory sites of NMDA receptors at high and low concentrations respectively (Stone and Darlington 2013). However, the abnormal build-up of kynurenic acid can induce glutamatergic hypofunction, possibly disturbing cognitive functioning (Fujigaki et al. 2017).

Accumulating evidence implicates the KP in AD progression and inflammatory responses (Hwu et al. 2000). Increased plasma concentrations of the cytotoxic quinolinic acid (from 192 nM to 334 nM) and reduced concentrations of tryptophan (from 29.83 mM to 22.09 mM) and neuroprotective kynurenic acid (from 30.94 nM to 20.85 nM) has been associated with AD patients in comparison to healthy controls (Gulaj et al. 2010). Unbalanced upregulation of the KP may trigger a degree of injury to the surrounding tissues, playing a role in neurodegeneration (Yu et al. 2015). Previous studies have found an inverse relationship between KP activation and cognitive performance (Ramos-Chávez et al. 2018).

In a cognitively healthy population, increased inflammatory markers are related to poor cognitive performance (Smith et al. 2012). In AD, indoleamine 2, 3-dioxygenase (IDO), the enzyme responsible for catabolising tryptophan into products that enter the KP, is stimulated through proinflammatory cytokine activity, including interferon-gamma (IFN- γ) (Yamada et al. 2009), interleukin-12 (IL-12), interleukin-18 (IL-18) (Liebau et al. 2002), and the A β 1-42 fragment (Solvang et al. 2019). Complex neuroinflammation in the CNS can contribute to AD development. Microglia and astrocytes, which contain all of the enzymes necessary for the KP, are the primary effectors of neuroinflammation in AD (Mithaiwala et al. 2021). The edge of senile plaques in the hippocampus of *post-mortem* AD brain tissue has the greatest amounts of IDO and quinolinic acid expressed by microglia and astrocytes (Guillemin et al. 2005). Activated microglia are the main source of quinolinic acid throughout neuroinflammation

(Feng et al. 2017). Quinolinic acid produces hyperphosphorylation of TAU in human cortical neurons, cytotoxicity in astrocytes and neurons, astrocytic activation and astrogliosis (Rahman et al. 2009; Yu et al. 2015). Together, these studies strongly suggest the involvement of IDO and KP metabolism in neuroinflammation and cognitive impairment.

Accordingly, the KP is a well-rationalised therapeutic target for improving cognition. Several proof-of-concept studies using known KP pathway modulators, such as the kynurenine monooxygenase (KMO) inhibitor JM6, prevent spatial memory deficits, anxiety-related behaviours, and synaptic loss in APP Tg mice (Zwilling et al. 2011). In addition, the IDO-1 inhibitor, coptisine, decreases the activation of microglia and astrocytes in APP/PS1 mice, preventing neuronal loss and improving cognitive function (Yu et al. 2015). However, the specific relationship between tryptophan depletion or supplementation and the modulation of KP intermediates remains unclear (van Donkelaar et al. 2011; Crockett et al. 2012; Hughes et al. 2012).

Serotonin Pathway and Cognitive Decline

Approximately 3% of dietary tryptophan is required to produce serotonin (5-hydroxytryptamine (5-HT)) and melatonin (Gao et al. 2018). 5-HT is primarily found in the GI tract, blood platelets and the CNS and is synthesised via a two-stage enzymatic reaction involving tryptophan hydroxylase and aromatic amino acid decarboxylase. Serotonin synthesised in the GI tract cannot cross over the BBB under healthy conditions (El-Merahbi et al. 2015). Tryptophan, on the other hand, can enter the CNS via carrier proteins (Höglund et al. 2019). Therefore, the gut microbiota importantly regulates tryptophan availability for serotonin synthesis in the CNS.

Enzymes such as tryptophan hydroxylase and IDO balance the ratio of tryptophan metabolism via the KP and serotonin pathways (Lovelace et al. 2017). A shift in tryptophan metabolism to the KP decreases the availability of tryptophan in the serotonin pathway, consequently reducing serotonin availability for the host (Oxenkrug 2013). Serotonin plays a vital role in behaviours requiring high cognitive demand (Jenkins et al. 2016). Reductions in serotonin, therefore, are frequently associated with declines in learning, memory consolidation (Cowen and Sherwood 2013) and long-term memory (Schmitt et al. 2006). As such, serotonin is associated with neurological disorders such as depression (Cowen and Browning 2015) and AD (Porter et al. 2000), resulting in treatment options such as selective serotonin reuptake inhibitors (SSRI) to increase 5-HT neurotransmission and improve mood in the context of depression. In rodents, administering tryptophan orally, thereby increasing 5-HT neurotransmission, was found to improve memory acquisition, consolidation and storage (Haider et al. 2007), whilst daily tryptophan injections improved spatial memory (Levkovitz et al. 1994). Together, this evidence strongly suggests a link between cognitive decline and tryptophan through changes in tryptophan metabolism.

Other Tryptophan Metabolites

Numerous studies have identified abnormal tryptophan metabolism in patients with cognitive decline (Kaddurah-Daouk et al. 2013; Liu et al. 2015; Clarke et al. 2020). Although most studies link this association with the KP and its intermediates, other tryptophan metabolites, such as indole and its derivatives, may play a role. Bacterial tryptophan catabolites tryptamine, skatole, indole, indole-3-acetic acid (IAA), indole-3-acrylic acid (IA), indole-3-aldehyde (IAld), indole propionic acid (IPA), indoxyl-3-sulfate (I3S) and indole-3-lactic acid (ILA) are ligands of the aryl hydrocarbon receptor (AhR) (Zelante et al. 2013; Cheng et al. 2015; Cervantes-Barragan et al. 2017; Schroeder et al. 2010; Hubbard et al. 2015). AhR is a transcription factor widely expressed by cells in the immune system and known to play a role in inflammation, a factor highly associated with ageing and cognitive decline (Ramos-García et al. 2020). Antibiotic-treated mice administered with indole, I3S, IPA and IAld were found to have reduced CNS inflammation via AhR activation in astrocytes (Rothhammer et al. 2016). Wei and colleagues discovered activation of the AhR by indole could promote neurogenesis in the adult mouse hippocampus (Wei et al. 2021). Interestingly, this result was found to be ligand-specific as kynurenine, another known AhR ligand, failed to replicate these findings.

Both *in vitro* and *in vivo* studies have associated indoles with enhancing intestinal barrier function by increasing gene expression associated with the maintenance of epithelial cell structure and function (Bansal et al. 2010; Shimada et al. 2013), thereby decreasing the concentration of neuroactive products in circulation (Sochocka et al. 2019). The activation of AhR also helps preserve epithelial barrier function by maintaining tight junction integrity (Yu et al. 2018). IA may also have anti-inflammatory and anti-oxidative effects in LPS-activated human peripheral blood mononuclear cells (PBMCs) by reducing IL-6 and IL-1 β secretion and activation of the NRF2-ARE pathway (Wlodarska et al. 2017), a pathway suggested to ameliorate cognitive deficits (Joshi and Johnson 2012; Tian et al. 2019).

Tryptophan & Derivatives as Risk Factors of Cognitive Decline

Although no research studies to date have exclusively investigated the use of tryptophan and its derivatives as a risk factor of cognitive decline, many reports have highlighted the potential use of tryptophan pathway imbalances to reveal signs of cognitive decline (Liu et al. 2014). Kaddurah-Daouk and colleagues concluded from studying CSF of AD patients that changes in tryptophan, as well as methionine, tyrosine, and purine metabolism occurred in MCI and AD, suggesting its potential use as a risk factor of cognitive decline (Kaddurah-Daouk et al. 2013). However, the authors concluded that these changes may not be detectable in plasma, as the amount to which metabolic changes in blood mirror fluctuations in CSF remains to be investigated. Nevertheless, plasma metabolic profiling revealed changes in tryptophan metabolism in early cognitive decline, along with alterations in progesterone, lysophosphatidylcholine, L-phenylalanine, dihydrosphingosine and phytosphingosine

(Liu et al. 2014). Despite a lack of studies into the use of tryptophan and its derivatives as a risk factor of cognitive decline, these studies highlight the possible future use of metabolomic profiling to detect early changes.

1.4.4 *p*-Cresol

Amino acids present in dietary protein serve (particularly if overconsumed) as a fermentation substrate for bacteria in the large intestine. *p*-Cresol is the product of the microbial conversion of tyrosine and phenylalanine, notably by the bacteria from the *Coriobacteriaceae* or *Clostridium* genera (Saito et al. 2018). *p*-Cresol is an exogenous uremic toxin primarily produced by the microbial conversion of tyrosine and phenylalanine in the colon. Due to its toxicity, *p*-cresol is further conjugated with sulfate or glucuronic acid by host cells such that it is almost entirely found as *p*-cresol sulfate (PCS) or *p*-cresol glucuronide (PCG), in circulation, promoting its removal by the kidneys (Liu et al. 2018a).

p-Cresol can increase endothelial permeability *in vitro* through modulation of the actin cytoskeleton and adherens junctions (Cerini et al. 2004), decreasing the gut's barrier function. In the brain, *p*-cresol has been found to modulate dopamine turnover in Autism Spectrum Disorder BTBR mice, significantly increasing anxiety-like and hyperactive behaviours (Pascucci et al. 2020). *p*-Cresol's derivative, PCS, has been detected in the CSF of Parkinson's disease patients, suggesting the metabolite may cross the BBB and have a pathogenic effect on the CNS (Sankowski et al. 2020). However, this relationship may in part be due to the increased permeability of the BBB seen in PD (Al-Bachari et al. 2020). Increases in PCS has been associated with a variety of detrimental processes, including cell death and dysfunction through oxidative stress, inflammation, impairment of mitochondrial dynamics and vascular disruption (Azevedo et al. 2016; Sun et al. 2017; Edamatsu et al. 2018; Tang et al. 2018). PCS also acts as a potent neurotoxin due to its ability to cross the BBB, with concentrations in the CNS positively correlated with circulatory levels (Sankowski et al. 2020). Its administration in mice with nephrectomy contributed to neurological dysfunction through impairment of cell survival and neurogenesis, supporting its potential role in cognitive decline (Sun et al. 2020).

While PCG has long been recognised to exist in circulation, its physiological role remains largely unknown. Recently, PCG has been found *in vitro* as an antagonist of the principal LPS receptor, the TLR4 complex, indicating an anti-inflammatory role and preventing the permeabilising effects of the endotoxin (Stachulski et al. 2023). Alternatively, as a uremic toxin, high PCG concentrations can induce endothelial ROS (Itoh et al. 2012), reduce endothelial succinate dehydrogenase function (Mutsaers et al. 2013) and potentiate some of the inflammatory effects of PCS upon leukocytes (Meert et al. 2012) and the endothelium (Itoh et al. 2012), suggesting high levels of PCG may be detrimental. Elevated PCG concentrations have also been previously linked with mortality in patients with chronic kidney disease (Liabeuf et al. 2013).

***p*-Cresol as a risk factor of cognitive decline**

Current research is uncovering the potential of *p*-cresol and its derivatives as a risk factor of cognitive decline. A rodent model of A β 25–35-induced AD identified 45 endogenous metabolites as potential biomarkers of AD, including PCS, PCG and *p*-cresol, suggesting a role of altered phenylalanine and tyrosine metabolism by the gut microbiota in AD (Liu et al. 2018b). In adults, PCG was negatively associated with brain age deviation and cognitive function derived from MRI markers (Gordon et al. 2024), highlighting its potential as a contributing risk factor of decline.

1.4.5 Other Emerging Microbial-Derived Metabolites

Although the metabolites discussed above represent the focus of this thesis, it is important to note that many metabolites produced from the gut may influence the brain. Dietary proteins are broken down into potentially active peptides (Needham et al. 2020) that are further transformed into bacterial products such as neurotransmitter amino acids such as glutamate, glycine, aspartate, serine and GABA or polyamines (Luan et al. 2019; Smith and Macfarlane 1997; Strandwitz 2018). Aromatic amino acids (tryptophan, tyrosine, and phenylalanine) and (poly)phenols yield a myriad of compounds during catabolism leading to the formation of simpler structures containing at least one phenol ring (phenols) which can then be further transformed by the host (sulfation, glucuronidation) before re-entering circulation (Nicholson et al. 2012; Needham et al. 2020). Additionally, dietary choline and niacin are substrates for the synthesis of molecules essential for cellular function in the brain namely acetylcholine and nicotinamide adenine dinucleotide (NAD⁺) precursors (Ferreira-Vieira et al. 2016; Phelan 2017; Fricker et al. 2018), some of which have recently been shown to be synthesised by the gut microbiota (Deng et al. 2021; Fricker et al. 2018; Kim et al. 2020; Luan et al. 2019; Strandwitz 2018).

Short-chain fatty acids (SCFAs), formed from microbial anaerobic fermentation of dietary fibres in the caecum and colon (Ho et al. 2018), have been associated with attenuating cognitive decline (Berding et al. 2021a). In the CNS, SCFAs can reduce neuroinflammatory processes by decreasing the expression of pro-inflammatory cytokines and modulating brain histone acetylation (Soliman et al. 2012). SCFAs may also improve brain hypometabolism, a known contributor to neuronal dysfunction and AD, by providing an alternate substrate for energy metabolism (Den Besten et al. 2013; Zilberter and Zilberter 2017). Select SCFAs may also moderate AD progression (Colombo et al. 2021) by interfering with protein-protein interactions necessary for A β assemblies, potentially reducing the formation of toxic aggregates *in vitro* (Ho et al. 2018). Yet, it remains unclear if SCFAs produced in the GI tract can play a role in protein misfolding *in vivo* (Ho et al. 2018). However, Colombo and colleagues found GF AD mice display reduced circulatory SCFA concentrations and A β deposition, yet when supplemented with SCFAs, show an increase in A β plaque deposition, suggesting SCFA mediation (Colombo et al. 2021). In line with this, a clinical study into elderly individuals with ranging cognitive performance found a

negative association between butyrate levels in the blood and brain amyloid deposition (Marizzoni et al. 2020). In summary, while the exact role of many gut-derived metabolites in neurodegenerative diseases remains to be fully elucidated, emerging evidence highlights their influence on brain function and pathology, warranting further investigation into their therapeutic implications for cognitive health.

1.5 Using Dietary Approaches to Modulate the Microbiota-Gut-Brain Axis

It has been estimated that delaying disease onset by as little as 2 to 5 years could result in a 20 to 35% reduction in predicted AD prevalence by 2050 (Lewis et al. 2014), highlighting how preventative measures could significantly lessen overall disease burden. Targeting lifestyle factors is an attractive option in the prevention of neurodegenerative disease given their modifiable nature and can be used to shift an individual to a more favourable status which promotes healthy brain ageing, whilst resisting aberrant changes (Figure 1.3).

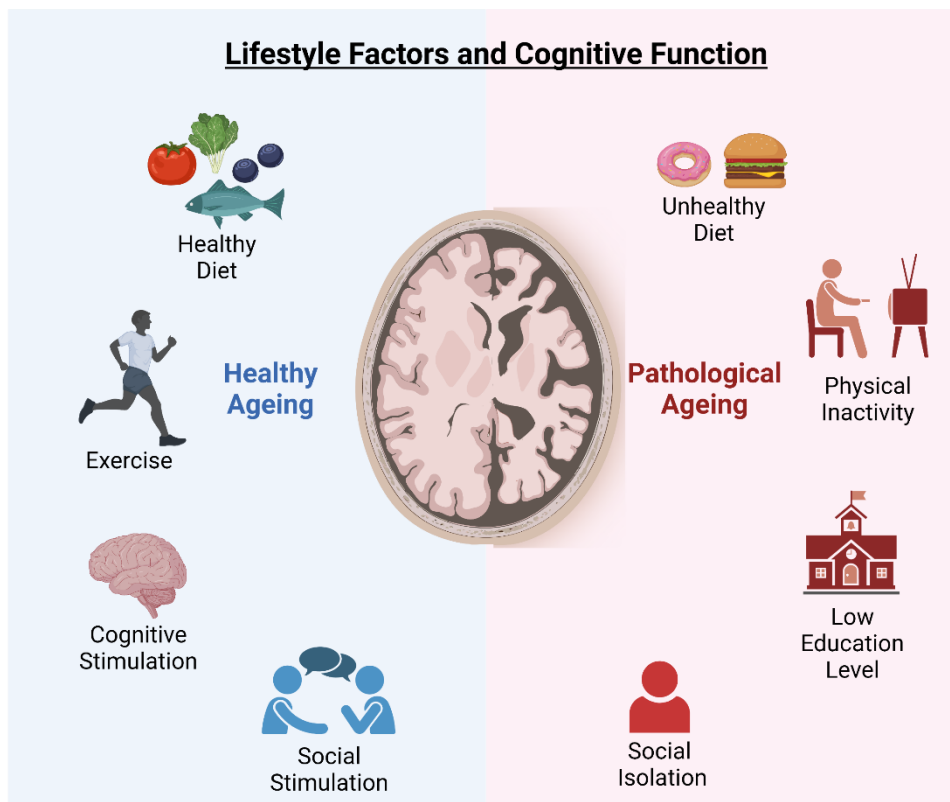


Figure 1.3: Lifestyle factors associated with healthy and pathological ageing.

Current evidence indicates that nutritional strategies can delay or ameliorate neurodegenerative disease progression (Trichopoulou et al. 2003; Dangour et al. 2010). As diet can account for up to 57% of changes in gut microbiota composition (Clark and Mach 2016), changes in diet can profoundly affect

the brain through the microbiota-gut-brain axis, modulating pathways involving the *vagus* nerve, immune system responses, and bacterial metabolites and byproducts.

The Western-style dietary pattern, high in saturated fat, animal protein, and refined carbohydrates but inadequate amounts of dietary fibre, shifts the composition of the microbiota to a more disease-associated type. Prolonged consumption of a Western diet in humans and animals can result in the extinction of beneficial microbes, a reduction in bacterial diversity, and promote a predominant *Bacteroides*-driven enterotype (Arumugam et al. 2011; Sonnenburg et al. 2016; Vangay et al. 2018; Precup and Vodnar 2019). Similarly, an increased *Firmicutes: Bacteroidetes* ratio and reductions in beneficial SCFA-producing bacteria (e.g., *Faecalibacterium prausnitzii*) are frequently observed (Agus et al. 2016; Severino et al. 2024).

Ultra-processed foods (sugary beverages, snacks, and fast foods), a hallmark of the Western diet, are detrimental to the microbiota, increasing the abundance of *Dialister*, *Coprococcus*, *Megasphaera*, *Oscillospira*, and *Blautia obeum* abundance in humans (Davis et al. 2017). The Western diet has been associated with poorer mental health (Lai et al. 2014; O'Neil et al. 2014), impaired cognitive function (Hayes et al. 2024), and increased risk of developing anxiety (Xu et al. 2021), depression (Jacka et al. 2010; Sánchez-Villegas et al. 2012), AD (Więckowska-Gacek et al. 2021), suggesting possible microbiota-gut-brain connections. However, the underlying mechanisms remain unknown.

Conversely, the Mediterranean diet, composed of a high intake of fruits, vegetables, olive oil, whole grains and unsaturated fatty acids (mono and poly-unsaturated), moderate intake of fish, low to moderate intake of dairy products (in the form of yoghurt and cheese) and restricted consumption of red meats, but regular consumption of alcohol (especially wine) (Trichopoulou et al. 2003), has been well recognised for various health benefits, including mental health and cognition (Loughrey et al. 2017). Adherence to the Mediterranean diet is associated with a slower decline in cognition (Tsigoulis et al. 2013), improved cognitive performance (Zbeida et al. 2014), decreased risk of cognitive impairment and reduced risk of MCI to AD conversion (Féart et al. 2010) (Table 1.2). Potential mechanisms underlying the protective effect of the Mediterranean diet include anti-inflammatory, antioxidant, and microbiome modulation due to the beneficial roles of major components of the dietary pattern, including fatty acids, (poly)phenols, vitamins, minerals and fibre (Figure 1.4). Indeed, recent human intervention studies support the beneficial impact of a Mediterranean diet on microbiota profiles, suggesting the modulation of the microbiota-gut-brain axis. Greater microbial diversity, as well as higher abundance of health-promoting bacterial taxa (i.e., *Clostridium cluster XIVa*, *F. prausnitzii*, *Roseburia*, *Eubacterium*, *B. thetaiotaomicron*, *Parabacteroides distasonis*, *Bifidobacterium adolescentis*, and *Bifidobacterium longum*), have been associated with consumption of the Mediterranean diet (Gutiérrez-Díaz et al. 2016; Jin et al. 2019; Meslier et al. 2020). Additionally, increased adherence to a Mediterranean diet was associated with beneficial microbiota-related

metabolomic profiles, such as increased levels of SCFAs and reductions in bile acids (De Filippis et al. 2016; Jin et al. 2019; Meslier et al. 2020).

Table 1.2: Impact of the Mediterranean dietary patterns on health and cognitive function.

Study	Participants	Findings
(Gkatzamanis et al. 2022)	The HELIAD Study: 1,226 adults over 65 years	Higher adherence to the Mediterranean dietary pattern was associated with more favourable trajectories in ageing.
(Tsvigoulis et al. 2013)	REGARDS Study: 7,478 participants 45 years and over with no history of cognitive impairment at baseline	Higher adherence to the Mediterranean diet correlated with lower incidences of cognitive impairment.
(Trichopoulou et al. 2003)	22,043 adults from Greece	A 44-month follow-up showed higher adherence to the Mediterranean diet was significantly associated with a reduction in mortality.
(Féart et al. 2009)	1,410 participants 65 years and older	Higher Mediterranean diet adherence was linked with slower cognitive decline on the Mini-Mental State Examination test only and was not associated with dementia.
(Wu and Sun 2017)	Systematic review and meta-analysis of 9 cohorts with 34,168 participants	A linear relationship was found between Mediterranean diet score and the incidence of cognitive decline.
(Rodríguez-Rejón et al. 2014)	PREDIMED trial: 2,866 non-diabetic participants	A Mediterranean diet supplemented with extra virgin olive oil or nuts lowers glycaemic load and glycaemic index.
(Berti et al. 2018)	70 participants (30-60 years old)	Lower Mediterranean diet adherence was associated with progressive AD brain biomarker abnormalities.
(Gu et al. 2015)	674 elderly adults without dementia	Mediterranean diet adherence was associated with less brain atrophy, equivalent to 5 years of ageing.
(Zbeida et al. 2014)	Analysis of the US National Health and Nutrition Survey (NHANES) 1999-2002 and from the Israeli National Health and Nutrition Survey (MABAT ZAHAV) 2005-2006.	Mediterranean diet adherence was associated with better health outcomes and cognitive functioning.
(Mosconi et al. 2014)	52 cognitively healthy adults (mean age 54 years)	Lower adherence to the Mediterranean diet was associated with cortical thinning in similar regions to AD patients.
(Shannon et al. 2019)	EPIC-Norfolk study: 8,009 adults from the UK	The Mediterranean diet improved global cognitive function equivalent to 1.7 fewer years of cognitive ageing.
(Psaltopoulou et al. 2008)	732 males and females from the EPIC-Greece cohort	Intake of PUFA was inversely associated with cognitive function. Adherence to the Mediterranean diet exhibited a weakly positive but not significant association.

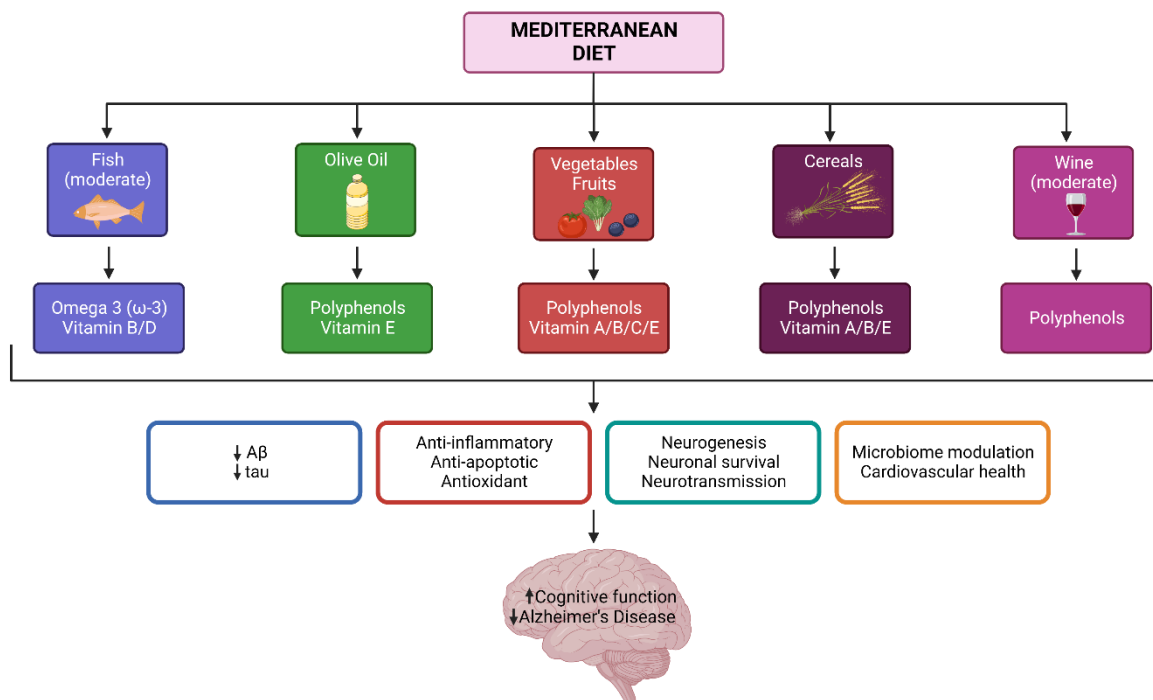


Figure 1.4: Components of a Mediterranean diet pattern and potential mechanisms underlying their cognitive benefits.

However, the relationship between the Mediterranean diet and cognition is disputed, with some research studies finding no correlation (Psaltopoulou et al. 2008; Féart et al. 2009). Contradictory findings may occur due to heterogeneity in research methods, including dietary intake, cognitive status methods, follow-up time and population characteristics, which can hinder comparisons. For example, a systematic review highlighted a 30% increase in positive significant findings in Mediterranean countries, in comparison to non-Mediterranean regions (Aridi et al. 2017).

1.6 Dietary Components

(Poly)phenols: The phytochemical class of (poly)phenols broadly encompasses flavonoids (i.e., flavan-3-ols, flavonols, isoflavones, anthocyanins, flavones and flavanones) and non-flavonoids (i.e., stilbenes, lignans, and phenolic acids). These bioactive compounds are abundant in fruit and vegetables, cocoa, spices, whole grains, nuts, and extra virgin olive oil, as well as beverages such as red wine, coffee, and green tea (Neveu et al. 2010). Over recent decades, (poly)phenols have attracted significant attention due to their protective capacity against age-related disorders via antioxidant, anti-inflammatory, antibacterial, anti-adipogenic, and neuroprotective activities (Rana et al. 2022; Hunt et al. 2024).

A recent meta-analysis of randomised controlled trials comprising of 5,519 participants underscored the cognitive benefits of (poly)phenol-rich foods. Cocoa ($g = 0.224$, $P = 0.036$), ginkgo ($g = 0.187$, $P \leq 0.001$) and berries ($g = 0.149$, $P = 0.009$) were shown to significantly improve long-term memory, processing speed and mood in middle-aged and older adults (Cheng et al. 2022). Furthermore, chronic consumption of flavan-3-ol-rich cranberries (*Vaccinium macrocarpon*) for 12 weeks improved episodic memory and regional brain perfusion in healthy older adults aged 50–80 (Flanagan et al. 2022). Epidemiological studies also suggest a positive association between high intake of total flavonoids and improved cognitive performance in older men and women (Nurk et al. 2009) and reduced rate of cognitive decline in adults aged 70 and over (Devore et al. 2012).

Approximately 90–95% of polyphenols escape absorption in the small intestine and are metabolised by gut microbes in the colon (Dueñas et al. 2015). Through this interaction, (poly)phenols can enrich beneficial bacteria such as *Akkermansia* and *Bifidobacterium*, reduce harmful bacteria like Proteobacteria, and enhance microbial diversity (Song et al. 2021). These gut microbiota shifts can positively modulate the microbiota-gut-brain axis, influencing the production of SCFAs, which possess anti-inflammatory properties and promote brain health (Zhou et al. 2016; Alves-Santos et al. 2020). SCFAs can cross the BBB, reduce neuroinflammation and influence microglial activation, providing neuroprotective benefits (Caetano-Silva et al. 2023).

Moreover, flavonols, such as quercetin, have been found to increase beneficial bacteria like *Barnesiella* and *Lactobacillus* while reducing detrimental taxa *Alistipes* and *Rikenella* in rodents (Xie et al. 2020). These microbial changes were accompanied by improved spatial memory and reduced amyloid-beta accumulation and tau phosphorylation, key features of AD pathology. Additionally, (poly)phenols and their metabolites activate cellular pathways that regulate oxidative stress and inflammation in both the gut and the brain (Shabbir et al. 2021), modulating the expression of anti-inflammatory cytokines and promoting the secretion of BDNF, which plays a crucial role in synaptic plasticity and cognitive function (Qi et al. 2017; Tayab et al. 2022). Moreover, (poly)phenols can suppress pro-inflammatory cytokines, such as TNF- α and IL-6, reducing cognitive decline associated with neuroinflammatory processes (Du et al. 2019; Li et al. 2020; Láng et al. 2024). This anti-inflammatory action, coupled with their ability to enhance BBB integrity and modulate the activity of astrocytes and microglia positions (poly)phenols as key modulators of the microbiota-gut-brain axis in the context of neurodegeneration (Du et al. 2019; Singh et al. 2020; Zhang et al. 2023; Balasubramanian et al. 2023).

Vitamins and Minerals: Vitamins are essential organic compounds crucial for the normal functioning of cellular and physiological processes, growth, and development. Except for vitamin D, all vitamins must be obtained from the diet. The gut microbiota can synthesise certain vitamins, most notably vitamin K and B-group vitamins (e.g., cobalamin (B12), folate, and riboflavin) (Hill 1997; Rowland et

al. 2018). However, most vitamins and minerals are absorbed in the upper GI tract and only small amounts reach the colon, serving as an important nutrient source for resident microbes (Sawaya et al. 2012). Many gut bacteria require minerals for growth and survival (Andrews et al. 2003).

Ageing is associated with an increased risk of lower vitamin and mineral intake (Thomas 2006; Vural et al. 2020). Balanced nutrients are essential for proper CNS neurotransmission and plasticity, but this requires appropriate transport to specific tissues/cells and metabolism through dedicated enzymes and signalling pathways, with vitamins and minerals playing a central role in catalysing nutrient utilisation and defending against cellular injury and dyshomeostasis caused by oxidised byproducts (Mason 2012). For example, adequate levels of folate and B12 are necessary for the remethylation of homocysteine, while B6 is essential for its metabolism to cysteine, with deficiencies in folate, B6, or B12 linked to increased dementia risk (Kennedy and Haskell 2011). Vitamin C acts as a redox catalyst and an excellent scavenger of free radicals generated during cellular metabolism (Gęgotek and Skrzydlewska 2023). Additionally, minerals and trace elements from dietary sources are essential as cofactors in enzymatic reactions, supporting metabolic processes, neurotransmission, and mitigating oxidative stress (Poljsak 2011). Current studies provide evidence that circulating levels of certain vitamins and minerals are markedly altered in people with AD compared to those in healthy individuals, raising a possibility that a gradual depletion/excess of these essential micronutrients may act as a contributing factor in AD pathogenesis (de Wilde et al. 2017). Supplementation of vitamins and minerals in humans has also been found to increase cognition and reduce A β -related biomarkers (Jama et al. 1996; Jia et al. 2019; Yang et al. 2020). However, current data is inconclusive, with some studies suggesting limited effects (O'Leary et al. 2012; Behrens et al. 2020).

Dietary Fibre: Consuming a high-fibre diet enhances bacterial diversity and promotes the growth of beneficial bacteria, such as *Bifidobacterium*, *Lactobacillus*, *Akkermansia*, *Faecalibacterium*, *Roseburia*, *Bacteroides*, and *Prevotella*, whilst reducing the presence of potentially pathogenic bacteria such as *Enterobacteriaceae* (Walker et al. 2011; Holscher et al. 2015; Tap et al. 2015; Kovatcheva-Datchary et al. 2015; Vanegas et al. 2017). Soluble, fermentable fibre enhances microbial enzymatic function to metabolise complex carbohydrates, leading to the production of beneficial SCFAs, namely acetate, propionate, and butyrate (Scott et al. 2013; So et al. 2018). Lowering the consumption of carbohydrates and wholegrain cereals reduces the abundance of crucial butyrate-producing microbes, including the probiotic bifidobacteria, and decreases SCFA levels (Russell et al. 2011; Staudacher et al. 2012). Greater fibre intake is associated with improved brain integrity (larger brain volume and minimal white matter damage) in older individuals (Prinelli et al. 2019) and post-weaned rodents (Torres-Velázquez et al. 2019). Fibre-rich diets are also associated with improved cognitive function across the lifespan (Milte et al. 2019; Sun et al. 2022; Beghelli et al. 2024). Mechanisms underlying cognitive

benefits range from microbiota-independent mechanisms, including promoting tight junction protein assembly or intestinal epithelial cell proliferation, regulation of cytokine and chemokine release, or microbiota-dependent mechanisms, such as the production of SCFAs (Berding et al. 2021a).

1.7 Literature review conclusions and research gaps

The concept of microbial-derived metabolites influencing cognitive decline is gaining traction, with implications in the fields of neuroscience, metabolomics and hepatology. However, due to the complexity of this relationship, the specific myriad of mechanisms responsible remain largely unknown, whilst defined roles of individual metabolites are only characterised for a select few (for a summary see Figure 1.5). Current evidence highlights dysregulation of the microbiota-gut-brain axis occurring early in AD progression, with possible changes in TMAO, tryptophan, bile acids, *p*-cresol and their derivatives accelerating or modulating this relationship. Identifying and understanding perturbed microbial-derived metabolites at a prodromal disease stage could further the current understanding of AD progression and provide a novel risk factor for disease progression, enabling earlier detection and mitigating interventions while prevention is still viable.

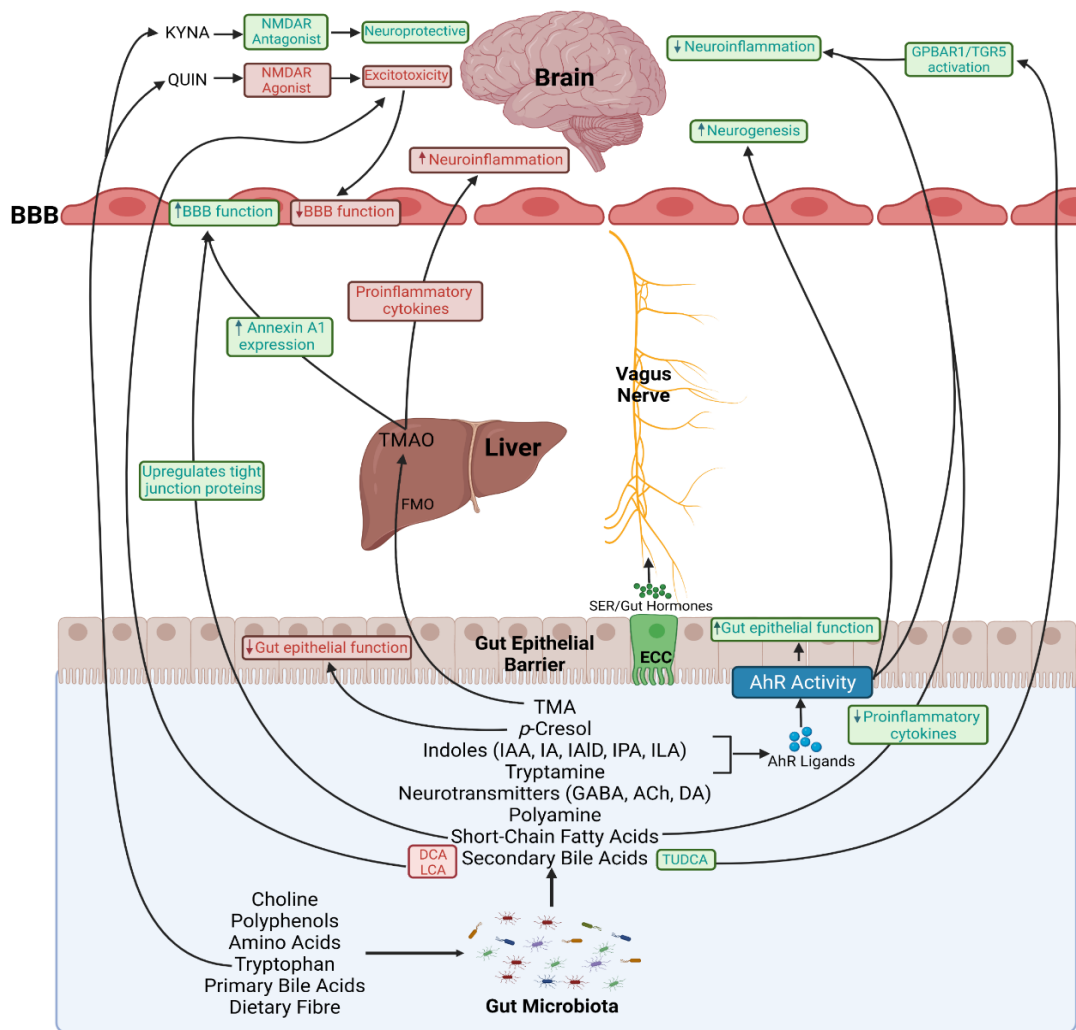


Figure 1.5: Key potential pathways through which microbial-derived metabolites influence cognitive function. An illustration of the main underlying mechanisms linking microbial metabolites and the brain. Dietary-derived precursor molecules can be metabolised by gut microbiota to form bioactive metabolites. These microbial-derived metabolites can influence gut permeability, blood-brain barrier function, neuroinflammation, *vagus* nerve activation, neurogenesis and excitotoxicity affecting the regulation of the microbiota-gut-brain axis and cognitive function. The green colour highlights a protective and beneficial effect, whereas red indicates a detrimental effect. Acronyms: BBB: blood-brain barrier; DCA: deoxycholic acid; ECC: enterochromaffin cells; FMO: flavin-containing monooxygenase; GABA: γ -aminobutyric acid; IA: indole-3- acrylic acid; IAA: indole-3- acetic acid; IAld: indole-3-aldehyde; ILA: indole-3-lactic acid; I3S: indoxyl-3-sulfate; KYNA; kynurenic acid; LCA: lithocholic acid; NMDAR: N-methyl-D-aspartate receptor; QUIN; quinolinic acid; TMA: trimethylamine; TMAO: trimethylamine N-oxide; TUDCA: tauroursodeoxycholic acid.

Understanding this communication system can also highlight potential targeted nutritional strategies to promote healthy ageing and resist aberrant neurological decline. From current evidence, reducing the intake of the highly refined Westernised-type diet and promoting the intake of the Mediterranean-like diet and its components such as (poly)phenols, carotenoids, fibres, vitamins and minerals appears to be associated with beneficial modulation of the gut and neuronal health. However, the complex connection between the gut and the brain, including the specific influence of dietary and microbial-derived metabolites, remains unknown. Understanding how nutritional strategies modulate metabolite-mediated pathways within the microbiota-gut-brain axis could provide valuable insights into dietary interventions that support cognitive health and mitigate the risk of AD progression.

1.8 Aims and outline of the thesis

The overall aim of this thesis is to investigate the modulatory interactions between key dietary and microbial-derived metabolites within the microbiota-gut-brain axis, focusing on their role in early cognitive decline and dementia, as well as their regulation by gut microbiota and their impact on brain health. Particular emphasis is placed on less-explored and recently identified metabolites associated with cognitive health and AD progression, including bile acids, TMAO, tryptophan, *p*-cresol and their derivatives, highlighting novel pathways that may influence brain health and contribute to neurodegenerative processes (Liu et al. 2014; Janeiro et al. 2018; MahmoudianDehkordi et al. 2019; Baloni et al. 2020; Whiley et al. 2021; Gordon et al. 2024). To achieve this, we aim to (1) build on existing knowledge of gut dysbiosis in early cognitive decline by using a targeted approach to assess whether changes in circulatory metabolites derived from dietary and microbial metabolism could serve as a novel composite risk factor for prodromal AD progression. Furthermore, we explore how nutritional approaches can modulate these metabolite-mediated communications along the microbiota-gut-brain axis to influence cognitive health and AD by assessing (2) the effect of a refined diet, consisting of highly processed carbohydrates and low fibre content, on bile acid signalling and detrimental processes in the brain, (3) the protective effects of a (poly)phenol-rich grape and blueberry extract against chronic low-grade inflammation, a hallmark of early AD progression, (4) the efficacy of a Mediterranean diet-inspired supplement as an early intervention against prodromal AD progression using the 5xFAD mouse model of AD. In the scope of this thesis, emphasis was placed on metabolites with emerging evidence in AD over those widely studied in microbiota-gut-brain interactions. For example, SCFAs have been extensively studied for their role in microbiota-gut-brain interactions and AD, as well as their association with dietary fibre, (poly)phenols, and the components of a Mediterranean diet (Edwards et al. 2017; Garcia-Mantrana et al. 2018; Nagpal et al. 2019; Zheng et al. 2021) and therefore was not the focus of this thesis.

Together, this thesis aims to highlight the powerful influence of metabolite-mediated pathways within the microbiota-gut-brain axis in modulating early cognitive decline and AD progression.

Hypothesis

We hypothesise that:

1. Circulatory microbial-derived metabolites released from the gut will be dysregulated in prodromal AD, increasing toxic metabolite concentrations.
2. Refined dietary intake, consisting of high sucrose, processed carbohydrates and low fibre content, will exacerbate the pathological processes in the brain through increasing cytotoxic bile acid concentrations and subsequent neuroinflammation.
3. (Poly)phenol-rich grape and blueberry extract and Mediterranean diet-inspired supplement will reduce cytotoxic metabolism and promote beneficial metabolites, providing a neuroprotective effect.

Chapter 2: Circulatory dietary and gut-derived metabolites as risk factors of prodromal Alzheimer's disease

This chapter has been prepared in the form of a research paper which has been submitted to Gut Microbes.

Title: Circulatory dietary and gut-derived metabolites predict prodromal Alzheimer's disease.

Authors: Emily Connell, Mizanur Khondoker, Saber Sami, Anne-Marie Minihane, Matthew G. Pontifex, Michael Müller, Gwenaëlle Le Gall and David Vauzour.

2.1 Introduction

Currently, an estimated 55.2 million people suffer from dementia worldwide, of which Alzheimer's disease (AD) is the main form (World Health Organization 2021). In the absence of an effective strategy to slow or prevent disease progression, dementia incidence is expected to increase to 152.8 million by 2050. By the time AD is typically diagnosed, substantial neuronal loss may have occurred across multiple brain regions. Identifying molecular precursors and biological risk factors at early disease stages would enable earlier detection and the targeting of regular monitoring and mitigating interventions while prevention is viable.

The contribution of lifestyle factors to cognitive decline and dementia is well documented (Flicker 2010; Livingston et al. 2024). Diet in particular has emerged as a key influencer of brain health and AD development, in part by modulating communication along the microbiota-gut-brain axis. This axis forms a bidirectional communication system comprising neuronal, endocrine, immune and metabolic signalling mechanisms linking the gut and the central nervous system (CNS) (Chakrabarti et al. 2022). Gut microbes can regulate this communication via the breakdown of dietary compounds into bioactive metabolites. Such microbial-derived metabolites subsequently modulate pathways affecting the CNS both directly, by crossing the blood-brain barrier and indirectly, via modulation of peripheral organ function or *vagus* nerve stimulation (Chapter 1). In the prodromal stages of AD, for example mild cognitive impairment (MCI), the microbiota-gut-brain axis becomes dysregulated (i.e., dysbiosis), a change associated with pathological processes such as neuroinflammation and neural injury, and thought to contribute to accelerating cognitive decline (Liu et al. 2019; Li et al. 2019; Nagpal et al. 2020). However, the mechanism(s) underlying these changes, and the role of microbial-derived metabolites in this process remains unknown.

Chapter 1 highlighted several examples of microbial-derived metabolites that have been associated with cognitive health, including trimethylamine N-oxide (TMAO) (Li et al. 2018a; Brunt et al. 2020; Hoyles et al. 2021; Zhuang et al. 2021), bile acids (BAs) (MahmoudianDehkordi et al. 2019; Nho et al. 2019;

Baloni et al. 2020), tryptophan (Schwarcz et al. 2012; Weaver et al. 2020; Whiley et al. 2021; Hestad et al. 2022), *p*-cresol and its derivatives (Sankowski et al. 2020; Shah et al. 2022). Notably, these same microbial-derived metabolites have been further linked to pathological processes known to be associated with AD, including neuroinflammation, synaptic damage and blood-brain barrier disruption (Smith et al. 2000; Tran et al. 2015; Azevedo et al. 2016; Edamatsu et al. 2018; Jena et al. 2018; Tang et al. 2018; Shah et al. 2022), but whether changes in these microbial-derived metabolites are drivers or correlates of disease processes requires comprehensive investigation.

Targeted metabolomics presents a powerful tool to comprehensively assess changes in the endogenous metabolome. Here, we present a targeted metabolomics approach employing liquid chromatography-tandem mass spectrometry (LC-MS/MS) to quantify TMAO, BAs, tryptophan and *p*-cresol metabolite profiles in the serum of healthy controls and participants in early cognitive decline. Early cognitive decline comprises individuals with subjective cognitive impairment (SCI) and mild cognitive impairment (MCI), the prodromal stages of AD progression. This study presents, for the first time, the prognostic value of key metabolites in combination and represents one of only a few studies characterising metabolic perturbations in the early stages of cognitive decline, including participants undergoing the earliest stage of AD, SCI.

2.2 Materials and Methods

2.2.1 Study samples

Human serum samples from the baseline measurements of two previously conducted clinical studies were used: (1) the impact of Cranberries On the Microbiome and Brain in healthy Ageing sTudy (COMBAT; NCT03679533) and (2) the Cognitive Ageing, Nutrition and Neurogenesis (CANN; NCT02525198) study. The COMBAT study recruited 60 adults, aged 50-80 years, with no subjective memory complaints as assessed by the Cognitive Change Index (CCI) questionnaire (Flanagan et al. 2022). The CANN study recruited 259 participants, aged ≥ 50 years, with subjective cognitive impairment (SCI) or mild cognitive impairment (MCI) based on criteria developed by the National Institute of Aging-Alzheimer's Association, with no indication of clinical dementia (Irvine et al. 2018). Cognitively healthy adults were selected from the COMBAT study as a control group, with all groups (controls, SCI and MCI, n=50 per group) matched for age, BMI and sex as these are key variables known to affect microbiome composition (Haro et al. 2016; Zhang et al. 2021b). Participants with chronic fatigue syndrome, liver disease, diabetes mellitus, or gall bladder abnormalities were excluded, as well as participants taking antidepressant or antipsychotic medications, medication that alters gastrointestinal function, or anticoagulant medications such as warfarin (Flanagan et al. 2022). Participants also completed the Patient Health Questionnaire-9 (PHQ9) and Generalised Anxiety Disorder Questionnaire 7 (GAD-7) which objectifies and assesses degree of depression and anxiety

severity respectively (Kroenke et al. 2001; Spitzer et al. 2006). Those with significant depression or anxiety were excluded.

Cognitive health was assessed using a variety of cognitive tests in both the COMBAT and CANN study. However, only the Trail Making Test (assessing visual processing speed, scanning, mental flexibility, as well as executive function) and the digit span test (assessing verbal short-term and working memory) were used across the COMBAT and CANN studies enabling comparisons. Participants also completed a validated, semi-quantitative Scottish Collaborative Group (SCG) food frequency questionnaire (version 6.6) to assess background diet (Hollis et al. 2017). Biochemical analyses of blood glucose, liver function (bilirubin, albumin, aspartate aminotransferase (AST), alanine aminotransferase (ALT) and AST/ALT ratio), kidney function (creatinine) and serum lipid concentrations (total-, LDL-, HDL-cholesterol and triglyceride) were conducted in all participants. Comparisons of biochemistry between groups (control, SCI and MCI) were calculated using one-way ANOVA with post hoc Tukey analysis. Faecal samples were collected by the participant up to 48h prior to their baseline visit using the collection vessels (NHS-approved Easy sampler collection kit supplied, Cover them Limited). The storage container was placed in a cool dry location prior to returning to the research facility at the earliest opportunity (i.e. study visit) and subsequently stored at -80°C until analysis. The protocols were approved by the UK National Research Ethics Service (NRES) Committee, (Study ID: 14/EE/0189) for CANN and by the University of East Anglia's Faculty of Medicine and Health Sciences Ethical Review Committee (Reference: 201819-039) and the UK Health Research Authority (IRAS number: 237251) for COMBAT. The participants provided written informed consent to participate.

2.2.2 Microbiome Profiling

Microbiome analysis was performed by 16S rRNA sequencing. DNA extraction was performed from approximately 50 mg of faecal content using the QIAamp PowerFecal Pro DNA Kit (Qiagen, Manchester, UK) as per the manufacturer's instructions. DNA quantity was evaluated using a Nanodrop 2000 Spectrophotometer (Fisher Scientific, UK). Quality assessment by agarose gel electrophoresis distinguished the DNA integrity, purity, fragment size and concentration. Illumina NovaSeq 6000 PE250 was used to amplify the V3-V4 hypervariable region. Sequence analysis was carried out using Uparse software (Uparse v7.0.1001) (Wang et al. 2007), incorporating all the effective tags. Sequences sharing a similarity of $\geq 97\%$ were grouped into the same Operational Taxonomic Unit (OTU). A representative OTU sequence was further analysed using the SSUrRNA database of SILVA Database 138 (Quast et al. 2013). OTU abundance data were normalised using a standard sequence number corresponding to the sample with the least sequences. Alpha diversity was assessed using both Chao1 and Shannon H diversity indices, whilst beta diversity was assessed using Bray-Curtis dissimilarity. Statistical significance was determined by Kruskal-Wallis or Permutational Multivariate Analysis of

Variance (PERMANOVA). Comparisons at the phylum and genus level were made using classical univariate analysis using Kruskal–Wallis combined with a false discovery rate (FDR) approach used to correct for multiple testing. P-values below 0.05 were considered statistically significant.

2.2.3 LC-MS/MS

Overnight fasted blood samples were drawn from participants during their baseline study visit of the COMBAT and CANN studies. After collection, blood was left to coagulate (in clot-activating gel tubes), followed by centrifugation at 2,000g for 10 min and removal of the resultant serum from the sub-fractions. Aliquoted serum was stored at -80°C until further analysis.

Serum samples were diluted with ice-cold methanol at a ratio of 1:10 (v/v) and placed on dry ice for 10 min. Samples were centrifuged (5 min, 16,000x g at room temp), supernatants filtered using a 0.45 μM PTFE syringe filter and evaporated to dryness using a Savant™ SpeedVac™ High-Capacity Concentrator (Cat. SC210A-230). For the detection of bile acids, dried samples were resuspended in 50 μL of methanol with 15 μL of lithocholic acid-d4, and cholic acid-d4 at 50 $\mu\text{g}/\text{mL}$ as the internal standards. For the detection of TMAO/TMA/choline, dried samples were resuspended in 50 μL water with TMA-d9 N-oxide, $^{13}\text{C}^{315}\text{N}$ TMA hydrochloride at 50 $\mu\text{g}/\text{mL}$ as the internal standards. Finally, for the detection of tryptophan and p-cresol-related metabolites, dried samples were resuspended in 50 μL water with 15 μL of L-methionine-3, 3, 4, 4 d4 and p-toluenesulfonic acid at 50 $\mu\text{g}/\text{mL}$ as the internal standards for tryptophan and p-cresol metabolites respectively.

Stock solutions of each metabolite were prepared in methanol (1mg/mL) and stored at -80°C . Calibration standards were prepared by pooling all relevant analytes for each method at eight concentrations and adding the respective internal standards at 50 $\mu\text{g}/\text{mL}$. Calibration standards were run at the beginning, middle and end of each analytical queue. The analyte: internal standard response ratio was used to create calibration curves and quantify each metabolite.

Metabolite quantification was performed using liquid chromatography-tandem mass spectrometry (LC-MS/MS) comprising of Waters Acquity UPLC system and Xevo TQ-S Cronos mass spectrometer controlled by MassLynx 4.1 software. For the detection of bile acids, the electrospray ionisation (ESI) operated in negative mode and chromatographic separations were performed with a Supelco Ascentis Express C18 column (150 x 4.6 mm, 2.7 μM) (adapted from (Blokker et al. 2019)). Eluent A (10mM ammonium acetate, 0.1% formic acid, water) and eluent B (10mM ammonium acetate, 0.1% formic acid, methanol) ran at a constant rate of 0.6 mL/min. The gradient began at 50% B and was held for 2 min before a linear increase to 95% B occurred at 20 min. This was held for 4 min before a linear

decrease in gradient back to 50% B occurred between 24 and 25 min. The gradient was held at 50% B for another 4 mins.

For the detection of TMAO, TMA and choline, ESI operated in positive mode (adapted from (Hoyles et al. 2018a; Anesi et al. 2019)). Chromatographic separation occurred using a BEH Amide (150 x 2.1 mm, 1.7 μ M) and 0.5mL/min using eluent A (10 mM ammonium formate, 0.2% formic acid, 50% acetonitrile) and eluent B (10mM ammonium formate, 0.2% formic acid, 95% acetonitrile) initially at 100% B to 60% B at 4 min and held until 4.2 min, before increasing back to initial conditions of 100% B at 4.21 min and being held until 5.4 min for equilibration.

ESI operated in positive mode for the detection of tryptophan and p-cresol-related metabolites and chromatographic separation occurred using an ACQUITY UPLC BEH C18 1.7 μ M (2.1 x 50mm) column at a rate of 0.3 mL/min and composition of eluent A (0.1% formic acid, water) and eluent B (0.1% formic acid, methanol) at a gradient of 5% B from 0 to 0.5 min, 10% B from 0.5 to 2.5 min, 15% B at 3.5 min, 35% B at 4.5 min, 45% B at 6.5 min, 55% B at 7 min, 100% B at 7.5 min, 100% B until 10 min, and 5% B at 10.1 min to return to initial conditions for equilibration until 14 mins. This method was adapted from Anesi and colleagues (Anesi et al. 2019). Chromatogram peak analysis was performed by the accompanying Waters® TargetLynx™ application manager and all further data analysis and calibration curve constructions were completed in Microsoft Excel (2019 version).

Excellent linear response range was ensured for each calibration curve with correlation coefficients (r^2) 0.99 or higher for all calibration curves generated. An Agilent high-performance autosampler with an injection program was used to minimise carry-over effects between samples. Samples were run in a random order and 20% of the whole set was re-run as a quality control for the method repeatability. No signal was also detected in blank samples run amongst the serum and calibration injections, or in blanks run after the highest calibration standard, indicating that there was little to no carry-over occurring.

2.2.4 Statistical Analyses

Significant associations of metabolites with cognitive status were identified using multiple linear regression analysis. Covariates known to affect metabolome or microbiome composition, including age, BMI, diet and markers of kidney function (creatinine) and liver function (AST/ALT ratio), were included in the model (Williams and Hoofnagle 1988; Giannini et al. 1999; Gowda et al. 2010; Leeming et al. 2019; Tavassol et al. 2023). Sex was not included as a covariate as all groups had an equal proportion of males and females. Diet was assessed using a validated, semi-quantitative Scottish Collaborative Group (SCG) food frequency questionnaire (version 6.6) (Hollis et al. 2017). Participants' dietary components were grouped (kcal, proteins, fats, carbohydrates, water, alcohol,

vitamins and minerals) and analysed using hierarchical clustering via Ward's linkage method to assemble individuals with similar dietary patterns (Supplementary Figure S2.1). This clustered participants into low, moderate and high intake of dietary components and was added to the model as a categorical variable, with participants with a moderate intake used as a reference group. Age, BMI, creatinine and AST/ALT ratio were added to the model as continuous variables. Finally, cognitive status (i.e., control, SCI and MCI) was added to the model as a categorical variable. Metabolite concentrations outside ± 2 standard deviations from the mean were excluded as outliers. The assumptions for multiple linear regression analysis including the existence of a linear relationship among the outcome and predictor variable, normality and homoscedasticity were assessed (Supplementary Figure S2.2). The model tested for significant associations between metabolite and cognitive status, adjusting for the included covariates. All multiple linear regression analyses were performed in R (v3.6.3; R Foundation: A Language and Environment for Statistical Computing).

2.2.5 Machine Learning

A Random Forest (RF) machine learning algorithm was implemented to assess whether metabolites could be predictive of early AD. The RF model was constructed using 100 decision trees and 6 random variables considered at each split. The number of variables considered per split corresponds to the square root of the total number of attributes in the data (Liaw and Wiener 2001) (as 32 variables were considered, this resulted in ~ 6 random variables per split). To create a composite panel to predict prodromal AD, metabolites were ranked according to the mean decrease Gini. This highlights the loss in model performance when permuting the predictor values, and can provide more robust results than mean decrease accuracy (Calle and Urrea 2011). The metabolites with the highest mean decrease Gini score producing the highest AUC values were retained in the model. To compare our model, Naive Bayes and AdaBoost machine learning models were also constructed (Rish 2001; Wang 2012). AdaBoost predictions were made by using a weighted average of weak classifiers. Our model contained 50 estimators, a learning rate of 1.00 and a SAMME classification algorithm which updated the base estimator's weights with classification results. The Naive Bayes method was applied based on applying Bayes' theorem with the "naive" assumption of conditional independence between every pair of features given the value of the target variable. The dataset for multi-class classification was randomly divided into training and testing, with 75% of the samples allocated to the training set and 25% to the testing set. Models were assessed by the average area under the receiver operator curve (AUC) (plotting the false positive rate against the true positive rate) over all classes (macro-average) as an indication of model performance. All machine learning models were built in Python (Python Software Foundation. Python Language Reference, version 3.8).

2.3 Results

2.3.1 Study population characteristics

A total of 150 individuals were included in the study of which 50 (33.3%) were cognitively healthy, 50 (33.3%) presented with SCI and 50 (33.3%) with MCI. The mean \pm SD age of all participants was 65.5 \pm 5.7 years, with a mean level of education of 14.6 \pm 3.5 years and 54% female (Table 2.1). Cognitive groups were matched for age, BMI and sex ($p=0.99$). Participants in both the COMBAT and CANN study undertook several cognitive assessments at their baseline visit (Irvine et al. 2018; Flanagan et al. 2022). Significant differences were found in the Trail Making Test B, digit span backward test and digit span total score between groups ($p<0.05$). There was a marginal difference between the three groups in the Trail Making Test A ($p=0.09$) and no significant difference occurred in the digit span forwards test ($p=0.21$). The prevalence of the *APO ε4* was lower in controls (18%) compared to SCI (26%) and MCI (38%) participants.

Table 2.2: Baseline characteristics of the participants. Mean (SD). P-value calculated using one-way ANOVA. Significant values at $p<0.05$ are in bold. SCI: subjective cognitive impairment, MCI: mild cognitive impairment, TMT: Trail Making Test A or B. Bold p-values represent $p<0.05$.

	Control (n=50)	SCI (n=50)	MCI (n=50)	P- value	Post Hoc Tukey's Test
Sex, M/ F (%F)	23/27 (54)	23/27 (54)	23/27 (54)	-	-
Age (years)	65.6 (5.3)	65.5 (6.1)	65.5 (5.8)	0.999	-
BMI (kg/m ²)	25.1 (3.1)	25.0 (2.9)	25.0 (2.8)	0.993	-
Education (years)	14.4 (2.6)	14.6 (4.0)	14.6 (3.9)	0.968	-
% <i>APOE4</i>	18	26	38	0.079	-
Cognitive tests					
TMT A	30.7 (6.2)	29.3 (8.1)	33.3 (12.1)	0.088	-
TMT B	66.4 (20.4)	62.3 (16.5)	74.9 (27.3)	0.015	SCI < MCI ($p=0.012$)
Digit Span Forwards	11.1 (2.2)	11.2 (1.8)	10.5 (2.6)	0.211	-
Digit Span Backwards	7.7 (2.0)	7.2 (1.8)	6.5 (2.1)	0.011	Control > MCI ($p=0.008$)
Digit Span Total	18.8 (3.8)	18.4 (3.0)	17.0 (4.2)	0.039	Control > MCI ($p=0.043$)
Biochemistry					
Creatinine ($\mu\text{mol/L}$)	73.90 (13.5)	72.5 (12.3)	73.5 (14.1)	0.871	-
Albumin (g/L)	40.4 (2.4)	30.0 (2.4)	39.4 (2.3)	<0.001	Control > SCI ($p<0.0001$); SCI > MCI ($p=0.010$)
Bilirubin ($\mu\text{mol/L}$)	12.8 (4.7)	8.9 (5.1)	9.1 (4.4)	<0.001	Control > SCI ($p<0.001$); Control > MCI ($p=0.001$)
AST (μL)	21.7 (3.9)	20.6 (5.9)	24.0 (13.1)	0.141	-
ALT (μL)	16.9 (5.4)	16.7 (9.0)	18.3 (11.3)	0.621	-
AST/ALT	1.4 (0.3)	1.4 (0.4)	1.4 (0.4)	0.548	-
Fasting Glucose (mmol/L)	4.8 (0.4)	5.0 (0.5)	5.3 (1.0)	<0.001	Control < MCI ($p<0.001$)
Triglyceride (mmol/L)	1.1 (0.5)	1.1 (0.4)	1.2 (0.5)	0.368	-
Cholesterol (mmol/L)	5.6 (1.1)	5.2 (1.1)	5.2 (1.0)	0.174	-
HDL Cholesterol (mmol/L)	1.6 (0.4)	1.5 (0.5)	1.5 (0.4)	0.297	-
LDL Cholesterol (mmol/L)	3.4 (0.1)	3.2 (0.9)	3.1 (0.8)	0.182	-

Albumin, bilirubin and fasting glucose ($p < 0.01$) differed according to cognitive status. Interestingly, both albumin and bilirubin were highest in controls and lowest in SCI participants. Although participants diagnosed with diabetes mellitus were excluded, fasting glucose increased in early AD, with the lowest concentrations in control individuals and the highest in MCI (Table 2.1).

2.3.2 Gut microbiome and metabolome shifts in prodromal AD

Faecal sample microbiome analysis revealed no significant differences in alpha diversity among groups, as measured by the Chao1 ($p = 0.21$) and Shannon H ($p = 0.70$) indices (Figure 2.1A-B). Conversely, beta diversity, as measured by Bray-Curtis dissimilarity, was significantly different (PERMANOVA F -value = 1.35, $p = 0.02$) (Figure 2.1C). Pairwise analysis suggested the shift was primarily driven by the differences between the control and SCI groups (FDR $q = 0.03$), rather than between SCI and MCI (FDR $q = 0.38$) or MCI and control (FDR $q = 0.15$) (Figure 1D). There was no significant difference in the gut microbiome at the phylum level (Figure 2.1E; Supplementary Table S2.1 for full abundance counts). However, 10 genera were modulated between groups (Figure 2.1F-O; Supplementary Table S2.2). The PLS-DA plot suggested similar patterns in participants' serum metabolomic profiles, with control separating from SCI and MCI (Figure 2.2A). The extent of this separation can be seen through the heatmap displaying shifts in metabolite concentrations between groups and clustering SCI and MCI together (Figure 2.2B).

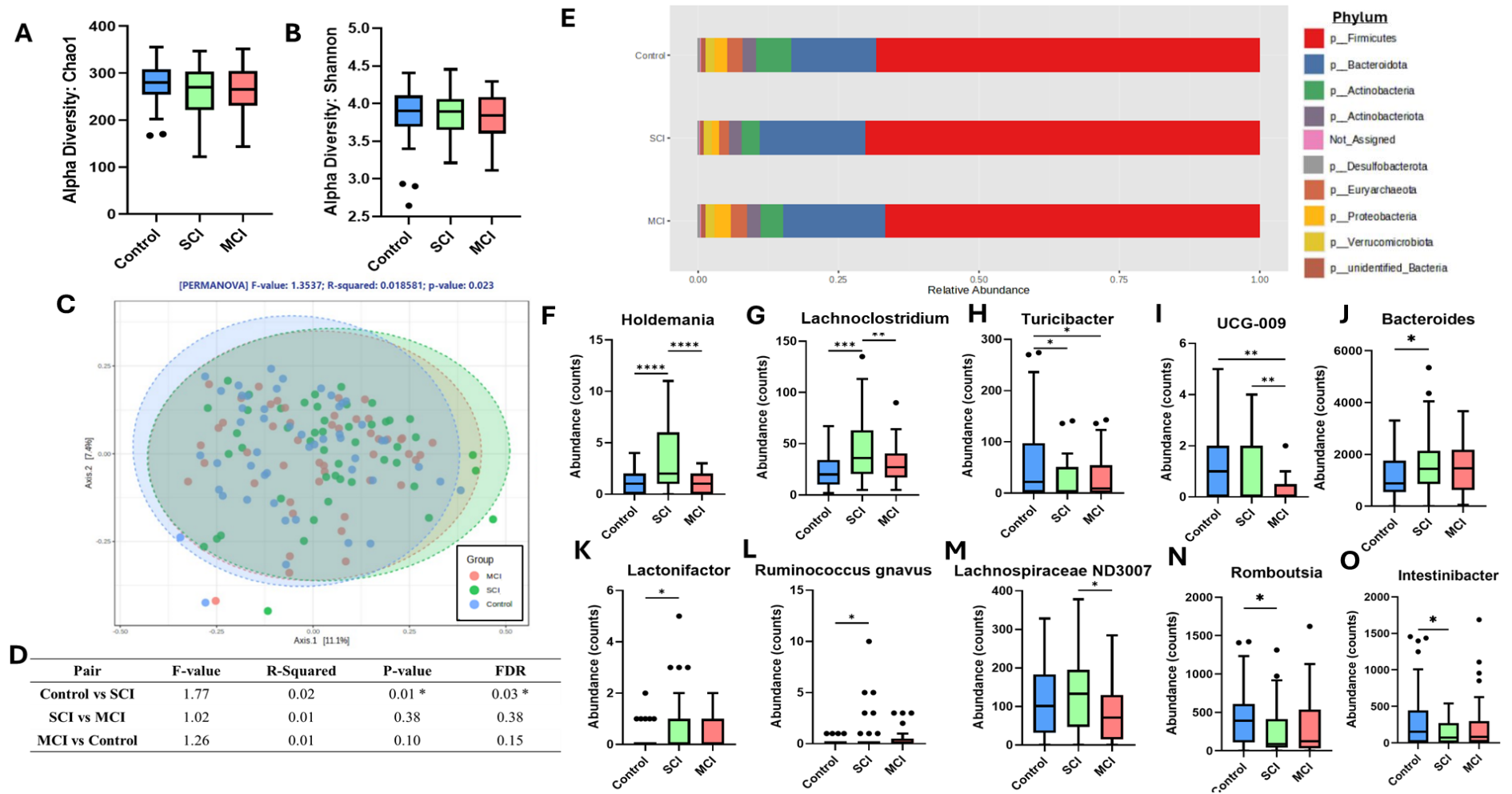


Figure 2.1: Faecal microbiome beta diversity is significantly altered in early cognitive decline. Alpha diversity measured by Chao1 (A) and Shannon H (B) index. (C) Beta diversity as measured by Bray-Curtis; p-value generated from PERMANOVA. (D) Pairwise comparisons of the beta diversity analysis. (E) Relative abundance of the gut microbiome at phylum level. (F-O) Abundance counts of microbiome genera significantly ($p < 0.05$) modulated between control, SCI and MCI. *= $p < 0.05$, **= $p < 0.01$.

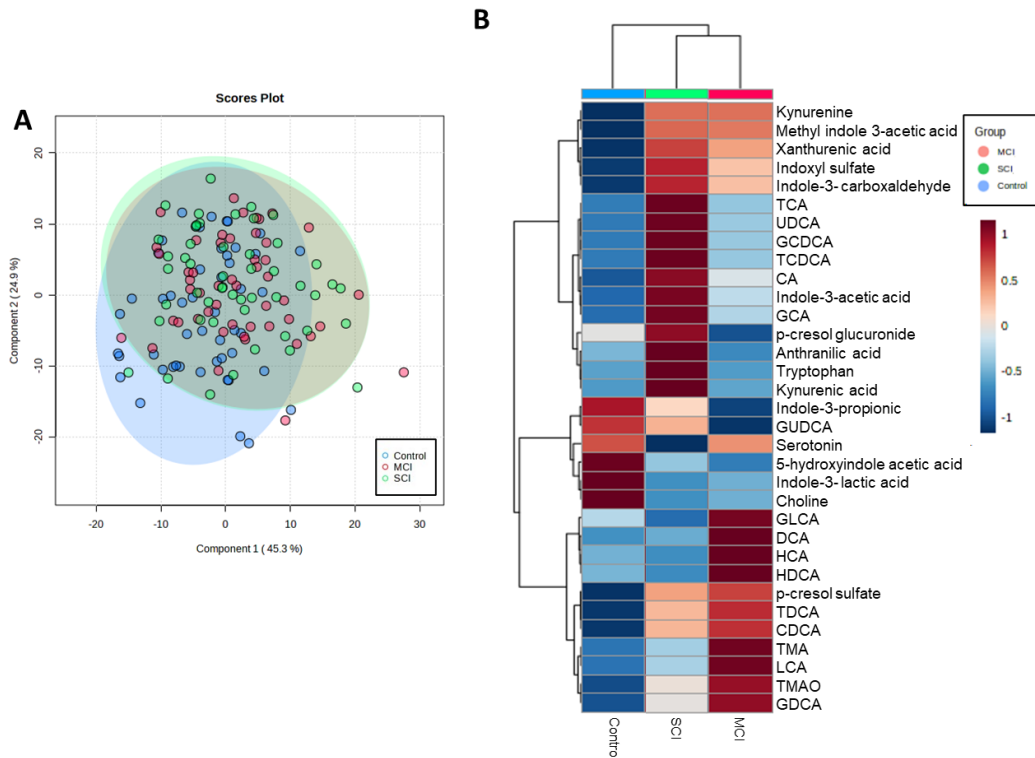


Figure 2.2: Serum metabolic shift occurs in early cognitive decline. (A) Partial least squares-discriminant analysis (PLS-DA) plot of the metabolomic profiles. (B) Heatmap displaying changes in concentrations of metabolites between the groups, with hierarchical clustering.

2.3.5 Serum dietary and microbial-derived metabolites and gut microbiome modulation in prodromal AD are significantly linked

Having identified a shift in both the gut microbiome and serum metabolome profiles, a Spearman correlation examined possible connections between the two datasets. Significantly modulated metabolites and microbiome genera between the three groups ($p < 0.05$) were correlated, revealing bacterial–metabolite interactions. Control and SCI participants displayed a negative relationship between 5-hydroxyindole acetic acid and *Lachnoclostridium* ($R = -0.29$, $p = 0.004$), indoxyl sulfate and *Turicibacter* ($R = -0.21$, $p = 0.038$), and choline and *Lachnoclostridium* ($R = -0.36$, $p = 0.0002$) and *Ruminococcus gnavus* group ($R = -0.28$, $p = 0.005$) (Figure 2.3A). Choline and *UCG-009* ($R = 0.316$, $p = 0.002$), anthranilic acid and *Lactonifactor* ($R = 0.24$, $p = 0.019$) and *Holdemanella* ($R = 0.24$, $p = 0.02$), indoxyl sulfate and *Holdemanella* ($R = 0.318$, $p = 0.001$) and *Lactonifactor* ($R = 0.33$, $p = 0.0008$) had a positive correlation. Between SCI and MCI participants, only IPA and *Lachnospiraceae ND3007* group had a positive correlation ($R = 0.26$, $p = 0.011$) (Figure 2.3B). The similarity between microbiome and metabolomic profiles was confirmed by conducting a Procrustes analysis to evaluate the congruence of the two datasets. The analysis revealed strong similarity between the metabolome and microbiome

results in control and SCI (R= 0.21, p= 0.03), SCI and MCI (R= 0.27, p= 0.002) and MCI and control (R= 0.26, p= 0.002) groups (Figure 2.3C-E).

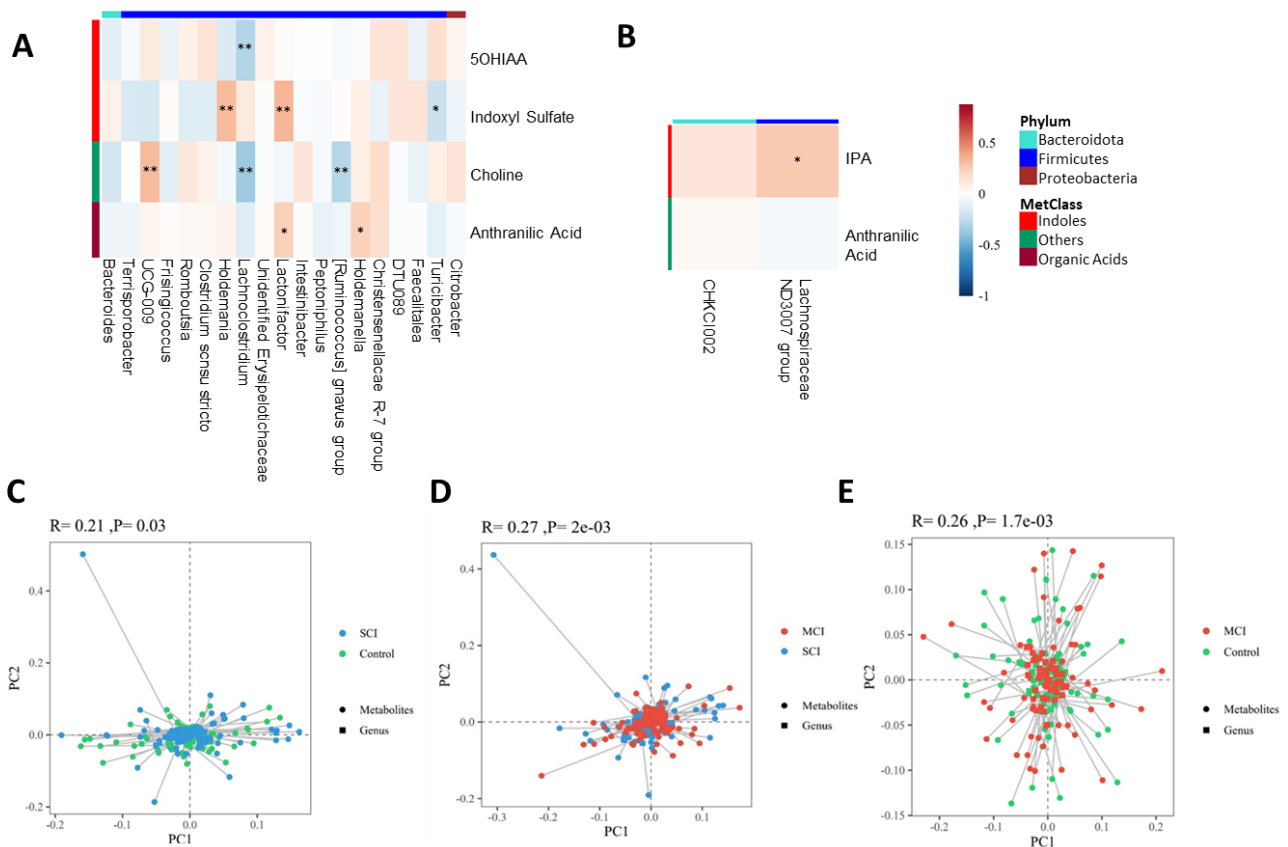


Figure 2.3: Serum metabolome and faecal microbiome profiles are linked. Spearman rank correlation analysis between metabolite and microbiome genera that are significantly modulated in early cognitive decline (A) between control and SCI and (B) between SCI and MCI. (C-E) Procrustes plot comparing the relationship between the microbiome and the metabolome profiles in control and SCI (C), SCI and MCI (D) and MCI and control (E). Longer lines indicate more within-subject dissimilarity.

2.3.3 Serum metabolites significantly associated with early cognitive decline in an adjusted multivariable model

Multiple linear regression analysis adjusted for liver function (AST/ALT ratio), kidney function (creatinine), age, BMI and background diet identified five serum metabolites significantly associated with early cognitive decline, including choline, 5-hydroxyindole acetic acid, indole-3- propionic acid (IPA), indoxyl sulfate and kynurenic acid (Table 2.2). Indoxyl sulfate, choline and 5-hydroxyindole acetic acid were associated with both SCI and MCI (p<0.05). Kynurenic acid was significantly associated with SCI (β = 0.007, 95% CI: <0.001, 0.014, p= 0.037) but not MCI (β = 0.001, 95% CI: -0.006, 0.007, p= 0.874). On the other hand, IPA was significantly associated with MCI (β = -0.558, 95% CI: -0.910, -0.206, p= 0.002), but not SCI (β = -0.181, 95% CI: -0.536, 0.174, p= 0.316).

Neuroprotective metabolites, including choline, 5-hydroxyindole acetic acid and indole propionic acid (Hwang et al. 2009; Blusztajn et al. 2017; Klein et al. 2018), exhibited lower concentrations in SCI and MCI participants in comparison to controls, while metabolites associated with cytotoxicity, including indoxyl sulfate, showed increasing levels (Leong and Sirich 2016). Kynurenic acid, a typically neuroprotective metabolite (Ostapiuk and Urbanska 2021), was higher in SCI and MCI in comparison to controls. Group means for all metabolite concentrations are given in Supplementary Table S2.1.

Table 2.2: Multiple linear regression model (adjusted for age, BMI, liver function (AST/ALT ratio), kidney function (creatinine) and diet) showing metabolites significantly associated with early cognitive decline. Diet was analysed using hierarchical clustering, ‘Ward’ method, to group individuals with similar dietary patterns. This grouped participants into three dietary groups (low, moderate and high intake of dietary components (Kcal, carbohydrates, fats, protein, water, alcohol, minerals, vitamins). Healthy controls and diet group 2 (moderate intake) were used as reference groups in the model. Bold p-values represent $p < 0.05$.

Explanatory Variable	Metabolite																			
	Indoxyl Sulfate				Choline				5-Hydroxyindole Acetic Acid				Indole Propionic Acid				Kynurenic Acid			
	Beta	P-value	95% CI		Beta	P-value	95% CI		Beta	P-value	95% CI		Beta	P-value	95% CI		Beta	P-value	95% CI	
			Low	High			Low	High			Low	High			Low	High			Low	High
Constant	-2.288	0.482	-8.705	4.128	29.690	0.011	6.938	52.443	0.068	0.020	0.011	0.125	3.094	0.009	0.790	5.397	0.017	0.448	-0.027	0.062
Age	0.057	0.115	-0.014	0.128	0.100	0.434	-0.152	0.351	0.001	0.058	0.000	0.001	-0.007	0.568	-0.033	0.018	<0.001	0.314	-0.001	<0.001
BMI	0.064	0.378	-0.079	0.207	-0.328	0.202	-0.835	0.178	-0.001	0.063	-0.003	0.000	-0.026	0.308	-0.077	0.025	0.001	0.039	<0.001	0.002
Creatinine	0.036	0.028	0.004	0.067	0.105	0.063	-0.006	0.217	0.000	0.493	0.000	0.000	-0.004	0.452	-0.016	0.007	0.001	<0.001	<0.001	0.001
AST/ALT	-1.437	0.011	-2.541	-0.332	0.812	0.681	-3.082	4.706	-0.002	0.710	-0.012	0.008	0.213	0.289	-0.182	0.607	-0.009	0.023	-0.017	-0.001
Diet Group 1	0.354	0.445	-0.559	1.267	1.247	0.445	-1.972	4.466	-0.002	0.690	-0.010	0.006	0.204	0.221	-0.124	0.532	-0.003	0.408	-0.009	0.004
Diet Group 3	0.130	0.829	-1.052	1.311	-0.706	0.740	-4.897	3.486	-0.001	0.826	-0.012	0.009	-0.128	0.568	-0.570	0.314	-0.003	0.450	-0.011	0.005
SCI	1.650	0.001	0.674	2.625	-5.635	0.002	-9.084	-2.187	-0.011	0.012	-0.020	-0.002	-0.181	0.316	-0.536	0.174	0.007	0.037	<0.001	0.014
MCI	1.308	0.008	0.342	2.274	-5.217	0.003	-8.645	-1.789	-0.015	0.001	-0.024	-0.007	-0.558	0.002	-0.910	-0.206	0.001	0.874	-0.006	0.007
Overall change in early cognitive decline	Increased				Decreased				Decreased				Decreased				Increased			

2.3.4 Machine learning models to identify risk factors predictive of prodromal AD

All 32 serum metabolites were initially evaluated as possible predictors of prodromal AD. RF achieved the highest classification AUC of 0.65, with AdaBoost and Naïve Bayes attaining 0.58 and 0.63 respectively (Table 2.3). Using the mean decrease Gini, the importance of each metabolite was assessed (Supplementary Figure S2.3). Six metabolites (5-hydroxyindole acetic acid, indole-3-propionic acid, choline, indoxyl sulfate, kynurenic acid and kynurenine) produced the highest AUC of 0.74 using the RF classification algorithm (Figure 2.4). In comparison, Naive Bayes achieved an AUC of 0.72 and AdaBoost attained 0.68. The RF ROC curve indicated the model’s predictive performance was highest for controls (AUC= 0.79), followed by MCI (AUC= 0.76) and SCI (AUC= 0.64). As such, we investigated whether the model performance would be improved by predicting only healthy ageing and MCI. Using the six serum metabolites from controls and MCI participants, the RF model showed improved predictive performance (AUC= 0.84) (Table S2.3). AdaBoost and Naive Bayes also demonstrated increased performance, attaining AUC of 0.87 and 0.90 respectively.

Table 2.3: Comparison of area under the receiver operator curve (AUC)

Machine Learning Model	Classification		
	Control vs. SCI vs. MCI (32 metabolites) AUC	Control vs. SCI vs. MCI (6 metabolites) AUC	Control vs. MCI (6 metabolites) AUC
Random Forest	0.65	0.74	0.84
AdaBoost	0.58	0.68	0.87
Naïve Bayes	0.63	0.72	0.90

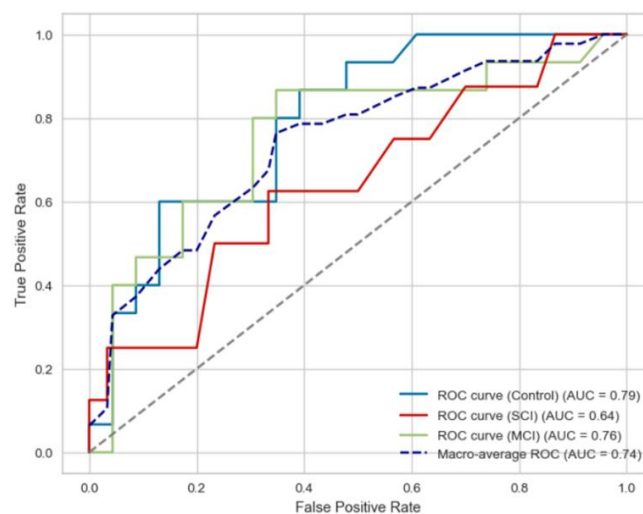


Figure 2.4: Six circulatory metabolites can distinguish stages of prodromal AD. Receiving Operating Characteristic (ROC) curve illustrating the performance of the Random Forest model for

classifying controls, SCI and MCI participants with the average area under the curve (AUC) of the multilevel classifier.

2.3.6 Bile acid ratios reflective of gut microbiome activity are significantly altered in early cognitive decline

Identifying a significant relationship between microbiome composition and serum metabolite levels suggests microbiome dysbiosis may be driving metabolite modulations. To ascertain whether enzymatic processes in BA metabolism are altered in early cognitive decline, we investigated differences in ratios reflective of bacterial enzymatic activity in the gut. These included (1) the CA: CDCA ratio to investigate whether BA synthesis shifted from the primary to the alternative BA pathway, (2) DCA: CA, GDCA: CA, TDCA: CA, LCA: CDCA, GLCA: CDCA, GUDCA: CDCA and UDCA: CDCA ratios reflective of gut microbiome enzymatic activity of primary to secondary BAs synthesis (Figure 2.5A), (3) GLCA: LCA, GDCA: DCA, GUDCA: UDCA and TDCA: DCA ratios to assess if the changes in secondary BA synthesis originated from enzymatic differences within their taurine and glycine conjugation.

The ratio CA: CDCA, representative of BA synthesis via the primary or alternative pathway, showed no significant difference between control, SCI and MCI participants (Figure 2.5A; $p=0.54$). The production of LCA (LCA: CDCA) significantly differed between groups ($p=0.05$), with a significant increase in LCA in MCI in comparison to controls. On the other hand, UDCA: CDCA and GUDCA: CDCA were unchanged between groups, suggesting higher concentrations of cytotoxic secondary BA production, but not neuroprotective, are evident in early cognitive decline. GLCA (GLCA: CDCA) was also unaffected by the cognitive group. No significant differences between the BA ratios reflective of enzymatic differences in taurine and glycine conjugation were found (Figure 2.5B). BA ratios reflective of secondary BA production were associated with 53 microbiome genera (Figure 2.5C).

reflective of BA synthesis via the primary and alternative pathway (blue) and BA ratios indicating primary to secondary BA synthesis reflective of the gut microbiome enzymatic activity (orange). Primary bile acids are highlighted in blue, and secondary BA are highlighted in red. Cytotoxic BAs are bordered with a red dashed line, neuroprotective BAs are bordered with a blue dashed line. (B) Changes in bile acids were not due to modulation of glycine and taurine conjugation (green). (C) Spearman rank correlation between bile acid ratios reflective of secondary BA production and gut microbiome genera. *= $p < 0.05$. Red highlights a positive correlation and blue represents a negative correlation.

2.4 Discussion

Identification of robust, inexpensive and non-invasive markers of cognitive status and its trajectory is currently an unmet medical need in AD research, with circulating gut-derived metabolites presenting a promising area. Metabolic alterations contain rich systemic information on the underlying physiology that connects the periphery to the CNS, likely affecting numerous pathways simultaneously. Thus, the simultaneous detection of numerous perturbed metabolites can provide a powerful detection tool. However, studies investigating composite markers are lacking.

16s rRNA sequencing indicated that significant shifts in gut microbiome composition occur during early cognitive decline, commencing as early as SCI, suggesting changes may already be apparent when memory complaints first appear, aligning with previous studies (Sheng et al. 2021; Chen et al. 2023). As cognitive decline progresses from SCI to MCI, gut microbiome modulation appears less significant. Circulatory metabolites also reflect this pattern, clustering SCI and MCI participants independently from the healthy controls. Individuals with SCI are likely at a higher risk of cognitive decline progression compared to those who are cognitively healthy (Reisberg et al. 2010), which may lead to greater alterations in biological markers, including the gut microbiome and its metabolites. Procrustes analysis showed significant congruence of the microbiome and metabolome datasets, suggesting the two are interlinked and provides the potential for microbial-derived metabolite predictors to be detected early in disease progression. Indeed, gut microbiome composition can account for up to 58% of the variation of circulatory metabolites communicating along the microbiota-gut-brain axis (Dekkers et al. 2022).

Targeted metabolomics quantifies metabolites with extremely high sensitivity and accuracy, providing an advantage over the relative responses yielded by untargeted approaches. RF and multiple linear regression models both revealed indoxyl sulfate, choline, 5-hydroxyindole acetic acid, IPA and kynurenic acid as key early indicators of cognitive decline, with RF presenting an AUC predictive performance of 0.74, strongly supporting a significant link between metabolic perturbations associated with the gut microbiome and prodromal AD progression. Previous studies have predominantly concentrated on binary classification approaches, primarily utilising MRI and PET imaging modalities,

to investigate AD progression (Subramanyam Rallabandi and Seetharaman 2023; Zubrikhina et al. 2023; Simfukwe et al. 2023). However, in clinical practice, multiclass classification of blood samples of patients with SCI, MCI and healthy controls could provide a useful approach. Tong and colleagues attained a similar predictive performance (AUC= 0.73) using RF and nonlinear graph fusion of multiple modalities (regional MRI volumes, voxel-based FDG-PET signal intensities, CSF biomarker measures and genetic information) to classify control, MCI and AD participants (Tong et al. 2017). AUC increased to 0.84 when predicting healthy ageing and MCI, likely due to the difficulty of diagnosing a patient undergoing SCI. Indeed, Purser and colleagues found no relationship between memory complaints and the progression of cognitive impairment over 10 years in individuals 65 years and over (Purser et al. 2006). However, others dispute this result (Geerlings et al. 1999). Adjusting our statistical analysis for confounding variables that heavily influence the host, such as age, BMI, kidney function, liver function and background diet, improves analysis robustness and sensitivity. Adjusting for background diet becomes particularly vital when examining microbial-derived metabolites as the diet can both modulate gut microbiome composition and provide a variety of bioactive precursor compounds; a factor which is often overlooked in metabolomic analyses (Playdon et al. 2016). Nevertheless, our results highlight the use of profiling select circulatory microbial-derived metabolites to identify higher-risk individuals of cognitive decline.

Of the five metabolites highlighted by both machine learning and multiple linear regression, all except choline are produced from tryptophan metabolism, indicating notable alterations in tryptophan metabolism may occur in prodromal AD progression. Alterations in tryptophan metabolism have previously been associated with AD (Weaver et al. 2020). Indeed, we find lower neuroprotective tryptophan-derived metabolites, including IPA and 5-hydroxyindole acetic acid, as cognitive decline progresses from controls to SCI and MCI. IPA is produced in the gut by the microbial conversion of tryptophan via the indole pathway and has previously been investigated as a possible treatment for AD (Bendheim et al. 2002) due to its potent antioxidant effect against A β 1-42 *in vitro* (Chyan et al. 1999) and its ability to prevent aggregation and deposition of A β monomers (Cheng and van Breemen 2005). IPA is anti-inflammatory, reducing the concentration of the proinflammatory TNF- α in activated microglia (Kim et al. 2023), lowering the expression of chemokine (CC Motif) ligand 2 (CCL2) and nitric oxide synthase 2 (NOS2) in interferon-beta (IFN- β) activated murine astrocytes (Rothhammer et al. 2016) and preventing increases in cytokines in LPS-induced human primary astrocytes (Garcez et al. 2020), and has previously been identified as a predictor of AD progression (Gao et al. 2021). 5-hydroxyindole acetic acid is often used as a surrogate marker for serotonin due to serotonin's rapid degradation. As such, our findings indicate lower peripheral serotonin breakdown as early cognitive decline progresses. Approximately 95% of all serotonin is localised in peripheral compartments where it is involved in the modulation of the enteric nervous system (ENS) development and neurogenesis, gut motility, secretion, inflammation, and epithelial development, suggesting these processes may be

disrupted in early cognitive decline (Terry and Margolis 2017). Indeed, MCI and AD patients have often been reported to suffer from gastrointestinal symptoms (Rao and Gershon 2016) and ENS dysregulation in AD has previously been described (Chalazonitis and Rao 2018). Decreased concentrations of 5-hydroxyindole acetic acid also suggest a shift in tryptophan metabolism towards the kynurenine pathway, reducing the availability of tryptophan for serotonin synthesis. This is supported by higher serum kynurenine concentrations in SCI and MCI participants in comparison to controls (Supplementary Table S1) and has previously been found in AD participants, linked to poor memory, executive function and global cognition (Willette et al. 2021). The kynurenine pathway is activated by an inflammatory stimulus, promoting indoleamine 2,3-dioxygenase, the rate-limiting enzyme that initiates the kynurenine pathway. Increased inflammation is a common feature of AD and as such may play a role in modulating tryptophan catabolites.

Both indoxyl sulfate and kynurenic acid concentrations were increased as cognitive decline progressed, even after adjusting for measures of liver and kidney function. As a uremic toxin, indoxyl sulfate can disrupt neuronal efflux transport systems, promote the production of free radicals, inflammation, endothelial cell dysfunction and disturb the circadian rhythm involved in clearing renal and CNS toxins (Iwata et al. 2007; Franco et al. 2019), likely contributing to cognitive decline. Serum levels of indoxyl sulfate, as well as albumin, have previously been identified as predictive of cognitive impairment in participants with end-stage renal disease (Hou et al. 2021). End-stage renal disease patients have also been reported to have an increased abundance of the gut bacteria *Holdemania*, in line with our results, suggesting his genera may be underlying the changes between control and SCI (Zheng et al. 2020). Rodent studies show increased kynurenic acid concentrations can impair cognitive function, including spatial working memory, and broad monitoring deficits (Pocivavsek et al. 2011; Hahn et al. 2018). However, data regarding this relationship in human studies is inconsistent (Chiappelli et al. 2014; Fazio et al. 2015). Kynurenic acid can play a protective role against the cytotoxic product of the kynurenine pathway, quinolinic acid, by acting as an NMDA antagonist for both glycine and glutamate modulatory sites (Stone and Darlington 2013). However, abnormal accumulation has previously been found to induce glutamatergic hypofunction and subsequently disrupt cognitive function (Fujigaki et al. 2017). In AD, increased blood concentrations of kynurenic acid have been hypothesised to relate to neuroinflammatory processes and may be produced as a protective response to neuronal damage (Marrugo-Ramírez et al. 2021).

Choline is required for numerous biological functions in the body (Zeisel and da Costa 2009), notably including hallmark AD-associated processes such as acetylcholine synthesis (Dave et al. 2023). As choline readily crosses the blood-brain barrier, peripheral concentrations typically mirror concentrations in the brain (Wurtman et al. 2009), thus lower concentrations in early cognitive decline may indicate decreased central acetylcholine production. Acetylcholine is intricately connected to neural networks regulating memory, and a reduction in this system is closely associated with learning

and memory deficits in AD (Poly et al. 2011). *Lachnoclostridium* and *Lactonifactor* were inversely correlated with choline levels, suggesting changes in these genera may modulate blood concentrations. Indeed, previous research has found *L. saccharolyticum* WM1, a representative strain of *Lachnoclostridium*, to be an efficient converter of choline to TMA *in vitro*, transforming at a rate near 100% (Cai et al. 2022). This metabolic process *in vivo* also elevated serum TMAO levels (Cai et al. 2022), which is supported by our results displaying a 1.6-fold higher TMAO in MCI compared to controls. Increases in *Lachnoclostridium* abundance may likely increase the metabolism of choline to TMAO, decreasing its concentration in circulation.

APOE, a major cholesterol carrier, plays a crucial role in lipid transport and neuronal repair, with its polymorphic alleles being primary genetic determinants of AD risk (Jeong et al. 2019). *APOE* ϵ 4 is a major genetic risk factor for AD, increasing risk by up to 15-fold in homozygotes, and is associated with impaired A β clearance, increased aggregation, and neuroinflammation, contributing to synaptic dysfunction and neurodegeneration (Strittmatter et al. 1993; Liu et al. 2013). *APOE* isoforms differentially regulate glucose metabolism, neuronal signalling, and mitochondrial function, further influencing AD progression and age-related cognitive decline (Raulin et al. 2022). Emerging evidence suggests that *APOE* ϵ 4 status may modulate gut microbiota composition and function, and therefore the production of microbial-derived metabolites (Tran et al. 2019). In this study, the prevalence of *APOE* ϵ 4 carriers was higher among patients with SCI compared to controls and further increased in those with MCI, consistent with previous research indicating *APOE* ϵ 4 carriers had an elevated risk of AD (Gharbi-Meliani et al. 2021). Therefore, the differing prevalence of *APOE* ϵ 4 in controls, SCI and MCI participants may contribute to the observed shifts in metabolite profiles across the groups. This study does not have the power to stratify participants by *APOE* ϵ 4 status. However, future research should investigate how *APOE4*-carrier status interacts with microbial-derived metabolites to influence cognitive trajectories.

As secondary BAs are synthesised from the microbial action of primary BAs (Dekkers et al. 2022), we investigated whether a change in the production of secondary BAs through enzymatic activities in the gut microbiome occurred in early cognitive decline. Higher concentrations of the cytotoxic secondary BAs, LCA (LCA: CDCA), DCA (DCA: CA), TDCA (TDCA: CA) and GDCA (GCDCA: CA) production were evident in early cognitive decline. No differences in the production of the neuroprotective BAs UDCA (UDCA: CDCA) and GUDCA (GUCDCA: CDCA) were evident. Several studies support this result, with dysregulation in the synthesis of BA ratios in AD participants, increasing the production of cytotoxic BAs (Nho et al. 2019; Baloni et al. 2020). BAs are cytotoxic when their concentration becomes abnormally high and varies between BAs due to their structure. Hydrophobic BAs, such as DCA and LCA, are more cytotoxic (Hofmann 1999). An *in vitro* study associated increased DCA with the modulation of mitochondrial pathways causing apoptosis and with the presence of cognitive symptoms (Ignacio Barrasa et al. 2011; Olazarán et al. 2015). Aligning with

our results, plasma LCA is also increased in AD participants (Vogt et al. 2018), suggesting that elevated levels of cytotoxic secondary BAs may contribute to the progression of cognitive decline and the pathogenesis of AD.

The gut microbiome analysis highlighted a significant relationship between secondary bile acid production and numerous bacterial genera. A decrease in the abundance of *Intestinibacter* was strongly associated with an increase in cytotoxic bile acid production, but not with neuroprotective bile acids. On the other hand, an increase in *Blautia* is positively correlated with cytotoxic bile acid production. *Blautia* contains many species of *Clostridium* and *Ruminococcus spp.*, of which many are closely related to human bile acid 7 α -dehydroxylating species (the enzymatic process converting primary BAs to secondary BAs) (Ridlon et al. 2013), which may contribute to higher cytotoxic BAs production in early AD. Interestingly, the primary BA ratio (CA: CDCA) was not significantly modulated in early cognitive decline suggesting there is no significant change in the synthesis of BAs via the primary or alternative pathway.

Pathophysiological progression of AD is apparent up to 20 years prior to clinical symptom onset, making it vital for prevention research to focus on uncovering novel prodromal risk factors. Scalable markers that enable the early detection of at-risk persons could permit the targeting of lifestyle interventions to lessen future risk and uncover novel mechanisms underpinning dementia. Our findings present new insights into the early progression of cognitive decline and dementia. We signify a major role for the gut in connection to the brain through the modulation of key microbial-derived metabolites. Furthermore, we lend strength to the hypothesis that individuals with higher risks of cognitive decline can be identified via a targeted metabolomic approach in the preceding stages of AD. These results suggest that dietary interventions, by influencing metabolite concentrations, could offer a promising therapeutic strategy to mitigate and potentially slow disease progression.

Chapter 3: Refined diet consumption increases neuroinflammatory signalling through bile acid dysmetabolism

This chapter has been prepared in the form of a research paper which is currently published in *Nutritional Neuroscience* (<https://doi.org/10.1080/1028415X.2023.2301165>).

Title: Refined diet consumption increases neuroinflammatory signalling through bile acid dysmetabolism

Authors: Emily Connell, Britt Blokker, Lee Kellingray, Gwénaëlle Le Gall, Mark Philo, Matthew G. Pontifex, Arjan Narbad, Michael Müller and David Vauzour.

3.1. Introduction

Modern society is experiencing a shift in dietary patterns in which the consumption of convenient, ultra-processed refined foods has increased dramatically. These calorie-dense foods are typically stripped of nutritional components, including dietary fibre, instead containing refined carbohydrates and fructose, starch and sucrose. Consequently, refined diets have been associated with deleterious health problems, including effects on brain health. Indeed, in mice, the long-term consumption of a refined diet leads to cognitive impairment relating to hippocampal synaptic loss mediated through gut microbial metabolites (Shi et al. 2021). Similarly, anxiety-related (Gomes et al. 2020) and compulsive-like behaviour have also been reported in response to a refined diet, resulting from metabolite-mediated neuroinflammation and nitric oxide activation, respectively (Gomes et al. 2018).

One proposed mechanism linking dietary intake to the brain is through modulation of a “microbiota-gut-brain” axis, a bidirectional signalling pathway connecting the gut and the brain that is modulated by the gut microbiome. Recent pre-clinical and clinical evidence has revealed the significance of diet on gut microbiota composition, which subsequently alters numerous microbial-derived metabolite, neuroendocrine, autonomic and neuroimmune pathways, which can both directly and indirectly influence brain function (Loughrey et al. 2017; Morrison et al. 2020). However, despite evidence that a refined diet can modulate gut microbiota composition (Morrison et al. 2020), the specific effects of a refined diet on the microbiota-gut-brain axis remain unknown.

Bile acids (BAs), which are produced by hepatic and bacterial enzymes from cholesterol to assist in digestion and regulate inflammatory signalling, form a key communication system along the microbiota-gut-brain axis and are one of the top microbial-derived metabolites associated with cognitive health (Nho et al. 2019; Baloni et al. 2020). Primary BAs are produced from cholesterol in the liver, of

which most (~95%) are secreted into the intestine by the gallbladder and are actively reabsorbed in the ileum via enterohepatic circulation. The remaining 5% are converted by gut microbial action to form secondary BAs in the colon and therefore their production is strongly associated with multiple bacterial species (Monteiro-Cardoso et al. 2021). The gut microbiome performs two essential roles in BA synthesis. Firstly, conjugated primary BAs reach the gut, and microbiota with bile salt hydrolase (BSH) activity deconjugate glycine or taurine residuals (Ridlon et al. 2014). Following this, selected members of the gut microbiota with 7 α -dehydroxylase activity convert these primary BAs to secondary BAs. BAs also regulate the gut microbiota due to their antimicrobial properties creating strong selectional forces (Zheng et al. 2017). More recently, over 20 conjugated and unconjugated BAs and their receptors have been found in both human and rodent brains, suggesting BAs can not only cross the blood-brain barrier (BBB) but also bind to nuclear receptors and initiate physiological responses (Pan et al. 2017; Baloni et al. 2020). Therefore, the composition of the brain BA pool is regulated by the action of the gut microbiota, with BAs forming part of a complex communication system between the gut and the brain. As such, cognition may be influenced by the dysregulation of BA synthesis and metabolism. Indeed, BA profiles are reportedly altered in cases of mild cognitive impairment and Alzheimer's disease, suggesting a role of the gut microbiome in disease progression (MahmoudianDehkordi et al. 2019).

Here, we investigate the impact of a refined low-fat diet on the microbiota-gut-brain axis. In particular, we explore changes in gut microbiota and metabolome profiles, including changes in BA profiles in the periphery and brain. Further, we provide a novel link between changes in neuronal BAs and detrimental neuronal signalling, suggesting a novel pathway between refined dietary intake and brain health.

3.2. Materials and Methods

3.2.1 Study approval

All experimental procedures and protocols used in this chapter were reviewed and approved by the Animal Welfare and Ethical Review Body (AWERB) and were conducted within the provisions of the Animals (Scientific Procedures) Act 1986 (Amendment Regulations 2012). Animal ethics approval reference PPL 70/8710. Reporting of the study outcomes complies with the ARRIVE (Animal Research: Reporting of In Vivo Experiments) guidelines (Sert et al. 2020).

3.2.2 Animals and Experimental Designs

Ten 10-week-old male wild-type C57BL/6J were sourced from the Disease Modelling Unit (DMU) at the University of East Anglia. Mice were maintained in individually ventilated cages (n=5 per cage) within a controlled environment (21 \pm 2°C; 12-h light-dark cycle; light from 07:00 hours) for the duration of the experiments. After feeding a standard chow diet (RM3; Special Diet Services, Essex, UK) for

two weeks, mice were assigned to either the RM3 diet or to a 10 kCal% low-fat diet (rLFD; Research Diet Inc., New Brunswick, USA) for another 8-weeks (Figure 3.1; Supplementary Table S3.1). This is in line with previous studies (Zheng et al. 2017), allowing sufficient time for the modulation of the gut microbiome and bile acid metabolism. Following this, mice were sedated with 4% isoflurane (IsoFlo®, Abbott, ND) in a mixture of nitrous oxide (70%) and oxygen (30%) and blood samples were collected by cardiac puncture into SST microtubes (Sarstedt, Leicester, UK) followed by trans-cardiac perfusion of ice-cold 0.9% NaCl solution containing heparin (10 units/ml; Sigma-Aldrich, Dorset, UK). Serum samples were isolated by centrifugation at 2,000 x g for 10 min. Organs were rapidly removed, rinsed with ice-cold NaCl (150 mmol/L), snap-frozen and stored at -80 °C until further analysis.

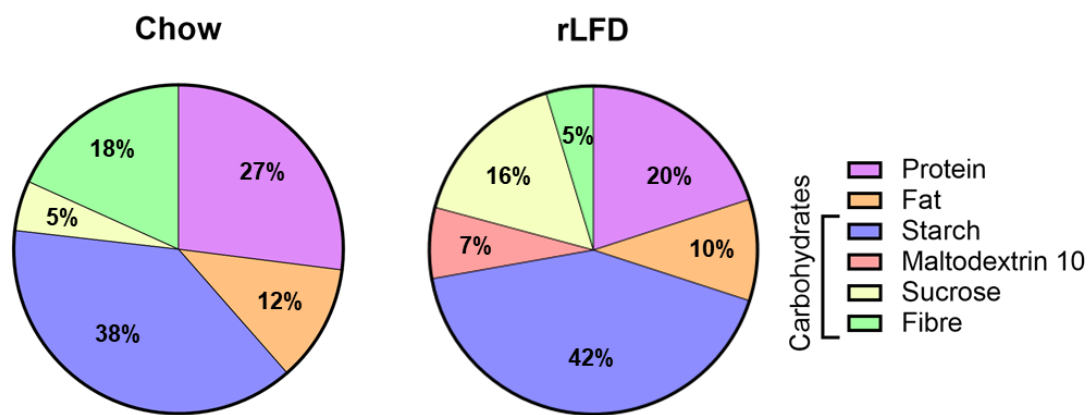


Figure 3.1. Composition of chow and rLFD.

3.2.3 Microbial 16S rRNA extraction and amplicon sequencing

Microbial DNA was isolated from approximately 50mg of colon content using a FastDNA SPIN Kit for Soil (MP Biomedicals) as previously described in Section 2.2.2. Alpha-diversity was assessed using Chao1, Simpson, observed species and Shannon H diversity index whilst beta diversity was assessed using Bray-Curtis. Statistical significance was determined by the Wilcoxon rank-sum test (Mann-Whitney-U) or analysis of similarities (ANOSIM).

3.2.4 ¹H NMR Metabolomics

20 mg of colonic faecal material was added to 1 mL of saline phosphate buffer (1.9 mM Na₂HPO₄, 8.1 mM NaH₂PO₄, 150 mM NaCl, and 1 mM TSP (sodium 3-(trimethylsilyl)-propionate-d₄) in D₂O (deuterium oxide), followed by centrifugation (18,000g, 1 min). Supernatants were removed, filtered through 0.2 μm membrane filters, and stored at -20 °C until required.

High-resolution ¹H NMR spectra were recorded on a 600 MHz Bruker Avance spectrometer fitted with a 5 mm TCI cryoprobe and a 60-slot autosampler (Bruker, Rheinstetten, Germany). Sample temperature

was controlled at 300 K. Each spectrum consisted of 128 scans of 32,768 complex data points with a spectral width of 14 ppm (acquisition time 1.95 s). The noesypr1d pre-saturation sequence was used to suppress the residual water signal with low-power selective irradiation at the water frequency during the recycle delay ($D1 = 2$ s) and mixing time ($D8 = 0.15$ s). A 90° pulse length of $8.8 \mu\text{s}$ was set for all samples. Spectra were transformed with a 0.3 Hz line broadening and zero filling, manually phased, baseline corrected, and referenced by setting the TSP methyl signal to 0 ppm. Metabolites were identified using the Human Metabolome Database (<http://www.hmdb.ca/>) and by use of the 2D-NMR methods, COSY, HSQC, and HMBC (Le Gall et al. 2011) and quantified using the software Chenomx® NMR Suite 8.6™.

3.2.5 Bile acid metabolism

Colon content and brain samples (50 mg) were homogenised in 1ml of 70% v/v methanol containing 25 μl of 40 $\mu\text{g/ml}$ d_4 -DCA (Sigma-Aldrich, USA; Cat# 614130) for 30 seconds at 6,000 rpm on a Precellys homogeniser (Bertin Technologies, UK). The slurry was then centrifuged at 3,000 rpm at 4°C and the supernatant was transferred to a new tube with the addition of 25 μl of 40 $\mu\text{g/ml}$ d_4 -CDCA (Sigma-Aldrich, USA; Cat# C-147). This was evaporated by centrifugal evaporation at 50°C for 70 minutes to almost dryness using a SpeedVac™ concentrator and then made to 1 ml volume with 5% v/v methanol and the addition of 25 μl of 40 $\mu\text{g/ml}$ d_4 -CA (Sigma-Aldrich, USA# Cat: 614149). The reconstituted sample was passed through a hydrophilic-lipophilic balance clean-up cartridge (Waters Oasis Prime HLB, 1cc, 30mg), washed with 1 ml of 5% methanol and eluted in 500 μl methanol and addition of 25 μl of 40 $\mu\text{g/ml}$ d_4 -GCA (Sigma-Aldrich, USA; Cat# 330277P) and d_4 -LCA (Sigma-Aldrich, USA; Cat# 589349). Samples were analysed using an Agilent 1260 binary HPLC coupled to an AB Sciex 4000 QTrap triple quadrupole mass spectrometer. HPLC was carried out using a binary gradient of solvent A (Water + 5mM Ammonium Acetate + 0.012% Formic acid) and solvent B (Methanol + 5mM Ammonium Acetate + 0.012% Formic acid) at a constant flow rate of 600 $\mu\text{l/min}$. Separation was achieved using a Supelco Ascentis Express C18 150 x 4.6, $2.7\mu\text{m}$ column maintained at 40°C . The mass spectrometer was operated in electrospray negative mode with a capillary voltage of -4500V at 550°C . Instrument-specific gas flow rates were 25ml/min curtain gas, GS1: 40 ml/min and GS2: 50 ml/min. Mass fragmentation was monitored in MRM mode. Quantification was applied using Analyst 1.6.2 software to integrate detected peak areas relative to the deuterated internal standards.

3.2.6 RNA isolation and qRT-PCR

Total RNA was isolated from both the cortex and hippocampus using the Qiazol reagent (Qiagen, UK). The hippocampus was investigated as it plays pivotal roles in learning and memory and is affected by a variety of neurological and psychiatric disorders (Anand and Dhikav 2012). The cortex was also

analysed as it is involved in numerous higher brain processes, including memory, thinking, learning, reasoning, the senses, and emotions (Jawabri and Sharma 2022). Two μg of total RNA was treated with DNase I (Invitrogen, UK) and used for cDNA synthesis using Invitrogen™ Oligo (dT) primers and M-MMLV reverse transcriptase. Quantitative real-time PCR (qRT-PCR) reactions were performed using SYBR green detection technology on the Applied Biosystems Viiia-7 Real-Time PCR system (Life Technologies). Results are expressed as relative fold change in rLFD in comparison to the standard chow diet, which has been scaled to the average across all samples per target gene and normalised to the reference genes, beta-2-microglobulin (*B2m*), TATA-box binding protein (*Tbp*) and glyceraldehyde-3-phosphate dehydrogenase (*Gapdh*) and presented as \log_2 fold change. The primer sequences are given in Supplementary Table S3.2.

3.2.7 Statistical analysis

Statistical analysis was carried out using GraphPad Prism version 9.5.1 (GraphPad Software, CA, USA) software packages. All values are presented as means \pm standard error of the means (SEM) unless otherwise stated. All data was checked for normal distribution using the Shapiro-Wilk test. The significant differences in alpha diversity and abundances of each taxonomic unit were detected using Mann-Whitney-U. Statistical analysis of metabolomics data was carried out using Metaboanalyst 5.0. Data was normalised by sum, scaled by autoscaling and square root transformed. Principal Component Analysis (PCA) was employed to illustrate the clustering of different metabolites across groups. Univariate Analysis was carried out by Wilcoxon rank-sum tests. Changes in BA concentrations and gene expression were detected using Mann-Whitney-U or unpaired t-test. All correlation analyses were performed using Spearman rank.

3.3. Results

3.3.1. Male C57BL/6J rLFD-fed mice display marked shifts in intestinal microbiota and metabolism

The impact of a rLFD on gut microbial composition was investigated by 16S rRNA sequencing. Alpha diversity was significantly reduced in rLFD-fed mice in comparison to standard chow, including Chao1 ($p=0.01$), Shannon index ($p=0.003$) and the number of observed species ($p=0.01$) (Figure 2.2A). The PCA component analysis displayed a clear separation between chow and rLFD microbiota composition (Figure 3.2B), which was confirmed by a significant ANOSIM ($p= 0.009$). At the phylum level, rLFD-fed mice showed a significant increase in Deferribacterota and Desulfobacterota (Supplementary Table S3.3). At the genus level, linear discrimination analysis (LDA) effect size (LEfSe) revealed significant differences in 35 genera between rLFD and the standard chow diet (Figure 3.2C). 17 genera were significantly increased in rLFD, including *Lachnospiraceae UCG 010*, *Eubacterium brachy group*, *XBB1006*, *Oscillospira*, *Lactococcus*, *Peptococcus*, *Tuzzerella*, *Ligilactobacillus*, *Rikenellaceae RC9*

gut group, *Mucispirillum*, *Intestinimonas*, *Colidextribacter*, GCA 900066575, *Lachnoclostridium*, *Turicibacter*, *Bilophila* and *Faecalibaculum*. Conversely, 18 genera were significantly decreased, including *Roseburia*, *Lachnospiraceae*, NK4A136 group, *Lachnospiraceae* UCG 001, A2, *Eubacterium xylanophilum* group, *Anaeroplasma*, ASF356, *Lachnospiraceae* FCS020 group, *Prevotellaceae* UCG 001, *Muribaculum*, *Anaerotruncus*, *Acetatifactor*, *Tyzzerella*, HT002, *Eubacterium siraeum* group, UCG 005 and Family XIII UCG 001.

These shifts in microbiome profile included changes in bacterial entities involved in BA metabolism (Figure 3.2D-E), including a significant shift in bacterial genera expressing both BSH capability (*Roseburia* and *Turicibacter* genera) and increases in enzymes involved in 7 α -dehydroxylation (Ruminococcaceae family and *Lachnoclostridium* genera) in rLFD.

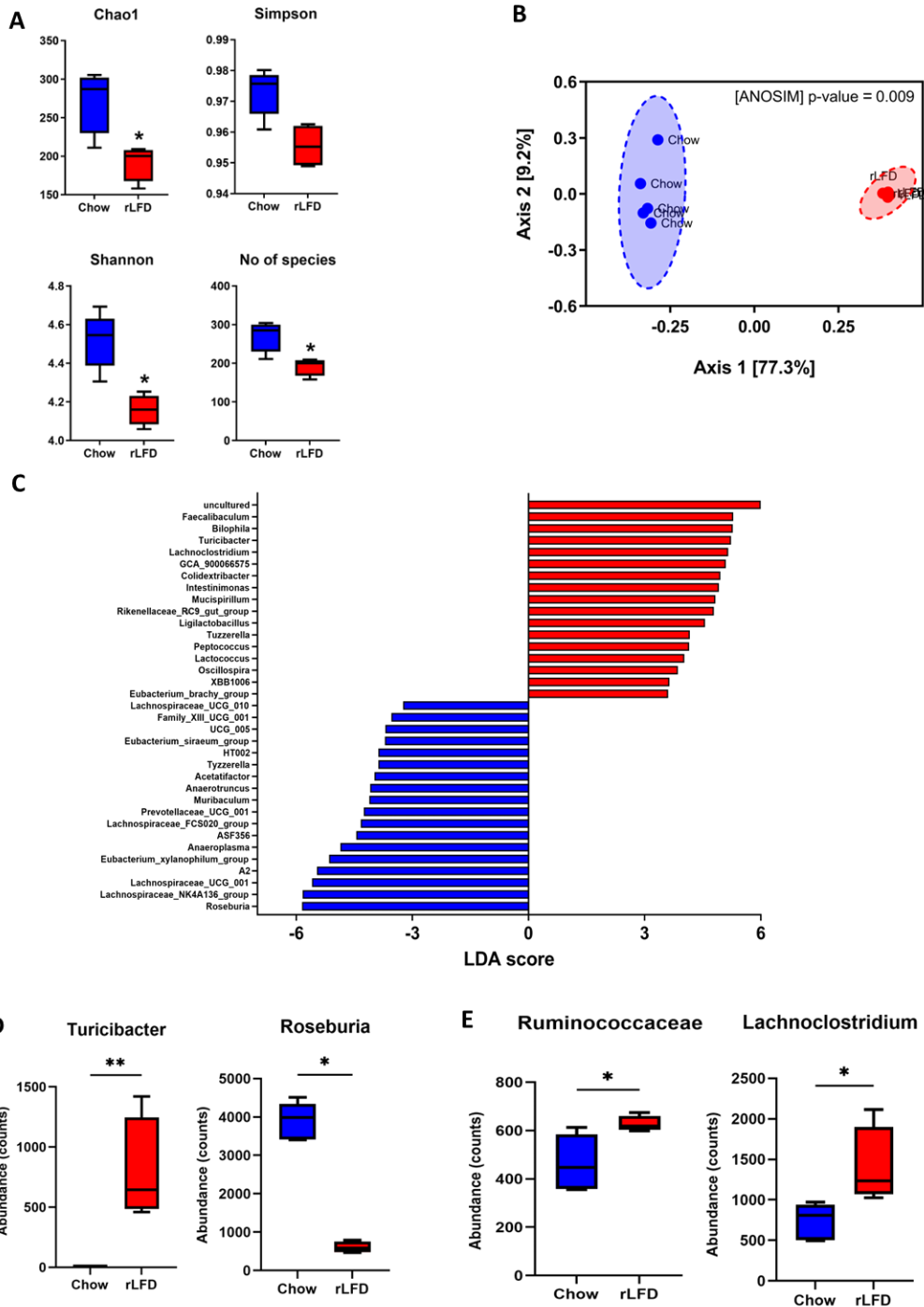


Figure 3.2. rLFD significantly modulates the gut microbiome diversity and composition in male C57BL/6J mice. (A) Alpha diversity using Chao1, Simpson's index, and the number of observed species was decreased in a rLFD compared to chow ($p < 0.05$). Shannon index was decreased near significance ($p = 0.06$). (B) Beta diversity measured through ANOSIM showed significant separation between the two groups. (C) Linear discrimination analysis (LDA) effect size (LEfSe) of significant differences (FDR adjusted $p < 0.05$) in genera between rLFD and standard chow diet. (D) abundance of gut microbiota genera with bile salt hydrolase capability modulated by rLFD. (E) abundance of gut

microbiota family Rumminococcaceae and genera *Lachnospirillum*, with 7 α -dehydroxylation capability. * = p < 0.05, ** = p < 0.01.

¹H-NMR metabolomic profiling of colonic faecal samples was conducted to gain insight into possible shifts in the production of bioactive metabolites. The PCA showed clear separations of the two diets, suggesting a shift in metabolic response to the rLFD (Figure 3.3A). Full NMR concentrations are given in Supplementary Table S3.4. This was confirmed by heatmap analysis showing relative changes in the abundance of 63 metabolites in both standard chow and rLFD (Figure 3.3B). This shift included reductions in short-chain fatty acids (SCFAs) (acetate, propionate and n-butyrate, p < 0.001) and an increase in i-butyrate (p=0.41) (Figure 3.3C).

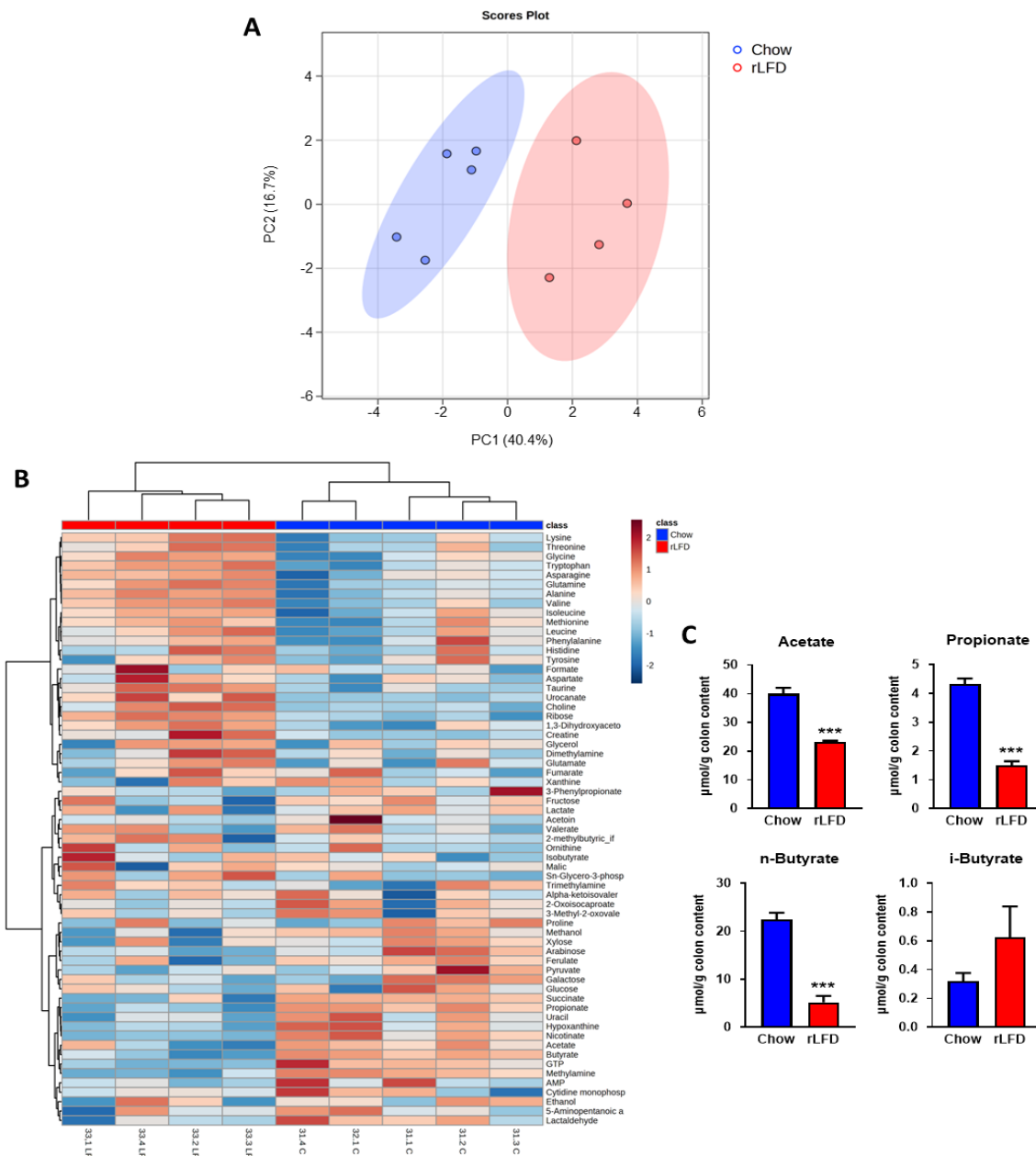


Figure 3.3. rLFD altered the metabolomic profile in male C57BL/6J mice. (A) Partial least squares-discriminant analysis (PLS-DA) showed separation between rLFD and chow diet, indicative of a

metabolic shift in response. (B) Heatmap depicting changes in each metabolite in chow and rLFD diet. (C) rLFD significantly modulates short-chain fatty acid concentrations, including a decrease in acetate, propionate, and n-butyrate and an increase in i-butyrate. *** = $p < 0.001$.

To clarify the relationship between the gut microbiome and the metabolome in the chow and rLFD, Procrustes analyses were conducted to evaluate the congruence of the two datasets. The analysis demonstrated that plots of both the metabolome and microbiome were separated by dietary intake, with a similarity between the metabolome and microbiome plots, suggesting an association between the two ($p=0.001$, Figure 3.4A). This was confirmed by a Spearman rank analysis, which correlated metabolites and microbiota genera that were significantly shifted in a rLFD in comparison to chow (FDR adjusted $p < 0.05$). This demonstrated a significant correlation between 17 metabolites with 9 of the gut microbiome genera (Figure 3.4B). BA concentrations also significantly correlated with 40 gut microbiome genera, suggesting a strong relationship between the two (Figure 3.4C).

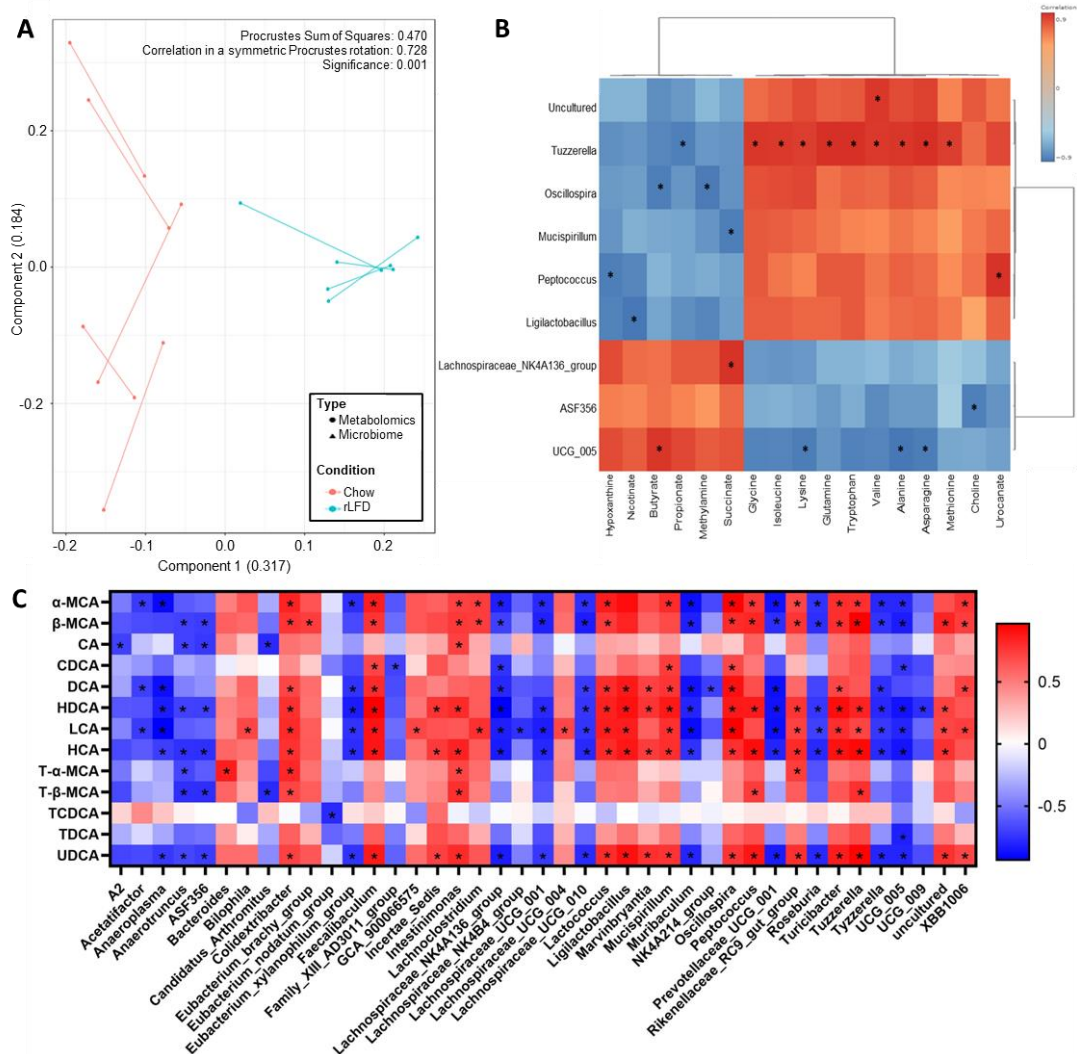


Figure 3.4. The gut microbiome and the metabolome profile of chow and rLFD male C57BL/6J mice are significantly related. (A) Procrustes plot comparing the relationship between the microbiome

and the metabolome profiles. Longer lines indicate more within-subject dissimilarity. (B) Spearman rank correlation showing the interaction between microbiota genus and metabolome that are significantly modulated by the rLFD. (C) Heatmap displaying Spearman rank correlation between bile acids in the colon and gut microbiome genera. * = $p < 0.05$. Red = positive correlation. Blue = negative correlation.

3.3.2 rLFD-fed mice display dysregulated bile acid metabolism

BA profiles were quantified from both colon and brain samples. BA profiles were significantly modulated in both the colon and the brain under rLFD challenge. Total colonic BA concentration significantly increased (Supplementary Table S3.5), predominantly from increases in alpha-muricholic acid (α -MCA), beta-muricholic acid (β -MCA) and ursodeoxycholic Acid (UDCA), hyodeoxycholic acid (HDCA) and hyocholic acid (HCA) ($p < 0.05$) (Figure 3.5A). Concentrations of tauro-alpha-muricholic acid (T- α -MCA), tauro- β -muricholic acid (T- β -MCA), deoxycholic acid (DCA) and lithocholic acid (LCA) were also increased. In the brain, BA profiles were also significantly modulated, with significant decreases in cholic acid (CA) and taurocholic acid (TCA) ($p < 0.05$) (Figure 3.5B). The chenodeoxycholic acid (CDCA): CA ratio was also calculated in both the colon ($p = 0.80$) and the brain ($p = 0.68$) and showed no significant difference, suggesting there was no shift in BA synthesis via the primary or alternative pathway (Supplementary Table S3.5). For detailed concentrations of BA in the colon and brain, see Supplementary Table S3.5.

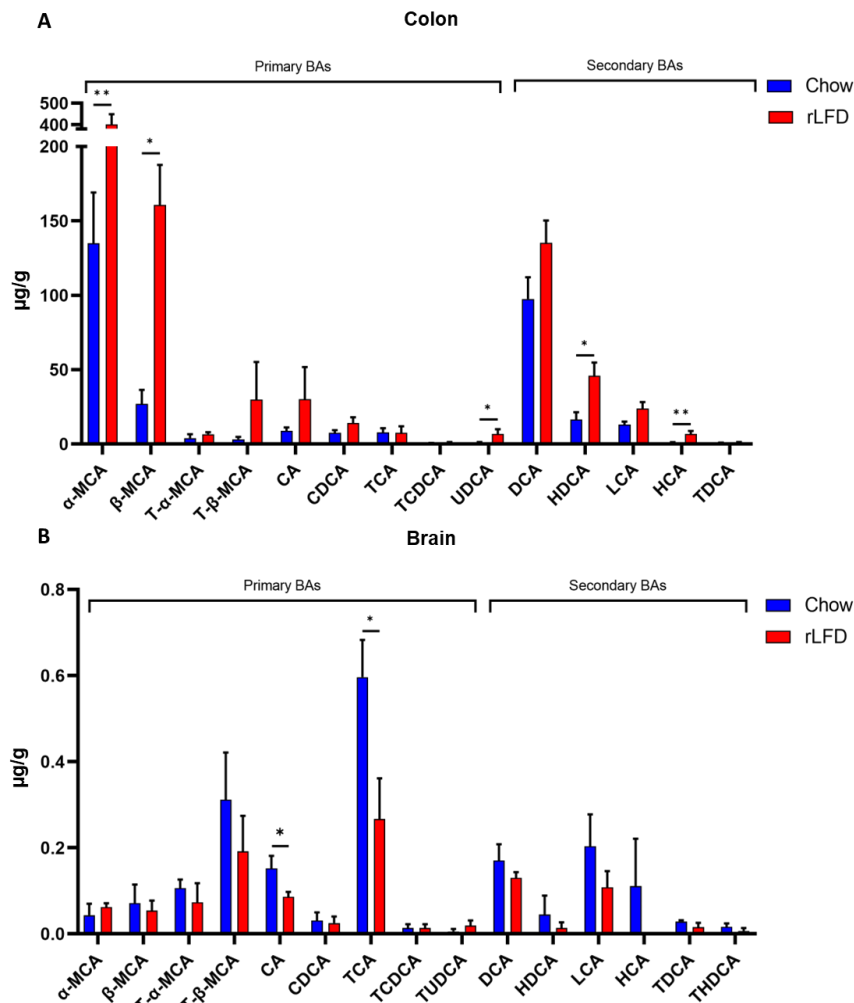


Figure 3.5. Bile acid profiles in both the colon and brain are modulated by a rLFD of C57BL/6J male mice. Bar plots represent the concentration of bile acids ($\mu\text{g/g}$) in the colon (A) and the brain (B). The blue bars represent the standard chow diet ($n = 5$), the red bars represent the rLFD diet ($n = 5$). Error bars = SEM. * = $p < 0.05$, ** = $p < 0.01$.

3.3.3 rLFD significantly modulates gene expression in the brain of C57BL/6J male mice

Given the extent of BA modulation within the brain in response to rLFD, we investigated the extent to which these changes influence neuronal gene expression/function. qRT-PCR suggested significant modulation of five genes in the hippocampus ($p < 0.05$). Three genes were upregulated, Mitogen-Activated Protein Kinase 8 (*Mapk8*), DNA Damage Inducible Transcript 3 (*Ddit3*) and nuclear factor κ -light-chain-enhancer of activated B cells (*NF κ B1*), whilst two genes were downregulated (Nitric Oxide Synthase 2 (*Nos2*) and Tyrosine 3-Monooxygenase/Tryptophan 5-Monooxygenase Activation Protein Theta (*Ywhaq*)) in the mice fed a rLFD in comparison to a chow diet (Figure 3.6A). In the cortex, two genes were upregulated (Activity Regulated Cytoskeleton Associated Protein (*Arc*) and *Ddit3*), whilst peptidylprolyl isomerase A (*Ppia*) was downregulated ($p < 0.05$) (Figure 3.6B). For a full

list of changes in gene expression in the cortex and hippocampus, see Supplementary Table S3.6 and S3.7 respectively.

To identify whether the significant changes in gene expression were associated with BA concentrations in the brain, a Spearman rank correlation analysis was performed (Figure 3.6C). Results showed a significant negative correlation between T- α -MCA ($p=0.037$, $R^2= -0.72$), TCA ($p= 0.006$, $R^2= -0.85$) and TDCA ($p= 0.034$, $R^2= -0.72$) and hippocampal *NF κ B1* gene expression. As the rLFD significantly modulated both TCA concentration and *NF κ B1* expression in the brain, this association was of particular interest (Figure 3.6D).

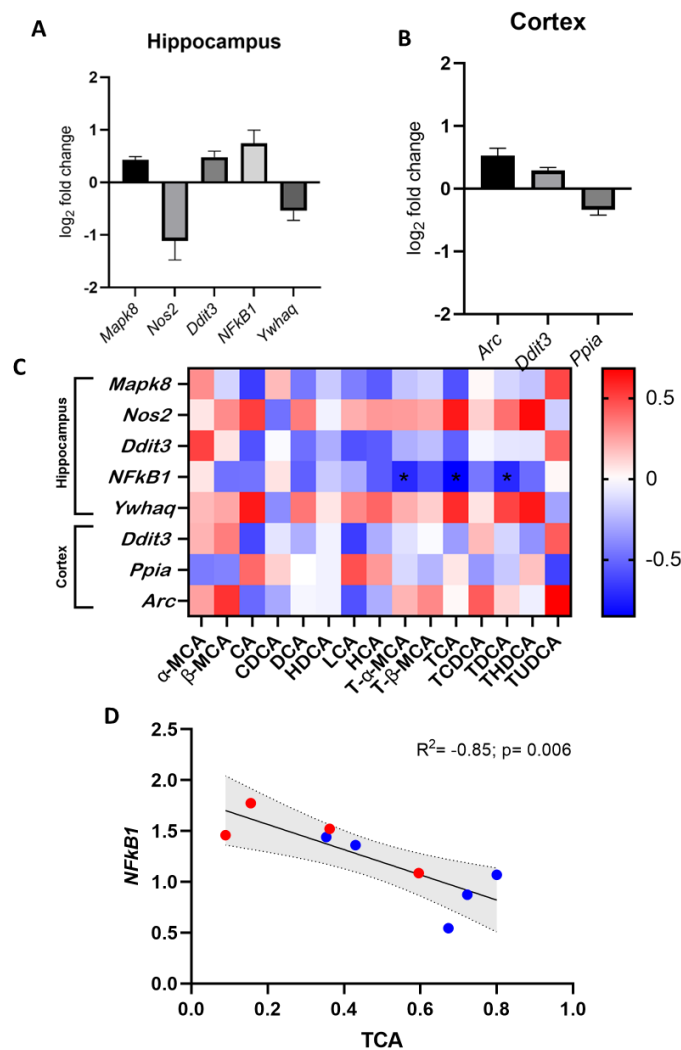


Figure 3.6. rLFD significantly modulates gene expression in the hippocampus and cortex of male mice. Significant log₂ fold changes in mRNA expression in a rLFD ($n = 5$) in comparison to a chow ($n = 5$) diet in the hippocampus (A) and the cortex (B) ($p < 0.05$). (C) Heatmap displaying Spearman rank correlation between genes significantly modulated by rLFD and bile acids in the brain. * = $p < 0.05$. (D) TCA concentration in the brain is significantly modulated by rLFD and is correlated with *NF- κ B1* signalling in the hippocampus. Blue = chow diet. Red = rLFD. Shaded region displays a 95% confidence interval.

3.4. Discussion

As the consumption of refined foods increases in western society, it is important we elucidate its effect on brain health. Diet represents one of the largest factors influencing intestinal microbiota activity, and therefore can modify the microbiota-gut-brain axis and affect many aspects of human health. These include metabolic disorders, cardiovascular health and neurological function (Berding et al. 2021b). The current study is to our knowledge the first to highlight the effects of a refined diet on BA profiles within the microbiota-gut-brain axis, including quantifying BA profiles in the brain; an area which is infrequently explored. Here, we demonstrated the feeding of a high sugar and fibre-poor rLFD to mice for eight weeks significantly shifted the gut microbiome profile, subsequently modulating BA composition in both the colon and the brain. These events, in part, upregulated *NFκB1* gene expression in the hippocampus, a key mediator of CNS inflammatory response (Rolova et al. 2014), which is associated with a significant decrease in three taurine-conjugated BAs (TDCA, TCA and T- α -MCA).

The consumption of a rLFD for eight weeks was found to modulate gut microbiota composition, significantly reducing microbial diversity. Previous studies investigating low-fibre intake have found similar decreases in microbial diversity, which can even be transferred between generations (Sonnenburg et al. 2016). The rLFD also modulated 35 bacterial genera, decreasing SCFA-producing bacteria such as *Roseburia*, *Eubacterium* and several genera belonging to the Lachnospiraceae family, aligning with reductions in peripheral SCFA concentrations. Similar changes have previously been reported by Pontifex and colleagues, highlighting the poor fermentation of insoluble fibres in the rLFD by the gut microbiota (Pontifex et al. 2021b). SCFAs provide a key energy source for colonocytes, promote the expansion of commensal microbiota, restrict the development of pathogenic bacteria and lessen local and systemic inflammation (Besten et al. 2013), processes that are likely reduced under rLFD consumption.

Since BA metabolism is modulated by the gut microbiota, the shift in gut microbiome composition likely in part contributes to the dysregulation of BA synthesis in the rLFD. This relationship was highlighted by a significant correlation between several colonic BAs and gut microbiota genera, including a shift in bacterial genera expressing BSH (*Roseburia* and *Turicibacter*) and 7 α -dehydroxylation enzymes (increases in Ruminococcaceae and *Lachnoclostridium*) in rLFD. These modulations likely underpin the increased concentration of colonic secondary BAs in the rLFD. Low-fibre intake shifts gut microbial metabolism towards the utilisation of less favourable substrates, particularly dietary and endogenously supplied proteins, which may be detrimental to the host and increase BA production (Zeng et al. 2019). Of the 35 bacterial genera modulated by the rLFD, 34 were Gram-positive bacteria. Although bile acid tolerance is overall strain-specific, Gram-positive bacteria

are typically more sensitive to bile acids than Gram-negative bacteria (Min et al. 2022). As such, these bacteria would likely be more responsive to increases in the bile acid concentrations.

In the colon, BA concentrations of α -MCA, β -MCA, HDCA and UDCA were significantly increased. These BAs are antagonists of the nuclear farnesoid receptor (FXR) (Sayin et al. 2013; Mueller et al. 2015; Kuang et al. 2023). Ileal FXR activation induces expression of the fibroblast growth factor 19 (FGF19; FGF15 in mice), which represses BA synthesis by inhibiting the rate-limiting enzyme CYP7A1 (Lee et al. 2006). As such, increases in these antagonists likely inhibit this signalling in a rLFD and contribute to the increase in peripheral BA concentrations. FGF19 can also cross the BBB (H et al. 2013). Fibroblast growth factor receptor (FGFR) 4, the target for FGF15/19, has been detected in the brain and reduces orexigenic AGRP/NPY neuron activity in the hypothalamic arcuate nucleus (Miyake and Itoh 1996; Marcelin et al. 2014). This process improves peripheral glucose homeostasis. Therefore, a reduction in ileal FXR signalling from rLFD may reduce FGF15 in the brain and worsen peripheral glucose homeostasis.

Despite our results suggesting dysregulation of BA levels in the colon and the brain in rLFD, the two locations show definitive differences. For example, UDCA was below our limit of detection, suggesting it is either not present in the brain or exists in small quantities. However, UDCA was found in the colon. These differences may arise due to the varying capabilities of BAs to cross the BBB or changes in local synthesis. Indeed, whilst some studies have demonstrated the influx of BAs across the BBB and identified BA transporters in the brain, it is unclear the extent to which *de novo* synthesis contributes to the pool. The genes encoding cytochrome P450 enzymes required for the alternative BA synthesis pathway (*CYP8B1*, *CYP27A1* and *CYP7B1*) are expressed in the brain (Nishimura et al. 2003). However, since *CYP7A1* is not found in the brain, BAs such as CA likely enter from the periphery. Furthermore, the presence of secondary BAs in the brain strongly suggests a role of the gut microbiota and transport to the CNS from the periphery. In terms of dietary-related modulation, our results show lower total BA in the brain of rLFD which may indicate disrupted BA transport from the periphery or a reduction in *de novo* synthesis compared with a chow diet.

Modulated BA concentrations in the brain suggest BA dysregulation occurs in rLFD. Brain BA dysmetabolism has been postulated as a factor for the pathogenesis of neurodegenerative diseases such as Alzheimer's disease (AD) and Parkinson's disease (PD) (Graham et al. 2018; Baloni et al. 2020). In particular, our results show significant decreases in CA and TCA, suggesting these BAs may be mostly modulated by a rLFD. TCA has previously been found to be decreased in the brain of AD patients and both CA and TCA concentrations are decreased in the brain of 12-month APP/PS1 mice (Pan et al. 2017). However, since behavioural outcome measures were not performed in this study, we cannot determine whether BA dysregulation from the rLFD affects cognition. CA is also an antagonist for the

N-methyl-D-aspartate (NMDA) receptor and γ -aminobutyric acid (GABA) type A (GABAA) receptor. NMDA receptors play a role in synaptic communication by generating a Ca^{2+} influx and initiating calmodulin to activate CaMKII, MAPK, CREB, and PI3K pathways (Montes de Oca B 2018). GABAA receptor activation triggers chloride ions release following neuron hyperpolarisation and neurotransmission inhibition (Çiçek 2020). These processes are likely modulated by a reduction in CA in a rLFD. Nevertheless, these results suggest BA dysmetabolism may also influence BA homeostasis and signalling in the brain.

Results from the qRT-PCR analysis showed an upregulation of pro-apoptotic genes in the rLFD through the cytochrome c mediated pathway (*Mapk8*) in the hippocampus and through the enhanced expression of autophagy genes (*Ddit3* and *Mapk8*) in the cortex and hippocampus; a process highly detrimental to neurons (Ajoalabady et al. 2022). *Ddit3* can also upregulate the *Txnip* gene, which in turn upregulates neuroinflammatory genes and promotes the formation of the NLR family pyrin domain containing 3 (NLRP3) inflammasome, leading to neuroinflammation. These changes have previously been associated with worsening pathology observed in AD (Ajoalabady et al. 2022). In the cortex, *Arc* gene expression was upregulated in the rLFD compared to the chow diet. Typically, ARC plays a role in the maintenance phase of long-term potentiation and spatial memory consolidation. However, chronic activation of the immune system alters ARC activity, which has been suggested as a mechanism of cognitive dysfunction associated with neuroinflammatory conditions (Rosi 2011). The rLFD also significantly downregulated *Ppia*, *Nos2* and *Ywhaq*. Inside cells, PPIA is suggested to play a beneficial role, promoting *de novo* protein folding and protecting against oxidative stress. However, when deficient, *Ppia* may increase neurodegenerative features similar to frontotemporal dementia, marked TDP-43 pathology and late-onset motor dysfunction (Pasetto et al. 2021). *Nos2* produces inducible NOS (iNOS), which can play a critical role in neuroinflammation by producing nitric oxide (NO), an important signalling and redox factor in the brain. Although NO is associated with tissue damage, it can also promote cell survival. In a mouse model of AD, a *Nos2* deletion was associated with multiple neuropathologies including increased neuronal degradation and caspase-3 activation (Colton et al. 2006). Finally, *Ywhaq* encodes the 14-3-3- θ protein which binds major histocompatibility complex (MHC) class II molecules and is implicated in various neurodegenerative diseases (Jia et al. 2014). While the exact impact of *Ywhaq* on brain health is still unclear, there is evidence to suggest that it may play an important role in protecting against oxidative stress (Pennington et al. 2018) and regulating mood and behaviour (Demars et al. 2020). Taken together, these results suggest a rLFD reduces the expression of several neuroprotective proteins in the hippocampus and cortex.

Only *NF- κ B1* gene expression was found to both be significantly modulated in a rLFD and correlated to BA concentrations in the brain. *NF- κ B1* was inversely correlated with three taurine-conjugated BAs (T- α -MCA, TCA and TDCA). Of these BAs, TCA was also significantly modulated by a rLFD in the

brain, suggesting the diet may decrease neuronal TCA concentrations which increases *NF-κB1* signalling. NFκB1 is a well-known regulator of inflammation, stress, and immune responses as well as cell survival. In glia, NF-κB regulates inflammatory processes that exacerbate diseases such as autoimmune encephalomyelitis, ischemia, and Alzheimer's disease (Kaltschmidt and Kaltschmidt 2009). Therefore, an increase in *NF-κB1* expression in rLFD likely highlights an increase in neuroinflammation, which is associated with a decrease in taurine-conjugated BAs. Taurine-conjugated BAs are known to play a neuroprotective role in the brain. *In vitro* evidence shows that TDCA can inhibit NF-κB1 activation in response to IL-1β (Ghaderpour et al. 2023). Taurine itself can also suppress inflammatory damage by acting on NF-κB expression (Agca et al. 2014). In some neurological disorders where inflammation plays a key role, taurine transport across the BBB is impaired, leading to reductions within the CNS (Csernansky et al. 1996; Baloni et al. 2020). Therefore, our results suggest a refined diet can significantly reduce TCA concentrations in the brain which likely reduces the inhibition of NF-κB1 activation and induces a neuroinflammatory response. However, as this is based on association data, further studies examining the link between TCA and neuroinflammation would be required. Particularly as the current understanding of specific BA roles within the brain is limited.

Overall, our results suggest a novel link between a refined diet and detrimental neuronal processes, likely in part through modulation of the microbiota-gut-brain axis and BA dysmetabolism. These results highlight the interconnected nature of dietary carbohydrates, gut microbiome composition and bile acids on brain health and function. BA dysregulation is becoming increasingly important in numerous neuropathological states, yet little is understood about its roles in the brain. Future research should focus on uncovering the origin and transport of BAs in the brain to improve our understanding of communication within the microbiota-gut-brain axis and identify potential therapeutic targets.

Chapter 4: (Poly)phenol-rich grape and blueberry extract prevents LPS-induced disruption of the blood-brain barrier through the modulation of the gut microbiota-derived uremic toxins

This chapter has been prepared in the form of a research paper which is currently published in *Neurochemistry International* (doi: 10.1016/j.neuint.2024.105878).

Title: (Poly)phenol-rich grape and blueberry extract prevents LPS-induced disruption of the blood-brain barrier through the modulation of the gut microbiota-derived uremic toxins.

Authors: Emily Connell, Gwénaëlle Le Gall, Simon McArthur, Leonie Lang, Bernadette Breeze, Matthew G. Pontifex, Saber Sami, Line Pourtau, David Gaudout, Michael Müller and David Vauzour.

4.1 Introduction

Changes in the immune system have long been recognised to occur with ageing, including increases in oxidative stress, cell senescence, immune system dysfunction and metabolic disturbances (Jang et al. 2024). These collective processes contribute to the development of chronic, low-grade inflammation, commonly referred to as "inflammageing" (Ferrucci and Fabbri 2018). Inflammageing is a prominent factor in the onset and progression of age-related chronic diseases, including cognitive decline and Alzheimer's disease (AD), as well as chronic conditions such as diabetes, atherosclerosis, and cardiovascular disease, which are established risk factors for AD (Kosyreva et al. 2022).

Previous research associates inflammageing with gut microbiota dysregulation, alterations in microbial-derived metabolites, and disrupted microbiota-gut-brain axis communication, contributing to neuroinflammation and negatively impacting brain health (Ownby 2010; Willette et al. 2021; Kosyreva et al. 2022). Lifestyle interventions such as diet may provide an effective strategy to reduce these effects due to their ability to directly modulate inflammation and gut microbiota composition (Delafuente 1991; Di Giosia et al. 2022). However, the effect of specific dietary components is not fully understood.

(Poly)phenols are a diverse group of phytochemicals abundant in fruits, vegetables, and other plant-based foods. Renowned for their potent antioxidant and anti-inflammatory properties, (poly)phenol intake has been associated with prevention of various chronic diseases, including cardiovascular diseases, cancers and neurodegenerative disorders, and are regarded as highly relevant modifiers of brain pathophysiology (Singh et al. 2008; Del Rio et al. 2013; Ramis et al. 2020; Mutha et al. 2021; Iqbal et al. 2023). Accordingly, dietary (poly)phenols are emerging as promising therapeutic strategies

to promote healthy ageing due to their accessibility and the minimal side effects compared to pharmacological treatments.

Dietary (poly)phenols have been shown to influence gut microbiota composition, promoting the growth of beneficial bacteria while suppressing pathogenic species (Mithul Aravind et al. 2021; Song et al. 2021; Romo-Vaquero et al. 2022; Láng et al. 2024). Modulation of the gut microbiome has the capability to alter numerous microbial-derived metabolite, neuroendocrine, autonomic and neuroimmune pathways, directly and indirectly influencing brain function (Chakrabarti et al. 2022).

Grapes and blueberries are rich sources of (poly)phenols. Blueberries, containing high concentrations of anthocyanins (Ma et al. 2018), and grapes, consisting of flavonoids (flavan-3-ols, flavonols, anthocyanins and flavones), and non-flavonoids (phenolic acids and stilbenes) (Garrido and Borges 2013), have been studied in both human (Krikorian et al. 2010a, b) and rodent models (Shukitt-Hale et al. 2006; Sarkaki et al. 2007; Rendeiro et al. 2012; Dal-Pan et al. 2017) for their potential to enhance cognitive performance and protect against cognitive decline. Supplements containing high concentrations of (poly)phenols are increasingly popular as a convenient method to boost the intake of beneficial compounds, which may enhance cognitive function (Troppmann et al. 2002). Memophenol™, a patented (WO/2017/072219) (poly)phenol-rich blueberry and grape extract, has been reported to prevent age-related spatial memory deficits in aged mice (Bensalem et al. 2016) and to improve recognition memory in 3xTg-AD mice, a model of Alzheimer's disease (Dal-Pan et al. 2017). Furthermore, consumption of Memophenol™ was reported to improve cognitive capabilities in healthy young adults (Philip et al. 2019), elderly individuals (Bensalem et al. 2019) and older adults with mild cognitive impairment (Lopresti et al. 2023). However, whether these effects are due to modulation of the microbiota-gut-brain axis remains unknown.

In this chapter, we present for the first time the effect of a (poly)phenol-rich grape and blueberry extract, Memophenol™, on the microbiota-gut-brain axis; exploring its effect on gut microbiota composition, quantifying key circulatory microbial-derived metabolites associated with cognitive health and underlying neuronal gene expression changes in the brain, in the context of a lipopolysaccharide (LPS) model of chronic low-grade inflammation. LPS, a component of the outer membrane of Gram-negative bacteria, triggers systemic inflammation by activating immune and inflammatory pathways.

4.2. Materials and Methods

4.2.1. Study approval

All experimental procedures and protocols performed were reviewed and approved by the Animal Welfare and Ethical Review Body (AWERB) of the University of East Anglia and were conducted in accordance with the United Kingdom Animals (Scientific Procedures) Act, 1986 (Amendment

Regulations 2012) under project licence PPL80/2533. Reporting of the study outcomes complies with the ARRIVE (Animal Research: Reporting of In Vivo Experiments) guidelines (Sert et al. 2020).

4.2.2. Overview of experimental procedure

Thirty male C57BL/6J mice sourced from Charles River (Margate, UK) were maintained in individually ventilated cages ($n = 5$ per cage), within a controlled environment (21 ± 2 °C; 12 h light/dark cycle; light from 7:00 AM). Mice were fed *ad libitum* on a standard diet (RM3-P; Special Diet Services (SDS, Horley UK)) up to the age of 10 weeks, ensuring normal development and stabilisation of the microbiota. Mice were subsequently divided into three groups ($n = 10$ per group): 1) the control group fed the standardised AIN93-M diet with a sham injection of saline, 2) the lipopolysaccharide (LPS) group formed of mice fed the standardised AIN93-M with LPS administration or 3) the LPS + Memophenol™, a (poly)phenol-rich grape and blueberry extract (Supplementary Table S4.1), group consisting of mice consuming the Memophenol™ diet (Activ'Inside, Beychac-et-Caillau, France) with LPS administration, for eight weeks. The Memophenol™ diet consisted of the background AIN93-M supplemented with 879 mg kg⁻¹ diet of Memophenol™ (see Supplementary Table S4.2 for full dietary composition). Diets were prepared by Research Diet Inc. (New Brunswick, USA) to comply with animal nutrition requirements. Chronic low-grade inflammation was initiated upon switching of the diets and was induced through weekly intraperitoneal injections (IP) of 0.5 mg kg⁻¹ LPS (*Escherichia coli* O111:B4, Merck Life Science, UK) for 8 weeks as described previously (Hoyles et al. 2021; Pontifex et al. 2022) or a sham injection consisting of 0.9% saline to control mice. At the end of the experiments, 5-month-old animals were sedated with isoflurane (1.5%) in 70% nitrous oxide/30% oxygen mix and transcardially perfused with ice-cold 0.9% saline containing 10 UI heparin (Sigma-Aldrich, UK). Whole blood was allowed to clot in ice for 30 minutes before isolating the serum by centrifugation at 4,000g for 10 min. Brains were rapidly removed, halved, snap-frozen and stored at -80 °C until biochemical, immunohistochemical and transcriptomic analyses. Additionally, caeca were removed, weighed and contents were extracted. Samples were then snap-frozen in liquid nitrogen and stored at -80 °C until further analysis.

4.2.3. Microbial 16S rRNA extraction and sequencing

Microbial DNA was isolated from approximately 50 mg of caecal content using the QIAamp PowerFecal Pro DNA Kit (Qiagen, Manchester, UK) from $n = 6$ randomly selected male C57BL/6J mice as described in Section 2.2.2.

Alpha diversity was assessed using both Chao1 and Shannon H diversity index whilst beta diversity was assessed using Bray–Curtis. Statistical significance was determined by Kruskal–Wallis or

Permutational Multivariate Analysis of Variance (PERMANOVA). Comparisons at the genus level were made using classical univariate analysis using Kruskal–Wallis combined with a false discovery rate (FDR) approach used to correct for multiple testing.

4.2.4 LC-MS/MS

LC-MS/MS was conducted to gain insight into possible shifts in the production of bioactive serum metabolites in 5-month-old male mice as previously described in Section 2.2.3.

4.2.5 Immunofluorescent staining

Coronal brain cryosections (20 μm) containing the hippocampus were processed from the left hemisphere of snap-frozen brain samples. For each animal, six coronal sections containing the hippocampus, spaced 120 μm apart, were analysed to ensure consistent and representative region coverage. Cryosections were mounted onto glass slides before being fixed in 4% formaldehyde in PBS for 15 minutes. Sections were washed in Tris-buffered saline (TBS; 50 mM Tris base, 150 mM NaCl, pH 7.4) containing 0.05% Triton X-100 for 10 min, followed by blocking with TBS containing 10% normal goat serum and incubated with the primary antibody for 1 hour at room temperature (polyclonal rabbit anti-mouse zonula occludens-1 (ZO-1), 1:100, Thermofisher Scientific, UK), diluted in TBS containing 0.1% normal goat serum. Nuclei were counterstained with DAPI (Sigma–Aldrich, UK). Images were collected from the hippocampus of each mouse using a Direct Fluorescence Leica Ctr 5000 Microscope at x10 magnification. Image analysis was performed using ImageJ (version 1.53) software (NIH, Washington DC, USA). ZO-1 signal intensity was quantified using densitometry, calculated as the mean grey value within the delineated ROI. The values were averaged across the six sections for each animal to provide a comprehensive measure of ZO-1 expression.

4.2.6 RNA isolation and sequencing

Total RNA was isolated from hippocampi ($n= 4$, randomly selected from each group) using the Qiazol reagent (Qiagen, UK). Messenger RNA was then purified from total RNA using poly-T oligo-attached magnetic beads. After fragmentation, the first strand cDNA was synthesized using random hexamer primers, followed by the second strand cDNA synthesis using either dUTP for a directional library or dTTP for non- directional library (Parkhomchuk et al. 2009). The libraries were checked with Qubit and real-time PCR for quantification and bioanalyzer for size distribution detection. Quantified libraries were pooled and sequenced on Illumina platforms, according to effective library concentration and data amount. Raw data (raw reads) of FASTQ format were first processed through in-house Perl scripts. All

the downstream analyses were based on clean data with high quality. The index of the reference genome was built using Hisat2 v2.0.5 (Mortazavi et al. 2008) and paired-end clean 1 reads were aligned to the reference genome using Hisat2 v2.0.5. FeatureCounts v1.5.0-p3 was used to count the reads numbers mapped to each gene (Liao et al. 2014). Then FPKM of each gene was calculated based on the length of the gene and the read count mapped to this gene.

4.2.7 qRT-PCR

RNA was prepared as outlined above. Two µg of total RNA was treated with DNase I (Invitrogen, UK) and used for cDNA synthesis using Invitrogen™ Oligo (dT) primers and M-MMLV reverse transcriptase. Quantitative real-time PCR (qRT-PCR) reactions were performed using SYBR green detection technology on the Applied Biosystems QuantStudio 5 Real-Time PCR system (Life Technologies). Results are expressed as relative fold change in LPS and LPS + Memophenol™ in comparison to the control group, which has been scaled to the average across all samples per target gene and normalised to the geometric mean of three reference genes, TATA-box binding protein (*Tbp*), glyceraldehyde-3-phosphate dehydrogenase (*Gapdh*) and hypoxanthine phosphoribosyltransferase 1 (*Hprt1*). The primer sequences are given in Supplementary Table S4.3.

4.2.8. Statistical analysis

Data analysis was performed in GraphPad Prism version 9.5.1 (GraphPad Software, CA, USA). All data are presented as means ± standard error of the means (SEM) unless otherwise stated. After identifying outliers using the ROUT method ($q = 1\%$), data were checked for normality/equal variances using the Shapiro–Wilk test. For analysis of dietary intervention, a one-way ANOVA or Kruskal Wallis test was used followed by Tukey or Dunns's multiple comparison depending on the normality of data. *P*-values of less than 0.05 were considered statistically significant.

Statistical analysis of metabolomics data was carried out using Metaboanalyst 5.0 (Pang et al. 2022). Partial Least-Squares Discriminant Analysis (PLS-DA) was employed to illustrate the clustering of different metabolites across groups. Univariate Analysis was carried out by one-way ANOVA, followed by Tukey HSD. Dendrogram and heatmaps were created with Spearman and Ward. Procrustes analysis (PA), investigating the congruence of the metabolomics and microbiome data, was conducted using M2IA (Ni et al. 2020). Correlation network analysis was performed to uncover complex relationships between microbial-derived metabolites and neuronal gene expression data. Correlations were calculated using the Spearman rank-order correlation coefficient. Significant correlations ($R > 0.5$; $p < 0.05$) were used to construct a network in which nodes represent significantly modulated metabolites ($p < 0.05$) and edges represent significant correlations. The network was visualised using Omics Analyst (Zhou et al.

2021). Modules were constructed using the label propagation algorithm. Functional enrichment analysis of network clusters was performed using KEGG pathway analysis to identify overrepresented biological processes and pathways. All other correlation analyses were conducted using Spearman's rank-order correlation analysis.

4.3. Results

4.3.1. Chronic low-dose LPS exposure and Memophenol™ supplementation does not impact body weight in male C57BL/6J mice

Although body weight significantly increased over the 8-week period ($F(7, 189) = 55.67$; $P < 0.0001$), this was comparable across all experimental groups ($F(2, 27) = 0.1197$; $p = 0.89$) (Figure 4.1A). Overall body weight gain throughout the experiment did not differ between groups ($F(2, 27) = 0.6681$; $p = 0.5220$) (Figure 4.1B). There was no significant difference in mean food intake throughout the study with mice consuming on average 3.21 ± 0.18 g per day per mouse, providing the animals with 97.2 ± 5.9 mg per kg bw per day of Memophenol™. Using allometric scaling based on body surface area (Nair and Jacob 2016), this dose equates to 472.2 ± 28.5 mg per day human equivalent dose for a person of 60 kg.

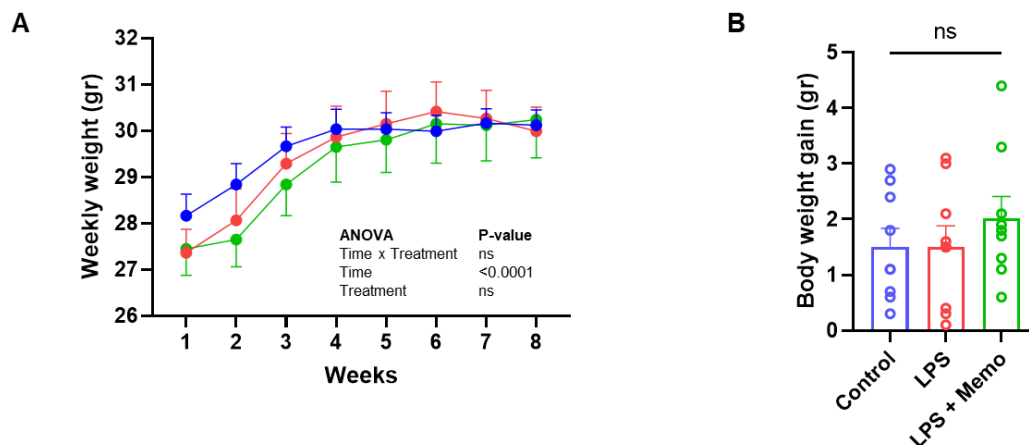


Figure 4.1: Administration of LPS (0.5 mg per kg bw per week) and LPS + Memophenol™ supplementation does not significantly impact body weight. (A) Average weekly weight of male mice from each group ($n=10$), which although increased significantly over the course of the experiment, did not significantly differ between groups. (B) The total average weight mice gained from each group during the experiment did not significantly differ ($n=10$). Error bars represent SEM. ns; no significant.

4.3.2 Chronic low-dose LPS exposure and Memophenol™ supplementation display modest shifts in intestinal microbiota and metabolism in male C57BL/6J mice

The impact of LPS and LPS + Memophenol™ on the gut microbiome was investigated using 16S rRNA sequencing of caecal samples. Alpha diversity was measured using Chao1 ($F(2, 15) = 2.16$; $p = 0.15$) and Shannon H ($F(2, 15) = 0.15$; $p = 0.86$) index and suggested no significant differences between treatment groups (Figure 4.2A). Conversely, PCoA as measured by Bray-Curtis, suggested beta diversity was significantly altered between groups (PERMANOVA F-value= 1.73; R-squared= 0.21; $p = 0.001$) (Figure 4.2B). Pairwise comparisons demonstrated this shift was most significant between control and LPS ($p = 0.005$, FDR $q = 0.015$). Conversely, the shift between LPS and LPS + Memophenol™ was more subtle ($p = 0.096$, FDR $q = 0.186$). At the genus level, seven genera were found to be significantly altered ($q < 0.05$) between treatment groups, including *Erysipelotrichaceae* ($q = 0.016$), *Muribaculum* ($q = 0.016$), *Rikenellaceae_RC9_group* ($q = 0.017$), *Butyricoccus* ($q = 0.017$), *Alistipes* ($q = 0.027$), *Lachnospiraceae_A2* ($q = 0.030$), *Desulfovibrio* ($q = 0.03$), *Muribaculaceae* ($q = 0.032$) and *Romboutsia* ($q = 0.034$) (For abundance concentrations, see Supplementary Table S4.4). *Muribaculum* abundance was significantly decreased by LPS in comparison to control. However, the abundance was partially restored by Memophenol™ supplementation (Figure 4.2C). Memophenol™ supplementation significantly increased beneficial short chain fatty acid producing bacteria *Eubacterium_brachy_group* and *Romboutsia* abundance in comparison to LPS (Figure 4.2D-E) (Mukherjee et al. 2020; Fan et al. 2024). LPS also induced significant increases in *Desulfovibrio* and the ratio of Firmicutes: Bacteroidota ($p < 0.05$) in comparison to controls (Figure 2F-G). However, Memophenol™ supplementation partially restored levels.

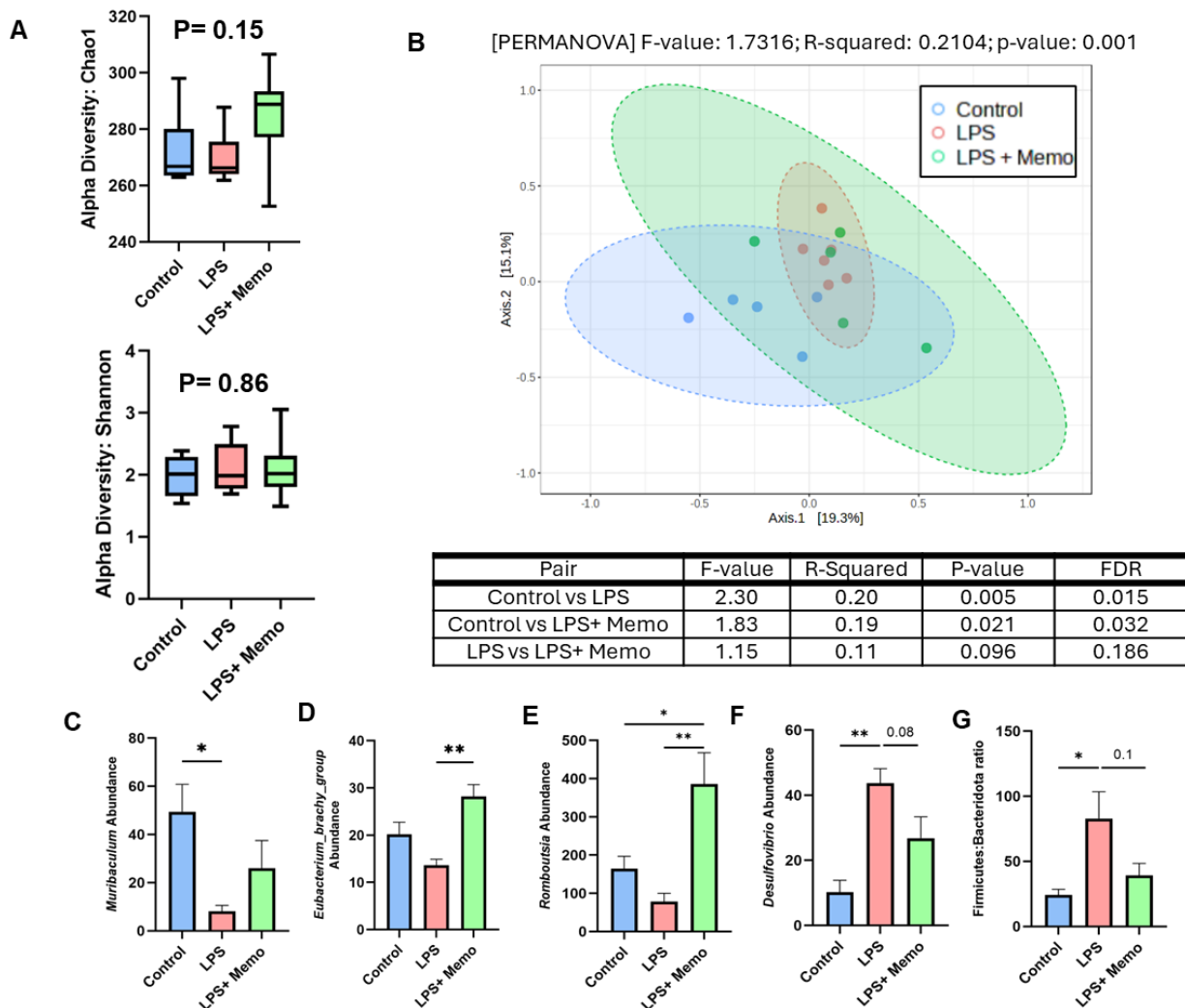


Figure 4.2: Administration of LPS and LPS + Memophenol™ altered beta, but not alpha diversity of the gut microbiome in male C57BL/6J mice. (A) Alpha diversity as measured by Chao1 and Shannon H index was not significantly modulated between groups ($n=6$). (B) Beta diversity as measured by Bray-Curtis; p-value generated from PERMANOVA and pairwise comparison ($n=6$). FDR= false discovery rate. Abundance of bacteria that are modulated by LPS and are in part restored by Memophenol™, including *Muribaculum* (C), *Eubacterium_brachy_group* (D), *Romboutsia* (E), *Desulfovibrio* (F) and Firmicutes: Bacteridota ratio (G) in control, LPS and LPS + Memophenol™ ($n=6$).

Partial Least-Squares Discriminant Analysis (PLS-DA) showed a shift in serum metabolomic profiles between the treatment groups, suggesting a change in metabolic response between control, LPS and LPS + Memophenol™ groups (Figure 4.3A). This was confirmed by hierarchical clustering highlighting relative changes in the abundance of 38 metabolites (Figure 4.3B). The concentration of four metabolites, trimethylamine N-oxide (TMAO; $F(2, 24) = 6.96$, $P = 0.004$), indoxyl sulfate (IS; F

(2, 24)= 5.12; P= 0.014), *p*-cresol sulfate (PCS; F (2, 24)= 4.68; P= 0.019) and *p*-cresol glucuronide (PCG; F (2, 24)= 5.36; P= 0.012) were significantly modulated between the three groups ($p < 0.05$). TMAO and IS were significantly increased in LPS in comparison to control. However, supplementation with Memophenol™ prevented the LPS-induced increase (Figure 4.3C). PCS and PCG were significantly decreased in LPS + Memophenol™ in comparison to LPS and PCG were also significantly decreased from controls (Figure 4.3D). Choline (F(2, 24)= 2.62; P= 0.093), indole-3-lactic acid (ILA; F(2, 24)= 5.41; P= 0.056), tryptophan (F(92, 24)= 2.90; P= 0.074) and indole-3-acetic acid (IAA; F(2, 24)= 2.85; P= 0.078) were modulated near statistical significance. A full list of serum metabolite concentrations is provided in Supplementary Table S4.5.

Spearman rank correlation analysis revealed a significant relationship between serum metabolites modulated across treatment groups ($p < 0.05$) and microbial genera (Figure 4.3E). Notably, TMAO was positively correlated with *Desulfovibrio*, a known converter of choline to TMA (Craciun and Balskus 2012), while IS was negatively correlated with *Romboutsia*, a bacterium involved in tryptophan metabolism via the kynurenine pathway (Vazquez-Medina et al. 2024) (Figure 4.3F-G). These findings aligned with Procrustes' analysis, which assessed global similarity between metabolome and microbiome datasets. Significant congruence was observed between the Control and LPS groups ($R = 0.6$, $p = 0.04$), with the LPS + Memophenol™ and LPS groups showing near-significant similarity ($R = 0.55$, $p = 0.08$) (Figure 4.4). In contrast, the Control and LPS + Memophenol™ groups were less congruent ($R = 0.46$, $p = 0.28$).

Correlation analysis between trimethylamine N-oxide (TMAO) and *Desulfovibrio*. (G) Correlation analysis between indoxyl sulfate and *Romboutsia* ($n=6$).

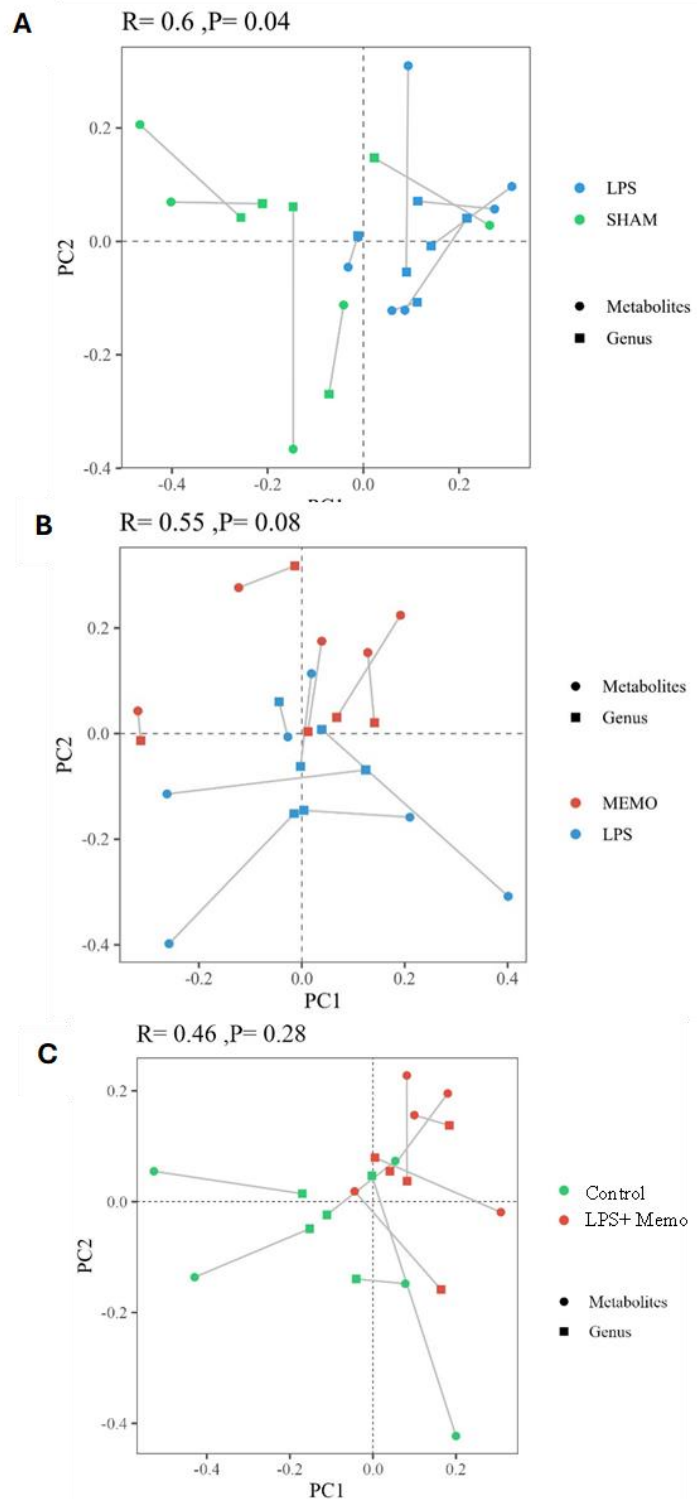


Figure 4.4: Procrustes analysis comparing to congruence of the gut microbiome and metabolome profile in male C57BL/6J mice. (A) Congruence between control SHAM and LPS, (B) LPS+ MemophenolTM and LPS and (C) control SHAM and LPS+ MemophenolTM ($n=6$).

4.3.3 Chronic low-dose LPS exposure in male C57BL/6J mice disrupts hippocampal endothelial tight junction, ZO-1, which is diminished by Memophenol™ supplementation

Blood-brain barrier (BBB) permeability is underpinned by inter-endothelial tight junctions that interact with the actin cytoskeleton and can be disrupted by chronic low-grade inflammation (Gan et al. 2023). As such, we examined the effect of the treatment groups on the key tight junction component zonula occludens-1 (ZO-1). Immunostaining revealed that in comparison with the control group, LPS disrupted the marginal localisation of ZO-1 in the hippocampus, resulting in fragmented and discontinuous ZO-1 signals endothelial tight junction, an effect not seen after treatment with Memophenol™ (Figure 4.5A). These findings consistent across multiple sections of the hippocampus within each experimental group. This was supported by a significant reduction in ZO-1 intensity in the LPS group in comparison to controls that was mitigated by the addition of Memophenol™ (Figure 4.5B) and downregulation of mRNA expression of the gene encoding the ZO-1 protein, tight junction protein 1 (*Tjp1*), under LPS in comparison to control ($p= 0.046$), which was subsequently increased by Memophenol™ ($p= 0.005$) (Figure 4.5C). Changes in *Tjp1* expression were found to negatively correlate with circulatory TMAO ($R= -0.88$; $p< 0.001$) and IS ($R= -0.45$; $p= 0.039$) concentrations (Supplementary Table S4.6). As IS and TMAO levels were significantly modulated between treatment groups, with LPS-induced increases prevented by Memophenol™ intake, these correlations were of particular interest (Figure 4.5D). Further markers of BBB permeability, including occludin ($F(2,9)= 1.20$; $p= 0.35$), annexin A1 ($F(2,9)= 2.02$; $p= 0.18$) and claudin 5 ($F(2,9)= 1.07$; $p= 0.38$), were not significantly modulated between treatment groups (Supplementary Figure S4.1).

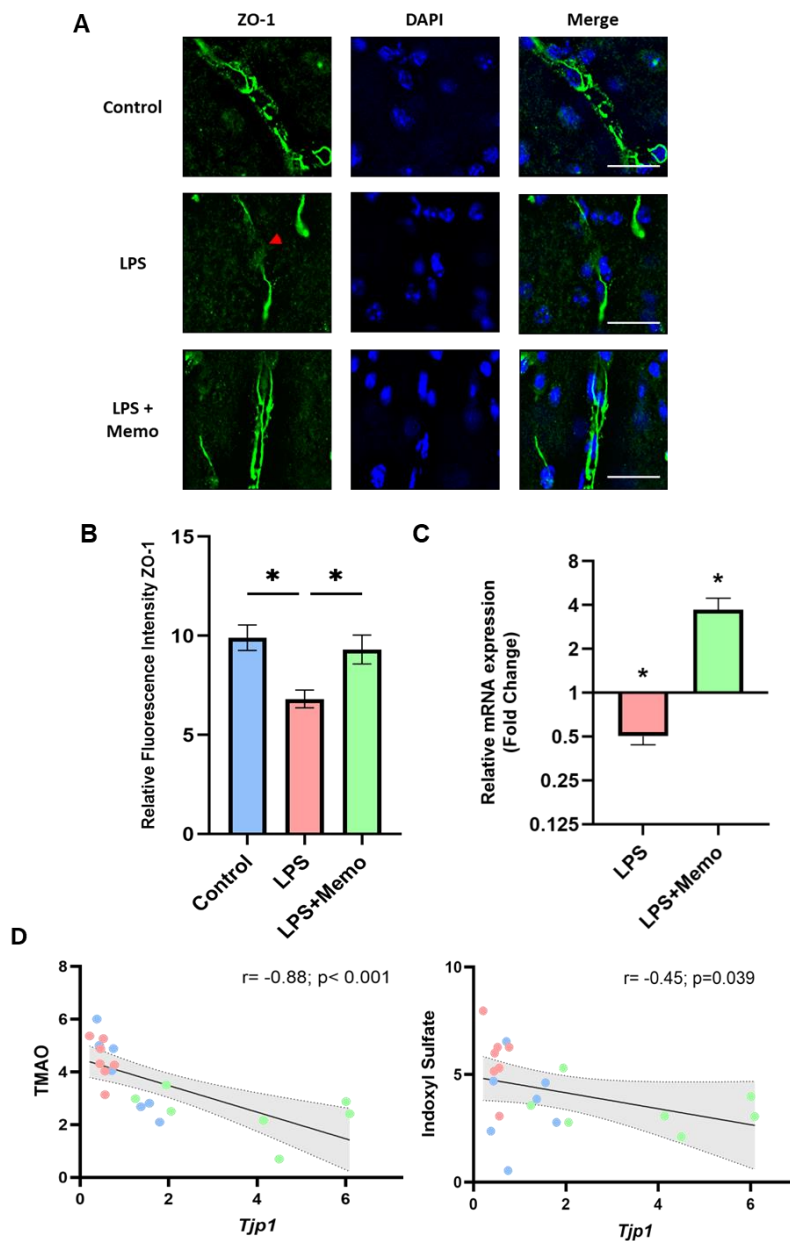


Figure 4.5: Memophenol™ recovers LPS-induced decreases in ZO-1 in the hippocampus of male C57BL/6J mice. (A) Representative images of expression of the tight junction component zona occludens-1 (ZO-1). Red arrowhead indicates an example site of ZO-1 disruption. Scale bar represents 10 μ m. Images are representative of at least four independent experiments. (B) Relative fluorescence intensity of ZO-1 images. (C) Fold change of *Tjp1* relative mRNA expression in LPS and LPS + Memophenol™ from control group ($n=6$). * = significant change from control group. (D) Correlation analysis between TMAO and indoxyl sulfate concentrations and *Tjp1* expression. Blue points represent control group, red points signify LPS and green points display LPS + Memophenol™.

4.3.4 Memophenol™ supplementation in male C57BL/6J mice prevented the LPS-induced increase in pathways of neurodegeneration in the hippocampus which was associated with changes in indoxyl sulfate

To examine the potential neuroprotective mechanisms of Memophenol™ in a model of LPS-induced low-grade inflammation, RNA sequencing analysis was conducted on the hippocampal brain region. Differentially expressed genes (DEG) were screened between pairwise comparisons of the three groups [(1) control SHAM vs. LPS, (2) control SHAM vs. LPS + Memophenol™, (3) LPS + Memophenol™ vs. LPS ($p < 0.05$)] (Figure 4.6A). A total of 2,730 genes were differentially expressed between groups, with 20 genes similarly differentially expressed between all three pairwise comparisons. Hierarchical clustering analysis displayed the expression of significant DEGs between all groups (Figure 4.6B). Correlation network analysis revealed significant associations between circulatory microbial-derived metabolites and neuronal gene expression (Figure 4.6C). Significant modulation of TMAO between groups correlated with 63 genes in the brain, including a negative correlation with 22 genes and a positive correlation with 41 genes. These genes were associated with modulation of cysteine and methionine metabolism ($p = 0.006$), selenocompound metabolism ($p = 0.037$), EGFR tyrosine kinase inhibitor resistance ($p = 0.039$), one carbon pool by folate ($p = 0.041$), maturity onset diabetes of the young ($p = 0.042$) and mannose type *O*-glycan biosynthesis ($p = 0.049$). PCG correlated with 451 genes, including 163 negatively correlated and 288 positively correlated. These genes were associated with oxidative phosphorylation ($p < 0.0001$), glutamatergic synapse ($p < 0.0001$), neurotrophin signalling ($p = 0.002$), ABC transporters ($p = 0.002$), pentose phosphate pathway ($p = 0.002$) and fructose and mannose metabolism ($p = 0.003$). PCS correlated with 268 genes, 107 were negatively correlated and 161 were positively correlated. These genes were mostly associated with pyruvate metabolism ($p = 0.002$), renin-angiotensin system ($p = 0.003$), fatty acid elongation ($p = 0.017$), neurotrophin signalling pathway ($p = 0.018$), calcium signalling pathway ($p = 0.047$) and cysteine and methionine metabolism ($p = 0.049$). IS concentrations were correlated with 52 genes, including 20 genes negatively correlated and 32 genes positively correlated. These genes were associated with hematopoietic cell lineage ($p = 0.0001$), complement and coagulation cascades ($p = 0.009$), graft-versus-host disease ($p = 0.009$), Notch signalling pathway ($p = 0.001$), D-glutamine and D-glutamate metabolism ($p = 0.01$) and pathways of neurodegeneration ($p = 0.01$). The correlation between IS and pathways of neurodegeneration was of particular interest as these genes may provide insight into the mechanisms associated with IS and the observed changes in ZO-1 expression. This pathway consisted of significant modulation of inducible nitric oxide synthase (*iNOS/Nos2*) and caspase-3 (*Casp3*), which were both upregulated by LPS in comparison to control, but the increase was prevented by Memophenol™ supplementation (Figure 4.6D). NOS2 is a known producer of nitric oxide (NO), a mediator implicated in neuroinflammatory processes and neurodegeneration (Colton et al. 2006) and caspase-3 is a critical executor of apoptosis (Brentnall et al. 2013). RNA sequencing also highlighted a significant decrease in the expression of the

ATP-binding cassette transporter subfamily G member 2 (*Abcg2*), an exporter of IS (Takada et al. 2018), under LPS challenge which was subsequently recovered by Memophenol™ supplementation (Figure 4.6E). Importantly, RNA sequencing results did not significantly differ from qPCR results on *Tjp1* expression and a randomly selected differentially expressed gene; *Slco1a4* (Supplementary Figure S4.2).

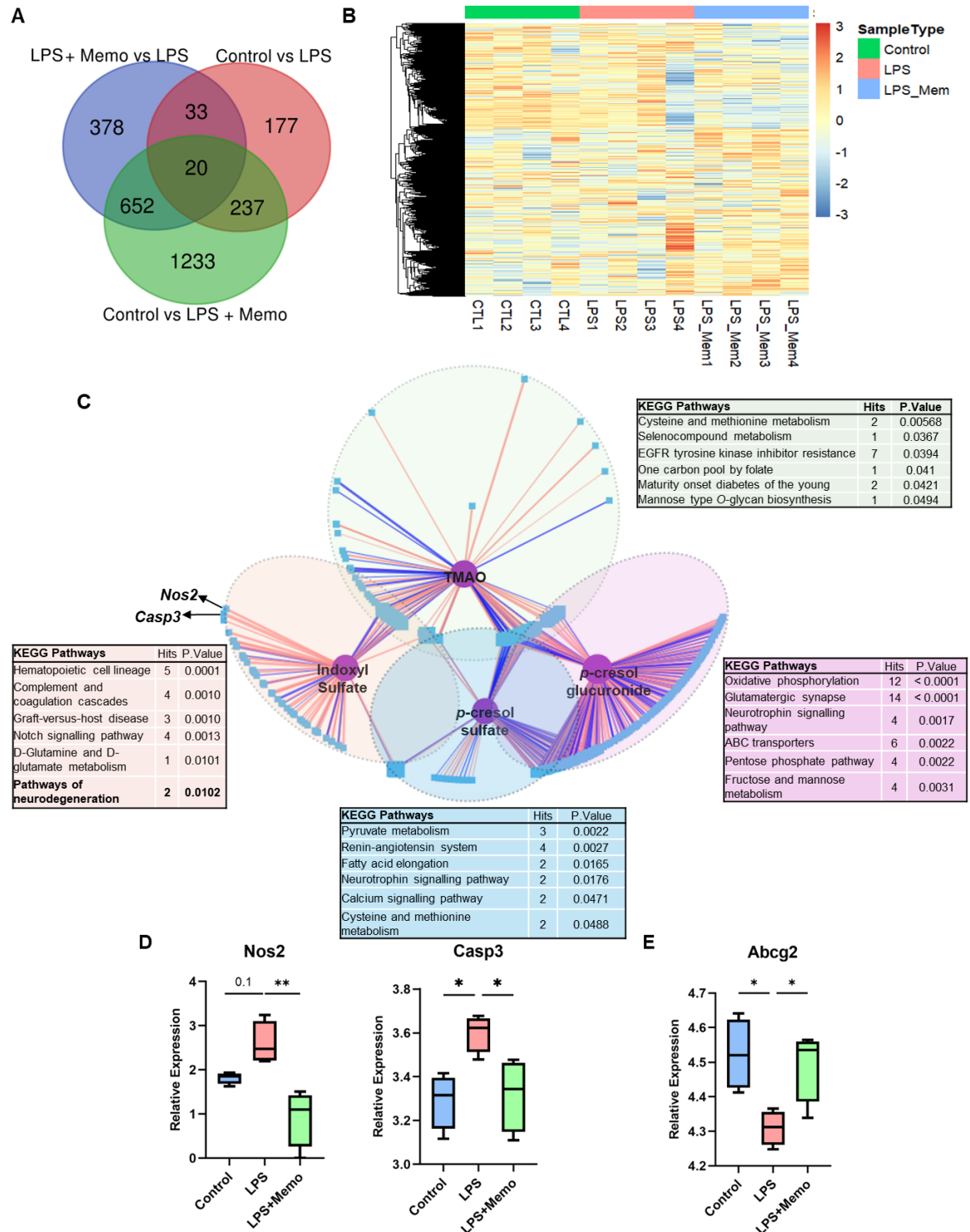


Figure 4.6: Memophenol™ alters the transcriptional profile in the hippocampus of C57BL/6J male mice. (A) Venn diagram displaying unique and overlapping significantly differentially expressed

genes between pairwise analysis of the groups (B) Heatmap displaying the expression of the differentially expressed genes between groups. (C) Correlation network analysis illustrating significant correlations ($R > 0.5$; $p < 0.05$) between modulated circulatory metabolites—indoxyl sulfate, TMAO, *p*-cresol sulfate, and *p*-cresol glucuronide, which serve as the central nodes of the networks—and differentially expressed genes ($p < 0.05$) identified through RNA sequencing analysis. Metabolites are depicted as purple circles, forming the core of the network, while genes are shown as blue square nodes. Red lines represent positive correlations, and blue lines indicate negative correlations. Correlations are clustered to form coloured nodules, which are further analysed using KEGG pathway analysis to identify significantly modulated pathways related to gene expression and metabolite changes, highlighting potential mechanistic links between specific metabolites and gene expression changes in response to experimental conditions. (D) Relative expression of *Nos2* and *Casp3* genes which represent the two genes positively correlated with indoxyl sulfate in the pathways of neurodegeneration KEGG pathway. (E) Relative abundance of the indoxyl sulfate efflux transporter, *Abcg2*.

4.4. Discussion

Diet represents one of the largest factors influencing intestinal microbiota activity, offering a promising therapeutic avenue to modulate many aspects of human health, including the CNS, via modulation of the microbiota-gut-brain axis (Moles and Otaegui 2020). Here, we investigated the effectiveness of a (poly)phenol-rich grape and blueberry extract, Memophenol™, in countering the harmful effects of chronic LPS-induced low-grade inflammation. Our results highlight a novel protective effect of Memophenol™, significantly reducing adverse effects of LPS on gut-derived uremic toxins, IS and TMAO, indicating modulation of metabolic pathways related to microbial or biosynthetic metabolism. Indeed, TMAO and IS concentrations correlated with *Desulfovibrio* and *Romboutsia* abundance, respectively. LPS also induced disruption of the endothelial tight junction protein, ZO-1. Concentrations of IS and TMAO were inversely correlated with the modulation of ZO-1 expression, with changes in IS positively associated with modulation of the neurodegeneration-related gene pathway, indicating potential protective effects within the microbiota-gut-brain axis.

16S rRNA sequencing indicated significant modulation of the gut microbiome by LPS and Memophenol™ supplementation in comparison to control. At the genus level, Memophenol™ prevented the LPS-induced decrease of *Eubacterium_brachy_group* and *Romboutsia* and partially restored the abundance of *Muribaculum*, *Desulfovibrio* and the Firmicutes: Bacteridota ratio to control level. Gut bacterial changes were associated with the modulation of circulatory microbial-derived metabolites, most notably PCS, PCG, TMAO and IS concentrations. PCS and PCG concentrations were similar in LPS and control. However, Memophenol™ supplementation alongside LPS decreased concentrations of PCS and PCG reaching significantly lower than both the LPS and control group.

These modulations negatively correlated with the abundance of *Lachnospiraceae* A2, *Butyricicoccus* and *Eubacterium brachy* bacterium, which were also significantly modulated between groups. *p*-Cresol is an exogenous uremic toxin primarily produced by the microbial conversion of tyrosine and phenylalanine in the colon. Due to its toxicity, *p*-cresol is further conjugated with sulfate or glucuronic acid by host cells such that it is almost entirely found as PCS or PCG in circulation and as such their concentrations are modulated by the gut microbiome (Liu et al. 2018a; Shah et al. 2022). Aligning with our results, (poly)phenols have previously been found to increase *Eubacterium brachy* abundances (Wang et al. 2021). *Eubacterium brachy* metabolises the *p*-cresol precursor, phenylalanine, into phenylpropionate, cinnamate and phenylacetate (Hamid et al. 1994). Therefore, Memophenol™-induced increases may enhance phenylalanine metabolism through alternative pathways, shifting away from *p*-cresol production. Unlike high concentrations of PCS, low levels are insufficient to induce detrimental effects such as vascular permeability, oxidative stress and neuroinflammation (Tang et al. 2018; Sun et al. 2020), suggesting a potential protective effect of Memophenol™.

LPS significantly increased the abundance of *Desulfovibrio*, a bacterium that converts choline to TMA (a precursor to TMAO) via the *CutC* gene cluster (Craciun and Balskus 2012). TMAO concentrations positively correlated with *Desulfovibrio* abundances suggesting a modulatory relationship between the two. Memophenol™ supplementation reduced *Desulfovibrio* in comparison to LPS ($p=0.08$), aligning with previous studies suggesting that (poly)phenols reduce the abundance of the intestinal microbiota with the *CutC* gene (Jiang et al. 2024). This reduction may play a role in decreased circulatory TMAO concentrations, which is also supported by a reduction in TMA with Memophenol™ supplementation (Supplementary Table S4.5). Of note, LPS can also upregulate the expression of flavin-containing monooxygenase 3 (FMO3) (Xiao et al. 2022), an enzyme that catalyses the oxidation of TMA into TMAO in the liver. (Poly)phenols can reduce FMO3 expression, reducing TMAO in the blood (Jiang et al. 2024). As such, modulation of TMAO may be due to changes in gut microbial or biosynthetic metabolism.

The mechanism(s) by which TMAO affects human physiology remains poorly understood. High plasma TMAO levels ($\sim 5\mu\text{M}$) may induce gut microbial dysbiosis and systemic inflammation in patients with common variable immunodeficiency (Macpherson et al. 2020) and cardiovascular diseases (Zheng and He 2022), though whether it is a cause or an effect remains unclear (Papandreou et al. 2020). While supraphysiological doses of TMAO have been associated with poor cardiovascular health, neuronal senescence, oxidative stress and mitochondrial dysfunction (Li et al. 2018a; Papandreou et al. 2020), it is improbable for TMAO to naturally reach these concentrations, even under adverse conditions. Naturally increasing TMAO levels via the consumption of TMAO-rich foods, such as fish or seafood (Wang et al. 2022), or TMAO precursors, such as the choline-rich leafy vegetables (Van Parys et al. 2022), are considered part of a healthy diet. Protective roles have been observed for TMAO in rodent models of hypertension (Huc et al. 2018), glucose homeostasis (Dumas et al. 2017), atherosclerosis

(Collins et al. 2016), non-alcoholic steatohepatitis (Zhao et al. 2019) and BBB integrity (Hoyles et al. 2021), with elevated levels acting as a compensatory mechanism to osmotic and hydrostatic stresses, processes that become elevated in inflammatory conditions such as those induced by LPS (Nakano et al. 2020). As such, it is plausible that TMAO modulation observed in LPS-induced inflammation is analogous to the increased levels of certain protective peptides, such as natriuretic peptide B, which serve as both markers of inflammatory stress and mediators of compensatory protective effects. This mechanism has been postulated to explain the strong positive correlation between TMAO and cardiovascular disease (Lundstrom and Racicot 1983; Park et al. 2022). Our results may therefore indicate that altered TMAO levels are a byproduct of metabolic deviations or an adaptive response aimed at mitigating the effects of LPS challenge. KEGG pathway analysis of TMAO-associated gene expression in the brain further emphasised processes associated with cellular homeostasis, redox balance, and protein synthesis (Waterland 2006; Stolwijk et al. 2020; Minich 2022; Jelleschitz et al. 2022), supporting the hypothesis that TMAO may play a role in buffering against inflammatory stress.

LPS was also associated with an increase in circulatory IS concentrations in comparison to control, which was mitigated by Memophenol™ supplementation. Modulation of IS was inversely correlated to the abundance of *Romboutsia*. *Romboutsia* has been associated with the functional kynB enzyme, which plays a central role within the kynurenine pathway of tryptophan metabolism (Vazquez-Medina et al. 2024). IS is formed via the indole pathway, in which tryptophan is converted to indole by gut microbiota, which is subsequently absorbed, oxidised, and sulfated in the liver to produce IS. Decreases in *Romboutsia* under LPS may highlight a reduction in tryptophan metabolism via the kynurenine pathway, increasing tryptophan availability for IS production. Indeed, circulatory tryptophan concentrations were reduced in LPS and LPS+ Memophenol™ in comparison to control. Memophenol™ supplementation significantly increased *Romboutsia*, abundance aligning with previous studies of the flavonoid-rich extract, Painong powder, in mice with colitis (Wang et al. 2022). As a uremic toxin, IS has been found to accumulate in the blood of chronic kidney disease patients and is a predictor of overall cardiovascular morbidity/ mortality (Hung et al. 2017). Renal impairment is associated with the accumulation of uremic toxins in circulation and the brain, leading to CNS dysfunction (Kelly and Rothwell 2022). IS displays pro-inflammatory effects by acting on CNS and glial cells (Adesso et al. 2017, 2018) and has been proposed as a microbiota-derived metabolic surrogate for the development of CNS diseases (Sun et al. 2021).

Under LPS challenge, the brain displayed disrupted marginal location of the endothelial tight junction ZO-1, as well as decreased ZO-1 fluorescent intensity and mRNA expression, which was recovered by Memophenol™ supplementation. LPS has previously been used as an *in vivo* model of BBB disruption in mice, increasing BBB leakage and permeability, which coincided with decreased ZO-1 mRNA and protein expression (Hoyles et al. 2021; Gan et al. 2023). The modulation of ZO-1 mRNA levels negatively correlated with TMAO and IS concentrations, suggesting that decreases in these circulatory

metabolites in the LPS+ Memophenol™ group in comparison to LPS may be associated with increased ZO-1 expression. Interestingly, TMAO has previously been found to enhance BBB integrity and protect it from the effects of inflammation (Hoyles et al. 2021).

IS also negatively correlated with ZO-1 gene expression. Due to its ability to accumulate in the brain tissue and contribute to the disruption of neuronal damage and CNS homeostasis, IS can be considered a neurotoxin (Karbowska et al. 2020), and has previously been found to disrupt BBB permeability in rodent models of chronic kidney disease (Bobot et al. 2020). When investigating the underlying mechanism between ZO-1 and IS levels, KEGG pathway analysis highlighted a significant association between IS concentrations and genes associated with neurodegeneration, including increases in *Nos2* and *Casp3*, which were restored by Memophenol™ supplementation. NOS2 (or iNOS) is the inducible isoform of the mammalian nitric oxide synthases. Excessive production of NO by iNOS in the brain can cause neurotoxicity and BBB disruption (Toda et al. 2009). Transcriptional upregulation of iNOS, as well as increased production of 3-nitrotyrosine, appears to be characteristic of BBB breakdown following cerebral trauma (Nag et al. 2001). iNOS-deficient mice also display significantly reduced disruption of the BBB following experimental bacterial induction of meningitis compared to wild-type mice (Winkler et al. 2001). IS has previously been found *in vitro* to increase the production of iNOS in astrocytes and mixed glial cells, inducing conditions of oxidative stress (Adesso et al. 2017). Caspase-3 is also involved in ZO-1 disruption during cerebral ischemia (Zehendner et al. 2011). Inducing an inflammatory response of the human brain endothelial cells (BEC) hCMEC/D3 with cytokines induced caspase-3 activation, which even at low concentrations of cytokines, led to the redistribution of ZO-1 and VE-cadherin (Lopez-Ramirez et al. 2012). Inhibitors of caspase-3, as well as caspase-9, also partially blocked cytokine-induced disruption of ZO-1 and BEC permeability. IS has previously been found to significantly increase caspase-3 expression in mononuclear blood cells (Pieniazek et al. 2023) and mesangial cells (Cheng et al. 2020). Memophenol™ also restored expression of the IS efflux transporter *Abcg2* (also known as breast cancer resistance protein, BCRP) in the brain to control levels, which was decreased under LPS challenge (Takada et al. 2018), suggesting IS may be more efficiently expelled from the brain.

Overall, our results suggest a novel neuroprotective effect of dietary Memophenol™ on the microbiota-gut-brain axis. Memophenol™ reduced concentrations of toxic microbial-derived metabolites, which was associated with moderate changes in gut microbiome composition, increased ZO-1 signalling and decreased *caspase-3* and *iNOS* gene expression. These results further highlight the interconnected nature of diet on the microbiota-gut-brain axis and brain health, providing further support for its use as a therapeutic intervention in a model of chronic low-grade inflammation.

Chapter 5: Neuroprotective Effects of a Mediterranean Diet-Inspired Supplement through the Microbiota-Gut-Brain Axis in 5xFAD Mice: Insights into Alzheimer's Disease Pathology

This chapter is formatted as a research paper, which has been submitted to Gut Microbes.

Title: Neuroprotective Effects of a Mediterranean Diet-Inspired Supplement through the Microbiota-Gut-Brain Axis in 5xFAD Mice: Insights into Alzheimer's Disease Pathology

Authors: Emily Connell, Gwénaëlle Le Gall, Simon McArthur, Leonie Lang, Marrium Liaquat, Matthew G. Pontifex, Saber Sami, Line Pourtau, David Gaudout, Michael Müller and David Vauzour

5.1 Introduction

Dementia, of which Alzheimer's disease (AD) is the most common form, is a major and growing public health concern, with an estimated 152.8 million cases predicted worldwide by 2050 (GBD 2019 Dementia Forecasting Collaborators 2022). Early therapeutic intervention during the prodromal phase, when neuropathological changes accumulate with minimal or no cognitive symptoms, has been proposed as an effective strategy to slow disease progression and delay the onset of cognitive impairment (Karran et al. 2011). Given the potential for early-stage interventions to prevent or delay AD, exploring modifiable factors such as diet has become a promising area of research.

Nutrition is a key influencer of cognitive function and can delay or ameliorate neurodegenerative disease progression (Trichopoulou et al. 2003; Dangour et al. 2010; Lefèvre-Arbogast et al. 2022; Puri et al. 2023). One proposed mechanism linking dietary intake to neuronal health and AD is through the modulation of the extensive bidirectional relationship between the gut microbiome and the brain known as the microbiota-gut-brain axis (Mohajeri 2019; Chakrabarti et al. 2022; Williams et al. 2024). Indeed, microbial fermentation of dietary bioactives in the gut produces numerous soluble metabolites that have been shown to exert anti-inflammatory and protective effects upon the blood-brain barrier (BBB) and the microglia, key actors in neurodegenerative disease (Schneider et al. 2024). Importantly, both these defences are known to be impaired early in the pathogenesis of AD, hence we hypothesise that strategies to promote their function may have considerable therapeutic benefit.

Mediterranean diet adherence, composed of a high intake of fruits, vegetables, olive oil, whole grains and unsaturated fatty acids, moderate intake of fish and restricted consumption of red meats (Trichopoulou et al. 2003), has been reported to improve cognitive function (Zbeida et al. 2014; Loughrey et al. 2017; Coelho-Júnior et al. 2021) and slow age-related cognitive decline (Tsivgoulis et al. 2013; Devranis et al. 2023). Potential mechanisms underlying the protective effects of the Mediterranean diet include a combination of anti-inflammatory, antioxidant, improved vascular health

and microbiome-modulating properties (Tuttolomondo et al. 2019; Merra et al. 2020; Barbouti and Goulas 2021). Given the growing evidence that the Mediterranean diet can influence gut microbiome composition (Merra et al. 2020), we hypothesised these effects may be related to the response of the microbiota-gut-brain axis.

Here, we explore the effects of consumption of a novel blend of bioactives commonly found in the Mediterranean diet, named 'Neurosyn240' thereafter, on the microbiota-gut-brain axis in male and female 5xFAD mice, determining its potential as an early preventative dietary intervention to delay AD progression. Our study investigates changes within the gut microbiome, serum metabolome, behaviour and brain, including microglia density and amyloid deposits in the hippocampus. As all of these components within the microbiota-gut-brain axis are found to be modulated by genotype between wild-type and 5xFAD mice without dietary effects, wild-type mice have not been included in this study (Forner et al. 2021; Dunham et al. 2022; Pandey et al. 2024; Pádua et al. 2024). Our study focuses on the prodromal stage of AD in this model, a critical period before cognitive symptoms appear, but when metabolic changes may influence future cognitive decline. This stage represents a key window for implementing nutritional strategies to slow disease progression. Beneficial effects of the Mediterranean diet have been shown to be sexually dimorphic, with greater protection against AD observed in women (Gregory et al. 2022; Pontifex et al. 2024b). However, most characterisation studies using 5xFAD mice either overlook sex-specific differences (Oakley et al. 2006) or including only one sex (Eimer and Vassar 2013), which might have significant consequences when translating the findings to humans. To address these shortcomings, the current study assessed changes in the microbiota-gut-brain axis and neuropathology in the prodromal stages of decline in both male and female 5xFAD mice (up to 5 months of age) (AlzBiomaker Database 2019).

5.2 Material and Methods

5.2.1 Study approvals

All experimental procedures and protocols performed were reviewed and approved by the Animal Welfare and Ethical Review Body (AWERB) and were conducted in accordance with the specifications of the United Kingdom Animal Scientific Procedures Act, 1986 (Amendment Regulations 2012). Reporting of the study outcomes complies with the ARRIVE (Animal Research: Reporting of In Vivo Experiments) guidelines (Sert et al. 2020).

5.2.2 Experimental procedure

5xFAD mice with a C57Bl/6 background overexpress human APP with three FAD mutations [the Swedish (K670N, M671L), Florida (I716V), and London (V717I) mutations] and human PSEN1 with

two FAD mutations (M146L and L286V) (Oblak et al. 2021). Mice display early-onset amyloid pathology including intraneuronal amyloid beta (A β) at 1.5 months, plaque deposition in the subiculum and cortex deep layers at 2 months, neuronal loss in the subiculum and cortical layer V at 9 months (Oakley et al. 2006) and hippocampal-dependent cognitive deficits from 6 to 13 months of age (Uddin et al. 2021; Poon et al. 2023). 16 males and 16 females 5xFAD mice (6 weeks old) sourced from Jackson Laboratories (Bar Harbor, US) were maintained in individually ventilated cages (n=4 per cage), in a controlled environment (21 \pm 2°C; 12h light/dark cycle; light from 7:00 AM) and fed *ad libitum* on a standard diet (RM3-P; Special Diet Services (SDS, Horley UK) for 2 weeks ensuring normal development and stabilisation of the microbiota (Laukens et al. 2016). After this time mice were transferred onto one of two diets, namely control (AIN93-M) or a Neurosyn240 supplemented diet for 12 weeks. The Neurosyn240 diet comprises of the background control diet (AIN93-M) supplemented with 2,157 mg/kg diet of Neurosyn240 (Activ'Inside, Beychac-et-Caillau, France). Neurosyn240 is a proprietary (patent pending) standardised blend of Memophenol™, a unique formula of French Grape (*Vitis vinifera* L.) and North-American Wild Blueberry (*Vaccinium angustifolium* A.) extract (patent WO/2017/072219), saffron extract (patent WO/2018/020013), green tea extract, olive leaf extract, trans-resveratrol, zinc, vitamins B5, B9, B12, C, D3 & E (comprising 15% of vitamins and mineral reference value), polyphenols (mainly flavan-3-ol monomers \geq 10% and resveratrol \geq 1%) and crocins carotenoids (mainly trans-4-galloyl-gallate, trans-3-galloyl-galocatechin, cis-4-galloyl-gallate, trans-2-galloyl) \geq 500 ppm as previously described (Pontifex et al. 2024a). The dietary fibre content of this mix is at trace amounts and therefore is unlikely to exert an effect upon either the gut microbes or host systems. Diets were prepared by Research Diets Inc. (New Brunswick, USA) to comply with animal nutrition requirements. At the end of the experiments, 5-month-old animals were anaesthetised with a mixture of isoflurane (1.5%) in nitrous oxide (70%) and oxygen (30%) and transcardially perfused with ice-cold saline containing 10 UI/ml heparin (Sigma-Aldrich, UK). Cardiac blood was allowed to clot for 30 mins on ice before sera were isolated via centrifugation at 4,000 x g for 10 min. Brains were rapidly removed, halved, snap frozen and stored at -80°C until biochemical analysis.

5.2.3 Behavioural assessment

All behavioural tests were performed at the experimental endpoint after the 12-week intervention, with mice remaining on the control or Neurosyn240 diet during the testing period. Prior to commencing, a visual placing test was performed on each mouse to ensure animals were not visually impaired (Pinto and Enroth-Cugell 2000). All behavioural tests were analysed using the Ethovision software (Tracksys Ltd, Nottingham, UK).

The Open Field (OF) task, a measure of anxiety-related behaviour (Tucker and McCabe 2021), was conducted as described previously (Yu et al. 2012). Mice were individually placed within the (50 cm × 50 cm × 50 cm) cubed arena illuminated with dim lighting (100 lux) and allowed to move freely for 10 minutes. They were tracked using Ethovision software, which determined travel distance, velocity, and time spent in the centre/periphery of the maze, respectively.

The novel object recognition (NOR) task, a measure of recognition memory, was conducted as previously described (Davis et al. 2013; Leger et al. 2013). All experiments were carried out under dim lighting conditions (100 lux). Briefly, on day 1 (habituation), mice were placed into an empty arena (50 cm × 50 cm × 50 cm) for 10 minutes. On day 2, mice were conditioned to two identical objects for 10 minutes. Half of the mice were conditioned with two identical golf balls and the other half with two green plastic toy bricks (4x4x6 cm). Following an inter-trial interval of one hour, mice were placed back within the testing arena now containing one familiar object and one novel object, with the position of the novel object (left or right) being randomised between each mouse and group tested. Mice conditioned with the golf balls had the plastic toy brick placed as the novel object and vice versa. Videos were analysed for a 5-minute period. If the mice did not accumulate a total of 8 seconds of object exploration within this time, the analysis continued for up to 10 minutes or until 8 seconds of exploration was reached. Mice not achieving 8 seconds of exploration were excluded from the analysis (Denninger et al. 2018). Discrimination index (DI) was calculated as follows $DI = (TN - TF)/(TN + TF)$, where TN is the time spent exploring the novel object and TF is the time spent exploring the familiar object.

The Y-maze spontaneous alternation test, a measure of spatial working memory, was conducted as previously described (Pontifex et al. 2021a). Ethovision software analysed each mouse for 7 minutes recording zone transitioning and locomotor activity. Spontaneous alternation, defined as the tendency of rodents to explore a new arm of the maze rather than returning to one previously visited, reflecting their working memory, was calculated using the formula: (number of alternations/max number of alternations × 100).

The Barnes maze, as previously described (Gawel et al. 2019), was performed with slight modifications to assess spatial retrieval memory. Briefly, the maze consisted of a brightly illuminated (800 lux lighting) circular platform (92 cm diameter), with 20 evenly distributed holes located around the circumference and visual cues (4 simple shapes) placed at the periphery. The experiment was conducted over a 5-day period. On day 1 (habituation) mice were placed into the centre of the maze for 2 minutes and were able to explore freely. If the mouse did not find the escape box within this time

frame the mouse was guided to it after which they remained in the box for a further 2 minutes. Following habituation each mouse was tested/trained on their ability to locate the escape box on days 1–4 with three trials per day. On day 5, a probe test was conducted, the maze was rotated 90°, the escape box was removed, and mice were placed in the centre of the maze in which they were free to navigate for 1 minute. Percentage time in the correct quadrant was determined using Ethovision software.

5.2.4. Microbial 16S rRNA extraction and amplicon sequencing

Microbial DNA was isolated from approximately 50 mg of caecum content using a FastDNA SPIN Kit for Soil (MP Biomedicals) as previously described in Section 2.2.2.

Alpha diversity was assessed using Chao1 and Shannon H diversity indices whilst beta diversity was assessed using Bray–Curtis. Statistical significance was determined by the Wilcoxon rank-sum test (Mann–Whitney-U) or a permutational multivariate analysis of variance (PERMANOVA).

5.2.5 LC-MS/MS

LC-MS/MS was conducted on serum samples (80 µL) as described in Section 2.2.3

5.2.6 Immunofluorescent staining

Coronal brain cryosections (20 µm) were processed from snap-frozen hemi-brain samples. Cryosections were mounted onto glass slides before being fixed in 4% formaldehyde in 0.1M PBS for 15 minutes. To detect amyloid deposits, tissue sections were incubated in 1% thioflavin S aqueous solution (Sigma-Aldrich) for 8 minutes. Sections were further washed twice in 80% ethanol, once in 95% ethanol and thrice in distilled water prior to mounting with Mowiol mounting medium and storage at -20°C.

To detect the microglial marker protein, Iba-1, sections were incubated for 30 min at room temperature in 10% normal goat serum (NGS) containing 0.05% Triton X-100 to permeabilise cells and block nonspecific secondary antibody binding. Sections were then incubated for 1 hour at room temperature in a rabbit anti-mouse Iba-1 polyclonal antibody (Synaptic Systems) diluted 1/1000 in 1% NGS containing 0.05% Triton X-100. Sections were further washed in 1% NGS and incubated for 1 hour with an AF555-conjugated goat anti-rabbit IgG secondary antibody (diluted 1/500) and washed twice in PBS. 4',6-diamidino-2-phenylindole (DAPI) was used as a counterstain to visualise cell nuclei. Tissue samples were mounted in an aqueous medium, Mowiol, dried and stored at -20°C.

Images of the hippocampus were collected for the analysis of amyloid deposit pathology and Iba-1 positive microglia using a Direct Fluorescence Leica Ctr 5000 Microscope at x10 magnification. The

hippocampus was chosen as it is a key brain region critically involved in learning, memory, and spatial navigation, and it is one of the earliest and most severely affected areas in AD (Rao et al. 2022).

Amyloid deposits were quantified by manually counting thioflavin S-positive plaques within the hippocampal region of each section using Fiji software (NIH, Washington, DC, USA). The number of amyloid deposits per section was recorded, and the average was calculated across six sections per mouse, collected in a 1-in-4 series. Microglia were quantified by manually counting Iba-1-positive cells within a randomly selected 200 μm^2 region of interest (ROI) in the hippocampus. The average number of microglia per ROI was determined across all sections, using the same 1-in-4 series approach.

5.2.6 RNA isolation and RNA sequencing

Total RNA was isolated from hippocampi ($n=3$ randomly selected per group and sex) using the Qiazol reagent (Qiagen, UK), as previously described in Section 4.2.6. Data was analysed using the DESeq2 package in R (version 4.3.2) to investigate the effects of diet and sex on gene expression. Raw count data were filtered to remove low-abundance genes, retaining those with a minimum count of 5 in at least 15% of the samples. Genes with less than 15% variance were excluded. A generalised linear model (GLM) assessed the main effects of diet and sex. Differential expression was tested for each factor, which captures differential responses to diet between sexes. P-values were adjusted using the Benjamini-Hochberg method to control the false discovery rate (FDR). Enrichr was used to perform Gene Ontology (GO) analysis of differentially expressed genes (DEGs) (Kuleshov et al. 2016; Liu et al. 2023).

5.2.7 Statistical analysis

Data analysis was performed in GraphPad Prism version 9.5.1 (GraphPad Software, CA, USA). All values are presented as means \pm standard error of the means (SEM) unless otherwise stated. Outlier detection was performed using the Robust Regression and Outlier Removal (ROUT) method with a false discovery rate (q) of 1% to identify potential extreme values in metabolite, microbiome, hippocampal amyloid deposit and Iba1 positive microglia. Data were checked for normality using the Shapiro–Wilk test. Analyses were conducted using two-way ANOVA with Tukey *post-hoc* analysis when appropriate to correct for multiple comparisons. Weekly body weights for all mice were analysed using repeated measured ANOVA to assess the effects of diet, sex, and time, as well as their interactions on body weight. Partial Least Squares Discriminant Analysis (PLS-DA) was employed to illustrate the clustering of different metabolites across groups using Metaboanalyst 5.0 (Pang et al. 2022). Dendrogram and heatmaps were created using Spearman's rank correlation for distance

measurement and Ward's method for hierarchical clustering. Procrustes analysis (PA), investigating the congruence of the metabolomics and microbiome data, was conducted using M2IA (Ni et al. 2020). All other correlation analyses were conducted using Spearman's rank-order correlation analysis. P values of less than 0.05 were considered statistically significant.

5.3 Results

5.3.1 Neurosyn240 supplementation does not affect body weight or food intake in both male and female mice

Whilst body weight increased over the 12-week intervention for both males and females, animals receiving Neurosyn240 supplementation did not significantly differ from the control group of the same sex (Figure 5.1A). A main effect of sex was detectable upon body weight ($F(1, 28) = 40.4$; $p < 0.0001$), but neither diet ($F(1, 28) = 1.16$; $p = 0.29$) nor the interaction between sex and diet ($F(1, 28) = 0.05$; $p = 0.82$) reached statistical significance (Figure 5.1B). There were also no significant differences in food intake throughout the study with both males and females consuming on average 2.9 ± 0.3 g per animal, per day, providing an average of 208 ± 21 mg/kg BW/day of Neurosyn240. Using allometric scaling based on body surface area (Nair and Jacob 2016), this dose equates to 1.18 ± 0.1 g/day human equivalent dose for a person of 70 kg.

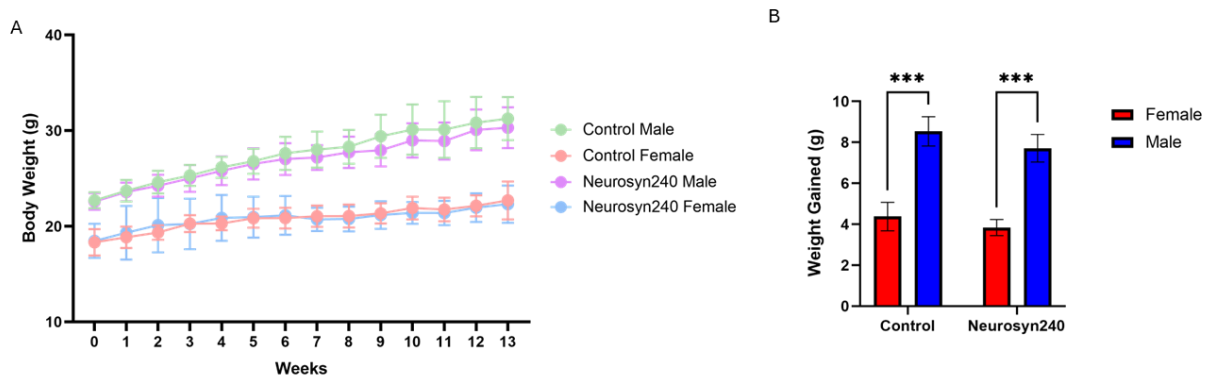


Figure 5.1: Supplementation of the Neurosyn240 diet for 12 weeks showed no significant difference in body weight to the control diet in both male and female 5xFAD mice. (A) weekly average body weight of males and females on the Neurosyn240 and control diet ($n = 8$ per sex per group). (B) Total weight gained by males and females on the control and Neurosyn240 diet over the course of the 12-week intervention ($n = 8$ per sex per group). Error bars represent SEM.

5.3.2 The Neurosyn240 containing diet does not significantly modulate cognitive decline in male and female 5xFAD mice

After 12 weeks of dietary intervention, cognitive performance was assessed in 5-month-old 5xFAD mice. There was a near significant effect of diet on time spent in the centre of the open field test as a measure of anxiety ($F(1, 27)= 4.09$; $p= 0.06$; Figure 5.2A), but no significant effect of distance travelled in the open field ($F(1,27)= 0.04$; $p= 0.83$; Figure 5.2B), or performance on the Y-maze ($F(1,27)= 2.9$; $p= 0.10$; Figure 5.2C), novel object recognition tests ($F(1,27)= 0.097$; $p= 0.76$; Figure 2D) or Barnes maze ($F(1,27)= 0.078$; $p= 0.78$; Figure 5.2E). No significant effects of sex were seen in the open field assessment on time spent in the centre ($F(1,27)= 0.90$; $p= 0.35$) or distance travelled in the open field ($F(1,27)= 2$; $p= 0.16$), as well as Y-maze ($F(1,27)= 0.79$; $p= 0.38$), novel object recognition ($F(1,27)= 0.0001$; $p= 0.99$) and Barnes maze ($F(1,27)= 0.028$; $p= 0.87$). No significant differences in interactions between diet and sex were detected in the behavioural measures.

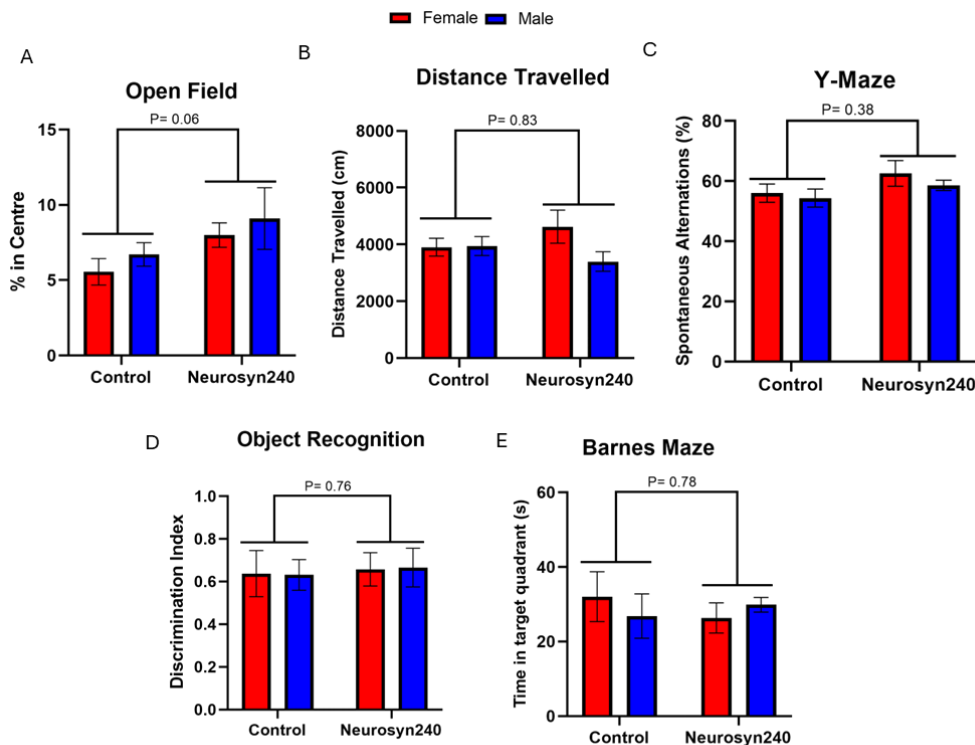


Figure 5.2: Neurosyn240 diet did not significantly alter hippocampal-dependent behavioural measures in male and female 5xFAD mice. (A) Percentage of time spent in the centre of the open field area in males and females consuming control and Neurosyn240 diet. (B) Distance travelled by mice during open field assessment. (C) Performance of mice on Y-maze measured by spontaneous alternation. (D) Performance of mice on novel object recognition assessment as measured by the discrimination index. (E) Percentage of time spent in the target quadrant on day 5 of the Barnes maze test. ($n= 8$ per sex per group). All p-values represent the main effect of diet on behavioural assessments.

5.3.3 Neurosyn240 diet significantly modulates the intestinal microbiota of male and female 5xFAD mice

The impact of Neurosyn240 on microbial composition was investigated by 16S rRNA sequencing. Alpha diversity, as measured by the Chao1 index, was not significantly affected by sex ($F(1,27)= 0.21$; $p= 0.65$), or diet ($F(1,27)= 0.53$; $p= 0.47$), nor was there an interaction between sex and diet ($F(1,27)= 0.21$; $p= 0.65$). Shannon H index displayed near significant effects of sex ($F(1,27)= 0.03$; $p= 0.06$), and diet ($F(1,27)= 3.87$; $p= 0.059$), but no significant interaction term ($F(1, 27)= 0.75$); $p= 0.39$) (Figure 5.3A). Principal coordinates of analysis (PCoA) highlighted significant differences in beta diversity metrics (PERMANOVA $F= 3.15$; $R^2= 0.26$; $p= 0.001$) between males and females in both control and Neurosyn240 groups (Figure 5.3B). Pairwise comparisons suggested both males ($F= 4.39$; $R^2 = 0.24$; FDR $q= 0.018$) and females ($F= 1.98$; $R^2= 0.13$; FDR $q= 0.09$) had significant differences in beta diversity with the consumption of Neurosyn240 ($P_{FDR}<0.1$) (Supplementary Table S5.1). At the genus level, linear discrimination analysis (LDA) effect size (LEfSe) revealed significant differences in 16 genera between groups (FDR $q< 0.05$; Supplementary Figure S5.1). Of these bacterium, a main effect of diet was detected in *Lactococcus* ($F(1,27)= 6.67$; $p= 0.016$), *Limosilactobacillus* ($F(1,27)= 12.12$; $p= 0.002$), *Marvinbryantia* ($F(1,27)= 17.22$; $p<0.001$), *Parvibacter* ($F(1,27)= 25.52$; $p<0.001$), *Romboutsia* ($F(1,27)= 12.69$; $p= 0.001$), *Sporosarcina* ($F(1,27)= 10.88$; $p= 0.003$), *Turicibacter* ($F(1,27)= 4.30$; $p= 0.048$), *Eubacterium_fissicatena_group* ($F(1,27)= 8.77$; $p= 0.006$), *Bifidobacterium* ($F(1,27)= 4.26$; $p= 0.049$), *Bifidobacterium* ($F(1,27)= 4.25$; $p= 0.049$) and *Dubosiella* ($F(1,27)= 13.14$; $p= 0.001$) (Figure 5.3C; Supplementary Table S5.2 for all genera abundances). Eight genera were significantly influenced by the main effect of sex, including *Lactococcus* ($F(1,27)= 4.28$; $p= 0.048$), *Limosilactobacillus* ($F(1,27) = 12.12$, $p = 0.0017$), *Marvinbryantia* ($F(1,27) = 7.407$, $p = 0.011$), *Sporosarcina* ($F(1,27) = 10.170$, $p = 0.004$), *Turibacter* ($F(1,27) = 15.22$, $p = 0.001$), *Enterococcus* ($F(1,27) = 6.766$, $p = 0.015$), *Enterorhabdus* ($F(1,27) = 5.444$, $p = 0.027$), and *Acetatifactor* ($F(1,27) = 6.77$, $p = 0.015$). Significant interaction effects were observed for *Lactococcus* ($F(1,27) = 5.43$, $p = 0.028$), *Limosilactobacillus* ($F(1,27) = 12.34$, $p = 0.0016$), *Enterococcus* ($F(1,27) = 7.008$, $p = 0.013$), *Marvinbryantia* ($F(1,27) = 8.424$, $p = 0.007$), *Romboutsia* ($F(1,27) = 4.163$, $p = 0.051$), *Sporosarcina* ($F(1,27) = 13.940$, $p = 0.001$) and *Turicibacter* ($F(1,27) = 4.296$, $p = 0.048$).

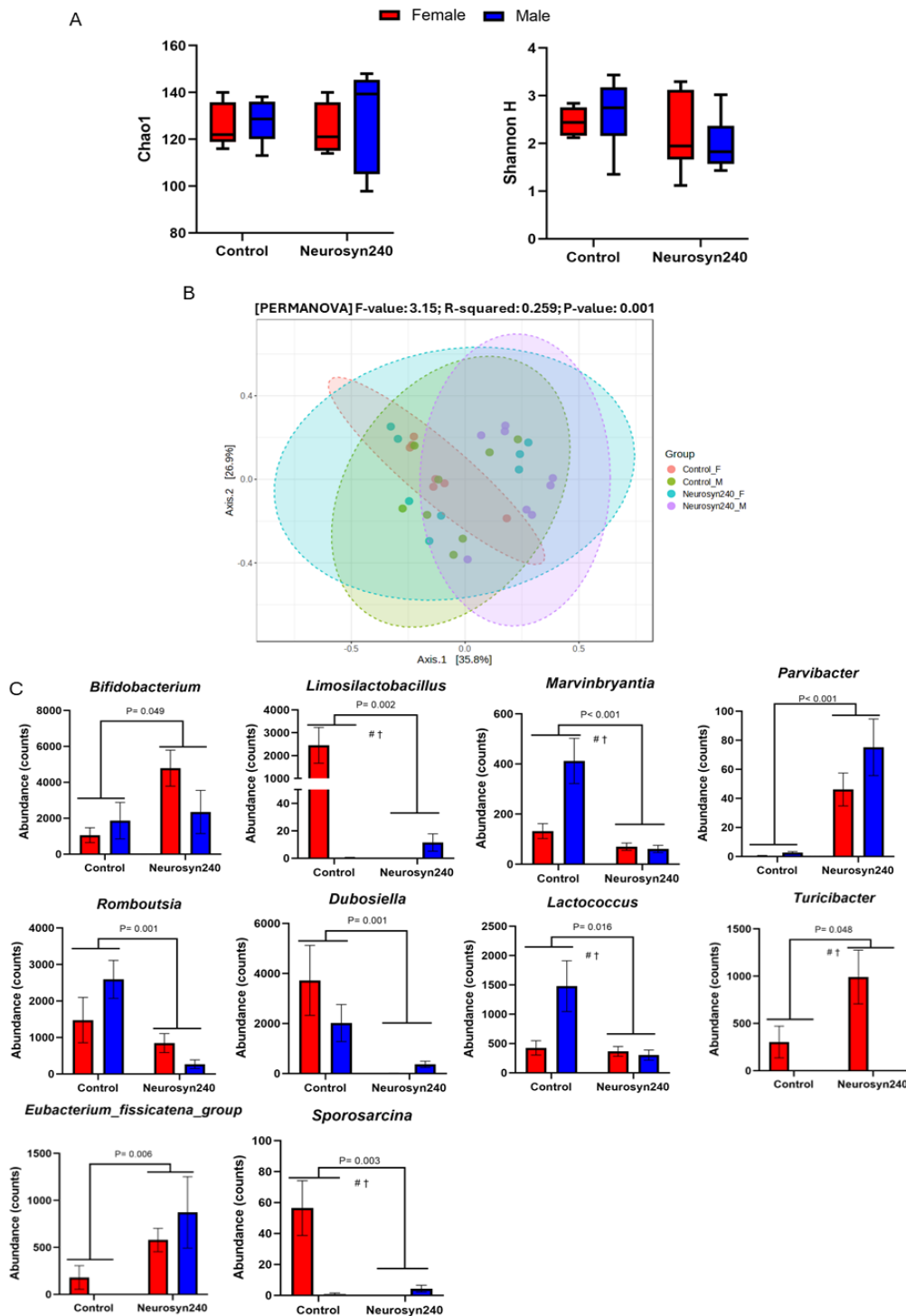


Figure 5.3: Neurosyn240 diet altered beta, but not alpha diversity of the gut microbiome in 5xFAD mice. (A) Alpha diversity as measured by Chao1 and Shannon H index was not significantly modulated by the main effect of diet, sex or their interaction. (B) Beta diversity as measured by Bray-Curtis; p-value generated from PERMANOVA. (C) Abundance of microbiome genera significantly affected by the main effect of diet ($p < 0.05$). P-value indicates the statistical significance of the main effect of diet. # denotes a significant main effect of sex. † indicates a significant interaction between sex and diet ($p < 0.05$). $n = 8$ per sex per group.

5.3.4 Sex Differences in the Modulation of Circulatory Microbial-Derived Metabolism by Neurosyn240 are Related to the Gut Microbiome

Targeted metabolomic profiling of serum samples was conducted to gain insight into possible shifts in the production of bioactive metabolites associated with cognitive health. PLS-DA showed a shift in metabolic response to the Neurosyn240 diet in both males and females (Figure 5.4A). This was further supported by heatmap analysis, which demonstrated alterations in the relative abundance of 33 metabolites in response to the Neurosyn240 diet compared to the control in males and females (Figure 5.4B). Seven metabolites were significantly impacted by the main effect of diet, including serotonin ($F(1, 27) = 13.14$; $p = 0.001$; Figure 5.4C), kynurenine ($F(1,27) = 6.46$; $p = 0.018$; Figure 5.4D), taurocholic acid (TCA; $F(1, 24) = 11.44$; $p = 0.002$; Figure 5.4E), hyodeoxycholic acid (HDCA; $F(1, 27) = 4.51$; $p = 0.044$; Figure 5.4F), taurodeoxycholic acid (TDCA; $F(1, 27) = 5.65$; $p = 0.025$; Figure 5.4G), chenodeoxycholic acid (CDCA; $F(1, 27) = 8.41$; $p = 0.008$; Figure 5.4H) and lithocholic acid (LCA; $F(1, 27) = 11.11$; $p = 0.003$; Figure 5.4I). See Supplementary Table S5.3 for all metabolite concentrations. To assess the relationship between dietary modulation of the gut microbiome and the circulatory metabolome, Spearman rank correlation analysis was performed on metabolites and microbiota genera modulated by the main effect diet ($p < 0.05$). This analysis revealed a significant correlation between the peripheral metabolome and the gut microbiome (Figure 5.4J). Procrustes analysis was conducted to evaluate the congruence of the two datasets. Significant similarities were observed between males ($R = 0.69$; $p < 0.001$; Figure 5.5A) and females ($R = 0.64$; $p < 0.001$; Figure 5.5B) on control and Neurosyn240 diet, suggesting similarity between microbiome and metabolome profiles.

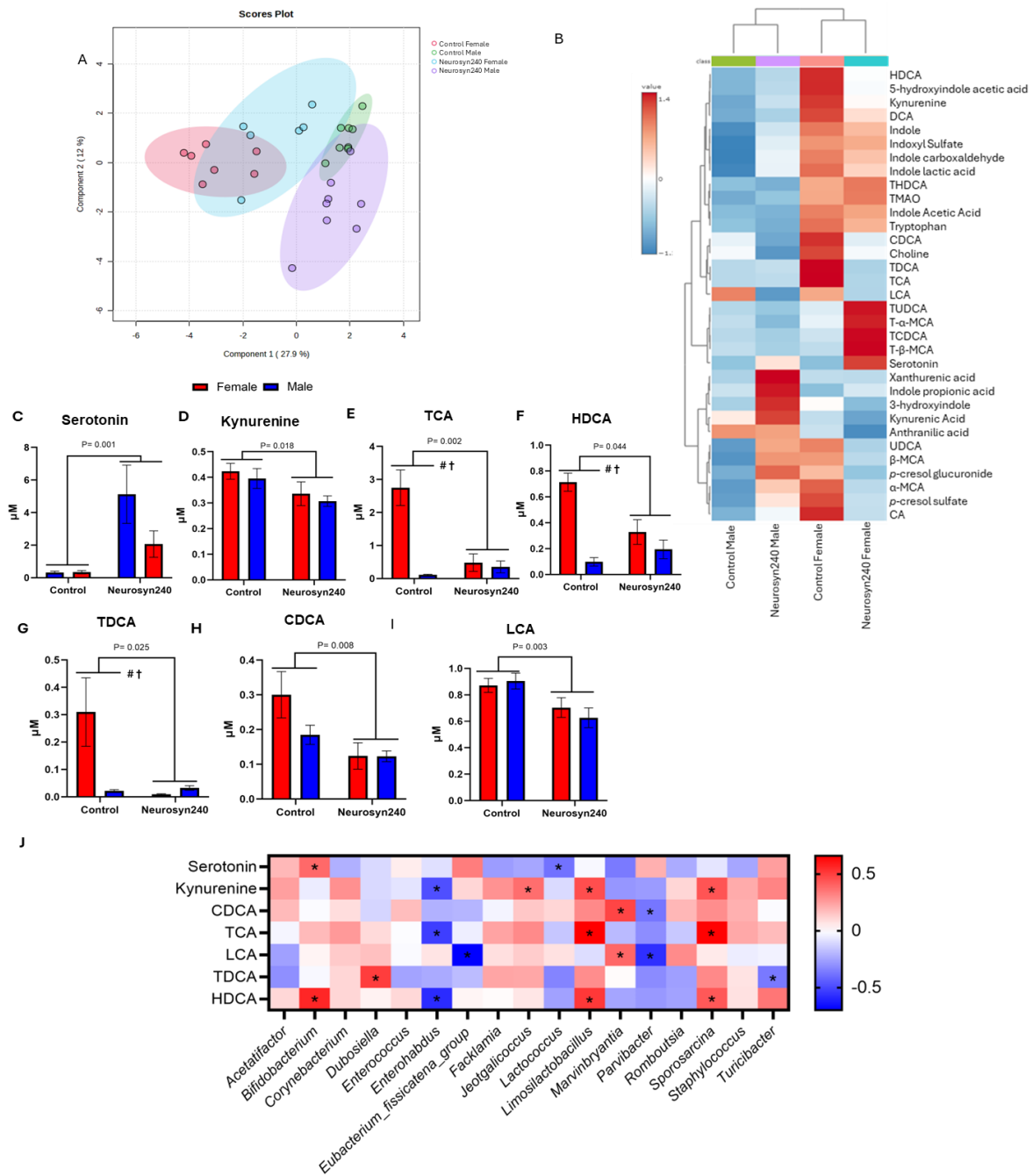


Figure 5.4: Neurosyn240 significantly modulated the circulatory metabolome profile in male and female 5xFAD mice which correlated with changes in the gut microbiome composition. (A) Partial least squares-discriminant analysis (PLS-DA) plot of the metabolomic profiles in both males and females ($n = 8$ per sex per group). (B) Heatmap displaying changes in concentrations of metabolites between the groups. (C-I) Concentrations of microbial-derived metabolites significantly modulated by the main effect of diet. P-value indicates the statistical significance of the main effect of diet. # denotes a significant main effect of sex. † indicates a significant interaction between sex and diet ($p < 0.05$). (J) Spearman rank correlation analysis between significantly modulated metabolites by diet and gut microbiome genera (FDR $q < 0.05$).

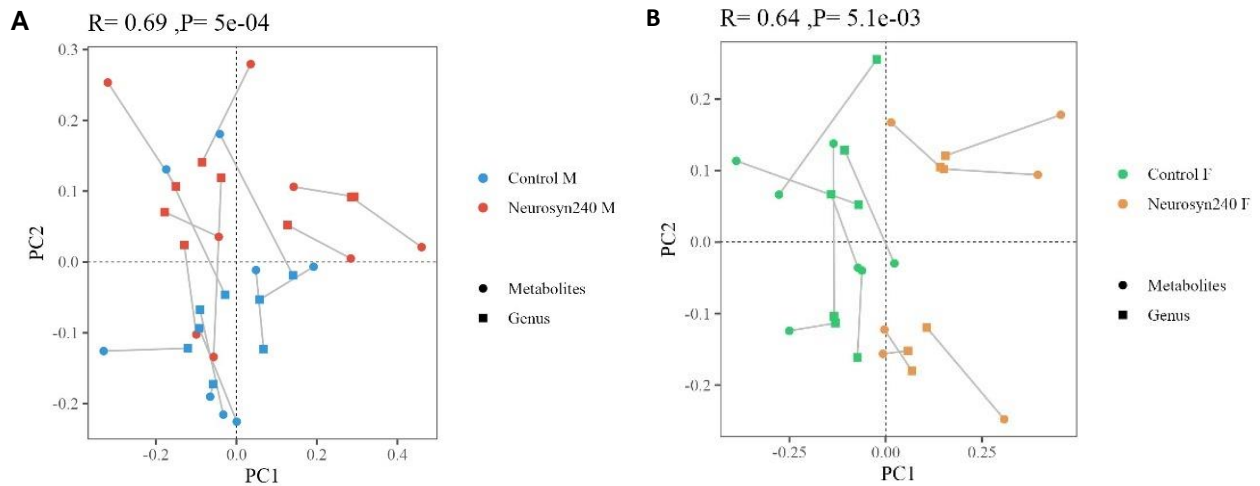


Figure 5.5: Procrustes analysis of the congruence of serum metabolite and microbiome profiles. (A) Congruence between males ($n = 8$ per group). (B) Congruence between females ($n = 8$ per group)

A main effect of sex was observed on numerous serum tryptophan-related metabolites, including tryptophan ($F(1,27) = 35.07$; $p < 0.001$), 5-hydroxyindole-acetic acid (5HIAA; $F(1, 27) = 11.93$; $p = 0.002$), anthranilic acid ($F(1,27) = 10.43$; $p = 0.004$), kynurenic acid ($F(1,27) = 5.20$; $p = 0.031$), indole acetic acid (IAA; $F(1,27) = 89.41$; $p < 0.001$), indole-3-lactic acid (ILA; $F(1,27) = 10.12$; $p = 0.004$), indole-3- carboxaldehyde (I3A; $F(1,27) = 8.69$; $p = 0.007$), indole ($F(1,27) = 12.72$; $p = 0.002$), indoxyl sulfate ($F(1,27) = 10.28$; $p = 0.004$) (Supplementary Figure S5.2). Trimethylamine-N-oxide (TMAO; $F(1,27) = 23.92$; $p < 0.001$), THDCA; ($F(1,24) = 7.14$; $p = 0.013$), cholic acid (CA; $F(1,27) = 7.01$; $p = 0.014$), HDCA ($F(1,27) = 30.39$; $p < 0.001$), DCA; $F(1,27) = 32.58$; $p < 0.001$), TCA ($F(1,27) = 21.24$; $p < 0.001$) and TDCA ($F(1,27) = 4.74$; $p = 0.039$) were also significantly influenced by sex (Supplementary Table S5.3). A significant interaction between sex and diet was observed in 5HIAA ($F(1,27) = 5.52$; $p = 0.027$), *p*-cresol sulfate ($F(1,27) = 9.18$; $p = 0.006$), *p*-cresol glucuronide ($F(1,27) = 26.31$; $p < 0.001$), alpha-muricholic acid (α -MCA; $F(1,27) = 5.14$; $p = 0.032$), CA ($F(1,27) = 12.44$; $p = 0.002$), ursodeoxycholic acid (UDCA; $F(1,27) = 5.42$; $p = 0.028$), HDCA ($F(1,27) = 12.47$; $p = 0.002$), DCA ($F(1,27) = 6.47$; $p = 0.018$), TCA ($F(1,27) = 17.51$; $p = 0.003$) and TDCA ($F(1,27) = 6.52$; $p = 0.017$) (Supplementary Table S5.3).

5.3.5 Male and female 5xFAD mice fed a Neurosyn240 diet showed reduced amyloid-beta plaque load and microglia in the hippocampus

In the hippocampus, there was a significant effect of diet on the percentage area of amyloid deposits ($F(1,27) = 4.33$; $p = 0.048$; Figure 5.6A) and a near significant effect of diet on the number of amyloid deposits ($F(1,27) = 3.68$; $p = 0.06$; Figure 5.6B-C). However, there was no effect of sex on the percentage of amyloid deposits ($F(1,27) = 2.20$; $p = 0.15$) or number of amyloid deposits ($F(1,27) = 1.06$; $p = 0.31$).

Similarly, no interaction was observed between sex and diet on the percentage area of amyloid deposits ($F(1,27)= 0.83$; $p= 0.37$) or number of amyloid deposits ($F(1,27)= 0.35$; $p= 0.56$). Given the absence of a significant main effect of sex or interaction between sex and diet, correlation analysis was conducted on all mice as a single group to examine the relationship between metabolites significantly modulated by diet ($p<0.05$) and amyloid deposits (Supplementary Figure S5.3). A significant positive association was found between serum LCA concentrations and the number of amyloid deposits in mice ($r = 0.39$; $p = 0.04$), suggesting that these changes may be linked to metabolite levels (Figure 5.6D).

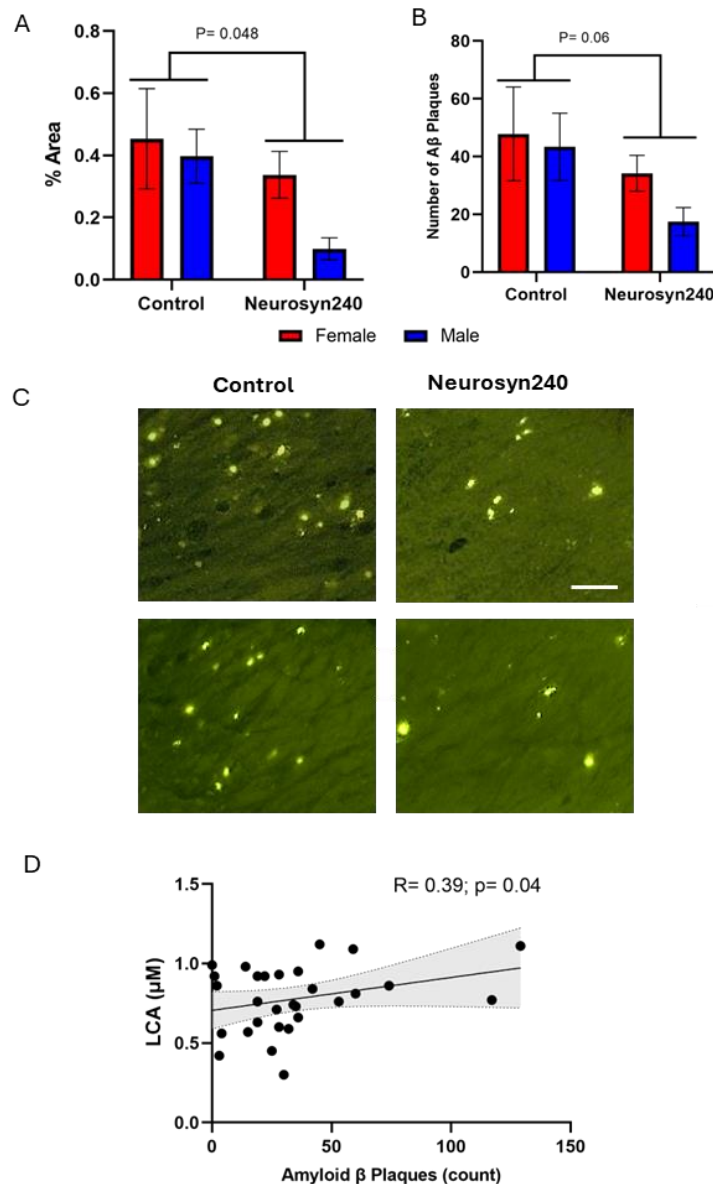


Figure 5.6: Male and female 5xFAD mice consuming a Neurosyn240 diet have reduced amyloid deposits in the hippocampus. (A) The main effect of diet significantly reduced the average percentage of the hippocampal area filled with amyloid. (B) The main effect of diet showed a trend towards significance on the number of amyloid deposits within the hippocampus. Bars represent average per section, with six sections recorded per mouse taken at 1 in 4 intervals. Error bars represent

SEM. (C) Representative images of the hippocampus of control and Neurosyn240 mice at x10 magnification. Scale bar represents 100 μ M. (D) Spearman rank correlation between circulatory LCA concentrations and the number of amyloid deposits in the hippocampus. $n=8$ per sex per group.

In the hippocampus, a significant main effect of diet was observed on the number of Iba-1 positive microglia ($F(1,27)=8.55$; $p=0.007$; Figure 5.7A-B), but no effect of sex ($F(1,27)=1.31$; $p=0.26$) or interaction between sex and diet ($F(1,27)=2.20$; $p=0.15$). Due to the absence of a significant effect of sex or interaction between sex and diet, correlation analysis was conducted on all mice as a single group focusing on metabolites significantly modulated by the main effect of diet to explore potential metabolite-microglia associations (Supplementary Figure 5.3). The number of hippocampal Iba-1 positive microglia negatively correlated with circulatory serotonin concentrations ($r=-0.38$; $p=0.045$) suggesting a possible gut-brain interaction (Figure 5.7C).

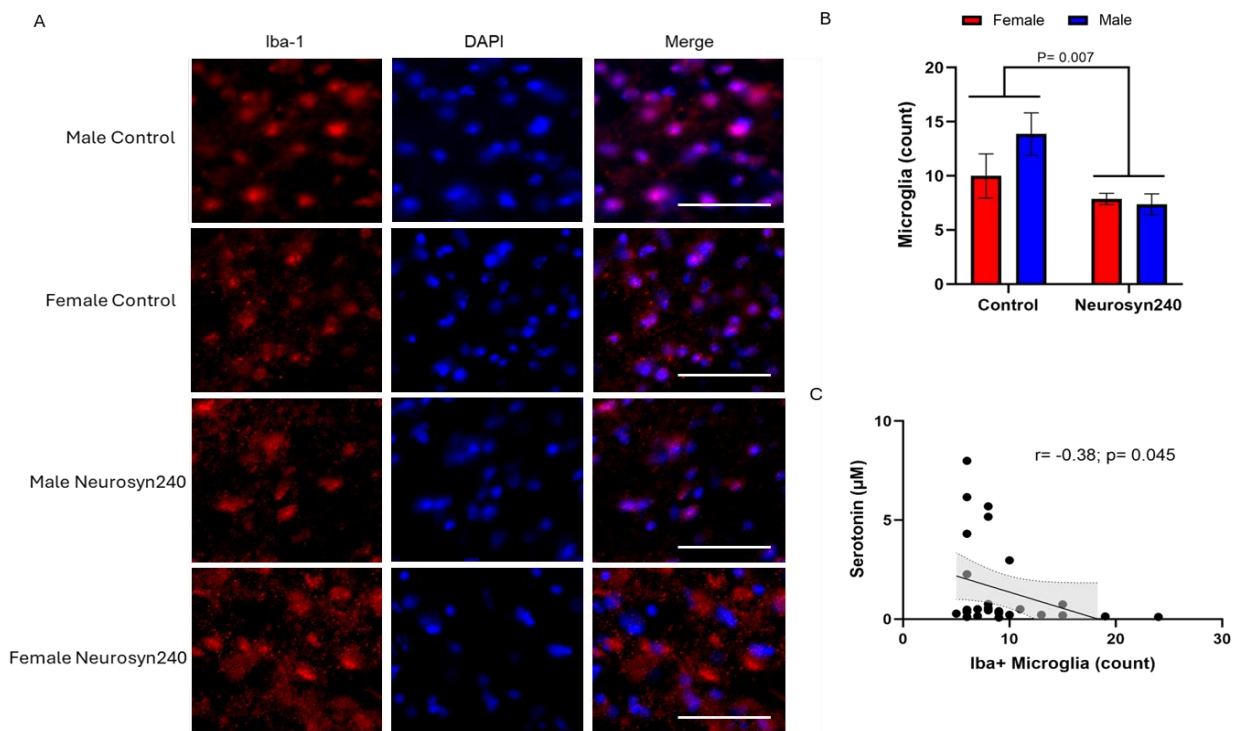


Figure 5.7: Male and female 5xFAD mice consuming a Neurosyn240 diet have reduced Iba-1 positive microglia in the hippocampus. (A) Representative images of Iba-1 positive microglia in the hippocampus of control and Neurosyn240 mice at x10 magnification. Scale bar represents 100 μ M. (B) Average number of Iba-1 positive microglia per section within a random 200 μ m² region of interest (ROI) within the hippocampus by sex and treatment groups ($n=8$ per sex per group). Six sections were taken per mouse at 1 in 4 intervals in the hippocampal region. P-value represents the statistical significance of the main effect of diet. Bars represent SEM. (C) Spearman rank correlation between circulatory serotonin concentrations and Iba-1 positive microglia in 5xFAD mice ($n=8$ per sex per group).

5.3.6 Neurosyn240 differently affects hippocampal gene expression in male and female 5xFAD mice

To examine the potential neuroprotective mechanisms of Neurosyn240, RNA sequencing analysis was conducted on the hippocampal brain region, a region significantly affected by AD (Kim et al. 2019). Using DESeq2 analysis, we identified 47 DEGs that were upregulated and 77 genes that were downregulated by the main effect of diet (Figure 5.8A). Additionally, 7 genes were upregulated, and 7 genes were downregulated by the main effect of sex. Hierarchical clustering analysis displayed the expression of significant DEGs (Figure 5.8B). GO analysis highlighted the functional properties of DEGs. The Neurosyn240 diet upregulated processes related to neuronal health, including positive regulation of biosynthetic processes (GO:0009891) and dopaminergic neuron differentiation (GO:0071542), critical for maintaining neuronal function, particularly as dopamine neuronal loss is observed in AD patients and 5xFAD mice, and can contribute to memory dysfunction (Figure 5.8C) (Nobili et al. 2017; Vorobyov et al. 2019). Additionally, pathways related to calcium-mediated signalling (GO:0019722, GO:0035584) and protein localisation to cell junctions (GO:1902414) were significantly upregulated, suggesting synaptic signalling and cellular communication may be improved ($P_{FDR} < 0.1$). Several key inflammatory and immune-related pathways were downregulated by Neurosyn240 consumption ($p < 0.05$). Notably, NF-kappaB signalling (GO:1901224), a central regulator of inflammation, along with pathways involved in the positive regulation of cytokine production (GO:1900017), were downregulated, including interleukin-6 production (GO:0032675). However, it should be noted these pathways did not reach significance at an FDR adjusted $q < 0.05$.

GO analysis revealed sexually dimorphic effects on histone modifications and signalling pathways (Figure 5.8D). Females showed upregulation of H3-K4 and histone lysine methylation, downregulation of histone lysine demethylation, and reduced androgen and steroid hormone receptor signalling compared to males, aligning with previous studies (Goldstein et al. 2001; Singh et al. 2019).

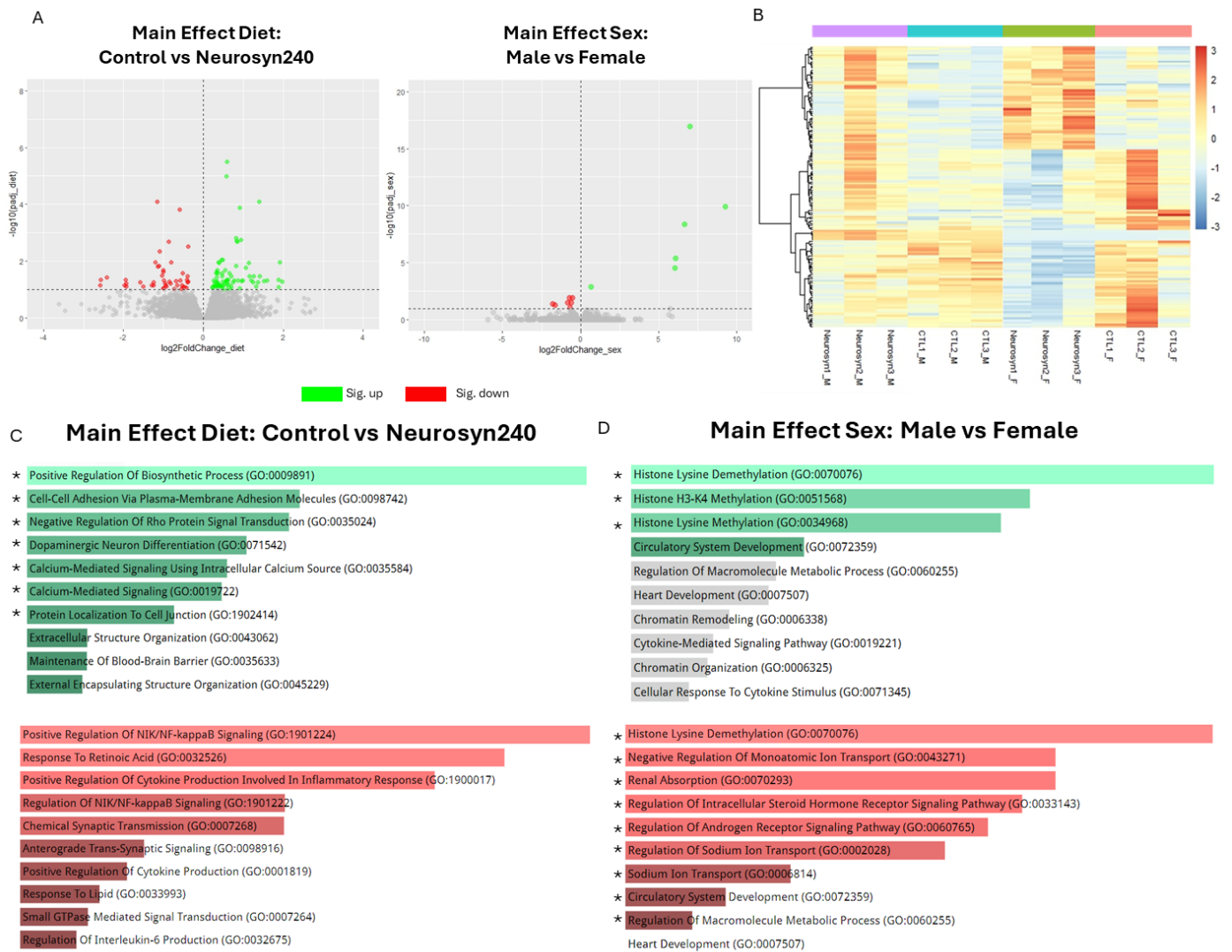


Figure 5.8: Neurosyn240 significantly modulated gene expression within the hippocampus of male and female 5xFAD mice. (A) Volcano plot displaying differentially expressed genes between males (left) and females (right) consuming control and Neurosyn240 diet. (B) Heatmap displaying the expression of the differentially expressed genes between treatment groups. (C) Gene Ontology pathway analysis of genes significantly upregulated (green) and downregulated (red) by the main effect of diet. (D) Gene Ontology analysis of genes significantly upregulated (green) and downregulated (red) by the main effect of sex. Red or green pathway colour indicates $p < 0.05$. Grey pathway indicates $p > 0.05$. * = FDR adjusted $q < 0.05$. $n = 3$ per sex per group.

To investigate potential pathways underlying hippocampal reductions in amyloid deposits, gene expression results were compared to a curated set of 155 genes associated with amyloid beta formation, binding, and clearance, identifying those consistently present across two functional genome databases (Ashburner et al. 2000; The Gene Ontology Consortium et al. 2023; Baldarelli et al. 2024). DESeq2 GLM analysis showed that the Neurosyn240 significantly ($P_{FDR} < 0.1$) upregulated expression

of genes associated with amyloid beta binding (*Clu*; $P_{FDR} = 0.051$), clearance (*Lrp2*; $P_{FDR} = 0.045$) and cellular response (*Vcam1*; $P_{FDR} = 0.027$), while downregulating the amyloid binding gene *Ager* $P_{FDR} = 0.07$ (Table 5.1; Supplementary Table S5.4 for full list of gene expression). No genes associated with amyloid beta formation, binding or clearance were significantly modulated by the main effect of sex (Supplementary Table S5.5). Correlating genes and circulatory metabolites significantly modulated by the main effect of diet highlighted a negative correlation between *Lrp2* and LCA concentrations ($r = -0.60$; $p = 0.041$; Figure 5.9), suggesting a potential link between the metabolome and the brain.

Table 5.1: Amyloid-associated gene expression modulated by the main effect of diet (Control vs Neurosyn240)

EntrezID	Gene	Description	Category	Log ₂ FC	Adjusted P-value
22329	<i>Vcam1</i>	vascular cellular adhesion molecule 1	cellular response to amyloid-beta	0.51	0.027
14725	<i>Lrp2</i>	low-density lipoprotein receptor-related protein 1	amyloid-beta clearance	1.73	0.045
12759	<i>Clu</i>	clusterin	amyloid-beta binding	0.85	0.051
11596	<i>Ager</i>	advanced glycosylation end product-specific receptor	amyloid-beta binding	-1.32	0.077

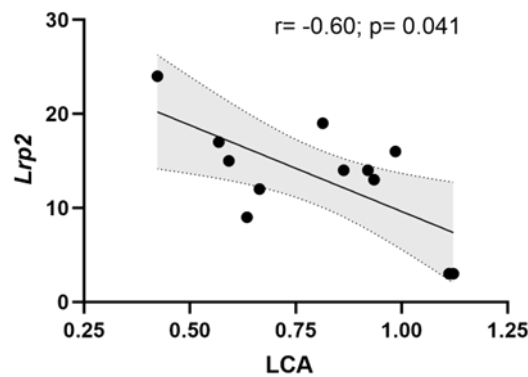


Figure 5.9: Correlation analysis between *Lrp2* expression and LCA in both control and Neurosyn240 males and females. $n=3$ per sex per group.

5.4 Discussion

The bioactive constituents of a Mediterranean-style diet are well-recognised for their neuroprotective properties (Féart et al. 2010). However, the mechanisms through which they may slow or reduce AD pathology are currently unclear. Using the 5xFAD mouse model of AD, we evaluated the protective effects of a Mediterranean diet-inspired bioactive blend, Neurosyn240, on modulating metabolite

communication within the microbiota-gut-brain axis in both sexes during the prodromal stage of decline (Manji et al. 2019; Keszycki et al. 2023; Pádua et al. 2024). Our results highlight novel protective effects of Neurosyn240 in mitigating early AD-related neuropathology in 5xFAD mice. Neurosyn240 consumption over twelve weeks significantly shifted the gut microbiome profile, which was associated with the modulation of the circulatory microbial-derived metabolome, including increased serotonin and reduced LCA levels. These changes were associated with a reduction in hippocampal Iba-1 positive microglia and amyloid deposits, respectively.

The 5xFAD model typically exhibits hippocampal-dependent cognitive deficits from 6 months of age (Poon et al. 2023), with some studies reporting only mild deficits as late as 13 months (Uddin et al. 2021). At 5 months, a prodromal stage of AD in this model (Poon et al. 2023), no significant difference in cognitive behaviour was present between the control and Neurosyn240 diet groups. However, both males and females showed trends towards reduced anxiety-related behaviour in the open field assessment following Neurosyn240 treatment. Given that anxiety is an early sign of AD, preceding cognitive decline (Johansson et al. 2020), these findings may suggest effects on early disease manifestations. In parallel with these behavioural trends, amyloid deposits in the hippocampus were also reduced with Neurosyn240 intake, indicating that while behavioural differences are subtle at this stage, there are early effects on amyloid pathology. This suggests that the diet may be influencing early disease processes before pronounced cognitive deficits emerge. Consistent with previous research in 5xFAD mice (Forner et al. 2021), no significant sex differences were detected across behavioural assessments.

Metabolite-mediated communication within the microbiota-gut-brain axis may contribute to the protective effects associated with the constituents of the Mediterranean diet (Merra et al. 2020). Neurosyn240 significantly reduced concentrations of TCA, HDCA and LCA; bile acids which are typically considered cytotoxic and are elevated in AD patients (Baloni et al. 2020). The bile salt hydrolase (BSH)-capable *Limosilactobacillus* (Kumar et al. 2013; Song et al. 2023), which can deconjugate bile acids, showed a positive correlation with reductions in TCA and HDCA. *Dubosiella*, a bacterium with 7- α -dehydroxylation capability to convert primary bile acids into secondary bile acids (Ojeda et al. 2023), was also significantly decreased with Neurosyn240 consumption and correlated with reductions in TDCA. The correlation between these microbial changes and metabolite levels suggests that gut microbiome modulation may play a critical role in the observed metabolic shifts. Increases in the beneficial microbe, *Parvibacter*, by Neurosyn240 inversely correlated with LCA concentrations. *Parvibacter* abundance, which can be increased by vitamin intake (Rajoka et al. 2021), upregulates the *baiA* gene, enhancing the metabolism of LCA to the less toxic form, 3-oxo-5 β -cholanate (Wang et al. 2024). Given that LCA can accumulate in the brain of AD patients due to increased serum levels and is associated with cognitive decline (Baloni et al. 2020), these reductions

induced by Neurosyn240 may offer neuroprotective benefits.

Reductions in LCA were associated with decreased amyloid deposits in the hippocampus, suggesting a possible connection between the peripheral metabolome and the brain. Hippocampal RNA sequencing revealed upregulation of A β clearance-related genes, including *Lrp2* and *Clu*, in mice receiving Neurosyn240. LRP2, a key A β transporter at the BBB, plays a critical role in clearing A β from the brain through binding with CLU (Nelson et al. 2017). LCA can strongly inhibit LRP2 expression *in vitro* (Erranz et al. 2004) via the activation of the vitamin D receptor (VDR) (Chapron et al. 2018), suggesting that the observed reductions in LCA may enhance the expression of LRP2, facilitating the clearance of A β from the brain. These findings align with evidence linking Mediterranean diet adherence to reduced A β accumulation via interactions with genes such as *Clu* (Radd-Vagenas et al. 2018; Rainey-Smith et al. 2018).

Neurosyn240 increased peripheral serotonin levels in comparison to controls. With approximately 95% of serotonin located in the periphery through tryptophan metabolism, its dysregulation is considered an early sign of Alzheimer's disease (see Chapter 2). AD patients often have reduced serum serotonin levels (Whiley et al. 2021) and exhibit dysregulated tryptophan metabolism (Pais et al. 2023), which can exacerbate inflammation (Liu et al. 2017; Metaxas et al. 2019; Willette et al. 2021). Thus, elevated circulatory serotonin from Neurosyn240 may help mitigate these effects. Notably, increased serotonin levels may be associated with the abundance of *Bifidobacterium*, which positively correlated with serotonin concentrations. Strains of *Bifidobacterium*, such as *Bifidobacterium dentium*, secrete products such as acetate that stimulate serotonin release from enterochromaffin cells, increasing circulatory concentrations (Engevik et al. 2021).

Neurosyn240 intake significantly reduced the number of hippocampal Iba-1 positive microglia. Phenolic components of the Mediterranean diet have previously been associated with mitigating microglial responses in the brain (Hornedo-Ortega et al. 2018). However, the specific mechanisms are poorly understood. Reductions in amyloid deposits in the hippocampus may decrease microglial activation, as these cells often respond to amyloid accumulation and can promote inflammation. Peripheral serotonin concentrations inversely correlated with the number of Iba-1 positive microglia. Serotonin is a potent immune modulator through receptors expressed on immune cells, inhibiting pro-inflammatory cytokine production, including tumour necrosis factor- α (TNF- α) and interleukin-1 β (IL-1 β) (Arreola et al. 2015). Microglial cells, as resident macrophage-like cells of the central nervous system, respond to signals from the peripheral immune system and induce neuroinflammation through the activation of pro-inflammatory cytokines (Hong et al. 2016). In AD, neuroinflammation plays a critical role in pathogenesis by increasing microglial cell and astrocyte activation. Dysregulation of the serotonergic system in AD patients can influence neuroinflammation, and immune system and

microglial activation (Neshan et al. 2020). As such, Neurosyn240-induced modulation of *Bifidobacterium*, serotonin, and Iba-1 microglia may play a neuroprotective role.

Overall, our results indicate novel interactions between a Mediterranean diet-inspired supplement and a neuroprotective response against early AD-associated pathology. This protective effect appears to be associated with metabolite-driven pathways of the microbiota-gut-brain axis. These findings enhance our understanding of how dietary components can influence brain health and support the potential benefits of therapeutic interventions during the prodromal stage of AD.

Chapter 6: General discussion

Main Findings

Pathophysiological progression of AD is apparent up to 20 years prior to clinical symptom onset, making it vital for research to focus on uncovering novel early risk factors and interventions to identify at-risk individuals and slow disease progression. However, despite decades of research, the mechanisms contributing to AD progression are still unclear and likely multifactorial. AD progression is associated with significant gut dysbiosis. Such dysregulation has been associated with an increase in inflammatory markers, cytokines and the permeability of the gut epithelial barrier ('leaky gut'), modulating the concentrations of bioactive metabolites released into circulation (see Chapter 1). As these metabolites can directly and indirectly influence the brain, their modulation provides a less explored mechanistic pathway for cognitive decline, warranting further exploration.

The findings of this thesis present new insights into the early progression of cognitive decline and dementia, signifying a major role for the gut in connection to the brain through the modulation of key microbial-derived metabolites. Metabolic alterations contain rich systemic information on the underlying physiology connecting the periphery to the CNS, affecting numerous pathways simultaneously. Since these compounds are derived from the diet, modulating these metabolites through nutritional strategies provides a theoretically cost-effective and straightforward approach to slow disease progression. As such, this thesis provides a composite assessment of the metabolites most recently associated with cognitive health in the current literature (TMAO, bile acids, tryptophan, *p*-cresol and their derivatives) as early risk factors of AD, as well as exploring their interaction with dietary patterns to influence cognitive health and AD; a previously under-researched area in the field.

6.1 Microbial-derived metabolites are associated with prodromal AD progression and form a novel composite risk factor for the early detection of AD

Over the last 20 years, research has sought to elucidate the complex mechanisms connecting the gut and the brain (Needham et al. 2020). As outlined in Chapter 1, this interaction can be mediated by bioactive signalling molecules derived from the gut metabolism of dietary compounds. However, while previous studies have connected individual metabolites, such as TMAO, tryptophan, bile acids, and *p*-cresol, in cognitive decline and accelerated AD progression, these metabolites have not been collectively examined as a composite risk factor. In Chapter 2, we address this gap by providing significant support for the link between metabolic perturbations, derived from both dietary and microbial metabolism, and prodromal AD progression through the quantification of gut microbiome profiles and 32 dietary and microbial-derived metabolites in 150 participants ranging from cognitively

healthy to SCI to MCI. To our knowledge, this analysis was the first to quantify tryptophan, bile acids, *p*-cresol, TMAO, and their derivatives in the early stages of AD, specifically in SCI patients. This enabled precise monitoring of metabolite levels and their progression from the initial stages of the decline. PLS-DA plot demonstrated a shift in metabolic profiles commenced as early as SCI and continued to MCI, suggesting changes may already be apparent when memory complaints first appear. Multiple linear regression adjusted for confounders of gut microbial metabolism and machine learning analysis both highlighted choline, 5-hydroxyindole acetic acid, indole-3-propionic acid, indoxyl sulfate and kynurenic acid as key metabolites significantly associated with prodromal AD progression. Neuroprotective metabolites, including choline, 5-hydroxyindole acetic acid and indole propionic acid (Hwang et al. 2009; Blusztajn et al. 2017; Klein et al. 2018), exhibited lower concentrations in SCI and MCI participants in comparison to controls, while cytotoxic metabolites, including indoxyl sulfate, showed increasing levels (Leong and Sirich 2016). Kynurenic acid, a typically neuroprotective metabolite (Ostapiuk and Urbanska 2021), was higher in SCI and MCI in comparison to healthy controls. However, its abnormal accumulation can disrupt cognitive function (Fujigaki et al. 2017). Of the five metabolites highlighted by both machine learning and multiple linear regression, all except choline are produced from tryptophan metabolism, indicating notable alterations in tryptophan metabolism in prodromal AD progression. These findings align with emerging evidence linking tryptophan metabolism to AD, suggesting its potential role in the disease's early stages (Weaver et al. 2020).

Procrustes analysis indicated that metabolic changes were congruent with shifts in gut microbiome composition, implying a significant modulatory relationship between the two. This supports previous findings that the gut microbiome composition is modulated from the early stages AD progression, such as MCI (Sheng et al. 2021; Chen et al. 2023). *Lachnoclostridium*, a converter of choline to TMA (Cai et al. 2022), inversely correlated with choline concentrations, suggesting increases in *Lachnoclostridium* abundance in prodromal AD may raise choline metabolism to TMA, decreasing circulatory concentrations. In line with this, TMAO concentrations were 1.6x higher in MCI patients than in healthy controls. *Holdemania* showed a positive correlation with indoxyl sulfate levels, consistent with findings in patients with end-stage renal disease; a known risk factor for dementia (Hung et al. 2017). This suggests that *Holdemania* may contribute to differences between control and SCI patients, potentially via the modulation of tryptophan metabolism (Zheng et al. 2020).

Together, these findings advance our current understanding of metabolic alterations in prodromal AD. Integrating both statistical and machine learning models improved the robustness of the metabolite features identified, including adjusting for confounding variables of metabolism such as age, BMI, sex, background diet, and markers of kidney and liver function; factors often overlooked in metabolomic analyses. Given that many of these metabolites are modifiable through diet, dietary interventions may offer a promising therapeutic strategy for slowing early AD progression.

6.2 Refined dietary intake can detrimentally alter metabolite-mediated pathways of the microbiota-gut-brain axis

The functions of the gut microbiota extend beyond the physical borders of the digestive tract. Microbial-derived metabolites released from the gut modulate pathways affecting the CNS both directly, by crossing the blood-brain barrier, and indirectly, via modulation of peripheral organ function or *vagus* nerve stimulation (see Chapter 1). Diet has a major influence on this communication by providing precursor compounds for bioactive metabolites and shaping gut microbiome composition; thereby having the ability to influence brain health.

A characteristic of the Western-type dietary pattern is the high intake of refined carbohydrates and low dietary fibre, which have been associated with alterations in gut microbiota and cognitive impairment in both humans and rodents, indicating potential microbiota-gut-brain interactions (Sonnenburg et al. 2016; Więckowska-Gacek et al. 2021). In Chapter 3, multi-omics approaches revealed that mice maintained on a rLFD consisting of high sucrose, processed carbohydrates, and low fibre content for eight weeks displayed significant decreases in microbial diversity and induced dysbiosis, aligning with previous findings (Morrison et al. 2020). Dietary fibre serves as a substrate for beneficial microbes such as *Roseburia*, *Eubacterium* and genera within the *Lachnospiraceae* family, which are known producers of SCFAs (Abdugheni et al. 2022; Song et al. 2022; Igudesman et al. 2022). These bacteria were notably reduced with rLFD consumption, corresponding with reductions in peripheral SCFA concentrations, as the gut microbiota relies on fibre to generate these metabolites (Sonnenburg et al. 2016). In contrast, pathobionts, such as *Bilophila* increased with rLFD consumption due to their ability to thrive in low-fibre environments by metabolising alternative substrates such as proteins and fats, disrupting the balance of the gut microbiome (Natividad et al. 2018; Wu et al. 2022). Increases in pathobionts like *Bilophila* are common in AD patients, suggesting a rLFD may shift gut composition into a more pathogenic state (Vogt et al. 2017).

Consumption of an rLFD was associated with alterations in gut composition that correlated with changes in colonic BA concentrations, suggesting that dysbiosis may contribute to BA dysmetabolism. Specifically, gut dysbiosis included a reduction in bacteria expressing bile salt hydrolase (BSH) activity, such as *Roseburia* and *Turicibacter*, which are responsible for bile acid deconjugation, while an increase was observed in bacteria with 7α -dehydroxylation enzymes, like *Ruminococcaceae* and *Lachnoclostridium*, which convert primary BAs to secondary BAs. Low-fibre intake shifts gut microbes to metabolise less favourable substrates, especially dietary and endogenous proteins, which can enhance BA production. Dietary fibre can also bind with bile acids, preventing their reabsorption and promoting their excretion, rather than returning them to the liver (Naumann et al. 2019). A rLFD may disrupt this process, leading to elevated BA concentrations in enterohepatic circulation; a phenomenon observed in AD patients, which can contribute to cognitive impairment (Ren et al. 2024). Additionally, the rLFD increased colonic concentrations of the nuclear farnesoid receptor (FXR) antagonists, including α -

MCA, β -MCA, HDCA and UDCA, which can inhibit BA synthesis by repressing enzyme CYP7A1 through the fibroblast growth factor 19 (FGF19; FGF15 in mice) (Lee et al. 2006). The accumulation of these antagonists under an rLFD may impair this signalling pathway, further contributing to elevated colonic BA levels.

rLFD consumption was associated with decreased BA concentrations in the brain, particularly levels of CA and TCA, indicating bile acid dysregulation- a hallmark of neurodegenerative diseases such as AD (as discussed in Chapter 2) (Graham et al. 2018; Baloni et al. 2020). These findings align with neuronal metabolic profiles in AD patients and 12-month APP/PS1 mice (Pan et al. 2017). Changes in neuronal bile acids are indicative of disrupted BA transport from the periphery or a reduction in local synthesis. However, genes involved in the production of CA and TCA have not been found in the brain samples, suggesting reductions are most likely due to disrupted peripheral transport, modulating microbiota-gut-brain axis signalling (Baloni et al. 2020). Furthermore, the rLFD-induced decrease in TCA levels was inversely correlated with *NF- κ B1* expression, a key neuroinflammatory transcription factor associated with AD progression (Jones and Kounatidis 2017), suggesting disruptions in the transport of TCA may promote neuroinflammation. Taurine-conjugated bile acids play a neuroprotective role in the brain as taurine itself can suppress inflammation by reducing NF- κ B1 activation (Agca et al. 2014; Ghaderpour et al. 2023). As a result, reduced TCA concentrations may lessen the inhibition of *NF- κ B1*, increasing neuroinflammation, a key accelerator of AD progression (Kiraly et al. 2023). As such, a refined diet could contribute to accelerated AD progression through microbial-mediated changes in the microbiota-gut-brain axis. This presents a novel connection linking a refined diet and detrimental neuroinflammatory processes, highlighting the interconnected nature of dietary carbohydrates, gut microbiome composition and bile acids on brain health (Summary Figure 6.1).

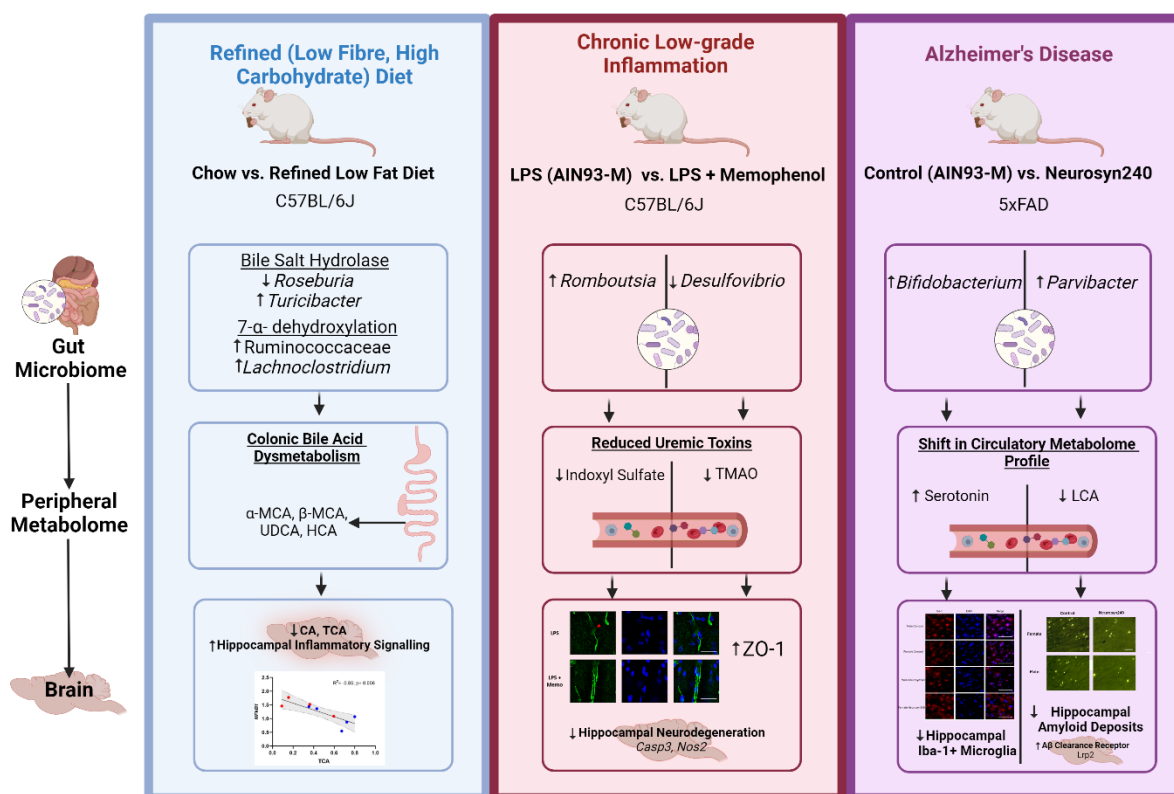


Figure 6.1 Summary of dietary modulation of metabolite-mediated pathways within the microbiota-gut-brain axis.

6.3 Dietary supplements can provide metabolite-mediated protective effects in a model of chronic low-grade inflammation and early AD neuropathology

Given the detrimental effects of a rLFD diet on microbial-derived metabolite pathways within the microbiota-gut-brain axis, we investigated whether dietary interventions could conversely provide protective benefits. Supplements containing high concentrations of dietary bioactives have recently gained popularity as a convenient method to boost the intake of beneficial compounds. Therefore, in Chapters 4 and 5, two dietary supplements were investigated: a (poly)phenol-rich grape and blueberry extract, Memophenol™, in a model of chronic low-grade inflammation, and a Mediterranean-inspired supplement, Neurosyn240, for its potential to mitigate AD neuropathology. Both (poly)phenols and the components of a Mediterranean diet are renowned for their potent antioxidant and anti-inflammatory properties, playing a crucial role in supporting cognitive health (Aridi et al. 2017; Singh et al. 2020; Láng et al. 2024). However, despite the knowledge that they can modulate the gut (Dueñas et al. 2015; De Filippis et al. 2016), whether these effects extend to metabolite-mediated communication of the microbiota-gut-brain axis remains unclear (Merra et al. 2020; Song et al. 2021; Romo-Vaquero et al. 2022; Láng et al. 2024).

As individuals age, increased inflammation driven by oxidative stress, metabolic dysregulation, and immune changes can accelerate neurodegeneration, a process referred to as ‘inflammaging’. As highlighted in Chapter 3, dietary patterns, such as a modern refined diet, can also exacerbate neuroinflammation. Ageing is associated with the increased production of LPS by the gut microbiota (Kim et al. 2016), which further amplifies the inflammatory response. Given these factors, we investigated the protective effects of Memophenol™ in a model of LPS-induced chronic low-grade inflammation.

Memophenol™ effectively protected against LPS-induced increases in the uremic toxins IS and TMAO, which were positively associated with *Desulfovibrio* and negatively associated with *Romboutsia* abundances, respectively, suggesting a role of the gut microbiome in this protective effect. (Poly)phenols can reduce the abundance of bacteria containing the *CutC* gene, such as *Desulfovibrio*, which encodes trimethylamine-lyase responsible for converting choline into TMA, a precursor of TMAO (Jiang et al. 2024). However, this study was the first to demonstrate this association in a model of chronic low-grade inflammation. Additionally, (poly)phenols can reduce the expression of FMO3, an enzyme catalysing the oxidation of TMA to TMAO in the liver, which is upregulated by LPS (Xiao et al. 2022; Jiang et al. 2024), suggesting biosynthetic modulation in the liver may also play a role.

(Poly)phenols can also enhance *Romboutsia* abundance, which increases the functional activity of the kynB enzyme in the kynurenine pathway of tryptophan metabolism (Vazquez-Medina et al. 2024). As IS is formed via the indole pathway of tryptophan metabolism, increased *Romboutsia* may promote a higher rate of tryptophan metabolism via the kynurenine pathway, decreasing tryptophan availability for IS production. Interestingly, IS was identified in Chapter 2 as a significant risk factor for early cognitive decline, indicating a potential beneficial role of Memophenol™ in mitigating prodromal AD risk through modulations of the gut microbiome. However, further investigations would be required.

In the brain, Memophenol™ intake prevented LPS-induced disruption of the endothelial tight junction ZO-1, which correlated with TMAO and IS concentrations. Elevated levels of TMAO, without a supraphysiological increase, can be protective against LPS-induced BBB disruption (Hoyles et al. 2021), acting as a compensatory mechanism for the osmotic and hydrostatic stress that LPS can induce (Nakano et al. 2020). Conversely, the neurotoxin IS can disrupt BBB permeability *in vivo* (Bobot et al. 2020). RNA sequencing suggested IS upregulated neurodegeneration-related genes, such as *Nos2* and *Casp3*, an association which has previously only been seen *in vitro* and may contribute to altered ZO-1 functioning (Adesso et al. 2017; Pieniasek et al. 2023). NOS2 (iNOS) produces nitric oxide in the brain, which can induce neurotoxicity and BBB disruption (Shukla et al. 1996). Caspase 3, a key regulator of apoptosis, can directly disrupt ZO-1 proteins, which can affect BBB function (Zehendner et al. 2011). However, it is unclear from this study alone whether the disruption of ZO-1 affected BBB permeability, as markers of BBB permeability were not measured and LPS did not significantly disrupt other BBB-

related genes, making this an important area for future research. Memophenol™ also prevented the LPS-induced decrease in expression of the IS efflux transporter *Abcg2* (also known as breast cancer resistance protein, BCRP) in the brain (Takada et al. 2018), potentially enhancing IS clearance from the brain, reducing neurotoxic buildup.

Building upon these neuroprotective properties of Memophenol™, we investigated Neurosyn240, a Mediterranean diet-inspired supplement combining Memophenol™ with carotenoids, minerals and vitamins. This supplement has previously been shown to ameliorate cognitive, microbial, and metabolic deficits in the same LPS mouse model of chronic low-grade inflammation (Pontifex et al. 2024a). Given the growing evidence supporting the Mediterranean diet's benefits for cognitive health (Chapter 1), our study focused on exploring the effects of Neurosyn240 on metabolite-mediated communication within the microbiota-gut-brain axis in the 5xFAD model of AD. Specifically, we examined the prodromal stages to assess the efficacy of Neurosyn240 in slowing AD-related neuropathologies.

Neurosyn240 significantly reduced *Dubosiella* abundance, a bacterium with 7- α -dehydroxylation capability (Ojeda et al. 2023), and correlated with reductions in TDCA, suggesting gut microbiome modulations may underlie changes in bile acid concentrations. The beneficial microbe *Parvibacter* was increased by Neurosyn240 intake, and its abundance was inversely correlated with LCA concentrations, suggesting a modulatory relationship. Indeed, *Parvibacter* abundance is associated with vitamin intake (Rajoka et al. 2021) and contributes to the upregulation of the *baiA* gene, which plays a role in metabolising LCA to 3-oxo-5 β -cholanate, thereby reducing its toxicity (Wang et al. 2024). As outlined in Chapter 2, bile acid dysmetabolism is a common feature of early AD progression, characterised by increased production of cytotoxic LCA and TDCA. As such, Neurosyn240 may offer therapeutic benefits by reducing LCA and TDCA.

Bifidobacterium abundance was increased by Neurosyn240 supplementation and positively correlated with peripheral serotonin concentrations. Serotonin is a neurotransmitter synthesised from the essential amino acid tryptophan by the sequential actions of tryptophan hydroxylase (TPH) and aromatic amino acid decarboxylase, of which most (~95%) is located in the periphery. Strains of *Bifidobacterium*, such as *Bifidobacterium dentium*, can modulate the serotonergic system by secreting products such as acetate, which stimulates serotonin release from enterochromaffin cells (Engevik et al. 2021), and therefore may increase serotonin concentrations. Chapter 2 highlighted decreased peripheral serotonin turnover in early AD progression, as indicated by the serotonin marker 5-hydroxyindole acetic acid. Neurosyn240 intake may be beneficial against early AD progression by enhancing peripheral serotonin turnover, with the potential to mitigate early serotonergic deficits.

In the brain, Neurosyn40 decreased early AD neuropathology, reducing amyloid deposits and Iba-1 positive microglia within the hippocampus, correlating with a reduction in LCA and an increase in serotonin, respectively. RNA sequencing analysis suggested upregulation of genes associated with the

prevention of amyloid binding and promoting clearance (aggregation inhibitors; *Clu*, and A β clearance transporter at the BBB; *Lrp2*) with Neurosyn240 intake in comparison to controls. These findings align with evidence linking Mediterranean diet adherence to reduced A β accumulation via interactions with genes like *Clu* (Radd-Vagenas et al. 2018; Rainey-Smith et al. 2018), through changes in microbial and metabolic metabolism. Decreased LCA levels with Neurosyn240 supplementation inversely correlated with expression of the A β transporter LRP2, required for efficient clearance of A β from the brain (Nelson et al. 2017). Clusterin (*Clu*) binds to LRP2 to mediate A β clearance across the BBB (Nelson et al. 2017). LCA can strongly inhibit LRP2 expression *in vitro* (Erranz et al. 2004), suggesting the Neurosyn240-induced reductions of LCA may decrease the inhibition of LRP2 and improve A β clearance from the brain.

Peripheral serotonin levels inversely correlated with hippocampal Iba-1 positive microglia. As a potent immune modulator, peripheral serotonin can modulate immunological events, such as chemotaxis, leukocyte activation, proliferation and cytokine secretion through serotonin (5-HT) receptor-expressing immune cells (Arreola et al. 2015). This immune regulation can reduce pro-inflammatory cytokine release, thereby limiting microglial recruitment and activation in response to neuroinflammatory signals. In AD, dysregulation of the serotonergic system is well-documented, contributing to immune system modulation, neuroinflammation, and heightened microglial activity (Neshan et al. 2020). Therefore, the increase in serotonin levels following Neurosyn240 supplementation may help attenuate microglial activation, offering a potential neuroprotective effect against AD-related inflammation.

Together, these findings highlight novel protective effects of dietary supplements on the microbiota-gut-brain axis, through the modulation of key metabolites, in mitigating the effects of chronic low-grade inflammation and prodromal AD neuropathology, accentuating their therapeutic potential against early AD progression (Summary Figure 6.1). These findings extend those in Chapter 2 by suggesting that microbial and metabolic alterations identified in early AD could be modulated through dietary intervention. In Chapter 2, *Turibacter* was significantly decreased during early cognitive decline, in line with previous studies in AD patients (Vogt et al. 2017). In Chapter 5, Neurosyn240 supplementation increased its abundance in female 5xFAD mice, suggesting potential sex-specific beneficial modulation of the gut microbiome.

In addition to microbial changes, key metabolic disruptions associated with early AD progression, particularly in tryptophan and bile acid metabolism, were identified in Chapter 2. Chapter 5 demonstrated that Neurosyn240 influenced similar metabolic pathways, reducing cytotoxic bile acids (LCA and TDCA) and increasing beneficial metabolites, such as serotonin, which were reduced in early AD, as suggested by reduced levels of 5-hydroxyindole acetic acid, indicating reduced serotonin turnover. The correlation between reductions in the bile acid LCA and hippocampal A β deposits and

inverse relationship between serotonin and Iba-1 positive microglia further supports the hypothesis from Chapter 2 that gut-derived metabolites may be associated with disease progression.

However, direct comparisons between human and mouse data remain challenging due to significant physiological and environmental differences, which influence gut microbiota composition, metabolism, immune responses and cognitive function (Hou et al. 2022), as discussed in more detail in section 6.5. Metabolic differences, such as differences in tryptophan metabolism have been observed in 5xFAD mice in comparison to AD patients, with 5xFAD mice exhibiting higher blood serotonin levels than wild-type mice, while AD patients show lower serotonin levels than age-matched controls (Dunham et al. 2022). Similarly, while bile acid dysregulation is observed in both AD patients and transgenic mouse models, specific bile acids and their gut microbiome interactions differ, possibly due to differences in diet and hepatic metabolism (MahmoudianDehkordi et al. 2019). The 5xFAD model also exhibits an aggressive amyloid pathology that progresses much faster than in humans, in which AD develops over decades with contributions from tau pathology, vascular dysfunction, and systemic metabolic alterations (Forner et al. 2021). This highlights the importance of integrating both preclinical and clinical findings to better understand disease progression and identify modifiable targets for intervention.

Chapter 5 also did not include a wild-type control group, as 5xFAD mice already exhibit significant microbiota and metabolic changes compared to wild-type mice, even in the absence of dietary intervention. Therefore, limiting the ability to distinguish dietary effects from genotypic differences already present between wild-type and 5xFAD mice. Instead, the study was designed to focus on whether Neurosyn240 could modify microbiota and metabolic pathways within an AD model and the resulting effect on AD pathology. However, this removed the study's ability to directly evaluate the effects of Neurosyn240 in non-AD mice, which may have provided additional comparisons to Chapter 2.

6.4 Discussion of the experimental models and methodology

Analysis of the COMBAT and CANN dietary and microbial-derived metabolites and gut microbiome profiles.

Our study in Chapter 2 offers several major strengths including simultaneously targeting key microbial and metabolic metabolites associated with cognitive decline, whilst carefully matching our participants and adjusting our analysis for key factors known to influence the metabolome (age, BMI, sex, liver function, kidney function and background diet), which are often overlooked in marker studies. Furthermore, our study identifies specific microbiota which may be closely associated with these

metabolic shifts, as well as investigating participants from the earliest stage of cognitive decline (SCI) and validating our results through machine learning and adjusted statistical approaches. However, despite our study adjusting results for key covariates, host metabolome profiles are influenced by a plethora of additional, largely environmental and biological factors. For example, factors such as stress levels, physical activity, and even circadian rhythms can significantly impact metabolomic profiles, potentially confounding the associations we observe between microbiota-derived metabolites and cognitive decline (Suárez et al. 2017). However, while our study is unable to establish causality from these analyses alone, it does not diminish the use of this metabolic signature as a risk factor of early AD progression. Future research should build on these insights through randomised controlled trials or by modulating relevant biosynthetic pathways in disease-relevant animal models, such as transgenic mouse models of AD, to clarify the mechanistic links contributing to cognitive decline.

Moreover, participants' background diet was adjusted for using data collected by SCG food frequency questionnaires, which can be prone to measurement error and may introduce inaccuracies due to recall bias and self-reporting issues. For example, in the Women's Health Initiative prospective cohort study, food frequency questionnaires explained only 3.8% of the variation in energy biomarkers and 8.4% of the variation in protein biomarkers, which was significantly less than food records and 24-hour food recalls (24HRs) (Prentice et al. 2011). However, it is cost-effective and efficient for large-scale studies, providing a practical alternative to resource-intensive methods such as weighed food diaries or 24-hour recalls. The SCG FFQ also provides high precision in comparison to non-quantitative FFQs by incorporating portion size estimates, enabling more accurate nutrient analysis. In particular, the SCG FFQ has been found to have reasonable repeatability and validity in ranking nutrient intakes in an older population (Jia et al. 2008), making it a suitable tool for our population in Chapter 2. However, it should be noted that impaired short-term memory or executive function may affect the validity of the FFQ, potentially making it less reliable for SCI and MCI participants. Since the FFQ relies on participants' memory, it is more susceptible to recall bias and misclassification in these populations. Furthermore, the SCG FFQ's fixed food list may omit some dietary items for participants. However, its cultural tailoring improves its relevance for UK populations compared to generic FFQs. Nevertheless, to enhance accuracy, future research should consider using 24HRs, which may offer less biased intake estimates compared to food frequency questionnaires (Gibson et al. 2017), or metabolomic dietary biomarkers, which provide an objective, unbiased measure of dietary intake (Rafiq et al. 2021).

Furthermore, like all studies utilising machine learning models, the larger the dataset, the more robust the predictive performance. With the current dataset including 150 individuals and 32 metabolites, we achieved significant predictive performance, utilising cohorts larger than some previous metabolite marker studies (Lin et al. 2023). However, our findings will require external validation in larger independent cohorts to improve the model.

***In vivo* assessment of nutritional strategies to modulate the microbiota-gut-brain axis**

Metabolites of Interest: Despite targeting some of the key metabolites currently associated with neuronal health (see Chapter 1), the gut microbiome is capable of directly and indirectly modifying a variety of metabolites which may contribute to the protective effects of Memophenol™ against chronic inflammation and Neurosyn240 with AD neuropathology or the detrimental effects of rLFD. For example, SCFAs produced from the microbiota through the anaerobic fermentation of indigestible polysaccharides play a role in enhancing and protecting the BBB (Braniste et al. 2014; Hoyles et al. 2018b; O’Riordan et al. 2022) and are protective against AD (Qian et al. 2022). SCFAs have been extensively studied for their role in microbiota-gut-brain interactions and early AD, as well as their association with dietary fibre, (poly)phenols, and the components of a Mediterranean diet (Edwards et al. 2017; Garcia-Mantrana et al. 2018; Nagpal et al. 2019; Zheng et al. 2021). Given these previous investigations, SCFAs were not the focus of this thesis. Furthermore, recent research has also revealed the capacity of the microbiome to produce new microbially conjugated BAs (MCBAs) that are conjugated with phenylalanine, leucine, and tyrosine on a cholic acid backbone (Quinn et al. 2020). Although the biological function of these new MCBAs remains unclear, future research may focus on uncovering their relationship within the microbiota-gut-brain axis and early cognitive decline. This is particularly relevant given the observed bile acid dysmetabolism in prodromal AD and the impact of refined dietary intake on this process.

Secondly, although the metabolite-mediated pathways of the microbiota-gut-brain axis were the focus of this thesis, this pathway is not the only form of communication along the axis. Immune, hormonal and *vagus* nerve-related pathways all contribute to the complex relationship between the gut and the brain and may have been contributing to the observed changes. For example, in Chapter 3, despite a rLFD modulating neuroinflammatory gene expression (*NF-κB1*) which correlated to changes in bile acid signalling, *Arc* signalling was also upregulated with rLFD in comparison to regular diet. ARC is detrimental to cognitive function through immune system activation, which can be triggered by the increased of pathobionts such as *Bilophila* via Th1-mediated immune response, suggesting further pathways may contribute to the negative effects of rLFD (Rosi 2011; Devkota and Chang 2015).

Furthermore, despite our results outlining numerous associations between the gut microbiome, circulatory metabolites and brain health, further work will be required to establish causality of the underlying mechanisms. Advances in this work are underway. For example, IS was positively correlated to caspase 3 expression in Chapter 4, and recent work has found the addition of IS to mononuclear blood cells increased the expression of caspase 3 via the mitochondrial pathway, strengthening the relationship and providing further mechanistic insight underlying the correlation (Erranz et al. 2004; Pieniazek et al. 2023). However, further *in vivo* investigations will be required.

Finally, in Chapters 3 and 4, the effect of a refined diet and Memophenol™ intake were investigated using only male mice. Gut microbiome composition and dietary metabolism, including fibre and (poly)phenol metabolism, can be sexually dimorphic (Pontifex et al. 2024b). As such, further studies investigating these results in females will be required.

LPS Model of Chronic Low-Grade Inflammation: A key strength of the LPS model of chronic low-grade inflammation is its simplicity and cost-effectiveness, offering a reliable method for studying the mechanisms and effects of chronic inflammation over time. However, while LPS-induced inflammation effectively simulates aspects of chronic inflammatory conditions, such as those seen in AD and ageing, it primarily activates the innate immune system via Toll-like receptor 4 (TLR4). This restrictive focus on innate immunity may not fully capture the complexity of chronic inflammation, which involves substantial interplay with the adaptive immune system. As a result, the model may not entirely reflect the intricate inflammatory processes that contribute to early AD progression and age-related immune dysregulation, where adaptive immune responses play a significant role (Weng 2006; Costa 2024). Additionally, there can be variability in responses depending on the species and strain used, which can limit the interpretation and generalisability of results, so comparisons with other studies should be made with caution.

5xFAD Mouse Model: The 5xFAD mouse model is widely utilised in AD research due to it replicating key pathological features observed in human AD, such as amyloid-beta accumulation from 2 months of age and neuroinflammation, with cognitive impairment commencing between 6-13 months (O’Leary et al. 2020; Forner et al. 2021). As such, this model uniquely allowed us to study the effectiveness of early dietary interventions within a prodromal disease progression at a relatively young age (5 months). This aligns with the key research hypothesis of this thesis, offering insights into the prevention of neuropathology as early AD manifestation progresses. However, while the model effectively recapitulates amyloid pathology, it does not capture the tau-related neurofibrillary tangles characteristic of later stages of AD. Therefore the study could not assess the modulation of tau phosphorylation, an aspect that has previously been found to be improved by anthocyanins, a (poly)phenol present in the Neurosyn240 diet (Ali et al. 2018). As such, further *in vivo* works with appropriate tau transgenic models, such as the P301S mutant human tau transgenic (Tg) mouse model, may be necessary. Furthermore, while the 5xFAD mouse model is a rapidly progressing transgenic model that effectively mimics aspects of AD, the accelerated disease development may differ from the more gradual progression seen in sporadic AD. Additionally, the genetic modifications in this model may influence other physiological pathways, potentially confounding the interpretation of therapeutic outcomes. Therefore, the replication of this method in another transgenic AD mouse model may be beneficial.

Dietary Interventions:

rLFD: The chow diet and rLFD diets not only exhibit significant differences in their carbohydrate composition, but these diets also vary in protein content and sources. The chow diet has a slightly higher protein content (26.9 kcal%) compared to the rLFD diet (20 kcal%) which was derived from plant-based sources such as soy, potato protein, hydrolysed wheat gluten, and maize gluten meal. In contrast, the rLFD diet's protein comes exclusively from casein, primarily sourced from dairy. The source and balance of protein and amino acids are known to influence gut microbiota and its metabolites. For example, plant proteins like soy protein have been associated with a greater abundance of *Bacteroidetes* and lower circulating LPS levels compared to proteins from meat, dairy, and casein (Prokopidis et al. 2020). Casein may also shift gut microbiota towards an increased abundance of *Lactococcus*, influencing gut microbiome composition (Irvin et al. 2017). The chow diet also includes dietary aryl hydrocarbon receptor (AhR) ligands from phytochemicals (daidzein and genistein) present in grains and soy oil, whereas the rLFD diet lacks these phytochemicals. Research by Schanz and colleagues has shown that dietary AhR ligands significantly impact intestinal immune cells and gut microbiota composition (Schanz et al. 2020). Consequently, the absence of dietary fibre and AhR ligands in the rLFD diet might contribute to the 'unhealthy' phenotype observed with this diet.

Neurosyn240 and Memophenol™: The Mediterranean dietary pattern features a high consumption of plant-based foods like fruits, vegetables, herbs, and spices; a modest intake of olive oil as the primary fat source, along with fish and red wine; and low consumption of red/processed meats and refined carbohydrates. While Memophenol™ is rich in (poly)phenols, and Neurosyn240 contains primarily (poly)phenols, carotenoids, vitamins, and minerals, these supplements only partially replicate the broader nutrient profile of the Mediterranean diet. For example, the Mediterranean diet is often described as a rich source of n-3 polyunsaturated fatty acids (PUFAs) derived from fish, seafood and nuts which have been associated with reductions in AD and improved cognitive function (Joseph et al. 2009; Dighriri et al. 2022). Future research should build upon this foundation by investigating additional components of the Mediterranean diet, such as n-3 polyunsaturated fatty acids from fish, seafood, and nuts, to potentially yield even greater neuroprotective benefits.

6.5 Future Directions

The novel data and concepts arising from this project open potential avenues for further research to address gaps and disparities.

Validation of dietary and microbial-derived metabolite risk factors for the early detection of AD

In Chapter 2, the identification of novel composite risk factors to detect at-risk persons in prodromal AD is a promising avenue. However, validating these risk factors in external populations to warrant they are robust, reliable, and applicable across diverse populations is essential, thereby enhancing their potential clinical utility. Without rigorous validation, there is a risk of false positives, which in a clinical

setting could result in incorrect evaluations of individual risk or inappropriate interventions. Additionally, it is important to understand longitudinal changes in plasma markers relative to the onset of AD hallmark neuropathology. Correlating the metabolite risk factors with markers of neuropathology of AD will be an important step in enhancing the monitoring of disease progression and assessing efficacy. For example, previous studies have correlated plasma markers with brain amyloid levels as measured with ¹¹C-Pittsburgh compound B (PiB) PET (Bilgel et al. 2023).

Establishing causality between identified microbiota-gut-brain axis connections

As described in the previous section, one limitation of our current dietary intervention studies is the reliance on correlation analyses, which cannot conclusively establish causality. These cross-sectional study designs were essential for identifying initial exploratory connections between gut microbiota, dietary and gut-derived metabolites, and neuropathology in the brain due to the large number of potential interactions. However, future research may need to focus on experimental approaches that directly test these relationships to move towards establishing causality. For example, studies may explore whether gut microbiota changes induced by a rLFD drive bile acid dysmetabolism and subsequent neuroinflammatory responses. To achieve this, faecal microbiota transplants (FMT) from rLFD-fed mice into germ-free mice could help determine whether these microbiota alterations alone can replicate the bile acid dysregulation and neuroinflammatory outcomes observed in previous studies, thus clarifying the gut microbiota's contribution.

Additionally, future research may investigate whether increased uremic toxins (e.g., TMAO and indoxyl sulfate) observed under LPS challenge contribute to BBB disruption, including extending our findings to investigate changes in BBB permeability. Administering these metabolites at physiologically relevant concentrations in mice would allow researchers to evaluate their direct impact on BBB integrity. Such studies could build on the work of Hoyles and colleagues, who demonstrated that TMAO administration in mice enhances BBB integrity under inflammatory stress (Hoyles et al. 2021). Further research into these areas will help clarify the precise mechanisms through which gut-derived metabolites contribute to brain health, thereby providing the mechanistic insights needed to move beyond correlation.

The ability of microbial-derived metabolites to penetrate the BBB

The microbiome's influence on cognition is shaped not just by the totality of gut metabolites produced, but also by their ability to cross the BBB (Sochocka et al. 2019). Consequently, the mechanisms used by many metabolites to cross the BBB are still unknown and some may even be synthesised *de novo*. For example, Chapter 2 highlighted bile acid dysmetabolism in the colon and the brain. However, the extent to which peripheral bile acid dysmetabolism affects brain bile acid concentrations is currently unknown as it remains unclear whether the extent to which bile acids observed in the brain are

synthesised locally within neural cells or originate from systemic circulation. While the liver is the primary site for the complete enzyme pathway required for classical bile acid synthesis, neurons can produce 24-hydroxycholesterol via the enzyme CYP46A1, which can contribute to the formation of neuronal bile acids through alternative pathways involving cholesterol metabolism. Bile acid transporters such as Bile Salt Export Pump (BSEP), Na⁺-Taurocholate Cotransporting Polypeptide (NTCP), and Apical Sodium-Dependent Bile Acid Transporter (ASBT), along with bile acid receptors, have been identified in the brain. Concentrations of some bile acids like CA, DCA, and CDCA in the brain also correlated with their serum levels, indicating the possibility of passive diffusion from the periphery into the brain (Higashi et al. 2017; Mertens et al. 2017; Shibuya et al. 2024). Future studies may wish to use intraperitoneally administered deuterium-labelled bile acids and monitor their expression in the brain to further determine the extent peripheral metabolism plays in neuronal concentrations. Current research is advancing in this area, with intraperitoneally injected deuterium-labelled CA and CDCA detected in rat brains (Higashi et al. 2017). Expanding this approach to other bile acids and animals could provide deeper insights into the role of peripheral metabolism in brain function and neurodegenerative processes.

Translational Perspective

From a translational perspective, aside from Chapter 2, much of the research described has been conducted in animals to gain key mechanistic insights that are difficult to obtain in humans. Translating these findings to humans is critical but presents significant challenges due to the complexity and individual variability shaped by environmental factors, which in turn influence each person's microbiome (Bray 2019). While mouse models offer a controlled setting that allows for precise manipulation of variables and observation of microbiota-gut-brain axis connections, key differences between species should be considered. Humans have more diverse diets, lifestyles, and genetic backgrounds, which introduce variables not fully represented in mouse models. Furthermore, mice exhibit distinct metabolic profiles. For example, in bile acid metabolism, humans primarily produce CA and CDCA as primary bile acids, whereas mice predominantly synthesise MCAs from CDCA. Additionally, UDCA is a primary bile acid in mice but a secondary, microbiota-derived bile acid in humans. These differences highlight the challenge of translating animal data into human outcomes (Straniero et al. 2020; Zheng et al. 2024).

To address these challenges, future research may focus on validating key pathways in humans through approaches like "humanised" mouse models or controlled clinical studies. For example, humanised mice colonised with human gut microbiota could be employed to examine whether specific microbial metabolites identified in mouse models, such as secondary bile acids, TMAO or indoxyl sulfate, replicate similar effects on the microbiota-gut-brain axis in a context more closely resembling human

physiology. Moreover, clinical trials using dietary interventions or supplements based on findings from animal research could track changes in gut microbiome, metabolomic and cognitive markers, ensuring that the results are translatable to human health outcomes. For example, a randomised controlled trial investigating the effects of dietary supplementation with Neurosyn240 in patients with SCI and MCI, compared to controls, could measure whether similar changes occur in microbial composition and metabolomic profiles. These steps can importantly assist in bridging the gap between preclinical studies and real-world applications.

6.6 Overall Conclusion

In this PhD project, we investigated the use of microbial-derived metabolites as risk factors and key mediators of the microbiota-gut-brain axis in early cognitive decline and dementia. We provide evidence supporting the notion that circulatory dietary and microbial-derived metabolites, in particular choline, 5-hydroxyindole acetic acid, indole-3-propionic acid, kynurenic acid and indoxyl sulfate, can identify individuals at greater risk for AD progression, presenting new insights into the early progression of cognitive decline and dementia. We highlight novel microbiota-gut-brain axis connections linking refined diets to increases in neuroinflammatory signalling through bile acid dysmetabolism. We demonstrate a novel protective pathway of a (poly)phenol-rich grape and blueberry extract against chronic low-grade inflammation through reducing circulatory uremic toxins (TMAO and indoxyl sulfate), which in turn was associated with restored ZO-1 localisation in the brain to control levels. Finally, we highlight potential metabolite-mediated protective effects of the Mediterranean diet-inspired supplement, Neurosyn240, in reducing AD neuropathology, including hippocampal amyloid deposits and Iba-1 positive microglia, in prodromal decline. Overall, our findings present new insights into the early progression of cognitive decline and dementia. We signify a major role for the gut in connection to the brain through the modulation of key microbial-derived metabolites. Furthermore, we lend strength to the hypothesis that individuals with higher risks of cognitive decline can be identified via a targeted metabolomic approach in the preceding stages of AD and highlight the interconnected nature of diet on the microbiota-gut-brain axis and brain health, providing further support for its use as a therapeutic intervention against early AD progression.

List of Communications

1. **Connell, E.**, Le Gall, G., Pontifex, M. G., Sami, S., Cryan, J. F., Clarke, G., Müller, M. & Vauzour, D., Microbial-derived metabolites as a risk factor of age-related cognitive decline and dementia, 2022, *Molecular Neurodegeneration*. 17, 43.
2. **Connell, E.**, Pontifex, M., Vauzour, D., Nutrition and the Ageing Brain, In: Evidence-based functional foods for prevention of age-related diseases, 2023, Springer Nature Publishers. DOI: 10.1007/978-981-99-0534-8_5.
3. **Connell E**, Sami S, Khondoker M, Minihane AM, Pontifex MG, Müller M, McArthur S, Le Gall G, Vauzour D., Circulatory dietary and gut-derived metabolites predict prodromal Alzheimer’s disease, 2024. Submitted to *Gut Microbes*.
4. **Connell, E.**, Blokker, B., Kellingray, L., Le Gall, G., Philo, M., Pontifex, M.G, Narbad, A, Müller, M.& Vauzour, D., Refined diet consumption increases neuroinflammatory signalling through bile acid dysmetabolism, 2024, *Nutritional Neuroscience*. 3, 1-14. DOI: 10.1080/1028415X.2023.2301165
5. **Connell, E.**, Le Gall, G., McArthur, S., Lang, L., Breeze, B., Pontifex, M.G, Sami, S., Pourtau, L., Gaudout, D., Müller, M.& Vauzour, D. (Poly)phenol-rich grape and blueberry extract prevents LPS-induced disruption of the blood-brain barrier through the modulation of the gut microbiota-derived uremic toxins, 2024, *Neurochemistry International*. DOI: 10.1016/j.neuint.2024.105878.
6. **Connell, E.**, Le Gall, G., McArthur, S., Lang, L., Liaquat, M., Pontifex, M.G, Sami, S., Pourtau, L., Gaudout, D., Müller, M.& Vauzour, D. Sexually Dimorphic Neuroprotective Effects of a Mediterranean Diet-Inspired Supplement through the Microbiota-Gut-Brain Axis in 5xFAD Mice: Insights into Alzheimer's Disease Pathology. Submitted to *Gut Microbes*.
7. Shah S, Knausenberger T, **Connell E**, Le Gall G, Hardy TAJ, Randall DW, McCafferty K, Yaqoob MM, Solito E, Müller M, Stachulski AV, Glen RC, Vauzour D, Hoyles L, McArthur S., Cerebrovascular damage caused by the gut microbe-derived uraemic toxin p-cresol sulfate is prevented by blockade of the epidermal growth factor receptor, 2024, *Gut Microbes*. DOI: 10.1080/19490976.2024.2431651.
8. Pontifex MG, **Connell E**, Le Gall G, Lang L, Pourtau L, Gaudout D, Angeloni C, Zallocco L, Ronci M, Giusti L, Müller M and Vauzour D., A novel bioactive blend resembling the Mediterranean diet ameliorates cognitive, microbial and metabolic deficits in a mouse model of low-grade inflammation, *Gut Microbes*, 2024.

9. Pontifex, M, **Connell, E**, Le Gall, G, Pourtau, L, Gaudout, D, Giusti, L, Ronci, M, Angeloni, C, Müller, M and Vauzour, D. Saffron extract (Safr'Inside™) improves anxiety related behaviour in a mouse model of low-grade inflammation through the modulation of the microbiota and gut derived metabolites, 2022, Food and Function. The Royal Society of Chemistry; 13:12219–33.
10. Vauzour, D., Rendeiro, C., D'Amato, A., Waffo-Téguo, P., Richard, T., Mérillon, J. M., Pontifex, M. G., **Connell, E.**, Müller, M., Butler, L. T., Williams, C. M. & Spencer, J. P. E., Anthocyanins promote learning through modulation of synaptic plasticity related proteins in an animal model of ageing, 2021, Antioxidants. 10, 8, 1235.
11. Pontifex, M. G., Malik, M. M. A. H., **Connell, E.**, Müller, M. & Vauzour, D., Citrus polyphenols in brain health and disease: Current perspectives, 2021, Frontiers in Neuroscience. 15, 640648.

References

- Abbott NJ, Patabendige AAK, Dolman DEM, et al (2010) Structure and function of the blood–brain barrier. *Neurobiology of Disease* 37:13–25. <https://doi.org/10.1016/j.nbd.2009.07.030>
- Abdugheni R, Wang W-Z, Wang Y-J, et al (2022) Metabolite profiling of human-originated Lachnospiraceae at the strain level. *iMeta* 1:e58. <https://doi.org/10.1002/imt2.58>
- Abreu MT, Fukata M, Arditi M (2005) TLR Signaling in the Gut in Health and Disease. *The Journal of Immunology* 174:4453–4460. <https://doi.org/10.4049/jimmunol.174.8.4453>
- Adesso S, Magnus T, Cuzzocrea S, et al (2017) Indoxyl Sulfate Affects Glial Function Increasing Oxidative Stress and Neuroinflammation in Chronic Kidney Disease: Interaction between Astrocytes and Microglia. *Front Pharmacol* 8:370. <https://doi.org/10.3389/fphar.2017.00370>
- Adesso S, Paterniti I, Cuzzocrea S, et al (2018) AST-120 Reduces Neuroinflammation Induced by Indoxyl Sulfate in Glial Cells. *J Clin Med* 7:365. <https://doi.org/10.3390/jcm7100365>
- Adluru N, Destiche DJ, Lu SY-F, et al (2014) White matter microstructure in late middle-age: Effects of apolipoprotein E4 and parental family history of Alzheimer’s disease. *Neuroimage Clin* 4:730–742. <https://doi.org/10.1016/j.nicl.2014.04.008>
- Agca CA, Tuzcu M, Hayirli A, Sahin K (2014) Taurine ameliorates neuropathy via regulating NF- κ B and Nrf2/HO-1 signaling cascades in diabetic rats. *Food Chem Toxicol* 71:116–121. <https://doi.org/10.1016/j.fct.2014.05.023>
- Agostoni E, Chinnock JE, Daly MDB, Murray JG (1957) Functional and histological studies of the vagus nerve and its branches to the heart, lungs and abdominal viscera in the cat. *J Physiol* 135:182–205
- Agus A, Clément K, Sokol H (2021) Gut microbiota-derived metabolites as central regulators in metabolic disorders. *Gut* 70:1174–1182. <https://doi.org/10.1136/gutjnl-2020-323071>
- Agus A, Denizot J, Thévenot J, et al (2016) Western diet induces a shift in microbiota composition enhancing susceptibility to Adherent-Invasive *E. coli* infection and intestinal inflammation. *Sci Rep* 6:19032. <https://doi.org/10.1038/srep19032>
- Agus A, Planchais J, Sokol H (2018) Gut Microbiota Regulation of Tryptophan Metabolism in Health and Disease. *Cell Host & Microbe* 23:716–724. <https://doi.org/10.1016/j.chom.2018.05.003>
- Ajoolabady A, Lindholm D, Ren J, Pratico D (2022) ER stress and UPR in Alzheimer’s disease: mechanisms, pathogenesis, treatments. *Cell Death Dis* 13:1–15. <https://doi.org/10.1038/s41419-022-05153-5>
- Al-Bachari S, Naish JH, Parker GJM, et al (2020) Blood–Brain Barrier Leakage Is Increased in Parkinson’s Disease. *Front Physiol* 11:. <https://doi.org/10.3389/fphys.2020.593026>
- Alexander GE, Bergfield KL, Chen K, et al (2012) Gray matter network associated with risk for Alzheimer’s disease in young to middle-aged adults. *Neurobiol Aging* 33:2723–2732. <https://doi.org/10.1016/j.neurobiolaging.2012.01.014>
- Ali T, Kim T, Rehman SU, et al (2018) Natural Dietary Supplementation of Anthocyanins via PI3K/Akt/Nrf2/HO-1 Pathways Mitigate Oxidative Stress, Neurodegeneration, and Memory

- Impairment in a Mouse Model of Alzheimer's Disease. *Mol Neurobiol* 55:6076–6093. <https://doi.org/10.1007/s12035-017-0798-6>
- Alves-Santos AM, Sugizaki CSA, Lima GC, Naves MMV (2020) Prebiotic effect of dietary polyphenols: A systematic review. *Journal of Functional Foods* 74:104169. <https://doi.org/10.1016/j.jff.2020.104169>
- AlzBiomaker Database (2019) 5xFAD (C57BL6). <https://www.alzforum.org/research-models/5xfad-c57bl6>. Accessed 20 Sep 2024
- Alzheimer's Association (2019) 2019 Alzheimer's disease facts and figures. *Alzheimer's & Dementia* 15:321–387. <https://doi.org/10.1016/j.jalz.2019.01.010>
- Anand KS, Dhikav V (2012) Hippocampus in health and disease: An overview. *Ann Indian Acad Neurol* 15:239–246. <https://doi.org/10.4103/0972-2327.104323>
- Andrews SC, Robinson AK, Rodríguez-Quñones F (2003) Bacterial iron homeostasis. *FEMS Microbiol Rev* 27:215–237. [https://doi.org/10.1016/S0168-6445\(03\)00055-X](https://doi.org/10.1016/S0168-6445(03)00055-X)
- Anesi A, Rubert J, Oluwagbemigun K, et al (2019) Metabolic Profiling of Human Plasma and Urine, Targeting Tryptophan, Tyrosine and Branched Chain Amino Acid Pathways. *Metabolites* 9:E261. <https://doi.org/10.3390/metabo9110261>
- Aridi YS, Walker JL, Wright ORL (2017) The Association between the Mediterranean Dietary Pattern and Cognitive Health: A Systematic Review. *Nutrients* 9:E674. <https://doi.org/10.3390/nu9070674>
- Arreola R, Becerril-Villanueva E, Cruz-Fuentes C, et al (2015) Immunomodulatory effects mediated by serotonin. *J Immunol Res* 2015:354957. <https://doi.org/10.1155/2015/354957>
- Arumugam M, Raes J, Pelletier E, et al (2011) Enterotypes of the human gut microbiome. *Nature* 473:174–180. <https://doi.org/10.1038/nature09944>
- Ashburner M, Ball CA, Blake JA, et al (2000) Gene Ontology: tool for the unification of biology. *Nat Genet* 25:25–29. <https://doi.org/10.1038/75556>
- Azevedo MLV, Bonan NB, Dias G, et al (2016) p-Cresyl sulfate affects the oxidative burst, phagocytosis process, and antigen presentation of monocyte-derived macrophages. *Toxicol Lett* 263:1–5. <https://doi.org/10.1016/j.toxlet.2016.10.006>
- Azpiroz F, Dubray C, Bernalier-Donadille A, et al (2017) Effects of scFOS on the composition of fecal microbiota and anxiety in patients with irritable bowel syndrome: a randomized, double blind, placebo controlled study. *Neurogastroenterol Motil* 29:. <https://doi.org/10.1111/nmo.12911>
- Badawy AA-B (2017) Kynurenine Pathway of Tryptophan Metabolism: Regulatory and Functional Aspects. *Int J Tryptophan Res* 10:1178646917691938. <https://doi.org/10.1177/1178646917691938>
- Baj G, Carlino D, Gardossi L, Tongiorgi E (2013) Toward a unified biological hypothesis for the BDNF Val66Met-associated memory deficits in humans: a model of impaired dendritic mRNA trafficking. *Front Neurosci* 7:188. <https://doi.org/10.3389/fnins.2013.00188>

- Balagopal P (Babu), de Ferranti SD, Cook S, et al (2011) Nontraditional Risk Factors and Biomarkers for Cardiovascular Disease: Mechanistic, Research, and Clinical Considerations for Youth. *Circulation* 123:2749–2769. <https://doi.org/10.1161/CIR.0b013e31821c7c64>
- Balasubramanian R, Bazaz MR, Pasam T, et al (2023) Involvement of Microbiome Gut-Brain Axis in Neuroprotective Effect of Quercetin in Mouse Model of Repeated Mild Traumatic Brain Injury. *Neuromolecular Med* 25:242–254. <https://doi.org/10.1007/s12017-022-08732-z>
- Baldarelli RM, Smith CL, Ringwald M, et al (2024) Mouse Genome Informatics: an integrated knowledgebase system for the laboratory mouse. *Genetics* 227:iyae031. <https://doi.org/10.1093/genetics/iyae031>
- Baloni P, Funk CC, Yan J, et al (2020) Metabolic Network Analysis Reveals Altered Bile Acid Synthesis and Metabolism in Alzheimer’s Disease. *Cell Rep Med* 1:100138. <https://doi.org/10.1016/j.xcrm.2020.100138>
- Bansal T, Alaniz RC, Wood TK, Jayaraman A (2010) The bacterial signal indole increases epithelial-cell tight-junction resistance and attenuates indicators of inflammation. *Proc Natl Acad Sci U S A* 107:228–233. <https://doi.org/10.1073/pnas.0906112107>
- Barbier P, Zejneli O, Martinho M, et al (2019) Role of Tau as a Microtubule-Associated Protein: Structural and Functional Aspects. *Front Aging Neurosci* 11:204. <https://doi.org/10.3389/fnagi.2019.00204>
- Barbouti A, Goulas V (2021) Dietary Antioxidants in the Mediterranean Diet. *Antioxidants (Basel)* 10:1213. <https://doi.org/10.3390/antiox10081213>
- Barrea L, Annunziata G, Muscogiuri G, et al (2018) Trimethylamine-N-oxide (TMAO) as Novel Potential Biomarker of Early Predictors of Metabolic Syndrome. *Nutrients* 10:1971. <https://doi.org/10.3390/nu10121971>
- Bazzari FH, Abdallah DM, El-Abhar HS (2019) Chenodeoxycholic Acid Ameliorates AlCl₃-Induced Alzheimer’s Disease Neurotoxicity and Cognitive Deterioration via Enhanced Insulin Signaling in Rats. *Molecules* 24:. <https://doi.org/10.3390/molecules24101992>
- Beghelli D, Giusti L, Zallocco L, et al (2024) Dietary fiber supplementation increases *Drosophila melanogaster* lifespan and gut microbiota diversity. *Food Funct* 15:7468–7477. <https://doi.org/10.1039/d4fo00879k>
- Behrens A, Graessel E, Pendergrass A, Donath C (2020) Vitamin B—Can it prevent cognitive decline? A systematic review and meta-analysis. *Syst Rev* 9:111. <https://doi.org/10.1186/s13643-020-01378-7>
- Bendheim PE, Poeggeler B, Neria E, et al (2002) Development of indole-3-propionic acid (OXIGON) for Alzheimer’s disease. *J Mol Neurosci* 19:213–217. <https://doi.org/10.1007/s12031-002-0036-0>
- Benedetti A, Di Sario A, Marucci L, et al (1997) Carrier-mediated transport of conjugated bile acids across the basolateral membrane of biliary epithelial cells. *Am J Physiol* 272:G1416-1424. <https://doi.org/10.1152/ajpgi.1997.272.6.G1416>
- Bensalem J, Dudonné S, Etchamendy N, et al (2019) Polyphenols From Grape and Blueberry Improve Episodic Memory in Healthy Elderly with Lower Level of Memory Performance: A Bicentric

- Double-Blind, Randomized, Placebo-Controlled Clinical Study. *J Gerontol A Biol Sci Med Sci* 74:996–1007. <https://doi.org/10.1093/gerona/gly166>
- Bensalem J, Servant L, Alfos S, et al (2016) Dietary Polyphenol Supplementation Prevents Alterations of Spatial Navigation in Middle-Aged Mice. *Front Behav Neurosci* 10:. <https://doi.org/10.3389/fnbeh.2016.00009>
- Bercik P, Denou E, Collins J, et al (2011a) The intestinal microbiota affect central levels of brain-derived neurotropic factor and behavior in mice. *Gastroenterology* 141:599–609, 609.e1–3. <https://doi.org/10.1053/j.gastro.2011.04.052>
- Bercik P, Park AJ, Sinclair D, et al (2011b) The anxiolytic effect of *Bifidobacterium longum* NCC3001 involves vagal pathways for gut–brain communication. *Neurogastroenterology & Motility* 23:1132–1139. <https://doi.org/10.1111/j.1365-2982.2011.01796.x>
- Berding K, Carbia C, Cryan JF (2021a) Going with the grain: Fiber, cognition, and the microbiota-gut-brain-axis. *Exp Biol Med (Maywood)* 246:796–811. <https://doi.org/10.1177/1535370221995785>
- Berding K, Vlckova K, Marx W, et al (2021b) Diet and the Microbiota-Gut-Brain Axis: Sowing the Seeds of Good Mental Health. *Adv Nutr* 12:1239–1285. <https://doi.org/10.1093/advances/nmaa181>
- Berg G, Rybakova D, Fischer D, et al (2020) Microbiome definition re-visited: old concepts and new challenges. *Microbiome* 8:103. <https://doi.org/10.1186/s40168-020-00875-0>
- Bernstein H, Bernstein C, Payne CM, Dvorak K (2009) Bile acids as endogenous etiologic agents in gastrointestinal cancer. *World J Gastroenterol* 15:3329–3340. <https://doi.org/10.3748/wjg.15.3329>
- Berti V, Walters M, Sterling J, et al (2018) Mediterranean diet and 3-year Alzheimer brain biomarker changes in middle-aged adults. *Neurology* 90:e1789–e1798. <https://doi.org/10.1212/WNL.0000000000005527>
- Besten G den, Eunen K van, Groen AK, et al (2013) The role of short-chain fatty acids in the interplay between diet, gut microbiota, and host energy metabolism. *Journal of Lipid Research* 54:2325–2340. <https://doi.org/10.1194/jlr.R036012>
- Bilgel M, An Y, Walker KA, et al (2023) Longitudinal changes in Alzheimer’s-related plasma biomarkers and brain amyloid. *medRxiv* 2023.01.12.23284439. <https://doi.org/10.1101/2023.01.12.23284439>
- Blinkouskaya Y, Caçoilo A, Gollamudi T, et al (2021) Brain aging mechanisms with mechanical manifestations. *Mech Ageing Dev* 200:111575. <https://doi.org/10.1016/j.mad.2021.111575>
- Blinkouskaya Y, Weickenmeier J (2021) Brain Shape Changes Associated With Cerebral Atrophy in Healthy Aging and Alzheimer’s Disease. *Front Mech Eng* 7:. <https://doi.org/10.3389/fmech.2021.705653>
- Blokker BA, Maijo M, Echeandia M, et al (2019) Fine-Tuning of Sirtuin 1 Expression Is Essential to Protect the Liver From Cholestatic Liver Disease. *Hepatology* 69:699–716. <https://doi.org/10.1002/hep.30275>

- Blusztajn JK, Slack BE, Mellott TJ (2017) Neuroprotective Actions of Dietary Choline. *Nutrients* 9:815. <https://doi.org/10.3390/nu9080815>
- Bobot M, Thomas L, Moyon A, et al (2020) Uremic Toxic Blood-Brain Barrier Disruption Mediated by AhR Activation Leads to Cognitive Impairment during Experimental Renal Dysfunction. *J Am Soc Nephrol* 31:1509–1521. <https://doi.org/10.1681/ASN.2019070728>
- Bolandzadeh N, Davis JC, Tam R, et al (2012) The association between cognitive function and white matter lesion location in older adults: a systematic review. *BMC Neurology* 12:126. <https://doi.org/10.1186/1471-2377-12-126>
- Bonaz B, Bazin T, Pellissier S (2018) The Vagus Nerve at the Interface of the Microbiota-Gut-Brain Axis. *Front Neurosci* 12:. <https://doi.org/10.3389/fnins.2018.00049>
- Bonfili L, Cecarini V, Berardi S, et al (2017) Microbiota modulation counteracts Alzheimer’s disease progression influencing neuronal proteolysis and gut hormones plasma levels. *Sci Rep* 7:2426. <https://doi.org/10.1038/s41598-017-02587-2>
- Bose S, Cho J (2017) Targeting chaperones, heat shock factor-1, and unfolded protein response: Promising therapeutic approaches for neurodegenerative disorders. *Ageing Research Reviews* 35:155–175. <https://doi.org/10.1016/j.arr.2016.09.004>
- Bostanciklioğlu M (2019) The role of gut microbiota in pathogenesis of Alzheimer’s disease. *Journal of Applied Microbiology* 127:954–967. <https://doi.org/10.1111/jam.14264>
- Braniste V, Al-Asmakh M, Kowal C, et al (2014) The gut microbiota influences blood-brain barrier permeability in mice. *Science translational medicine* 6:263ra158. <https://doi.org/10.1126/scitranslmed.3009759>
- Bravo JA, Forsythe P, Chew MV, et al (2011) Ingestion of Lactobacillus strain regulates emotional behavior and central GABA receptor expression in a mouse via the vagus nerve. *Proceedings of the National Academy of Sciences* 108:16050–16055. <https://doi.org/10.1073/pnas.1102999108>
- Brentnall M, Rodriguez-Menocal L, De Guevara RL, et al (2013) Caspase-9, caspase-3 and caspase-7 have distinct roles during intrinsic apoptosis. *BMC Cell Biol* 14:32. <https://doi.org/10.1186/1471-2121-14-32>
- Bron B, Waldram R, Silk DB, Williams R (1977) Serum, cerebrospinal fluid, and brain levels of bile acids in patients with fulminant hepatic failure. *Gut* 18:692–696. <https://doi.org/10.1136/gut.18.9.692>
- Brunt VE, LaRocca TJ, Bazzoni AE, et al (2020) The gut microbiome-derived metabolite trimethylamine N-oxide modulates neuroinflammation and cognitive function with aging. *GeroScience*. <https://doi.org/10.1007/s11357-020-00257-2>
- Burokas A, Arboleya S, Moloney RD, et al (2017) Targeting the Microbiota-Gut-Brain Axis: Prebiotics Have Anxiolytic and Antidepressant-like Effects and Reverse the Impact of Chronic Stress in Mice. *Biol Psychiatry* 82:472–487. <https://doi.org/10.1016/j.biopsych.2016.12.031>
- Buttó LF, Haller D (2016) Dysbiosis in intestinal inflammation: Cause or consequence. *Int J Med Microbiol* 306:302–309. <https://doi.org/10.1016/j.ijmm.2016.02.010>

- Caetano-Silva ME, Rund L, Hutchinson NT, et al (2023) Inhibition of inflammatory microglia by dietary fiber and short-chain fatty acids. *Sci Rep* 13:2819. <https://doi.org/10.1038/s41598-022-27086-x>
- Cai Y-Y, Huang F-Q, Lao X, et al (2022) Integrated metagenomics identifies a crucial role for trimethylamine-producing *Lachnoclostridium* in promoting atherosclerosis. *npj Biofilms Microbiomes* 8:1–12. <https://doi.org/10.1038/s41522-022-00273-4>
- Calle ML, Urrea V (2011) Letter to the editor: Stability of Random Forest importance measures. *Brief Bioinform* 12:86–89. <https://doi.org/10.1093/bib/bbq011>
- Carabotti M, Scirocco A, Maselli MA, Severi C (2015) The gut-brain axis: interactions between enteric microbiota, central and enteric nervous systems. *Ann Gastroenterol* 28:203–209
- Cattaneo A, Cattane N, Galluzzi S, et al (2017) Association of brain amyloidosis with pro-inflammatory gut bacterial taxa and peripheral inflammation markers in cognitively impaired elderly. *Neurobiol Aging* 49:60–68. <https://doi.org/10.1016/j.neurobiolaging.2016.08.019>
- Cerini C, Dou L, Anfosso F, et al (2004) P-cresol, a uremic retention solute, alters the endothelial barrier function in vitro. *Thromb Haemost* 92:140–150. <https://doi.org/10.1160/TH03-07-0491>
- Cervantes-Barragan L, Chai JN, Tianero MD, et al (2017) *Lactobacillus reuteri* induces gut intraepithelial CD4+CD8 $\alpha\alpha$ + T cells. *Science* 357:806–810. <https://doi.org/10.1126/science.aah5825>
- Chakrabarti A, Geurts L, Hoyles L, et al (2022) The microbiota-gut-brain axis: pathways to better brain health. Perspectives on what we know, what we need to investigate and how to put knowledge into practice. *Cell Mol Life Sci* 79:80. <https://doi.org/10.1007/s00018-021-04060-w>
- Chakraborty N (2024) Metabolites: a converging node of host and microbe to explain meta-organism. *Front Microbiol* 15:. <https://doi.org/10.3389/fmicb.2024.1337368>
- Chalazonitis A, Rao M (2018) Enteric nervous system manifestations of neurodegenerative disease. *Brain Res* 1693:207–213. <https://doi.org/10.1016/j.brainres.2018.01.011>
- Chapron BD, Chapron A, Phillips B, et al (2018) Reevaluating the Role of Megalin in Renal Vitamin D Homeostasis Using a Human Cell-Derived Microphysiological System. *ALTEX* 35:504. <https://doi.org/10.14573/altex.1803161>
- Chelakkot C, Ghim J, Ryu SH (2018) Mechanisms regulating intestinal barrier integrity and its pathological implications. *Exp Mol Med* 50:1–9. <https://doi.org/10.1038/s12276-018-0126-x>
- Chen G, Zhou X, Zhu Y, et al (2023) Gut microbiome characteristics in subjective cognitive decline, mild cognitive impairment and Alzheimer’s disease: a systematic review and meta-analysis. *Eur J Neurol* 30:3568–3580. <https://doi.org/10.1111/ene.15961>
- Chen M-L, Zhu X-H, Ran L, et al (2017) Trimethylamine-N-Oxide Induces Vascular Inflammation by Activating the NLRP3 Inflammasome Through the SIRT3-SOD2-mtROS Signaling Pathway. *J Am Heart Assoc* 6:. <https://doi.org/10.1161/JAHA.117.006347>

- Cheng N, Bell L, Lamport DJ, Williams CM (2022) Dietary Flavonoids and Human Cognition: A Meta-Analysis. *Mol Nutr Food Res* 66:e2100976. <https://doi.org/10.1002/mnfr.202100976>
- Cheng T-H, Ma M-C, Liao M-T, et al (2020) Indoxyl Sulfate, a Tubular Toxin, Contributes to the Development of Chronic Kidney Disease. *Toxins* 12:684. <https://doi.org/10.3390/toxins12110684>
- Cheng X, Maher J, Chen C, Klaassen CD (2005) Tissue Distribution and Ontogeny of Mouse Organic Anion Transporting Polypeptides (oatps). *Drug Metab Dispos* 33:1062–1073. <https://doi.org/10.1124/dmd.105.003640>
- Cheng X, van Breemen RB (2005) Mass spectrometry-based screening for inhibitors of beta-amyloid protein aggregation. *Anal Chem* 77:7012–7015. <https://doi.org/10.1021/ac050556a>
- Cheng Y, Jin U-H, Allred CD, et al (2015) Aryl Hydrocarbon Receptor Activity of Tryptophan Metabolites in Young Adult Mouse Colonocytes. *Drug Metab Dispos* 43:1536–1543. <https://doi.org/10.1124/dmd.115.063677>
- Chiang JYL (2013) Bile Acid Metabolism and Signaling. *Compr Physiol* 3:1191–1212. <https://doi.org/10.1002/cphy.c120023>
- Chiappelli J, Pocivavsek A, Nugent KL, et al (2014) Stress-induced increase in kynurenic acid as a potential biomarker for patients with schizophrenia and distress intolerance. *JAMA Psychiatry* 71:761–768. <https://doi.org/10.1001/jamapsychiatry.2014.243>
- Chyan YJ, Poeggeler B, Omar RA, et al (1999) Potent neuroprotective properties against the Alzheimer beta-amyloid by an endogenous melatonin-related indole structure, indole-3-propionic acid. *J Biol Chem* 274:21937–21942. <https://doi.org/10.1074/jbc.274.31.21937>
- Clark A, Mach N (2016) Exercise-induced stress behavior, gut-microbiota-brain axis and diet: a systematic review for athletes. *J Int Soc Sports Nutr* 13:43. <https://doi.org/10.1186/s12970-016-0155-6>
- Clarke G, Grenham S, Scully P, et al (2013) The microbiome-gut-brain axis during early life regulates the hippocampal serotonergic system in a sex-dependent manner. *Molecular Psychiatry* 18:666–673. <https://doi.org/10.1038/mp.2012.77>
- Clarke G, Villalobos-Manriquez F, Marin DC (2020) Tryptophan Metabolism and the Microbiome-Gut-Brain Axis. *The Oxford Handbook of the Microbiome-Gut-Brain Axis*. <https://doi.org/10.1093/oxfordhb/9780190931544.013.13>
- Coelho-Júnior HJ, Trichopoulou A, Panza F (2021) Cross-sectional and longitudinal associations between adherence to Mediterranean diet with physical performance and cognitive function in older adults: A systematic review and meta-analysis. *Ageing Res Rev* 70:101395. <https://doi.org/10.1016/j.arr.2021.101395>
- Collins HL, Drazul-Schrader D, Sulpizio AC, et al (2016) L-Carnitine intake and high trimethylamine N-oxide plasma levels correlate with low aortic lesions in ApoE(-/-) transgenic mice expressing CETP. *Atherosclerosis* 244:29–37. <https://doi.org/10.1016/j.atherosclerosis.2015.10.108>
- Colombo AV, Sadler RK, Llovera G, et al (2021) Microbiota-derived short chain fatty acids modulate microglia and promote A β plaque deposition. *Elife* 10:e59826. <https://doi.org/10.7554/eLife.59826>

- Colton CA, Vitek MP, Wink DA, et al (2006) NO synthase 2 (NOS2) deletion promotes multiple pathologies in a mouse model of Alzheimer's disease. *Proceedings of the National Academy of Sciences* 103:12867–12872. <https://doi.org/10.1073/pnas.0601075103>
- Cosacak MI, Bhattarai P, Kizil C (2019) Alzheimer's disease, neural stem cells and neurogenesis: cellular phase at single-cell level. *Neural Regen Res* 15:824–827. <https://doi.org/10.4103/1673-5374.268896>
- Costa MR (2024) Switch of innate to adaptive immune responses in the brain of patients with Alzheimer's disease correlates with tauopathy progression. *npj Aging* 10:1–6. <https://doi.org/10.1038/s41514-024-00145-5>
- Costabile G, Vetrani C, Bozzetto L, et al (2021) Plasma TMAO increase after healthy diets: results from 2 randomized controlled trials with dietary fish, polyphenols, and whole-grain cereals. *The American Journal of Clinical Nutrition*. <https://doi.org/10.1093/ajcn/nqab188>
- Cowen P, Sherwood A (2013) The role of serotonin in cognitive function: Evidence from recent studies and implications for understanding depression. *Journal of psychopharmacology (Oxford, England)* 27:. <https://doi.org/10.1177/0269881113482531>
- Cowen PJ, Browning M (2015) What has serotonin to do with depression? *World Psychiatry* 14:158–160. <https://doi.org/10.1002/wps.20229>
- Craciun S, Balskus EP (2012) Microbial conversion of choline to trimethylamine requires a glycol radical enzyme. *Proceedings of the National Academy of Sciences* 109:21307–21312. <https://doi.org/10.1073/pnas.1215689109>
- Crockett MJ, Clark L, Roiser JP, et al (2012) Converging evidence for central 5-HT effects in acute tryptophan depletion. *Mol Psychiatry* 17:121–123. <https://doi.org/10.1038/mp.2011.106>
- Cryan JF, O'Riordan KJ, Cowan CSM, et al (2019) The Microbiota-Gut-Brain Axis. *Physiol Rev* 99:1877–2013. <https://doi.org/10.1152/physrev.00018.2018>
- Csernansky JG, Bardgett ME, Sheline YI, et al (1996) CSF excitatory amino acids and severity of illness in Alzheimer's disease. *Neurology* 46:1715–1720. <https://doi.org/10.1212/wnl.46.6.1715>
- Dal-Pan A, Dudonné S, Bourassa P, et al (2017) Cognitive-Enhancing Effects of a Polyphenols-Rich Extract from Fruits without Changes in Neuropathology in an Animal Model of Alzheimer's Disease. *J Alzheimers Dis* 55:115–135. <https://doi.org/10.3233/JAD-160281>
- Dangour AD, Whitehouse PJ, Rafferty K, et al (2010) B-vitamins and fatty acids in the prevention and treatment of Alzheimer's disease and dementia: a systematic review. *J Alzheimers Dis* 22:205–224. <https://doi.org/10.3233/JAD-2010-090940>
- Dave N, Judd JM, Decker A, et al (2023) Dietary choline intake is necessary to prevent systems-wide organ pathology and reduce Alzheimer's disease hallmarks. *Aging Cell* 22:e13775. <https://doi.org/10.1111/accel.13775>
- Davis KE, Eacott MJ, Easton A, Gigg J (2013) Episodic-like memory is sensitive to both Alzheimer's-like pathological accumulation and normal ageing processes in mice. *Behav Brain Res* 254:73–82. <https://doi.org/10.1016/j.bbr.2013.03.009>

- Davis SC, Yadav JS, Barrow SD, Robertson BK (2017) Gut microbiome diversity influenced more by the Westernized dietary regime than the body mass index as assessed using effect size statistic. *Microbiologyopen* 6:e00476. <https://doi.org/10.1002/mbo3.476>
- De Filippis F, Pellegrini N, Vannini L, et al (2016) High-level adherence to a Mediterranean diet beneficially impacts the gut microbiota and associated metabolome. *Gut* 65:1812–1821. <https://doi.org/10.1136/gutjnl-2015-309957>
- De S, Wirthensohn DC, Flagmeier P, et al (2019) Different soluble aggregates of A β 42 can give rise to cellular toxicity through different mechanisms. *Nat Commun* 10:1541. <https://doi.org/10.1038/s41467-019-09477-3>
- de Wilde MC, Vellas B, Girault E, et al (2017) Lower brain and blood nutrient status in Alzheimer's disease: Results from meta-analyses. *Alzheimers Dement (N Y)* 3:416–431. <https://doi.org/10.1016/j.trci.2017.06.002>
- Dehghani M, Kazemi Shariat Panahi H, Guillemin GJ (2019) Microorganisms, Tryptophan Metabolism, and Kynurenine Pathway: A Complex Interconnected Loop Influencing Human Health Status. *Int J Tryptophan Res* 12:1178646919852996. <https://doi.org/10.1177/1178646919852996>
- Dekkers KF, Sayols-Baixeras S, Baldanzi G, et al (2022) An online atlas of human plasma metabolite signatures of gut microbiome composition. *Nat Commun* 13:5370. <https://doi.org/10.1038/s41467-022-33050-0>
- Del Rio D, Rodriguez-Mateos A, Spencer JPE, et al (2013) Dietary (poly)phenolics in human health: structures, bioavailability, and evidence of protective effects against chronic diseases. *Antioxid Redox Signal* 18:1818–1892. <https://doi.org/10.1089/ars.2012.4581>
- Del Rio D, Zimetti F, Caffarra P, et al (2017) The Gut Microbial Metabolite Trimethylamine-N-Oxide Is Present in Human Cerebrospinal Fluid. *Nutrients* 9:. <https://doi.org/10.3390/nu9101053>
- Delafuente JC (1991) Nutrients and immune responses. *Rheum Dis Clin North Am* 17:203–212
- Demars F, Kebir O, Marzo A, et al (2020) Dysregulation of peripheral expression of the YWHA genes during conversion to psychosis. *Sci Rep* 10:9863. <https://doi.org/10.1038/s41598-020-66901-1>
- Den Besten G, Van Eunen K, Groen AK, et al (2013) The role of short-chain fatty acids in the interplay between diet, gut microbiota, and host energy metabolism. *J Lipid Res* 54:2325–2340. <https://doi.org/10.1194/jlr.R036012>
- Deng P, Valentino T, Flythe MD, et al (2021) Untargeted Stable Isotope Probing of the Gut Microbiota Metabolome Using ¹³C-Labeled Dietary Fibers. *J Proteome Res* 20:2904–2913. <https://doi.org/10.1021/acs.jproteome.1c00124>
- Deng Q, Wu C, Parker E, et al (2024) Microglia and Astrocytes in Alzheimer's Disease: Significance and Summary of Recent Advances. *Aging Dis* 15:1537–1564. <https://doi.org/10.14336/AD.2023.0907>
- Denninger JK, Smith BM, Kirby ED (2018) Novel Object Recognition and Object Location Behavioral Testing in Mice on a Budget. *J Vis Exp*. <https://doi.org/10.3791/58593>

- Derrien M, Belzer C, de Vos WM (2017) *Akkermansia muciniphila* and its role in regulating host functions. *Microbial Pathogenesis* 106:171–181. <https://doi.org/10.1016/j.micpath.2016.02.005>
- Desbonnet L, Clarke G, Traplin A, et al (2015) Gut microbiota depletion from early adolescence in mice: Implications for brain and behaviour. *Brain Behav Immun* 48:165–173. <https://doi.org/10.1016/j.bbi.2015.04.004>
- DeTure MA, Dickson DW (2019) The neuropathological diagnosis of Alzheimer’s disease. *Molecular Neurodegeneration* 14:32. <https://doi.org/10.1186/s13024-019-0333-5>
- Devkota S, Chang EB (2015) Interactions between diet, bile acid metabolism, gut microbiota, and Inflammatory Bowel Diseases. *Dig Dis* 33:351–356. <https://doi.org/10.1159/000371687>
- Devore EE, Kang JH, Breteler MMB, Grodstein F (2012) Dietary intakes of berries and flavonoids in relation to cognitive decline. *Ann Neurol* 72:135–143. <https://doi.org/10.1002/ana.23594>
- Devranis P, Vassilopoulou E, Tsironis V, et al (2023) Mediterranean Diet, Ketogenic Diet or MIND Diet for Aging Populations with Cognitive Decline: A Systematic Review. *Life (Basel)* 13:173. <https://doi.org/10.3390/life13010173>
- Di Giosia P, Stamerra CA, Giorgini P, et al (2022) The role of nutrition in inflammaging. *Ageing Research Reviews* 77:101596. <https://doi.org/10.1016/j.arr.2022.101596>
- Diaz Heijtz R, Wang S, Anuar F, et al (2011) Normal gut microbiota modulates brain development and behavior. *Proc Natl Acad Sci U S A* 108:3047–3052. <https://doi.org/10.1073/pnas.1010529108>
- Dighriri IM, Alsubaie AM, Hakami FM, et al (2022) Effects of Omega-3 Polyunsaturated Fatty Acids on Brain Functions: A Systematic Review. *Cureus* 14:e30091. <https://doi.org/10.7759/cureus.30091>
- DiNicolantonio JJ, McCarty M, O’Keefe J (2019) Association of moderately elevated trimethylamine N-oxide with cardiovascular risk: is TMAO serving as a marker for hepatic insulin resistance. *Open Heart* 6:e000890. <https://doi.org/10.1136/openhrt-2018-000890>
- Dionísio PA, Amaral JD, Ribeiro MF, et al (2015) Amyloid- β pathology is attenuated by tauroursodeoxycholic acid treatment in APP/PS1 mice after disease onset. *Neurobiol Aging* 36:228–240. <https://doi.org/10.1016/j.neurobiolaging.2014.08.034>
- Donaldson GP, Lee SM, Mazmanian SK (2016) Gut biogeography of the bacterial microbiota. *Nat Rev Microbiol* 14:20–32. <https://doi.org/10.1038/nrmicro3552>
- Dröge W, Schipper HM (2007) Oxidative stress and aberrant signaling in aging and cognitive decline. *Ageing Cell* 6:361–370. <https://doi.org/10.1111/j.1474-9726.2007.00294.x>
- Du L, Li J, Zhang X, et al (2019) Pomegranate peel polyphenols inhibits inflammation in LPS-induced RAW264.7 macrophages via the suppression of TLR4/NF- κ B pathway activation. *Food Nutr Res* 63:10.29219/fnr.v63.3392. <https://doi.org/10.29219/fnr.v63.3392>
- Dueñas M, Muñoz-González I, Cueva C, et al (2015) A survey of modulation of gut microbiota by dietary polyphenols. *Biomed Res Int* 2015:850902. <https://doi.org/10.1155/2015/850902>

- Dumas M-E, Rothwell AR, Hoyles L, et al (2017) Microbial-Host Co-metabolites Are Prodromal Markers Predicting Phenotypic Heterogeneity in Behavior, Obesity, and Impaired Glucose Tolerance. *Cell Rep* 20:136–148. <https://doi.org/10.1016/j.celrep.2017.06.039>
- Dunham SJB, McNair KA, Adams ED, et al (2022) Longitudinal Analysis of the Microbiome and Metabolome in the 5xfAD Mouse Model of Alzheimer’s Disease. *mBio* 13:e0179422. <https://doi.org/10.1128/mbio.01794-22>
- Duyckaerts C, Dickson D (2011) Neuropathology of Alzheimer’s Disease and its Variants. In: *Neurodegeneration: The Molecular Pathology of Dementia and Movement Disorders*. John Wiley & Sons, Ltd, pp 62–91
- Dye L, Boyle NB, Champ C, Lawton C (2017) The relationship between obesity and cognitive health and decline. *Proceedings of the Nutrition Society* 76:443–454. <https://doi.org/10.1017/S0029665117002014>
- Edamatsu T, Fujieda A, Itoh Y (2018) Phenyl sulfate, indoxyl sulfate and p-cresyl sulfate decrease glutathione level to render cells vulnerable to oxidative stress in renal tubular cells. *PLOS ONE* 13:e0193342. <https://doi.org/10.1371/journal.pone.0193342>
- Edwards CA, Havlik J, Cong W, et al (2017) Polyphenols and health: Interactions between fibre, plant polyphenols and the gut microbiota. *Nutr Bull* 42:356–360. <https://doi.org/10.1111/nbu.12296>
- Eimer WA, Vassar R (2013) Neuron loss in the 5XFAD mouse model of Alzheimer’s disease correlates with intraneuronal A β 42 accumulation and Caspase-3 activation. *Mol Neurodegener* 8:2. <https://doi.org/10.1186/1750-1326-8-2>
- El-Merahbi R, Löffler M, Mayer A, Sumara G (2015) The roles of peripheral serotonin in metabolic homeostasis. *FEBS Letters* 589:1728–1734. <https://doi.org/10.1016/j.febslet.2015.05.054>
- Engevik MA, Luck B, Visuthranukul C, et al (2021) Human-Derived *Bifidobacterium dentium* Modulates the Mammalian Serotonergic System and Gut–Brain Axis. *Cellular and Molecular Gastroenterology and Hepatology* 11:221–248. <https://doi.org/10.1016/j.jcmgh.2020.08.002>
- Erranz B, Miquel JF, Argraves WS, et al (2004) Megalin and cubilin expression in gallbladder epithelium and regulation by bile acids. *Journal of Lipid Research* 45:2185–2198. <https://doi.org/10.1194/jlr.M400235-JLR200>
- Eshkoor SA, Hamid TA, Mun CY, Ng CK (2015) Mild cognitive impairment and its management in older people. *Clin Interv Aging* 10:687–693. <https://doi.org/10.2147/CIA.S73922>
- Fan Z, Ke X, Jiang L, et al (2024) Genomic and biochemical analysis reveals fermented product of a putative novel *Romboutsia* species involves the glycometabolism of tilapia. *Aquaculture* 581:740483. <https://doi.org/10.1016/j.aquaculture.2023.740483>
- Farhangi MA, Javid AZ, Sarmadi B, et al (2018) A randomized controlled trial on the efficacy of resistant dextrin, as functional food, in women with type 2 diabetes: Targeting the hypothalamic-pituitary-adrenal axis and immune system. *Clin Nutr* 37:1216–1223. <https://doi.org/10.1016/j.clnu.2017.06.005>

- Farso M, Ménard C, Colby-Milley J, Quirion R (2013) The immune marker CD68 correlates with cognitive impairment in normally aged rats. *Neurobiology of Aging* 34:1971–1976. <https://doi.org/10.1016/j.neurobiolaging.2013.02.008>
- Fazio F, Lionetto L, Curto M, et al (2015) Xanthurenic Acid Activates mGlu2/3 Metabotropic Glutamate Receptors and is a Potential Trait Marker for Schizophrenia. *Sci Rep* 5:17799. <https://doi.org/10.1038/srep17799>
- Féart C, Samieri C, Barberger-Gateau P (2010) Mediterranean diet and cognitive function in older adults. *Curr Opin Clin Nutr Metab Care* 13:14–18. <https://doi.org/10.1097/MCO.0b013e3283331fe4>
- Féart C, Samieri C, Rondeau V, et al (2009) Adherence to a Mediterranean diet, cognitive decline, and risk of dementia. *JAMA* 302:638–648. <https://doi.org/10.1001/jama.2009.1146>
- Feng W, Wang Y, Liu Z-Q, et al (2017) Microglia activation contributes to quinolinic acid-induced neuronal excitotoxicity through TNF- α . *Apoptosis* 22:696–709. <https://doi.org/10.1007/s10495-017-1363-5>
- Ferreira-Vieira TH, Guimaraes IM, Silva FR, Ribeiro FM (2016) Alzheimer's Disease: Targeting the Cholinergic System. *Curr Neuropharmacol* 14:101–115. <https://doi.org/10.2174/1570159X13666150716165726>
- Ferrucci L, Fabbri E (2018) Inflammageing: chronic inflammation in ageing, cardiovascular disease, and frailty. *Nature reviews Cardiology* 15:505. <https://doi.org/10.1038/s41569-018-0064-2>
- Flanagan E, Cameron D, Sobhan R, et al (2022) Chronic Consumption of Cranberries (*Vaccinium macrocarpon*) for 12 Weeks Improves Episodic Memory and Regional Brain Perfusion in Healthy Older Adults: A Randomised, Placebo-Controlled, Parallel-Groups Feasibility Study. *Frontiers in Nutrition* 9:
- Flicker L (2010) Modifiable Lifestyle Risk Factors for Alzheimer's Disease. *Journal of Alzheimer's Disease* 20:803–811. <https://doi.org/10.3233/JAD-2010-091624>
- Forner S, Kawauchi S, Balderrama-Gutierrez G, et al (2021) Systematic phenotyping and characterization of the 5xFAD mouse model of Alzheimer's disease. *Sci Data* 8:270. <https://doi.org/10.1038/s41597-021-01054-y>
- Foster JA, Rinaman L, Cryan JF (2017) Stress & the gut-brain axis: Regulation by the microbiome. *Neurobiology of Stress* 7:124–136. <https://doi.org/10.1016/j.ynstr.2017.03.001>
- Franco Á de O, Starosta RT, Roriz-Cruz M (2019) The specific impact of uremic toxins upon cognitive domains: a review. *J Bras Nefrol* 41:103–111. <https://doi.org/10.1590/2175-8239-JBN-2018-0033>
- Fricker RA, Green EL, Jenkins SI, Griffin SM (2018) The Influence of Nicotinamide on Health and Disease in the Central Nervous System. *Int J Tryptophan Res* 11:1. <https://doi.org/10.1177/1178646918776658>
- Fröhlich EE, Farzi A, Mayerhofer R, et al (2016) Cognitive impairment by antibiotic-induced gut dysbiosis: Analysis of gut microbiota-brain communication. *Brain Behav Immun* 56:140–155. <https://doi.org/10.1016/j.bbi.2016.02.020>

- Fujigaki H, Yamamoto Y, Saito K (2017) L-Tryptophan-kynurenine pathway enzymes are therapeutic target for neuropsychiatric diseases: Focus on cell type differences. *Neuropharmacology* 112:264–274. <https://doi.org/10.1016/j.neuropharm.2016.01.011>
- Gan N, Zhou Y, Li J, et al (2023) Propofol Suppresses LPS-induced BBB Damage by Regulating miR-130a-5p/ZO-1 Axis. *Mol Biotechnol*. <https://doi.org/10.1007/s12033-023-00835-7>
- Gao J, Guo X, Wei W, et al (2021) The Association of Fried Meat Consumption With the Gut Microbiota and Fecal Metabolites and Its Impact on Glucose Homeostasis, Intestinal Endotoxin Levels, and Systemic Inflammation: A Randomized Controlled-Feeding Trial. *Diabetes Care* 44:1970–1979. <https://doi.org/10.2337/dc21-0099>
- Gao J, Xu K, Liu H, et al (2018) Impact of the Gut Microbiota on Intestinal Immunity Mediated by Tryptophan Metabolism. *Front Cell Infect Microbiol* 8:. <https://doi.org/10.3389/fcimb.2018.00013>
- Gao Q, Wang Y, Wang X, et al (2019) Decreased levels of circulating trimethylamine N-oxide alleviate cognitive and pathological deterioration in transgenic mice: a potential therapeutic approach for Alzheimer’s disease. *Aging* 11:. <https://doi.org/10.18632/aging.102352>
- Gao X, Liu X, Xu J, et al (2014) Dietary trimethylamine N-oxide exacerbates impaired glucose tolerance in mice fed a high fat diet. *J Biosci Bioeng* 118:476–481. <https://doi.org/10.1016/j.jbiosc.2014.03.001>
- Garcez ML, Tan VX, Heng B, Guillemin GJ (2020) Sodium Butyrate and Indole-3-propionic Acid Prevent the Increase of Cytokines and Kynurenine Levels in LPS-induced Human Primary Astrocytes. *Int J Tryptophan Res* 13:1178646920978404. <https://doi.org/10.1177/1178646920978404>
- Garcia-Mantrana I, Selma-Royo M, Alcantara C, Collado MC (2018) Shifts on Gut Microbiota Associated to Mediterranean Diet Adherence and Specific Dietary Intakes on General Adult Population. *Front Microbiol* 9:. <https://doi.org/10.3389/fmicb.2018.00890>
- Gareau MG (2014) Microbiota-Gut-Brain Axis and Cognitive Function. In: Lyte M, Cryan JF (eds) *Microbial Endocrinology: The Microbiota-Gut-Brain Axis in Health and Disease*. Springer, New York, NY, pp 357–371
- Gareau MG, Wine E, Rodrigues DM, et al (2011) Bacterial infection causes stress-induced memory dysfunction in mice. *Gut* 60:307–317. <https://doi.org/10.1136/gut.2009.202515>
- Garrido J, Borges F (2013) Wine and grape polyphenols — A chemical perspective. *Food Research International* 54:1844–1858. <https://doi.org/10.1016/j.foodres.2013.08.002>
- Gawel K, Gibula E, Marszalek-Grabska M, et al (2019) Assessment of spatial learning and memory in the Barnes maze task in rodents—methodological consideration. *Naunyn Schmiedebergs Arch Pharmacol* 392:1–18. <https://doi.org/10.1007/s00210-018-1589-y>
- GBD 2019 Dementia Forecasting Collaborators (2022) Estimation of the global prevalence of dementia in 2019 and forecasted prevalence in 2050: an analysis for the Global Burden of Disease Study 2019. *Lancet Public Health* 7:e105–e125. [https://doi.org/10.1016/S2468-2667\(21\)00249-8](https://doi.org/10.1016/S2468-2667(21)00249-8)

- Geerlings MI, Jonker C, Bouter LM, et al (1999) Association between memory complaints and incident Alzheimer's disease in elderly people with normal baseline cognition. *Am J Psychiatry* 156:531–537. <https://doi.org/10.1176/ajp.156.4.531>
- Gęgotek A, Skrzydlewska E (2023) Ascorbic acid as antioxidant. *Vitam Horm* 121:247–270. <https://doi.org/10.1016/bs.vh.2022.10.008>
- Geng S, Yang L, Cheng F, et al (2020) Gut Microbiota Are Associated With Psychological Stress-Induced Defections in Intestinal and Blood–Brain Barriers. *Front Microbiol* 10:. <https://doi.org/10.3389/fmicb.2019.03067>
- Ghaderpour A, Jeong J-Y, Kim Y-H, et al (2023) Taurodeoxycholate, a GPCR19 agonist, ameliorates atopic dermatitis in Balb/c mice. *European Journal of Immunology* n/a:2250048. <https://doi.org/10.1002/eji.202250048>
- Gharbi-Meliani A, Dugravot A, Sabia S, et al (2021) The association of APOE ε4 with cognitive function over the adult life course and incidence of dementia: 20 years follow-up of the Whitehall II study. *Alzheimer's Research & Therapy* 13:5. <https://doi.org/10.1186/s13195-020-00740-0>
- Ghosh TS, Shanahan F, O'Toole PW (2022) The gut microbiome as a modulator of healthy ageing. *Nat Rev Gastroenterol Hepatol* 19:565–584. <https://doi.org/10.1038/s41575-022-00605-x>
- Giannini E, Botta F, Fasoli A, et al (1999) Progressive liver functional impairment is associated with an increase in AST/ALT ratio. *Dig Dis Sci* 44:1249–1253. <https://doi.org/10.1023/a:1026609231094>
- Gibson RS, Charrondiere UR, Bell W (2017) Measurement Errors in Dietary Assessment Using Self-Reported 24-Hour Recalls in Low-Income Countries and Strategies for Their Prevention. *Adv Nutr* 8:980–991. <https://doi.org/10.3945/an.117.016980>
- Gkatzamanis V, Panagiotakos D, Yannakoulia M, et al (2022) Trajectories of healthy aging and their association with the Mediterranean diet: The HELIAD Study. *Maturitas* 159:33–39. <https://doi.org/10.1016/j.maturitas.2022.01.003>
- Goldstein FC, Ashley AV, Endeshaw Y, et al (2008) Effects of Hypertension and Hypercholesterolemia on Cognitive Functioning in Patients with Alzheimer's Disease. *Alzheimer Dis Assoc Disord* 22:336–342
- Goldstein JM, Seidman LJ, Horton NJ, et al (2001) Normal sexual dimorphism of the adult human brain assessed by in vivo magnetic resonance imaging. *Cereb Cortex* 11:490–497. <https://doi.org/10.1093/cercor/11.6.490>
- Gomes JAS, Oliveira MC, Gobira PH, et al (2018) A high-refined carbohydrate diet facilitates compulsive-like behavior in mice through the nitric oxide pathway. *Nitric Oxide* 80:61–69. <https://doi.org/10.1016/j.niox.2018.08.008>
- Gomes JAS, Silva JF, Marçal AP, et al (2020) High-refined carbohydrate diet consumption induces neuroinflammation and anxiety-like behavior in mice. *J Nutr Biochem* 77:108317. <https://doi.org/10.1016/j.jnutbio.2019.108317>
- Gordon S, Lee JS, Scott TM, et al (2024) Metabolites and MRI-Derived Markers of AD/ADRD Risk in a Puerto Rican Cohort. *Res Sq* rs.3.rs-3941791. <https://doi.org/10.21203/rs.3.rs-3941791/v1>

- Govindarajulu M, Pinky PD, Steinke I, et al (2020) Gut Metabolite TMAO Induces Synaptic Plasticity Deficits by Promoting Endoplasmic Reticulum Stress. *Front Mol Neurosci* 13:.
<https://doi.org/10.3389/fnmol.2020.00138>
- Gowda S, Desai PB, Kulkarni SS, et al (2010) Markers of renal function tests. *N Am J Med Sci* 2:170–173
- Graham SF, Rey NL, Yilmaz A, et al (2018) Biochemical Profiling of the Brain and Blood Metabolome in a Mouse Model of Prodromal Parkinson’s Disease Reveals Distinct Metabolic Profiles. *J Proteome Res* 17:2460–2469. <https://doi.org/10.1021/acs.jproteome.8b00224>
- Gregory S, Ritchie CW, Ritchie K, et al (2022) Mediterranean diet score is associated with greater allocentric processing in the EPAD LCS cohort: A comparative analysis by biogeographical region. *Front Aging* 3:1012598. <https://doi.org/10.3389/fragi.2022.1012598>
- Greicius MD, Srivastava G, Reiss AL, Menon V (2004) Default-mode network activity distinguishes Alzheimer’s disease from healthy aging: Evidence from functional MRI. *Proc Natl Acad Sci U S A* 101:4637–4642. <https://doi.org/10.1073/pnas.0308627101>
- Grundke-Iqbal I, Iqbal K, Tung YC, et al (1986) Abnormal phosphorylation of the microtubule-associated protein tau (tau) in Alzheimer cytoskeletal pathology. *Proc Natl Acad Sci U S A* 83:4913–4917
- Gu L, Guo Z (2013) Alzheimer’s A β 42 and A β 40 peptides form interlaced amyloid fibrils. *J Neurochem* 126:305–311. <https://doi.org/10.1111/jnc.12202>
- Gu Y, Brickman AM, Stern Y, et al (2015) Mediterranean diet and brain structure in a multiethnic elderly cohort. *Neurology* 85:1744–1751. <https://doi.org/10.1212/WNL.0000000000002121>
- Guillemin GJ, Brew BJ, Noonan CE, et al (2005) Indoleamine 2,3 dioxygenase and quinolinic acid immunoreactivity in Alzheimer’s disease hippocampus. *Neuropathol Appl Neurobiol* 31:395–404. <https://doi.org/10.1111/j.1365-2990.2005.00655.x>
- Gulaj E, Pawlak K, Bien B, Pawlak D (2010) Kynurenine and its metabolites in Alzheimer’s disease patients. *Advances in Medical Sciences* 55:204–211. <https://doi.org/10.2478/v10039-010-0023-6>
- Gutiérrez-Díaz I, Fernández-Navarro T, Sánchez B, et al (2016) Mediterranean diet and faecal microbiota: a transversal study. *Food Funct* 7:2347–2356.
<https://doi.org/10.1039/c6fo00105j>
- Guzior DV, Quinn RA (2021) Review: microbial transformations of human bile acids. *Microbiome* 9:140. <https://doi.org/10.1186/s40168-021-01101-1>
- H H, W P, Aj K (2013) Fibroblast growth factor 19 entry into brain. *Fluids and barriers of the CNS* 10:.
<https://doi.org/10.1186/2045-8118-10-32>
- Haase S, Wilck N, Haghikia A, et al (2020) The role of the gut microbiota and microbial metabolites in neuroinflammation. *European Journal of Immunology* 50:1863–1870.
<https://doi.org/10.1002/eji.201847807>

- Hahn B, Reneski CH, Pocivavsek A, Schwarcz R (2018) Prenatal kynurenine treatment in rats causes schizophrenia-like broad monitoring deficits in adulthood. *Psychopharmacology (Berl)* 235:651–661. <https://doi.org/10.1007/s00213-017-4780-9>
- Haider S, Khaliq S, Haleem DJ (2007) Enhanced serotonergic neurotransmission in the hippocampus following tryptophan administration improves learning acquisition and memory consolidation in rats. *Pharmacol Rep* 59:53–57
- Hamid MA, Iwaku M, Hoshino E (1994) The metabolism of phenylalanine and leucine by a cell suspension of *Eubacterium brachy* and the effects of metronidazole on metabolism. *Arch Oral Biol* 39:967–972. [https://doi.org/10.1016/0003-9969\(94\)90080-9](https://doi.org/10.1016/0003-9969(94)90080-9)
- Haran JP, Bhattarai SK, Foley SE, et al (2019) Alzheimer's Disease Microbiome Is Associated with Dysregulation of the Anti-Inflammatory P-Glycoprotein Pathway. *mBio* 10:e00632-19. <https://doi.org/10.1128/mBio.00632-19>
- Harmsen HJM, Raangs GC, He T, et al (2002) Extensive set of 16S rRNA-based probes for detection of bacteria in human feces. *Appl Environ Microbiol* 68:2982–2990. <https://doi.org/10.1128/AEM.68.6.2982-2990.2002>
- Haro C, Rangel-Zúñiga OA, Alcalá-Díaz JF, et al (2016) Intestinal Microbiota Is Influenced by Gender and Body Mass Index. *PLOS ONE* 11:e0154090. <https://doi.org/10.1371/journal.pone.0154090>
- Hayes AMR, Lauer LT, Kao AE, et al (2024) Western diet consumption impairs memory function via dysregulated hippocampus acetylcholine signaling. *Brain, Behavior, and Immunity* 118:408–422. <https://doi.org/10.1016/j.bbi.2024.03.015>
- He W, Luo Y, Liu J-P, et al (2020) Trimethylamine N-Oxide, a Gut Microbiota-Dependent Metabolite, is Associated with Frailty in Older Adults with Cardiovascular Disease. *Clin Interv Aging* 15:1809–1820. <https://doi.org/10.2147/CIA.S270887>
- Heijtz RD, Wang S, Anuar F, et al (2011) Normal gut microbiota modulates brain development and behavior. *PNAS* 108:3047–3052. <https://doi.org/10.1073/pnas.1010529108>
- Heise V, Filippini N, Ebmeier KP, Mackay CE (2011) The APOE ϵ 4 allele modulates brain white matter integrity in healthy adults. *Mol Psychiatry* 16:908–916. <https://doi.org/10.1038/mp.2010.90>
- Hestad K, Alexander J, Rootwelt H, Aaseth JO (2022) The Role of Tryptophan Dysmetabolism and Quinolinic Acid in Depressive and Neurodegenerative Diseases. *Biomolecules* 12:998. <https://doi.org/10.3390/biom12070998>
- Heylen A, Vermeiren Y, Kema IP, et al (2023) Brain Kynurenine Pathway Metabolite Levels May Reflect Extent of Neuroinflammation in ALS, FTD and Early Onset AD. *Pharmaceuticals* 16:615. <https://doi.org/10.3390/ph16040615>
- Higashi T, Watanabe S, Tomaru K, et al (2017) Unconjugated bile acids in rat brain: Analytical method based on LC/ESI-MS/MS with chemical derivatization and estimation of their origin by comparison to serum levels. *Steroids* 125:107–113. <https://doi.org/10.1016/j.steroids.2017.07.001>
- Hill MJ (1997) Intestinal flora and endogenous vitamin synthesis. *Eur J Cancer Prev* 6 Suppl 1:S43-45. <https://doi.org/10.1097/00008469-199703001-00009>

- Ho L, Ono K, Tsuji M, et al (2018) Protective roles of intestinal microbiota derived short chain fatty acids in Alzheimer's disease-type beta-amyloid neuropathological mechanisms. *Expert Review of Neurotherapeutics* 18:83–90. <https://doi.org/10.1080/14737175.2018.1400909>
- Hofmann AF (1999) The Continuing Importance of Bile Acids in Liver and Intestinal Disease. *Archives of Internal Medicine* 159:2647–2658. <https://doi.org/10.1001/archinte.159.22.2647>
- Höglund E, Øverli Ø, Winberg S (2019) Tryptophan Metabolic Pathways and Brain Serotonergic Activity: A Comparative Review. *Front Endocrinol* 10:. <https://doi.org/10.3389/fendo.2019.00158>
- Hollis JL, Craig LC, Whybrow S, et al (2017) Assessing the relative validity of the Scottish Collaborative Group FFQ for measuring dietary intake in adults. *Public Health Nutrition* 20:449–455. <https://doi.org/10.1017/S1368980016002421>
- Holscher HD, Caporaso JG, Hooda S, et al (2015) Fiber supplementation influences phylogenetic structure and functional capacity of the human intestinal microbiome: follow-up of a randomized controlled trial. *Am J Clin Nutr* 101:55–64. <https://doi.org/10.3945/ajcn.114.092064>
- Hong H, Kim BS, Im H-I (2016) Pathophysiological Role of Neuroinflammation in Neurodegenerative Diseases and Psychiatric Disorders. *Int Neurourol J* 20:S2-7. <https://doi.org/10.5213/inj.1632604.302>
- Hornedo-Ortega R, Cerezo AB, de Pablos RM, et al (2018) Phenolic Compounds Characteristic of the Mediterranean Diet in Mitigating Microglia-Mediated Neuroinflammation. *Front Cell Neurosci* 12:373. <https://doi.org/10.3389/fncel.2018.00373>
- Hou K, Wu Z-X, Chen X-Y, et al (2022) Microbiota in health and diseases. *Sig Transduct Target Ther* 7:1–28. <https://doi.org/10.1038/s41392-022-00974-4>
- Hou Y-C, Lu K-C, Huang C-L, et al (2021) Serum albumin and indoxyl sulfate were predictive of cognitive impairment via amyloid beta and tauopathy, respectively, in end-stage renal disease patients. *Alzheimer's & Dementia* 17:e053921. <https://doi.org/10.1002/alz.053921>
- Hoyle L, Jiménez-Pranteda ML, Chilloux J, et al (2018a) Metabolic retroconversion of trimethylamine N-oxide and the gut microbiota. *Microbiome* 6:73. <https://doi.org/10.1186/s40168-018-0461-0>
- Hoyle L, Pontifex M, Rodriguez-Ramiro I, et al (2021) Regulation of blood-brain barrier integrity and cognition by the microbiome-associated methylamines trimethylamine N-oxide and trimethylamine. <https://doi.org/10.1101/2021.01.28.428430>
- Hoyle L, Snelling T, Umlai U-K, et al (2018b) Microbiome–host systems interactions: protective effects of propionate upon the blood–brain barrier. *Microbiome* 6:55. <https://doi.org/10.1186/s40168-018-0439-y>
- Hubbard T, Murray I, Bisson W, et al (2015) Adaptation of the human aryl hydrocarbon receptor to sense microbiota-derived indoles. *Scientific Reports* 5:. <https://doi.org/10.1038/srep12689>
- Huc T, Drapala A, Gawrys M, et al (2018) Chronic, low-dose TMAO treatment reduces diastolic dysfunction and heart fibrosis in hypertensive rats. *Am J Physiol Heart Circ Physiol* 315:H1805–H1820. <https://doi.org/10.1152/ajpheart.00536.2018>

- Hughes MM, Carballedo A, McLoughlin DM, et al (2012) Tryptophan depletion in depressed patients occurs independent of kynurenine pathway activation. *Brain Behav Immun* 26:979–987. <https://doi.org/10.1016/j.bbi.2012.05.010>
- Hung P-H, Yeh C-C, Hsiao C-Y, et al (2017) End stage renal disease is associated with development of dementia. *Oncotarget* 8:107348–107355. <https://doi.org/10.18632/oncotarget.22458>
- Hunt T, Pontifex MG, Vauzour D (2024) (Poly)phenols and brain health – beyond their antioxidant capacity. *FEBS Letters* n/a: <https://doi.org/10.1002/1873-3468.14988>
- Hwang IK, Yoo K-Y, Li H, et al (2009) Indole-3-propionic acid attenuates neuronal damage and oxidative stress in the ischemic hippocampus. *J Neurosci Res* 87:2126–2137. <https://doi.org/10.1002/jnr.22030>
- Hwu P, Du MX, Lapointe R, et al (2000) Indoleamine 2,3-dioxygenase production by human dendritic cells results in the inhibition of T cell proliferation. *J Immunol* 164:3596–3599. <https://doi.org/10.4049/jimmunol.164.7.3596>
- Ignacio Barrasa J, Olmo N, Pérez-Ramos P, et al (2011) Deoxycholic and chenodeoxycholic bile acids induce apoptosis via oxidative stress in human colon adenocarcinoma cells. *Apoptosis* 16:1054–1067. <https://doi.org/10.1007/s10495-011-0633-x>
- Igudesman D, Crandell J, Corbin KD, et al (2022) The Intestinal Microbiota and Short-Chain Fatty Acids in Association with Advanced Metrics of Glycemia and Adiposity Among Young Adults with Type 1 Diabetes and Overweight or Obesity. *Current Developments in Nutrition* 6:nzac107. <https://doi.org/10.1093/cdn/nzac107>
- Iqbal I, Wilairatana P, Saqib F, et al (2023) Plant Polyphenols and Their Potential Benefits on Cardiovascular Health: A Review. *Molecules* 28:. <https://doi.org/10.3390/molecules28176403>
- Irvin A, Cockburn A, Primerano DA, et al (2017) Diet-Induced Alteration of the Murine Intestinal Microbiome Following Antibiotic Ablation. *Advances in Microbiology* 7:545–564. <https://doi.org/10.4236/aim.2017.77043>
- Irvine MA, Scholey A, King R, et al (2018) The Cognitive Ageing, Nutrition and Neurogenesis (CANN) trial: Design and progress. *Alzheimers Dement (N Y)* 4:591–601. <https://doi.org/10.1016/j.trci.2018.08.001>
- Irwin K, Sexton C, Daniel T, et al (2018) Healthy Aging and Dementia: Two Roads Diverging in Midlife? *Front Aging Neurosci* 10:275. <https://doi.org/10.3389/fnagi.2018.00275>
- Itoh Y, Ezawa A, Kikuchi K, et al (2012) Protein-bound uremic toxins in hemodialysis patients measured by liquid chromatography/tandem mass spectrometry and their effects on endothelial ROS production. *Anal Bioanal Chem* 403:1841–1850. <https://doi.org/10.1007/s00216-012-5929-3>
- Iwata K, Watanabe H, Morisaki T, et al (2007) Involvement of indoxyl sulfate in renal and central nervous system toxicities during cisplatin-induced acute renal failure. *Pharm Res* 24:662–671. <https://doi.org/10.1007/s11095-006-9183-2>

- Jacka FN, Kremer PJ, Leslie ER, et al (2010) Associations between diet quality and depressed mood in adolescents: results from the Australian Healthy Neighbourhoods Study. *Aust N Z J Psychiatry* 44:435–442. <https://doi.org/10.3109/00048670903571598>
- Jacobs HIL, Becker JA, Kwong K, et al (2021) In vivo and neuropathology data support locus coeruleus integrity as indicator of Alzheimer’s disease pathology and cognitive decline. *Sci Transl Med* 13:eabj2511. <https://doi.org/10.1126/scitranslmed.abj2511>
- Jama JW, Launer LJ, Witteman JC, et al (1996) Dietary antioxidants and cognitive function in a population-based sample of older persons. The Rotterdam Study. *Am J Epidemiol* 144:275–280. <https://doi.org/10.1093/oxfordjournals.aje.a008922>
- Janeiro MH, Ramírez MJ, Milagro FI, et al (2018) Implication of Trimethylamine N-Oxide (TMAO) in Disease: Potential Biomarker or New Therapeutic Target. *Nutrients* 10:. <https://doi.org/10.3390/nu10101398>
- Jang D, Shin J, Shim E, et al (2024) The connection between aging, cellular senescence and gut microbiome alterations: A comprehensive review. *Aging Cell* 23:e14315. <https://doi.org/10.1111/accel.14315>
- Jawabri KH, Sharma S (2022) Physiology, Cerebral Cortex Functions. In: StatPearls. StatPearls Publishing, Treasure Island (FL)
- Jelleschitz J, Zhang Y, Grune T, et al (2022) Methionine restriction - Association with redox homeostasis and implications on aging and diseases. *Redox Biol* 57:102464. <https://doi.org/10.1016/j.redox.2022.102464>
- Jena PK, Sheng L, Di Lucente J, et al (2018) Dysregulated bile acid synthesis and dysbiosis are implicated in Western diet-induced systemic inflammation, microglial activation, and reduced neuroplasticity. *FASEB J* 32:2866–2877. <https://doi.org/10.1096/fj.201700984RR>
- Jenkins TA, Nguyen JCD, Polglaze KE, Bertrand PP (2016) Influence of Tryptophan and Serotonin on Mood and Cognition with a Possible Role of the Gut-Brain Axis. *Nutrients* 8:. <https://doi.org/10.3390/nu8010056>
- Jeong W, Lee H, Cho S, Seo J (2019) ApoE4-Induced Cholesterol Dysregulation and Its Brain Cell Type-Specific Implications in the Pathogenesis of Alzheimer’s Disease. *Mol Cells* 42:739–746. <https://doi.org/10.14348/molcells.2019.0200>
- Jia B, Wu Y, Zhou Y (2014) 14-3-3 and aggresome formation: implications in neurodegenerative diseases. *Prion* 8:173–177. <https://doi.org/10.4161/pri.28123>
- Jia J, Hu J, Huo X, et al (2019) Effects of vitamin D supplementation on cognitive function and blood A β -related biomarkers in older adults with Alzheimer’s disease: a randomised, double-blind, placebo-controlled trial. *J Neurol Neurosurg Psychiatry* 90:1347–1352. <https://doi.org/10.1136/jnnp-2018-320199>
- Jia S, Lu Z, Gao Z, et al (2016) Chitosan oligosaccharides alleviate cognitive deficits in an amyloid- β 1-42-induced rat model of Alzheimer’s disease. *Int J Biol Macromol* 83:416–425. <https://doi.org/10.1016/j.ijbiomac.2015.11.011>

- Jia X, Craig LCA, Aucott LS, et al (2008) Repeatability and validity of a food frequency questionnaire in free-living older people in relation to cognitive function. *The Journal of nutrition, health and aging* 12:735–741. <https://doi.org/10.1007/BF03028622>
- Jiang C, Wang S, Wang Y, et al (2024) Polyphenols from hickory nut reduce the occurrence of atherosclerosis in mice by improving intestinal microbiota and inhibiting trimethylamine N-oxide production. *Phytomedicine* 128:155349. <https://doi.org/10.1016/j.phymed.2024.155349>
- Jin Q, Black A, Kales SN, et al (2019) Metabolomics and Microbiomes as Potential Tools to Evaluate the Effects of the Mediterranean Diet. *Nutrients* 11:207. <https://doi.org/10.3390/nu11010207>
- Johansson M, Stomrud E, Lindberg O, et al (2020) Apathy and anxiety are early markers of Alzheimer's disease. *Neurobiol Aging* 85:74–82. <https://doi.org/10.1016/j.neurobiolaging.2019.10.008>
- Joly A, Leulier F, Vadder FD (2021) Microbial Modulation of the Development and Physiology of the Enteric Nervous System. *Trends in Microbiology* 29:686–699. <https://doi.org/10.1016/j.tim.2020.11.007>
- Jones DT, Machulda MM, Vemuri P, et al (2011) Age-related changes in the default mode network are more advanced in Alzheimer disease. *Neurology* 77:1524–1531. <https://doi.org/10.1212/WNL.0b013e318233b33d>
- Jones SV, Kounatidis I (2017) Nuclear Factor-Kappa B and Alzheimer Disease, Unifying Genetic and Environmental Risk Factors from Cell to Humans. *Front Immunol* 8:1805. <https://doi.org/10.3389/fimmu.2017.01805>
- Joo SS, Won TJ, Lee DI (2004) Potential role of ursodeoxycholic acid in suppression of Nuclear factor kappa B in microglial cell line (BV-2). *Arch Pharm Res* 27:954. <https://doi.org/10.1007/BF02975850>
- Joseph J, Cole G, Head E, Ingram D (2009) Nutrition, brain aging, and neurodegeneration. *J Neurosci* 29:12795–12801. <https://doi.org/10.1523/JNEUROSCI.3520-09.2009>
- Joshi G, Johnson JA (2012) The Nrf2-ARE pathway: a valuable therapeutic target for the treatment of neurodegenerative diseases. *Recent Pat CNS Drug Discov* 7:218–229. <https://doi.org/10.2174/157488912803252023>
- Kaddurah-Daouk R, Zhu H, Sharma S, et al (2013) Alterations in metabolic pathways and networks in Alzheimer's disease. *Transl Psychiatry* 3:e244. <https://doi.org/10.1038/tp.2013.18>
- Kaltschmidt B, Kaltschmidt C (2009) NF-kappaB in the nervous system. *Cold Spring Harb Perspect Biol* 1:a001271. <https://doi.org/10.1101/cshperspect.a001271>
- Kamp F, Hamilton JA, Kamp F, et al (1993) Movement of fatty acids, fatty acid analogues, and bile acids across phospholipid bilayers. *Biochemistry* 32:11074–11086. <https://doi.org/10.1021/bi00092a017>
- Karbowska M, Hermanowicz JM, Tankiewicz-Kwedlo A, et al (2020) Neurobehavioral effects of uremic toxin–indoxyl sulfate in the rat model. *Sci Rep* 10:9483. <https://doi.org/10.1038/s41598-020-66421-y>

- Karran E, Mercken M, Strooper BD (2011) The amyloid cascade hypothesis for Alzheimer's disease: an appraisal for the development of therapeutics. *Nat Rev Drug Discov* 10:698–712. <https://doi.org/10.1038/nrd3505>
- Keller J, Gomez R, Williams G, et al (2017) HPA axis in major depression: cortisol, clinical symptomatology and genetic variation predict cognition. *Mol Psychiatry* 22:527–536. <https://doi.org/10.1038/mp.2016.120>
- Kelly DM, Rothwell PM (2022) Disentangling the Relationship Between Chronic Kidney Disease and Cognitive Disorders. *Front Neurol* 13:. <https://doi.org/10.3389/fneur.2022.830064>
- Kennedy DO, Haskell CF (2011) Vitamins and Cognition. *Drugs* 71:1957–1971. <https://doi.org/10.2165/11594130-000000000-00000>
- Keszycki R, Rodriguez G, Dunn JT, et al (2023) Characterization of apathy-like behaviors in the 5xFAD mouse model of Alzheimer's disease. *Neurobiology of Aging* 126:113–122. <https://doi.org/10.1016/j.neurobiolaging.2023.02.012>
- Kim C-S, Jung S, Hwang G-S, Shin D-M (2023) Gut microbiota indole-3-propionic acid mediates neuroprotective effect of probiotic consumption in healthy elderly: A randomized, double-blind, placebo-controlled, multicenter trial and in vitro study. *Clinical Nutrition* 42:1025–1033. <https://doi.org/10.1016/j.clnu.2023.04.001>
- Kim DK, Han D, Park J, et al (2019) Deep proteome profiling of the hippocampus in the 5XFAD mouse model reveals biological process alterations and a novel biomarker of Alzheimer's disease. *Exp Mol Med* 51:1–17. <https://doi.org/10.1038/s12276-019-0326-z>
- Kim K-A, Jeong J-J, Yoo S-Y, Kim D-H (2016) Gut microbiota lipopolysaccharide accelerates inflammaging in mice. *BMC Microbiol* 16:9. <https://doi.org/10.1186/s12866-016-0625-7>
- Kim L-J, Chalmers TJ, Smith GC, et al (2020) Nicotinamide mononucleotide (NMN) deamidation by the gut microbiome and evidence for indirect upregulation of the NAD+ metabolome. *bioRxiv* 2020.09.10.289561. <https://doi.org/10.1101/2020.09.10.289561>
- Kiraly M, Foss JF, Giordano T (2023) Neuroinflammation, Its Role in Alzheimer's Disease and Therapeutic Strategies. *J Prev Alzheimers Dis* 10:686–698. <https://doi.org/10.14283/jpad.2023.109>
- Kivipelto M, Helkala E-L, Laakso MP, et al (2001) Midlife vascular risk factors and Alzheimer's disease in later life: longitudinal, population based study. *BMJ* 322:1447–1451. <https://doi.org/10.1136/bmj.322.7300.1447>
- Klein C, Roussel G, Brun S, et al (2018) 5-HIAA induces neprilysin to ameliorate pathophysiology and symptoms in a mouse model for Alzheimer's disease. *Acta Neuropathologica Communications* 6:136. <https://doi.org/10.1186/s40478-018-0640-z>
- Knopman D, Boland LL, Mosley T, et al (2001) Cardiovascular risk factors and cognitive decline in middle-aged adults. *Neurology* 56:42–48. <https://doi.org/10.1212/WNL.56.1.42>
- Koeth RA, Wang Z, Levison BS, et al (2013) Intestinal microbiota metabolism of L-carnitine, a nutrient in red meat, promotes atherosclerosis. *Nat Med* 19:576–585. <https://doi.org/10.1038/nm.3145>

- Kosyreva AM, Sentyabreva AV, Tsvetkov IS, Makarova OV (2022) Alzheimer's Disease and Inflammaging. *Brain Sci* 12:1237. <https://doi.org/10.3390/brainsci12091237>
- Kotti TJ, Ramirez DMO, Pfeiffer BE, et al (2006) Brain cholesterol turnover required for geranylgeraniol production and learning in mice. *Proc Natl Acad Sci U S A* 103:3869–3874. <https://doi.org/10.1073/pnas.0600316103>
- Kovatcheva-Datchary P, Nilsson A, Akrami R, et al (2015) Dietary Fiber-Induced Improvement in Glucose Metabolism Is Associated with Increased Abundance of *Prevotella*. *Cell Metab* 22:971–982. <https://doi.org/10.1016/j.cmet.2015.10.001>
- Kowalski K, Mulak A (2019) Brain-Gut-Microbiota Axis in Alzheimer's Disease. *J Neurogastroenterol Motil* 25:48–60. <https://doi.org/10.5056/jnm18087>
- Krikorian R, Nash TA, Shidler MD, et al (2010a) Concord grape juice supplementation improves memory function in older adults with mild cognitive impairment. *Br J Nutr* 103:730–734. <https://doi.org/10.1017/S0007114509992364>
- Krikorian R, Shidler MD, Nash TA, et al (2010b) Blueberry supplementation improves memory in older adults. *J Agric Food Chem* 58:3996–4000. <https://doi.org/10.1021/jf9029332>
- Kroenke K, Spitzer RL, Williams JBW (2001) The PHQ-9: Validity of a Brief Depression Severity Measure. *Journal of General Internal Medicine* 16:606. <https://doi.org/10.1046/j.1525-1497.2001.016009606.x>
- Kuang J, Wang J, Li Y, et al (2023) Hyodeoxycholic acid alleviates non-alcoholic fatty liver disease through modulating the gut-liver axis. *Cell Metab* 35:1752-1766.e8. <https://doi.org/10.1016/j.cmet.2023.07.011>
- Kuleshov MV, Jones MR, Rouillard AD, et al (2016) Enrichr: a comprehensive gene set enrichment analysis web server 2016 update. *Nucleic Acids Res* 44:W90–W97. <https://doi.org/10.1093/nar/gkw377>
- Kumar R, Rajkumar H, Kumar M, et al (2013) Molecular cloning, characterization and heterologous expression of bile salt hydrolase (Bsh) from *Lactobacillus fermentum* NCDO394. *Mol Biol Rep* 40:5057–5066. <https://doi.org/10.1007/s11033-013-2607-2>
- Lai JS, Hiles S, Bisquera A, et al (2014) A systematic review and meta-analysis of dietary patterns and depression in community-dwelling adults. *Am J Clin Nutr* 99:181–197. <https://doi.org/10.3945/ajcn.113.069880>
- Láng L, McArthur S, Lazar AS, et al (2024) Dietary (Poly)phenols and the Gut–Brain Axis in Ageing. *Nutrients* 16:1500. <https://doi.org/10.3390/nu16101500>
- Laukens D, Brinkman BM, Raes J, et al (2016) Heterogeneity of the gut microbiome in mice: guidelines for optimizing experimental design. *FEMS Microbiol Rev* 40:117–132. <https://doi.org/10.1093/femsre/fuv036>
- Lay C, Sutren M, Rochet V, et al (2005) Design and validation of 16S rRNA probes to enumerate members of the *Clostridium leptum* subgroup in human faecal microbiota. *Environ Microbiol* 7:933–946. <https://doi.org/10.1111/j.1462-2920.2005.00763.x>

- Le Gall G, Noor SO, Ridgway K, et al (2011) Metabolomics of fecal extracts detects altered metabolic activity of gut microbiota in ulcerative colitis and irritable bowel syndrome. *J Proteome Res* 10:4208–4218. <https://doi.org/10.1021/pr2003598>
- Lee FY, Lee H, Hubbert ML, et al (2006) FXR, a multipurpose nuclear receptor. *Trends Biochem Sci* 31:572–580. <https://doi.org/10.1016/j.tibs.2006.08.002>
- Leeming ER, Johnson AJ, Spector TD, Le Roy CI (2019) Effect of Diet on the Gut Microbiota: Rethinking Intervention Duration. *Nutrients* 11:2862. <https://doi.org/10.3390/nu11122862>
- Lefèvre-Arbogast S, Thomas A, Samieri C (2022) Dietary factors and brain health. *Curr Opin Lipidol* 33:25–30. <https://doi.org/10.1097/MOL.0000000000000803>
- Leger M, Quiedeville A, Bouet V, et al (2013) Object recognition test in mice. *Nat Protoc* 8:2531–2537. <https://doi.org/10.1038/nprot.2013.155>
- Leloup C, Magnan C, Benani A, et al (2006) Mitochondrial reactive oxygen species are required for hypothalamic glucose sensing. *Diabetes* 55:2084–2090. <https://doi.org/10.2337/db06-0086>
- Leong SC, Sirich TL (2016) Indoxyl Sulfate—Review of Toxicity and Therapeutic Strategies. *Toxins* 8:358. <https://doi.org/10.3390/toxins8120358>
- Levkovitz Y, Richter-Levin G, Segal M (1994) Effect of 5-hydroxytryptophane on behavior and hippocampal physiology in young and old rats. *Neurobiol Aging* 15:635–641. [https://doi.org/10.1016/0197-4580\(94\)00058-1](https://doi.org/10.1016/0197-4580(94)00058-1)
- Lewis F, Karlsberg Schaffer S, Sussex J, et al (2014) The Trajectory of Dementia in the UK - Making a Difference. Office of Health Economics
- Li B, He Y, Ma J, et al (2019) Mild cognitive impairment has similar alterations as Alzheimer’s disease in gut microbiota. *Alzheimer’s & Dementia* 15:1357–1366. <https://doi.org/10.1016/j.jalz.2019.07.002>
- Li D, Ke Y, Zhan R, et al (2018a) Trimethylamine-N-oxide promotes brain aging and cognitive impairment in mice. *Aging Cell* 17:. <https://doi.org/10.1111/accel.12768>
- Li S, Shao Y, Li K, et al (2018b) Vascular Cognitive Impairment and the Gut Microbiota. *J Alzheimers Dis* 63:1209–1222. <https://doi.org/10.3233/JAD-171103>
- Li Y, Hao Y, Zhu J, Owyang C (2000) Serotonin released from intestinal enterochromaffin cells mediates luminal non-cholecystokinin-stimulated pancreatic secretion in rats. *Gastroenterology* 118:1197–1207. [https://doi.org/10.1016/S0016-5085\(00\)70373-8](https://doi.org/10.1016/S0016-5085(00)70373-8)
- Li Y, Rahman SU, Huang Y, et al (2020) Green tea polyphenols decrease weight gain, ameliorate alteration of gut microbiota, and mitigate intestinal inflammation in canines with high-fat-diet-induced obesity. *J Nutr Biochem* 78:108324. <https://doi.org/10.1016/j.jnutbio.2019.108324>
- Liabeuf S, Glorieux G, Lenglet A, et al (2013) Does P-Cresylglucuronide Have the Same Impact on Mortality as Other Protein-Bound Uremic Toxins? *PLOS ONE* 8:e67168. <https://doi.org/10.1371/journal.pone.0067168>

- Liao Y, Smyth GK, Shi W (2014) featureCounts: an efficient general purpose program for assigning sequence reads to genomic features. *Bioinformatics* 30:923–930. <https://doi.org/10.1093/bioinformatics/btt656>
- Liaw A, Wiener M (2001) Classification and Regression by RandomForest. *Forest* 23:
- Liebau C, Baltzer AWA, Schmidt S, et al (2002) Interleukin-12 and interleukin-18 induce indoleamine 2,3-dioxygenase (IDO) activity in human osteosarcoma cell lines independently from interferon-gamma. *Anticancer Res* 22:931–936
- Lin C-H, Lin Y-N, Lane H-Y, Chen C-J (2023) The identification of a potential plasma metabolite marker for Alzheimer’s disease by LC-MS untargeted metabolomics. *Journal of Chromatography B* 1222:123686. <https://doi.org/10.1016/j.jchromb.2023.123686>
- Lin X, Liu Y, Ma L, et al (2021) Constipation induced gut microbiota dysbiosis exacerbates experimental autoimmune encephalomyelitis in C57BL/6 mice. *J Transl Med* 19:317. <https://doi.org/10.1186/s12967-021-02995-z>
- Ling Z, Zhu M, Yan X, et al (2021) Structural and Functional Dysbiosis of Fecal Microbiota in Chinese Patients With Alzheimer’s Disease. *Frontiers in Cell and Developmental Biology* 8:
- Liu C-C, Kanekiyo T, Xu H, Bu G (2013) Apolipoprotein E and Alzheimer disease: risk, mechanisms, and therapy. *Nat Rev Neurol* 9:106–118. <https://doi.org/10.1038/nrneurol.2012.263>
- Liu M, Wang J, Zeng J, He Y (2017) Relationship between serum uric acid level and mild cognitive impairment in Chinese community elderly. *BMC Neurology* 17:146. <https://doi.org/10.1186/s12883-017-0929-8>
- Liu P, Ewald J, Pang Z, et al (2023) ExpressAnalyst: A unified platform for RNA-sequencing analysis in non-model species. *Nat Commun* 14:2995. <https://doi.org/10.1038/s41467-023-38785-y>
- Liu P, Wu L, Peng G, et al (2019) Altered microbiomes distinguish Alzheimer’s disease from amnesic mild cognitive impairment and health in a Chinese cohort. *Brain, Behavior, and Immunity* 80:633–643. <https://doi.org/10.1016/j.bbi.2019.05.008>
- Liu S, Gao J, Zhu M, et al (2020) Gut Microbiota and Dysbiosis in Alzheimer’s Disease: Implications for Pathogenesis and Treatment. *Mol Neurobiol* 57:5026–5043. <https://doi.org/10.1007/s12035-020-02073-3>
- Liu W, Tomino Y, Lu K (2018a) Impacts of Indoxyl Sulfate and p-Cresol Sulfate on Chronic Kidney Disease and Mitigating Effects of AST-120. *Toxins* 10:.. <https://doi.org/10.3390/toxins10090367>
- Liu X, Cao S, Zhang X (2015) Modulation of Gut Microbiota–Brain Axis by Probiotics, Prebiotics, and Diet. *J Agric Food Chem* 63:7885–7895. <https://doi.org/10.1021/acs.jafc.5b02404>
- Liu Y, Li N, Zhou L, et al (2014) Plasma metabolic profiling of mild cognitive impairment and Alzheimer’s disease using liquid chromatography/mass spectrometry. *Cent Nerv Syst Agents Med Chem* 14:113–120. <https://doi.org/10.2174/1871524915666141216161246>
- Liu Y, Wei M, Yue K, et al (2018b) Study on Urine Metabolic Profile of A β 25–35-Induced Alzheimer’s Disease Using UHPLC-Q-TOF-MS. *Neuroscience* 394:30–43. <https://doi.org/10.1016/j.neuroscience.2018.10.001>

- Livingston G, Huntley J, Liu KY, et al (2024) Dementia prevention, intervention, and care: 2024 report of the Lancet standing Commission. *The Lancet* 404:572–628. [https://doi.org/10.1016/S0140-6736\(24\)01296-0](https://doi.org/10.1016/S0140-6736(24)01296-0)
- Lo AC, Callaerts-Vegh Z, Nunes AF, et al (2013) Tauroursodeoxycholic acid (TUDCA) supplementation prevents cognitive impairment and amyloid deposition in APP/PS1 mice. *Neurobiology of Disease* 50:21–29. <https://doi.org/10.1016/j.nbd.2012.09.003>
- Lopez-Ramirez MA, Fischer R, Torres-Badillo CC, et al (2012) Role of Caspases in Cytokine-Induced Barrier Breakdown in Human Brain Endothelial Cells. *The Journal of Immunology* 189:3130–3139. <https://doi.org/10.4049/jimmunol.1103460>
- Lopresti AL, Smith SJ, Pouchieu C, et al (2023) Effects of a polyphenol-rich grape and blueberry extract (Memophenol™) on cognitive function in older adults with mild cognitive impairment: A randomized, double-blind, placebo-controlled study. *Front Psychol* 14:1144231. <https://doi.org/10.3389/fpsyg.2023.1144231>
- Loughrey DG, Lavecchia S, Brennan S, et al (2017) The Impact of the Mediterranean Diet on the Cognitive Functioning of Healthy Older Adults: A Systematic Review and Meta-Analysis. *Adv Nutr* 8:571–586. <https://doi.org/10.3945/an.117.015495>
- Lovelace MD, Varney B, Sundaram G, et al (2017) Recent evidence for an expanded role of the kynurenine pathway of tryptophan metabolism in neurological diseases. *Neuropharmacology* 112:373–388. <https://doi.org/10.1016/j.neuropharm.2016.03.024>
- Lu K, Abo RP, Schlieper KA, et al (2014) Arsenic exposure perturbs the gut microbiome and its metabolic profile in mice: an integrated metagenomics and metabolomics analysis. *Environ Health Perspect* 122:284–291. <https://doi.org/10.1289/ehp.1307429>
- Luan H, Wang X, Cai Z (2019) Mass spectrometry-based metabolomics: Targeting the crosstalk between gut microbiota and brain in neurodegenerative disorders. *Mass Spectrom Rev* 38:22–33. <https://doi.org/10.1002/mas.21553>
- Luczynski P, McVey Neufeld K-A, Oriach CS, et al (2016) Growing up in a Bubble: Using Germ-Free Animals to Assess the Influence of the Gut Microbiota on Brain and Behavior. *International Journal of Neuropsychopharmacology* 19:. <https://doi.org/10.1093/ijnp/pyw020>
- Lugo-Huitrón R, Ugalde Muñiz P, Pineda B, et al (2013) Quinolinic Acid: An Endogenous Neurotoxin with Multiple Targets. *Oxid Med Cell Longev* 2013:. <https://doi.org/10.1155/2013/104024>
- Lukić I, Getselter D, Koren O, Elliott E (2019) Role of Tryptophan in Microbiota-Induced Depressive-Like Behavior: Evidence From Tryptophan Depletion Study. *Frontiers in Behavioral Neuroscience* 13:123. <https://doi.org/10.3389/fnbeh.2019.00123>
- Lundstrom RC, Racicot LD (1983) Gas chromatographic determination of dimethylamine and trimethylamine in seafoods. *J Assoc Off Anal Chem* 66:1158–1163
- Lupp C, Robertson ML, Wickham ME, et al (2007) Host-mediated inflammation disrupts the intestinal microbiota and promotes the overgrowth of Enterobacteriaceae. *Cell Host Microbe* 2:119–129. <https://doi.org/10.1016/j.chom.2007.06.010>

- Lyte JM, Gheorghe CE, Goodson MS, et al (2020) Gut-brain axis serotonergic responses to acute stress exposure are microbiome-dependent. *Neurogastroenterology & Motility* 32:e13881. <https://doi.org/10.1111/nmo.13881>
- Ma L, Sun Z, Zeng Y, et al (2018) Molecular Mechanism and Health Role of Functional Ingredients in Blueberry for Chronic Disease in Human Beings. *Int J Mol Sci* 19:2785. <https://doi.org/10.3390/ijms19092785>
- Macpherson ME, Hov JR, Ueland T, et al (2020) Gut Microbiota-Dependent Trimethylamine N-Oxide Associates With Inflammation in Common Variable Immunodeficiency. *Front Immunol* 11:574500. <https://doi.org/10.3389/fimmu.2020.574500>
- MahmoudianDehkordi S, Arnold M, Nho K, et al (2019) Altered bile acid profile associates with cognitive impairment in Alzheimer's disease-An emerging role for gut microbiome. *Alzheimer's & Dementia: The Journal of the Alzheimer's Association* 15:76–92. <https://doi.org/10.1016/j.jalz.2018.07.217>
- Manji Z, Rojas A, Wang W, et al (2019) 5xFAD mice display sex-dependent inflammatory gene induction during the prodromal stage of Alzheimer's disease. *J Alzheimers Dis* 70:1259–1274. <https://doi.org/10.3233/JAD-180678>
- Mano N, Goto T, Uchida M, et al (2004) Presence of protein-bound unconjugated bile acids in the cytoplasmic fraction of rat brain. *J Lipid Res* 45:295–300. <https://doi.org/10.1194/jlr.M300369-JLR200>
- Mapstone M, Cheema AK, Fiandaca MS, et al (2014) Plasma phospholipids identify antecedent memory impairment in older adults. *Nature Medicine* 20:415–418. <https://doi.org/10.1038/nm.3466>
- Marcelin G, Jo Y-H, Li X, et al (2014) Central action of FGF19 reduces hypothalamic AGRP/NPY neuron activity and improves glucose metabolism. *Molecular Metabolism* 3:19–28. <https://doi.org/10.1016/j.molmet.2013.10.002>
- Marizzoni M, Cattaneo A, Mirabelli P, et al (2020) Short-Chain Fatty Acids and Lipopolysaccharide as Mediators Between Gut Dysbiosis and Amyloid Pathology in Alzheimer's Disease. *J Alzheimers Dis* 78:683–697. <https://doi.org/10.3233/JAD-200306>
- Marksteiner J, Blasko I, Kemmler G, et al (2017) Bile acid quantification of 20 plasma metabolites identifies lithocholic acid as a putative biomarker in Alzheimer's disease. *Metabolomics* 14:1. <https://doi.org/10.1007/s11306-017-1297-5>
- Marrugo-Ramírez J, Rodríguez-Núñez M, Marco M-P, et al (2021) Kynurenic Acid Electrochemical Immunosensor: Blood-Based Diagnosis of Alzheimer's Disease. *Biosensors* 11:20. <https://doi.org/10.3390/bios11010020>
- Marshall KE, Vadukul DM, Dahal L, et al (2016) A critical role for the self-assembly of Amyloid- β 1-42 in neurodegeneration. *Sci Rep* 6:30182. <https://doi.org/10.1038/srep30182>
- Martini-Stoica H, Cole AL, Swartzlander DB, et al (2018) TFEB enhances astroglial uptake of extracellular tau species and reduces tau spreading. *J Exp Med* 215:2355–2377. <https://doi.org/10.1084/jem.20172158>

- Marx W, Scholey A, Firth J, et al (2020) Prebiotics, probiotics, fermented foods and cognitive outcomes: A meta-analysis of randomized controlled trials. *Neuroscience & Biobehavioral Reviews* 118:472–484. <https://doi.org/10.1016/j.neubiorev.2020.07.036>
- Mason J (2012) *Vitamins, Trace Minerals, and Other Micronutrients*. pp 1397–1406
- Matsumoto M, Kibe R, Ooga T, et al (2013) Cerebral low-molecular metabolites influenced by intestinal microbiota: a pilot study. *Front Syst Neurosci* 7:9. <https://doi.org/10.3389/fnsys.2013.00009>
- Mayer EA, Knight R, Mazmanian SK, et al (2014) Gut Microbes and the Brain: Paradigm Shift in Neuroscience. *J Neurosci* 34:15490–15496. <https://doi.org/10.1523/JNEUROSCI.3299-14.2014>
- Mazmanian SK, Liu CH, Tzianabos AO, Kasper DL (2005) An Immunomodulatory Molecule of Symbiotic Bacteria Directs Maturation of the Host Immune System. *Cell* 122:107–118. <https://doi.org/10.1016/j.cell.2005.05.007>
- McArthur S, Carvalho A, Fonseca S, et al (2018) Effects of gut-derived trimethylamines on the blood-brain barrier
- McMillin M, DeMorrow S (2016) Effects of bile acids on neurological function and disease. *FASEB J* 30:3658–3668. <https://doi.org/10.1096/fj.201600275R>
- Medeiros R, Baglietto-Vargas D, LaFerla FM (2010) The Role of Tau in Alzheimer’s Disease and Related Disorders. *CNS Neurosci Ther* 17:514–524. <https://doi.org/10.1111/j.1755-5949.2010.00177.x>
- Meert N, Schepers E, Glorieux G, et al (2012) Novel method for simultaneous determination of p -cresylsulphate and p -cresylglucuronide: clinical data and pathophysiological implications. *Nephrology Dialysis Transplantation* 27:2388–2396. <https://doi.org/10.1093/ndt/gfr672>
- Merra G, Noce A, Marrone G, et al (2020) Influence of Mediterranean Diet on Human Gut Microbiota. *Nutrients* 13:7. <https://doi.org/10.3390/nu13010007>
- Mertens KL, Kalsbeek A, Soeters MR, Eggink HM (2017) Bile Acid Signaling Pathways from the Enterohepatic Circulation to the Central Nervous System. *Front Neurosci* 11:. <https://doi.org/10.3389/fnins.2017.00617>
- Meslier V, Laiola M, Roager HM, et al (2020) Mediterranean diet intervention in overweight and obese subjects lowers plasma cholesterol and causes changes in the gut microbiome and metabolome independently of energy intake. *Gut* 69:1258–1268. <https://doi.org/10.1136/gutjnl-2019-320438>
- Metaxas A, Anzalone M, Vaitheeswaran R, et al (2019) Neuroinflammation and amyloid-beta 40 are associated with reduced serotonin transporter (SERT) activity in a transgenic model of familial Alzheimer’s disease. *Alzheimer’s Research & Therapy* 11:38. <https://doi.org/10.1186/s13195-019-0491-2>
- Miller MI, Ratnanather JT, Tward DJ, et al (2015) Network Neurodegeneration in Alzheimer’s Disease via MRI Based Shape Diffeomorphometry and High-Field Atlasing. *Frontiers in Bioengineering and Biotechnology* 3:54. <https://doi.org/10.3389/fbioe.2015.00054>

- Milte CM, Ball K, Crawford D, McNaughton SA (2019) Diet quality and cognitive function in mid-aged and older men and women. *BMC Geriatr* 19:361. <https://doi.org/10.1186/s12877-019-1326-5>
- Min YW, Rezaie A, Pimentel M (2022) Bile Acid and Gut Microbiota in Irritable Bowel Syndrome. *J Neurogastroenterol Motil* 28:549–561. <https://doi.org/10.5056/jnm22129>
- Minich WB (2022) Selenium Metabolism and Biosynthesis of Selenoproteins in the Human Body. *Biochemistry (Mosc)* 87:S168–S177. <https://doi.org/10.1134/S0006297922140139>
- Miquel S, Martín R, Rossi O, et al (2013) Faecalibacterium prausnitzii and human intestinal health. *Curr Opin Microbiol* 16:255–261. <https://doi.org/10.1016/j.mib.2013.06.003>
- Missailidis C, Hällqvist J, Qureshi AR, et al (2016) Serum Trimethylamine-N-Oxide Is Strongly Related to Renal Function and Predicts Outcome in Chronic Kidney Disease. *PLOS ONE* 11:e0141738. <https://doi.org/10.1371/journal.pone.0141738>
- Mitchell SC, Zhang AQ, Smith RL (2002) Chemical and Biological Liberation of Trimethylamine from Foods. *Journal of Food Composition and Analysis* 15:277–282. <https://doi.org/10.1006/jfca.2002.1068>
- Mithaiwala MN, Santana-Coelho D, Porter GA, O'Connor JC (2021) Neuroinflammation and the Kynurenine Pathway in CNS Disease: Molecular Mechanisms and Therapeutic Implications. *Cells* 10:1548. <https://doi.org/10.3390/cells10061548>
- Mithul Aravind S, Wichienchot S, Tsao R, et al (2021) Role of dietary polyphenols on gut microbiota, their metabolites and health benefits. *Food Research International* 142:110189. <https://doi.org/10.1016/j.foodres.2021.110189>
- Miyake A, Itoh N (1996) Rat fibroblast growth factor receptor-4 mRNA in the brain is preferentially expressed in cholinergic neurons in the medial habenular nucleus. *Neurosci Lett* 203:101–104. [https://doi.org/10.1016/0304-3940\(95\)12272-9](https://doi.org/10.1016/0304-3940(95)12272-9)
- Mohajeri MH (2019) Brain Aging and Gut–Brain Axis. *Nutrients* 11:424. <https://doi.org/10.3390/nu11020424>
- Moheet A, Mangia S, Seaquist E (2015) Impact of diabetes on cognitive function and brain structure. *Ann N Y Acad Sci* 1353:60–71. <https://doi.org/10.1111/nyas.12807>
- Moles L, Otaegui D (2020) The Impact of Diet on Microbiota Evolution and Human Health. Is Diet an Adequate Tool for Microbiota Modulation? *Nutrients* 12:1654. <https://doi.org/10.3390/nu12061654>
- Monteiro-Cardoso VF, Corliano M, Singaraja RR (2021) Bile Acids: A Communication Channel in the Gut-Brain Axis. *Neuromol Med* 23:99–117. <https://doi.org/10.1007/s12017-020-08625-z>
- Montes de Oca B P (2018) Flux-Independent NMDAR Signaling: Molecular Mediators, Cellular Functions, and Complexities. *International Journal of Molecular Sciences* 19:3800. <https://doi.org/10.3390/ijms19123800>
- Moreira PI, Carvalho C, Zhu X, et al (2010) Mitochondrial dysfunction is a trigger of Alzheimer's disease pathophysiology. *Biochim Biophys Acta* 1802:2–10. <https://doi.org/10.1016/j.bbadis.2009.10.006>

- Morrison KE, Jašarević E, Howard CD, Bale TL (2020) It's the fiber, not the fat: significant effects of dietary challenge on the gut microbiome. *Microbiome* 8:15. <https://doi.org/10.1186/s40168-020-0791-6>
- Mortamet B, Zeng D, Gerig G, et al (2005) Effects of Healthy Aging Measured By Intracranial Compartment Volumes Using a Designed MR Brain Database. *Med Image Comput Comput Assist Interv* 8:383–391
- Mortazavi A, Williams BA, McCue K, et al (2008) Mapping and quantifying mammalian transcriptomes by RNA-Seq. *Nat Methods* 5:621–628. <https://doi.org/10.1038/nmeth.1226>
- Mosconi L, Murray J, Tsui WH, et al (2014) Mediterranean Diet and Magnetic Resonance Imaging-Assessed Brain Atrophy in Cognitively Normal Individuals at Risk for Alzheimer's Disease. *J Prev Alzheimers Dis* 1:23–32
- Mueller M, Thorell A, Claudel T, et al (2015) Ursodeoxycholic acid exerts farnesoid X receptor-antagonistic effects on bile acid and lipid metabolism in morbid obesity. *J Hepatol* 62:1398–1404. <https://doi.org/10.1016/j.jhep.2014.12.034>
- Mukherjee A, Lordan C, Ross RP, Cotter PD (2020) Gut microbes from the phylogenetically diverse genus *Eubacterium* and their various contributions to gut health. *Gut Microbes* 12:1802866. <https://doi.org/10.1080/19490976.2020.1802866>
- Murman DL (2015) The Impact of Age on Cognition. *Semin Hear* 36:111–121. <https://doi.org/10.1055/s-0035-1555115>
- Mutha RE, Tatiya AU, Surana SJ (2021) Flavonoids as natural phenolic compounds and their role in therapeutics: an overview. *Futur J Pharm Sci* 7:25. <https://doi.org/10.1186/s43094-020-00161-8>
- Mutsaers HAM, Wilmer MJG, Reijnders D, et al (2013) Uremic toxins inhibit renal metabolic capacity through interference with glucuronidation and mitochondrial respiration. *Biochimica et Biophysica Acta (BBA) - Molecular Basis of Disease* 1832:142–150. <https://doi.org/10.1016/j.bbadis.2012.09.006>
- Nag S, Picard P, Stewart DJ (2001) Expression of nitric oxide synthases and nitrotyrosine during blood-brain barrier breakdown and repair after cold injury. *Lab Invest* 81:41–49. <https://doi.org/10.1038/labinvest.3780210>
- Nagpal R, Neth BJ, Wang S, et al (2020) Gut mycobiome and its interaction with diet, gut bacteria and alzheimer's disease markers in subjects with mild cognitive impairment: A pilot study. *EBioMedicine* 59:102950. <https://doi.org/10.1016/j.ebiom.2020.102950>
- Nagpal R, Neth BJ, Wang S, et al (2019) Modified Mediterranean-ketogenic diet modulates gut microbiome and short-chain fatty acids in association with Alzheimer's disease markers in subjects with mild cognitive impairment. *EBioMedicine* 47:529–542. <https://doi.org/10.1016/j.ebiom.2019.08.032>
- Nair AB, Jacob S (2016) A simple practice guide for dose conversion between animals and human. *J Basic Clin Pharm* 7:27–31. <https://doi.org/10.4103/0976-0105.177703>
- Nakano D, Kitada K, Wan N, et al (2020) Lipopolysaccharide induces filtrate leakage from renal tubular lumina into the interstitial space via a proximal tubular Toll-like receptor 4–

- dependent pathway and limits sensitivity to fluid therapy in mice. *Kidney International* 97:904–912. <https://doi.org/10.1016/j.kint.2019.11.024>
- Natividad JM, Lamas B, Pham HP, et al (2018) *Bilophila wadsworthia* aggravates high fat diet induced metabolic dysfunctions in mice. *Nat Commun* 9:2802. <https://doi.org/10.1038/s41467-018-05249-7>
- Naumann S, Schweiggert-Weisz U, Eglmeier J, et al (2019) In Vitro Interactions of Dietary Fibre Enriched Food Ingredients with Primary and Secondary Bile Acids. *Nutrients* 11:1424. <https://doi.org/10.3390/nu11061424>
- Needham BD, Funabashi M, Adame MD, et al (2022) A gut-derived metabolite alters brain activity and anxiety behaviour in mice. *Nature* 602:647–653. <https://doi.org/10.1038/s41586-022-04396-8>
- Needham BD, Kaddurah-Daouk R, Mazmanian SK (2020) Gut microbial molecules in behavioural and neurodegenerative conditions. *Nat Rev Neurosci* 21:717–731. <https://doi.org/10.1038/s41583-020-00381-0>
- Nelson AR, Sagare AP, Zlokovic BV (2017) Role of clusterin in the brain vascular clearance of amyloid- β . *Proceedings of the National Academy of Sciences* 114:8681–8682. <https://doi.org/10.1073/pnas.1711357114>
- Neshan M, Campbell A, Malakouti SK, et al (2020) Gene expression of serotonergic markers in peripheral blood mononuclear cells of patients with late-onset Alzheimer’s disease. *Heliyon* 6:e04716. <https://doi.org/10.1016/j.heliyon.2020.e04716>
- Neufeld KM, Kang N, Bienenstock J, Foster JA (2011) Reduced anxiety-like behavior and central neurochemical change in germ-free mice. *Neurogastroenterol Motil* 23:255–264, e119. <https://doi.org/10.1111/j.1365-2982.2010.01620.x>
- Neveu V, Perez-Jiménez J, Vos F, et al (2010) Phenol-Explorer: an online comprehensive database on polyphenol contents in foods. *Database (Oxford)* 2010:bap024. <https://doi.org/10.1093/database/bap024>
- Nho K, Kueider-Paisley A, MahmoudianDehkordi S, et al (2019) Altered Bile Acid Profile in Mild Cognitive Impairment and Alzheimer’s Disease: Relationship to Neuroimaging and CSF Biomarkers. *Alzheimers Dement* 15:232–244. <https://doi.org/10.1016/j.jalz.2018.08.012>
- Ni Y, Yu G, Chen H, et al (2020) M2IA: a web server for microbiome and metabolome integrative analysis. *Bioinformatics* 36:3493–3498. <https://doi.org/10.1093/bioinformatics/btaa188>
- Nicholson JK, Holmes E, Kinross J, et al (2012) Host-gut microbiota metabolic interactions. *Science* 336:1262–1267. <https://doi.org/10.1126/science.1223813>
- Nishimura M, Yaguti H, Yoshitsugu H, et al (2003) Tissue distribution of mRNA expression of human cytochrome P450 isoforms assessed by high-sensitivity real-time reverse transcription PCR. *Yakugaku Zasshi* 123:369–375. <https://doi.org/10.1248/yakushi.123.369>
- Nizamutdinov D, DeMorrow S, McMillin M, et al (2017) Hepatic alterations are accompanied by changes to bile acid transporter-expressing neurons in the hypothalamus after traumatic brain injury. *Scientific Reports* 7:40112. <https://doi.org/10.1038/srep40112>

- Nobili A, Latagliata EC, Viscomi MT, et al (2017) Dopamine neuronal loss contributes to memory and reward dysfunction in a model of Alzheimer's disease. *Nat Commun* 8:14727. <https://doi.org/10.1038/ncomms14727>
- Nunes AF, Amaral JD, Lo AC, et al (2012) TUDCA, a bile acid, attenuates amyloid precursor protein processing and amyloid- β deposition in APP/PS1 mice. *Mol Neurobiol* 45:440–454. <https://doi.org/10.1007/s12035-012-8256-y>
- Nurk E, Refsum H, Drevon CA, et al (2009) Intake of flavonoid-rich wine, tea, and chocolate by elderly men and women is associated with better cognitive test performance. *J Nutr* 139:120–127. <https://doi.org/10.3945/jn.108.095182>
- Nutaitis AC, Tharwani SD, Serra MC, et al (2019) Diet as a Risk Factor for Cognitive Decline in African Americans and Caucasians with a Parental History of Alzheimer's Disease: A Cross-Sectional Pilot Study Dietary Patterns. *J Prev Alzheimers Dis* 6:50–55. <https://doi.org/10.14283/jpad.2018.44>
- Oakley H, Cole SL, Logan S, et al (2006) Intraneuronal β -Amyloid Aggregates, Neurodegeneration, and Neuron Loss in Transgenic Mice with Five Familial Alzheimer's Disease Mutations: Potential Factors in Amyloid Plaque Formation. *J Neurosci* 26:10129–10140. <https://doi.org/10.1523/JNEUROSCI.1202-06.2006>
- Oblak AL, Lin PB, Kotredes KP, et al (2021) Comprehensive Evaluation of the 5XFAD Mouse Model for Preclinical Testing Applications: A MODEL-AD Study. *Frontiers in Aging Neuroscience* 13:
- Obrenovich MEM (2018) Leaky Gut, Leaky Brain? *Microorganisms* 6:107. <https://doi.org/10.3390/microorganisms6040107>
- Odamaki T, Kato K, Sugahara H, et al (2016) Age-related changes in gut microbiota composition from newborn to centenarian: a cross-sectional study. *BMC Microbiology* 16:90. <https://doi.org/10.1186/s12866-016-0708-5>
- Ojeda ML, Nogales F, López JAC, et al (2023) Microbiota-Liver-Bile Salts Axis, a Novel Mechanism Involved in the Contrasting Effects of Sodium Selenite and Selenium-Nanoparticle Supplementation on Adipose Tissue Development in Adolescent Rats. *Antioxidants* 12:. <https://doi.org/10.3390/antiox12051123>
- Olazarán J, Gil-de-Gómez L, Rodríguez-Martín A, et al (2015) A blood-based, 7-metabolite signature for the early diagnosis of Alzheimer's disease. *J Alzheimers Dis* 45:1157–1173. <https://doi.org/10.3233/JAD-142925>
- O'Leary F, Allman-Farinelli M, Samman S (2012) Vitamin B12 status, cognitive decline and dementia: a systematic review of prospective cohort studies. *British Journal of Nutrition* 108:1948–1961. <https://doi.org/10.1017/S0007114512004175>
- O'Leary TP, Mantolino HM, Stover KR, Brown RE (2020) Age-related deterioration of motor function in male and female 5xFAD mice from 3 to 16 months of age. *Genes Brain Behav* 19:e12538. <https://doi.org/10.1111/gbb.12538>
- O'Neil A, Quirk SE, Housden S, et al (2014) Relationship between diet and mental health in children and adolescents: a systematic review. *Am J Public Health* 104:e31-42. <https://doi.org/10.2105/AJPH.2014.302110>

- Org E, Blum Y, Kasela S, et al (2017) Relationships between gut microbiota, plasma metabolites, and metabolic syndrome traits in the METSIM cohort. *Genome Biol* 18:70. <https://doi.org/10.1186/s13059-017-1194-2>
- O’Riordan KJ, Collins MK, Moloney GM, et al (2022) Short chain fatty acids: Microbial metabolites for gut-brain axis signalling. *Molecular and Cellular Endocrinology* 546:111572. <https://doi.org/10.1016/j.mce.2022.111572>
- Ostapiuk A, Urbanska EM (2021) Kynurenic acid in neurodegenerative disorders—unique neuroprotection or double-edged sword? *CNS Neurosci Ther* 28:19–35. <https://doi.org/10.1111/cns.13768>
- O’Toole PW, Jeffery IB (2015) Gut microbiota and aging. *Science* 350:1214–1215. <https://doi.org/10.1126/science.aac8469>
- Ouweland AC, Salminen S, Isolauri E (2002) Probiotics: an overview of beneficial effects. *Antonie Van Leeuwenhoek* 82:279–289
- Ownby RL (2010) Neuroinflammation and cognitive aging. *Curr Psychiatry Rep* 12:39–45. <https://doi.org/10.1007/s11920-009-0082-1>
- Oxenkrug G (2013) Serotonin-kynurenine hypothesis of depression: historical overview and recent developments. *Curr Drug Targets* 14:514–521. <https://doi.org/10.2174/1389450111314050002>
- Pádua MS, Guil-Guerrero JL, Lopes PA (2024) Behaviour Hallmarks in Alzheimer’s Disease 5xFAD Mouse Model. *International Journal of Molecular Sciences* 25:6766. <https://doi.org/10.3390/ijms25126766>
- Pais ML, Martins J, Castelo-Branco M, Gonçalves J (2023) Sex Differences in Tryptophan Metabolism: A Systematic Review Focused on Neuropsychiatric Disorders. *International Journal of Molecular Sciences* 24:6010. <https://doi.org/10.3390/ijms24066010>
- Pan X, Elliott CT, McGuinness B, et al (2017) Metabolomic Profiling of Bile Acids in Clinical and Experimental Samples of Alzheimer’s Disease. *Metabolites* 7:. <https://doi.org/10.3390/metabo7020028>
- Pandey RS, Arnold M, Batra R, et al (2024) Metabolomics profiling reveals distinct, sex-specific signatures in serum and brain metabolomes in mouse models of Alzheimer’s disease. *Alzheimer’s & Dementia* 20:3987–4001. <https://doi.org/10.1002/alz.13851>
- Pang Z, Zhou G, Ewald J, et al (2022) Using MetaboAnalyst 5.0 for LC–HRMS spectra processing, multi-omics integration and covariate adjustment of global metabolomics data. *Nat Protoc* 17:1735–1761. <https://doi.org/10.1038/s41596-022-00710-w>
- Papandreou C, Moré M, Bellamine A (2020) Trimethylamine N-Oxide in Relation to Cardiometabolic Health—Cause or Effect? *Nutrients* 12:1330. <https://doi.org/10.3390/nu12051330>
- Park G-H, Cho J-H, Lee D, Kim Y (2022) Association between Seafood Intake and Cardiovascular Disease in South Korean Adults: A Community-Based Prospective Cohort Study. *Nutrients* 14:4864. <https://doi.org/10.3390/nu14224864>

- Parkhomchuk D, Borodina T, Amstislavskiy V, et al (2009) Transcriptome analysis by strand-specific sequencing of complementary DNA. *Nucleic Acids Res* 37:e123. <https://doi.org/10.1093/nar/gkp596>
- Pascucci T, Colamartino M, Fiori E, et al (2020) P-cresol Alters Brain Dopamine Metabolism and Exacerbates Autism-Like Behaviors in the BTBR Mouse. *Brain Sciences* 10:233. <https://doi.org/10.3390/brainsci10040233>
- Pasetto L, Grassano M, Pozzi S, et al (2021) Defective cyclophilin A induces TDP-43 proteinopathy: implications for amyotrophic lateral sclerosis and frontotemporal dementia. *Brain* 144:3710–3726. <https://doi.org/10.1093/brain/awab333>
- Pennington KL, Chan TY, Torres MP, Andersen JL (2018) The dynamic and stress-adaptive signaling hub of 14-3-3: emerging mechanisms of regulation and context-dependent protein–protein interactions. *Oncogene* 37:5587–5604. <https://doi.org/10.1038/s41388-018-0348-3>
- Persson J, Lind J, Larsson A, et al (2006) Altered brain white matter integrity in healthy carriers of the APOE epsilon4 allele: a risk for AD? *Neurology* 66:1029–1033. <https://doi.org/10.1212/01.wnl.0000204180.25361.48>
- Phelan M (2017) Phase II Clinical Trial of Nicotinamide for the Treatment of Mild to Moderate Alzheimer’s Disease. *Journal of Geriatric Medicine and Gerontology* 3:. <https://doi.org/10.23937/2469-5858/1510021>
- Philip P, Sagaspe P, Taillard J, et al (2019) Acute Intake of a Grape and Blueberry Polyphenol-Rich Extract Ameliorates Cognitive Performance in Healthy Young Adults During a Sustained Cognitive Effort. *Antioxidants (Basel)* 8:650. <https://doi.org/10.3390/antiox8120650>
- Phillips JC (2019) Why A β 42 Is Much More Toxic than A β 40. *ACS Chem Neurosci* 10:2843–2847. <https://doi.org/10.1021/acscchemneuro.9b00068>
- Pieniazek A, Bernasinska-Slomczewska J, Hikisz P (2023) Indoxyl sulfate induces apoptosis in mononuclear blood cells via mitochondrial pathway. *Sci Rep* 13:14044. <https://doi.org/10.1038/s41598-023-40824-z>
- Pinto LH, Enroth-Cugell C (2000) Tests of the mouse visual system. *Mamm Genome* 11:531–536. <https://doi.org/10.1007/s003350010102>
- Pinto-Sanchez MI, Hall GB, Ghajar K, et al (2017) Probiotic *Bifidobacterium longum* NCC3001 Reduces Depression Scores and Alters Brain Activity: A Pilot Study in Patients With Irritable Bowel Syndrome. *Gastroenterology* 153:448-459.e8. <https://doi.org/10.1053/j.gastro.2017.05.003>
- Playdon MC, Sampson JN, Cross AJ, et al (2016) Comparing metabolite profiles of habitual diet in serum and urine. *Am J Clin Nutr* 104:776–789. <https://doi.org/10.3945/ajcn.116.135301>
- Pocivavsek A, Hq W, Mc P, et al (2011) Fluctuations in endogenous kynurenic acid control hippocampal glutamate and memory. *Neuropsychopharmacology : official publication of the American College of Neuropsychopharmacology* 36:. <https://doi.org/10.1038/npp.2011.127>
- Poljsak B (2011) Strategies for Reducing or Preventing the Generation of Oxidative Stress. *Oxid Med Cell Longev* 2011:194586. <https://doi.org/10.1155/2011/194586>

- Poly C, Massaro JM, Seshadri S, et al (2011) The relation of dietary choline to cognitive performance and white-matter hyperintensity in the Framingham Offspring Cohort. *Am J Clin Nutr* 94:1584–1591. <https://doi.org/10.3945/ajcn.110.008938>
- Pontifex MG, Connell E, Gall GL, et al (2022) Saffron extract (Safr'Inside™) improves anxiety related behaviour in a mouse model of low-grade inflammation through the modulation of the microbiota and gut derived metabolites. *Food Funct* 13:12219–12233. <https://doi.org/10.1039/D2FO02739A>
- Pontifex MG, Connell E, Gall GL, et al (2024a) A novel Mediterranean diet-inspired supplement ameliorates cognitive, microbial, and metabolic deficits in a mouse model of low-grade inflammation. *Gut Microbes* 16:. <https://doi.org/10.1080/19490976.2024.2363011>
- Pontifex MG, Martinsen A, Saleh RNM, et al (2021a) APOE4 genotype exacerbates the impact of menopause on cognition and synaptic plasticity in APOE-TR mice. *FASEB J* 35:e21583. <https://doi.org/10.1096/fj.202002621RR>
- Pontifex MG, Mushtaq A, Le Gall G, et al (2021b) Differential Influence of Soluble Dietary Fibres on Intestinal and Hepatic Carbohydrate Response. *Nutrients* 13:4278. <https://doi.org/10.3390/nu13124278>
- Pontifex MG, Vauzour D, Muller M (2024b) Sexual dimorphism in the context of nutrition and health. *Proceedings of the Nutrition Society* 83:109–119. <https://doi.org/10.1017/S0029665123003610>
- Poon CH, Wong STN, Roy J, et al (2023) Sex Differences between Neuronal Loss and the Early Onset of Amyloid Deposits and Behavioral Consequences in 5xFAD Transgenic Mouse as a Model for Alzheimer's Disease. *Cells* 12:780. <https://doi.org/10.3390/cells12050780>
- Porter RJ, Lunn BS, Walker LLM, et al (2000) Cognitive Deficit Induced by Acute Tryptophan Depletion in Patients With Alzheimer's Disease. *AJP* 157:638–640. <https://doi.org/10.1176/appi.ajp.157.4.638>
- Precup G, Vodnar D-C (2019) Gut Prevotella as a possible biomarker of diet and its eubiotic versus dysbiotic roles: a comprehensive literature review. *Br J Nutr* 122:131–140. <https://doi.org/10.1017/S0007114519000680>
- Prentice RL, Mossavar-Rahmani Y, Huang Y, et al (2011) Evaluation and Comparison of Food Records, Recalls, and Frequencies for Energy and Protein Assessment by Using Recovery Biomarkers. *Am J Epidemiol* 174:591–603. <https://doi.org/10.1093/aje/kwr140>
- Prinelli F, Fratiglioni L, Kalpouzos G, et al (2019) Specific nutrient patterns are associated with higher structural brain integrity in dementia-free older adults. *Neuroimage* 199:281–288. <https://doi.org/10.1016/j.neuroimage.2019.05.066>
- Profenno LA, Porsteinsson AP, Faraone SV (2010) Meta-Analysis of Alzheimer's Disease Risk with Obesity, Diabetes, and Related Disorders. *Biological Psychiatry* 67:505–512. <https://doi.org/10.1016/j.biopsych.2009.02.013>
- Prokopidis K, Cervo MM, Gandham A, Scott D (2020) Impact of Protein Intake in Older Adults with Sarcopenia and Obesity: A Gut Microbiota Perspective. *Nutrients* 12:2285. <https://doi.org/10.3390/nu12082285>

- Psaltopoulou T, Kyrozis A, Stathopoulos P, et al (2008) Diet, physical activity and cognitive impairment among elders: the EPIC-Greece cohort (European Prospective Investigation into Cancer and Nutrition). *Public Health Nutr* 11:1054–1062. <https://doi.org/10.1017/S1368980007001607>
- Puri S, Shaheen M, Grover B (2023) Nutrition and cognitive health: A life course approach. *Front Public Health* 11:1023907. <https://doi.org/10.3389/fpubh.2023.1023907>
- Purser JL, Fillenbaum GG, Wallace RB (2006) Memory complaint is not necessary for diagnosis of mild cognitive impairment and does not predict 10-year trajectories of functional disability, word recall, or short portable mental status questionnaire limitations. *J Am Geriatr Soc* 54:335–338. <https://doi.org/10.1111/j.1532-5415.2005.00589.x>
- Qi G, Mi Y, Wang Y, et al (2017) Neuroprotective action of tea polyphenols on oxidative stress-induced apoptosis through the activation of the TrkB/CREB/BDNF pathway and Keap1/Nrf2 signaling pathway in SH-SY5Y cells and mice brain. *Food Funct* 8:4421–4432. <https://doi.org/10.1039/C7FO00991G>
- Qian X, Xie R, Liu X, et al (2022) Mechanisms of Short-Chain Fatty Acids Derived from Gut Microbiota in Alzheimer's Disease. *Aging Dis* 13:1252–1266. <https://doi.org/10.14336/AD.2021.1215>
- Quast C, Pruesse E, Yilmaz P, et al (2013) The SILVA ribosomal RNA gene database project: improved data processing and web-based tools. *Nucleic Acids Res* 41:D590-596. <https://doi.org/10.1093/nar/gks1219>
- Quinn M, McMillin M, Galindo C, et al (2014) Bile acids permeabilize the blood brain barrier after bile duct ligation in rats via Rac1-dependent mechanisms. *Digestive and Liver Disease* 46:527–534. <https://doi.org/10.1016/j.dld.2014.01.159>
- Quinn RA, Melnik AV, Vrbanac A, et al (2020) Global chemical effects of the microbiome include new bile-acid conjugations. *Nature* 579:123–129. <https://doi.org/10.1038/s41586-020-2047-9>
- Radd-Vagenas S, Duffy SL, Naismith SL, et al (2018) Effect of the Mediterranean diet on cognition and brain morphology and function: a systematic review of randomized controlled trials. *The American Journal of Clinical Nutrition* 107:389–404. <https://doi.org/10.1093/ajcn/nqx070>
- Rafiq T, Azab SM, Teo KK, et al (2021) Nutritional Metabolomics and the Classification of Dietary Biomarker Candidates: A Critical Review. *Advances in Nutrition* 12:2333. <https://doi.org/10.1093/advances/nmab054>
- Rahman A, Ting K, Cullen KM, et al (2009) The Excitotoxin Quinolinic Acid Induces Tau Phosphorylation in Human Neurons. *PLOS ONE* 4:e6344. <https://doi.org/10.1371/journal.pone.0006344>
- Rainey-Smith SR, Gu Y, Gardener SL, et al (2018) Mediterranean diet adherence and rate of cerebral A β -amyloid accumulation: Data from the Australian Imaging, Biomarkers and Lifestyle Study of Ageing. *Transl Psychiatry* 8:1–7. <https://doi.org/10.1038/s41398-018-0293-5>
- Rajoka MSR, Thirumdas R, Mehwish HM, et al (2021) Role of Food Antioxidants in Modulating Gut Microbial Communities: Novel Understandings in Intestinal Oxidative Stress Damage and Their Impact on Host Health. *Antioxidants* 10:. <https://doi.org/10.3390/antiox10101563>

- Ramalho RM, Nunes AF, Dias RB, et al (2013) Tauroursodeoxycholic acid suppresses amyloid β -induced synaptic toxicity in vitro and in APP/PS1 mice. *Neurobiology of Aging* 34:551–561. <https://doi.org/10.1016/j.neurobiolaging.2012.04.018>
- Ramalho RM, Ribeiro PS, Solá S, et al (2004) Inhibition of the E2F-1/p53/Bax pathway by tauroursodeoxycholic acid in amyloid beta-peptide-induced apoptosis of PC12 cells. *J Neurochem* 90:567–575. <https://doi.org/10.1111/j.1471-4159.2004.02517.x>
- Ramis MR, Sarubbo F, Tejada S, et al (2020) Chronic Polyphenon-60 or Catechin Treatments Increase Brain Monoamines Syntheses and Hippocampal SIRT1 LEVELS Improving Cognition in Aged Rats. *Nutrients* 12:326. <https://doi.org/10.3390/nu12020326>
- Ramos-Chávez LA, Roldán-Roldán G, García-Juárez B, et al (2018) Low Serum Tryptophan Levels as an Indicator of Global Cognitive Performance in Nondemented Women over 50 Years of Age. *Oxid Med Cell Longev* 2018:. <https://doi.org/10.1155/2018/8604718>
- Ramos-García NA, Orozco-Ibarra M, Estudillo E, et al (2020) Aryl Hydrocarbon Receptor in Post-Mortem Hippocampus and in Serum from Young, Elder, and Alzheimer's Patients. *International Journal of Molecular Sciences* 21:1983. <https://doi.org/10.3390/ijms21061983>
- Rana A, Samtiya M, Dhewa T, et al (2022) Health benefits of polyphenols: A concise review. *J Food Biochem* 46:e14264. <https://doi.org/10.1111/jfbc.14264>
- Rao M, Gershon MD (2016) The bowel and beyond: the enteric nervous system in neurological disorders. *Nat Rev Gastroenterol Hepatol* 13:517–528. <https://doi.org/10.1038/nrgastro.2016.107>
- Rao YL, Ganaraja B, Murlimanju BV, et al (2022) Hippocampus and its involvement in Alzheimer's disease: a review. *3 Biotech* 12:55. <https://doi.org/10.1007/s13205-022-03123-4>
- Raulin A-C, Doss SV, Trottier ZA, et al (2022) ApoE in Alzheimer's disease: pathophysiology and therapeutic strategies. *Molecular Neurodegeneration* 17:72. <https://doi.org/10.1186/s13024-022-00574-4>
- Raz N, Rodrigue KM (2006) Differential aging of the brain: Patterns, cognitive correlates and modifiers. *Neuroscience & Biobehavioral Reviews* 30:730–748. <https://doi.org/10.1016/j.neubiorev.2006.07.001>
- Reisberg B, Shulman MB, Torossian C, et al (2010) Outcome over seven years of healthy adults with and without subjective cognitive impairment. *Alzheimers Dement* 6:10.1016/j.jalz.2009.10.002. <https://doi.org/10.1016/j.jalz.2009.10.002>
- Reitz C, Tang M-X, Manly J, et al (2007) Hypertension and the Risk of Mild Cognitive Impairment. *Archives of Neurology* 64:1734–1740. <https://doi.org/10.1001/archneur.64.12.1734>
- Ren Z, Zhao L, Zhao M, et al (2024) Increased intestinal bile acid absorption contributes to age-related cognitive impairment. *CR Med* 5:. <https://doi.org/10.1016/j.xcrm.2024.101543>
- Rendeiro C, Vauzour D, Kean RJ, et al (2012) Blueberry supplementation induces spatial memory improvements and region-specific regulation of hippocampal BDNF mRNA expression in young rats. *Psychopharmacology* 223:319–330. <https://doi.org/10.1007/s00213-012-2719-8>

- Richard DM, Dawes MA, Mathias CW, et al (2009) L-Tryptophan: Basic Metabolic Functions, Behavioral Research and Therapeutic Indications. *Int J Tryptophan Res* 2:45–60. <https://doi.org/10.4137/ijtr.s2129>
- Ridlon JM, Alves JM, Hylemon PB, Bajaj JS (2013) Cirrhosis, bile acids and gut microbiota: unraveling a complex relationship. *Gut Microbes* 4:382–387. <https://doi.org/10.4161/gmic.25723>
- Ridlon JM, Kang DJ, Hylemon PB, Bajaj JS (2014) Bile Acids and the Gut Microbiome. *Curr Opin Gastroenterol* 30:332–338. <https://doi.org/10.1097/MOG.0000000000000057>
- Ríos-Covián D, Ruas-Madiedo P, Margolles A, et al (2016) Intestinal Short Chain Fatty Acids and their Link with Diet and Human Health. *Front Microbiol* 7:185. <https://doi.org/10.3389/fmicb.2016.00185>
- Rish I (2001) An Empirical Study of the Naive Bayes Classifier. *IJCAI 2001 Work Empir Methods Artif Intell* 3:
- Roager HM, Licht TR (2018) Microbial tryptophan catabolites in health and disease. *Nat Commun* 9:3294. <https://doi.org/10.1038/s41467-018-05470-4>
- Roberts LM, Black DS, Raman C, et al (2008) Subcellular localization of transporters along the rat blood–brain barrier and blood–cerebral-spinal fluid barrier by in vivo biotinylation. *Neuroscience* 155:423–438. <https://doi.org/10.1016/j.neuroscience.2008.06.015>
- Rodrigues CMP, Spellman SR, Solá S, et al (2002) Neuroprotection by a Bile Acid in an Acute Stroke Model in the Rat. *J Cereb Blood Flow Metab* 22:463–471. <https://doi.org/10.1097/00004647-200204000-00010>
- Rodríguez-Rejón AI, Castro-Quezada I, Ruano-Rodríguez C, et al (2014) Effect of a Mediterranean Diet Intervention on Dietary Glycemic Load and Dietary Glycemic Index: The PREDIMED Study. *Journal of Nutrition and Metabolism* 2014:e985373. <https://doi.org/10.1155/2014/985373>
- Rolova T, Puli L, Magga J, et al (2014) Complex regulation of acute and chronic neuroinflammatory responses in mouse models deficient for nuclear factor kappa B p50 subunit. *Neurobiology of Disease* 64:16–29. <https://doi.org/10.1016/j.nbd.2013.12.003>
- Romo-Vaquero M, Fernández-Villalba E, Gil-Martinez A-L, et al (2022) Urolithins: potential biomarkers of gut dysbiosis and disease stage in Parkinson’s patients. *Food Funct* 13:6306–6316. <https://doi.org/10.1039/d2fo00552b>
- Rosi S (2011) Neuroinflammation and the plasticity-related immediate-early gene Arc. *Brain Behav Immun* 25:S39–S49. <https://doi.org/10.1016/j.bbi.2011.02.003>
- Roth W, Zadeh K, Vekariya R, et al (2021) Tryptophan Metabolism and Gut-Brain Homeostasis. *International Journal of Molecular Sciences* 22:2973. <https://doi.org/10.3390/ijms22062973>
- Rothhammer V, Mascanfroni ID, Bunse L, et al (2016) Type I interferons and microbial metabolites of tryptophan modulate astrocyte activity and CNS inflammation via the aryl hydrocarbon receptor. *Nat Med* 22:586–597. <https://doi.org/10.1038/nm.4106>
- Rothschild D, Weissbrod O, Barkan E, et al (2018) Environment dominates over host genetics in shaping human gut microbiota. *Nature* 555:210–215. <https://doi.org/10.1038/nature25973>

- Rowland I, Gibson G, Heinken A, et al (2018) Gut microbiota functions: metabolism of nutrients and other food components. *Eur J Nutr* 57:1–24. <https://doi.org/10.1007/s00394-017-1445-8>
- Russell WR, Gratz SW, Duncan SH, et al (2011) High-protein, reduced-carbohydrate weight-loss diets promote metabolite profiles likely to be detrimental to colonic health. *Am J Clin Nutr* 93:1062–1072. <https://doi.org/10.3945/ajcn.110.002188>
- Saito Y, Sato T, Nomoto K, Tsuji H (2018) Identification of phenol- and p-cresol-producing intestinal bacteria by using media supplemented with tyrosine and its metabolites. *FEMS Microbiology Ecology* 94:. <https://doi.org/10.1093/femsec/fiy125>
- Saji N, Murotani K, Hisada T, et al (2019) The relationship between the gut microbiome and mild cognitive impairment in patients without dementia: a cross-sectional study conducted in Japan. *Sci Rep* 9:19227. <https://doi.org/10.1038/s41598-019-55851-y>
- Samuel BS, Shaito A, Motoike T, et al (2008) Effects of the gut microbiota on host adiposity are modulated by the short-chain fatty-acid binding G protein-coupled receptor, Gpr41. *Proceedings of the National Academy of Sciences* 105:16767–16772. <https://doi.org/10.1073/pnas.0808567105>
- Sánchez-Villegas A, Toledo E, de Irala J, et al (2012) Fast-food and commercial baked goods consumption and the risk of depression. *Public Health Nutr* 15:424–432. <https://doi.org/10.1017/S1368980011001856>
- Sankowski B, Książarczyk K, Raćkowska E, et al (2020) Higher cerebrospinal fluid to plasma ratio of p-cresol sulfate and indoxyl sulfate in patients with Parkinson’s disease. *Clinica Chimica Acta* 501:165–173. <https://doi.org/10.1016/j.cca.2019.10.038>
- Šarenac TM, Mikov M (2018) Bile Acid Synthesis: From Nature to the Chemical Modification and Synthesis and Their Applications as Drugs and Nutrients. *Frontiers in Pharmacology* 9:939. <https://doi.org/10.3389/fphar.2018.00939>
- Sarkaki A, Farbood Y, Badavi M (2007) The effect of grape seed extract (GSE) on spatial memory in aged male rats. *Pakistan Journal of Medical Sciences* 23:561–565
- Savitz J (2020) The kynurenine pathway: a finger in every pie. *Mol Psychiatry* 25:131–147. <https://doi.org/10.1038/s41380-019-0414-4>
- Sawaya RA, Jaffe J, Friedenber L, Friedenber FK (2012) Vitamin, mineral, and drug absorption following bariatric surgery. *Curr Drug Metab* 13:1345–1355. <https://doi.org/10.2174/138920012803341339>
- Sayin SI, Wahlström A, Felin J, et al (2013) Gut microbiota regulates bile acid metabolism by reducing the levels of tauro-beta-muricholic acid, a naturally occurring FXR antagonist. *Cell Metab* 17:225–235. <https://doi.org/10.1016/j.cmet.2013.01.003>
- Schanz O, Chijiwa R, Cengiz SC, et al (2020) Dietary AhR Ligands Regulate AhRR Expression in Intestinal Immune Cells and Intestinal Microbiota Composition. *Int J Mol Sci* 21:3189. <https://doi.org/10.3390/ijms21093189>
- Schmitt JAJ, Wingen M, Ramaekers JG, et al (2006) Serotonin and Human Cognitive Performance. *Current Pharmaceutical Design* 12:2473–2486. <https://doi.org/10.2174/138161206777698909>

- Schneider E, O’Riordan KJ, Clarke G, Cryan JF (2024) Feeding gut microbes to nourish the brain: unravelling the diet–microbiota–gut–brain axis. *Nat Metab* 6:1454–1478. <https://doi.org/10.1038/s42255-024-01108-6>
- Schroeder JC, DiNatale BC, Murray IA, et al (2010) The Uremic Toxin 3-Indoxyl Sulfate Is a Potent Endogenous Agonist for the Human Aryl Hydrocarbon Receptor. *Biochemistry* 49:393–400. <https://doi.org/10.1021/bi901786x>
- Schubring SR, Fleischer W, Lin JS, et al (2012) The bile steroid chenodeoxycholate is a potent antagonist at NMDA and GABAA receptors. *Neuroscience Letters* 506:322–326. <https://doi.org/10.1016/j.neulet.2011.11.036>
- Schwarcz R, Bruno JP, Muchowski PJ, Wu H-Q (2012) KYNURENINES IN THE MAMMALIAN BRAIN: WHEN PHYSIOLOGY MEETS PATHOLOGY. *Nat Rev Neurosci* 13:465–477. <https://doi.org/10.1038/nrn3257>
- Scott KP, Gratz SW, Sheridan PO, et al (2013) The influence of diet on the gut microbiota. *Pharmacol Res* 69:52–60. <https://doi.org/10.1016/j.phrs.2012.10.020>
- Seldin MM, Meng Y, Qi H, et al (2016) Trimethylamine N-Oxide Promotes Vascular Inflammation Through Signaling of Mitogen-Activated Protein Kinase and Nuclear Factor- κ B. *J Am Heart Assoc* 5:. <https://doi.org/10.1161/JAHA.115.002767>
- Sert NP du, Hurst V, Ahluwalia A, et al (2020) The ARRIVE guidelines 2.0: Updated guidelines for reporting animal research. *PLOS Biology* 18:e3000410. <https://doi.org/10.1371/journal.pbio.3000410>
- Severino A, Tohumcu E, Tamai L, et al (2024) The microbiome-driven impact of western diet in the development of noncommunicable chronic disorders. *Best Practice & Research Clinical Gastroenterology* 101923. <https://doi.org/10.1016/j.bpg.2024.101923>
- Shabbir U, Tyagi A, Elahi F, et al (2021) The Potential Role of Polyphenols in Oxidative Stress and Inflammation Induced by Gut Microbiota in Alzheimer’s Disease. *Antioxidants (Basel)* 10:1370. <https://doi.org/10.3390/antiox10091370>
- Shah SN, Knausenberger TB-A, Connell E, et al (2022) Cerebrovascular damage caused by the gut microbe-derived uraemic toxin p-cresol sulfate is prevented by blockade of the epidermal growth factor receptor. 2022.11.12.516113
- Shannon OM, Stephan BCM, Granic A, et al (2019) Mediterranean diet adherence and cognitive function in older UK adults: the European Prospective Investigation into Cancer and Nutrition-Norfolk (EPIC-Norfolk) Study. *Am J Clin Nutr* 110:938–948. <https://doi.org/10.1093/ajcn/nqz114>
- Sheng C, Lin L, Lin H, et al (2021) Altered Gut Microbiota in Adults with Subjective Cognitive Decline: The SILCODE Study. *J Alzheimers Dis* 82:513–526. <https://doi.org/10.3233/JAD-210259>
- Shi H, Ge X, Ma X, et al (2021) A fiber-deprived diet causes cognitive impairment and hippocampal microglia-mediated synaptic loss through the gut microbiota and metabolites. *Microbiome* 9:223. <https://doi.org/10.1186/s40168-021-01172-0>
- Shibuya T, Sato A, Nishimoto-Kusunose S, et al (2024) Further evidence for blood-to-brain influx of unconjugated bile acids by passive diffusion: Determination of their brain-to-serum

- concentration ratios in rats by LC/MS/MS. *Steroids* 204:109397. <https://doi.org/10.1016/j.steroids.2024.109397>
- Shimada Y, Kinoshita M, Harada K, et al (2013) Commensal bacteria-dependent indole production enhances epithelial barrier function in the colon. *PLoS One* 8:e80604. <https://doi.org/10.1371/journal.pone.0080604>
- Shin N-R, Whon TW, Bae J-W (2015) Proteobacteria: microbial signature of dysbiosis in gut microbiota. *Trends Biotechnol* 33:496–503. <https://doi.org/10.1016/j.tibtech.2015.06.011>
- Shukitt-Hale B, Carey A, Simon L, et al (2006) Effects of Concord grape juice on cognitive and motor deficits in aging. *Nutrition* 22:295–302. <https://doi.org/10.1016/j.nut.2005.07.016>
- Shukla A, Dikshit M, Srimal RC (1996) Nitric oxide-dependent blood-brain barrier permeability alteration in the rat brain. *Experientia* 52:136–140. <https://doi.org/10.1007/BF01923358>
- Simen AA, Bordner KA, Martin MP, et al (2011) Cognitive dysfunction with aging and the role of inflammation. *Ther Adv Chronic Dis* 2:175–195. <https://doi.org/10.1177/2040622311399145>
- Simfukwe C, Youn YC, Kim M-J, et al (2023) CNN for a Regression Machine Learning Algorithm for Predicting Cognitive Impairment Using qEEG. *Neuropsychiatric Disease and Treatment* 19:851–863. <https://doi.org/10.2147/NDT.S404528>
- Singh A, Yau YF, Leung KS, et al (2020) Interaction of Polyphenols as Antioxidant and Anti-Inflammatory Compounds in Brain–Liver–Gut Axis. *Antioxidants* 9:669. <https://doi.org/10.3390/antiox9080669>
- Singh G, Singh V, Schneider JS (2019) Post-translational histone modifications and their interaction with sex influence normal brain development and elaboration of neuropsychiatric disorders. *Biochimica et Biophysica Acta (BBA) - Molecular Basis of Disease* 1865:1968–1981. <https://doi.org/10.1016/j.bbadis.2018.10.016>
- Singh M, Arseneault M, Sanderson T, et al (2008) Challenges for research on polyphenols from foods in Alzheimer’s disease: bioavailability, metabolism, and cellular and molecular mechanisms. *J Agric Food Chem* 56:4855–4873. <https://doi.org/10.1021/jf0735073>
- Smith EA, Macfarlane GT (1997) Dissimilatory amino Acid metabolism in human colonic bacteria. *Anaerobe* 3:327–337. <https://doi.org/10.1006/anae.1997.0121>
- Smith JA, Das A, Ray SK, Banik NL (2012) Role of pro-inflammatory cytokines released from microglia in neurodegenerative diseases. *Brain Res Bull* 87:10–20. <https://doi.org/10.1016/j.brainresbull.2011.10.004>
- Smith K, McCoy KD, Macpherson AJ (2007) Use of axenic animals in studying the adaptation of mammals to their commensal intestinal microbiota. *Seminars in Immunology* 19:59–69. <https://doi.org/10.1016/j.smim.2006.10.002>
- Smith M, Crowther RA, Goedert M (2000) The natural osmolyte trimethylamine N-oxide (TMAO) restores the ability of mutant tau to promote microtubule assembly. *FEBS letters* 484:265–70. [https://doi.org/10.1016/S0014-5793\(00\)02169-4](https://doi.org/10.1016/S0014-5793(00)02169-4)

- So D, Whelan K, Rossi M, et al (2018) Dietary fiber intervention on gut microbiota composition in healthy adults: a systematic review and meta-analysis. *Am J Clin Nutr* 107:965–983. <https://doi.org/10.1093/ajcn/nqy041>
- Soares R, Ribeiro FF, Xapelli S, et al (2018) Tauroursodeoxycholic Acid Enhances Mitochondrial Biogenesis, Neural Stem Cell Pool, and Early Neurogenesis in Adult Rats. *Mol Neurobiol* 55:3725–3738. <https://doi.org/10.1007/s12035-017-0592-5>
- Sochocka M, Donskow-Lysoniewska K, Diniz BS, et al (2019) The Gut Microbiome Alterations and Inflammation-Driven Pathogenesis of Alzheimer’s Disease—a Critical Review. *Mol Neurobiol* 56:1841–1851. <https://doi.org/10.1007/s12035-018-1188-4>
- Solá S, Amaral JD, Borralho PM, et al (2006) Functional modulation of nuclear steroid receptors by tauroursodeoxycholic acid reduces amyloid beta-peptide-induced apoptosis. *Mol Endocrinol* 20:2292–2303. <https://doi.org/10.1210/me.2006-0063>
- Solá S, Castro RE, Laires PA, et al (2003) Tauroursodeoxycholic Acid Prevents Amyloid- β Peptide-Induced Neuronal Death Via a Phosphatidylinositol 3-Kinase-Dependent Signaling Pathway. *Mol Med* 9:226–234. <https://doi.org/10.2119/2003-00042.Rodrigues>
- Soliman ML, Smith MD, Houdek HM, Rosenberger TA (2012) Acetate supplementation modulates brain histone acetylation and decreases interleukin-1 β expression in a rat model of neuroinflammation. *J Neuroinflammation* 9:51. <https://doi.org/10.1186/1742-2094-9-51>
- Solvang S-EH, Nordrehaug JE, Tell GS, et al (2019) The kynurenine pathway and cognitive performance in community-dwelling older adults. The Hordaland Health Study. *Brain Behav Immun* 75:155–162. <https://doi.org/10.1016/j.bbi.2018.10.003>
- Song C, Zhang Y, Cheng L, et al (2021) Tea polyphenols ameliorates memory decline in aging model rats by inhibiting brain TLR4/NF- κ B inflammatory signaling pathway caused by intestinal flora dysbiosis. *Exp Gerontol* 153:111476. <https://doi.org/10.1016/j.exger.2021.111476>
- Song L, Sun Q, Zheng H, et al (2022) Roseburia hominis Alleviates Neuroinflammation via Short-Chain Fatty Acids through Histone Deacetylase Inhibition. *Mol Nutr Food Res* 66:e2200164. <https://doi.org/10.1002/mnfr.202200164>
- Song Z, Feng S, Zhou X, et al (2023) Taxonomic identification of bile salt hydrolase-encoding lactobacilli: Modulation of the enterohepatic bile acid profile. *iMeta* 2:e128. <https://doi.org/10.1002/imt2.128>
- Sonnenburg ED, Smits SA, Tikhonov M, et al (2016) Diet-induced extinctions in the gut microbiota compound over generations. *Nature* 529:212–215. <https://doi.org/10.1038/nature16504>
- Soontornmalai A, Vlaming MLH, Fritschy J-M (2006) Differential, strain-specific cellular and subcellular distribution of multidrug transporters in murine choroid plexus and blood–brain barrier. *Neuroscience* 138:159–169. <https://doi.org/10.1016/j.neuroscience.2005.11.011>
- Spichak S, Bastiaanssen TFS, Berding K, et al (2021) Mining microbes for mental health: Determining the role of microbial metabolic pathways in human brain health and disease. *Neuroscience & Biobehavioral Reviews* 125:698–761. <https://doi.org/10.1016/j.neubiorev.2021.02.044>

- Spitzer RL, Kroenke K, Williams JBW, Löwe B (2006) A Brief Measure for Assessing Generalized Anxiety Disorder: The GAD-7. *Archives of Internal Medicine* 166:1092–1097. <https://doi.org/10.1001/archinte.166.10.1092>
- Stachulski AV, Knausenberger TB-A, Shah SN, et al (2023) A host-gut microbial amino acid co-metabolite, p-cresol glucuronide, promotes blood-brain barrier integrity in vivo. *Tissue Barriers* 11:2073175. <https://doi.org/10.1080/21688370.2022.2073175>
- Staudacher HM, Lomer MCE, Anderson JL, et al (2012) Fermentable carbohydrate restriction reduces luminal bifidobacteria and gastrointestinal symptoms in patients with irritable bowel syndrome. *J Nutr* 142:1510–1518. <https://doi.org/10.3945/jn.112.159285>
- Stolwijk JM, Garje R, Sieren JC, et al (2020) Understanding the Redox Biology of Selenium in the Search of Targeted Cancer Therapies. *Antioxidants (Basel)* 9:420. <https://doi.org/10.3390/antiox9050420>
- Stone TW, Darlington LG (2013) The kynurenine pathway as a therapeutic target in cognitive and neurodegenerative disorders. *Br J Pharmacol* 169:1211–1227. <https://doi.org/10.1111/bph.12230>
- Strader AD, Woods SC (2005) Gastrointestinal hormones and food intake. *Gastroenterology* 128:175–191. <https://doi.org/10.1053/j.gastro.2004.10.043>
- Strandwitz P (2018) Neurotransmitter modulation by the gut microbiota. *Brain Res* 1693:128–133. <https://doi.org/10.1016/j.brainres.2018.03.015>
- Straniero S, Laskar A, Savva C, et al (2020) Of mice and men: murine bile acids explain species differences in the regulation of bile acid and cholesterol metabolism. *J Lipid Res* 61:480–491. <https://doi.org/10.1194/jlr.RA119000307>
- Stremmel W, Schmidt KV, Schuhmann V, et al (2017) Blood Trimethylamine-N-Oxide Originates from Microbiota Mediated Breakdown of Phosphatidylcholine and Absorption from Small Intestine. *PLoS One* 12:e0170742. <https://doi.org/10.1371/journal.pone.0170742>
- Strittmatter WJ, Saunders AM, Schmechel D, et al (1993) Apolipoprotein E: high-avidity binding to beta-amyloid and increased frequency of type 4 allele in late-onset familial Alzheimer disease. *Proc Natl Acad Sci U S A* 90:1977–1981. <https://doi.org/10.1073/pnas.90.5.1977>
- Suárez M, Caimari A, del Bas JM, Arola L (2017) Metabolomics: An emerging tool to evaluate the impact of nutritional and physiological challenges. *TrAC Trends in Analytical Chemistry* 96:79–88. <https://doi.org/10.1016/j.trac.2017.06.003>
- Subramanian J, Savage JC, Tremblay M-È (2020) Synaptic Loss in Alzheimer’s Disease: Mechanistic Insights Provided by Two-Photon in vivo Imaging of Transgenic Mouse Models. *Front Cell Neurosci* 14:592607. <https://doi.org/10.3389/fncel.2020.592607>
- Subramanyam Rallabandi VP, Seetharaman K (2023) Deep learning-based classification of healthy aging controls, mild cognitive impairment and Alzheimer’s disease using fusion of MRI-PET imaging. *Biomedical Signal Processing and Control* 80:104312. <https://doi.org/10.1016/j.bspc.2022.104312>
- Sullivan EV, Pfefferbaum A (2006) Diffusion tensor imaging and aging. *Neurosci Biobehav Rev* 30:749–761. <https://doi.org/10.1016/j.neubiorev.2006.06.002>

- Sun C-Y, Cheng M-L, Pan H-C, et al (2017) Protein-bound uremic toxins impaired mitochondrial dynamics and functions. *Oncotarget* 8:77722–77733. <https://doi.org/10.18632/oncotarget.20773>
- Sun C-Y, Li J-R, Wang Y-Y, et al (2020) p-Cresol Sulfate Caused Behavior Disorders and Neurodegeneration in Mice with Unilateral Nephrectomy Involving Oxidative Stress and Neuroinflammation. *Int J Mol Sci* 21:E6687. <https://doi.org/10.3390/ijms21186687>
- Sun C-Y, Li J-R, Wang Y-Y, et al (2021) Indoxyl sulfate caused behavioral abnormality and neurodegeneration in mice with unilateral nephrectomy. *Aging (Albany NY)* 13:6681–6701. <https://doi.org/10.18632/aging.202523>
- Sun W, Li S, Chen C, et al (2022) Dietary fiber intake is positively related with cognitive function in US older adults. *Journal of Functional Foods* 90:104986. <https://doi.org/10.1016/j.jff.2022.104986>
- Suzuki N, Cheung TT, Cai XD, et al (1994) An increased percentage of long amyloid beta protein secreted by familial amyloid beta protein precursor (beta APP717) mutants. *Science* 264:1336–1340. <https://doi.org/10.1126/science.8191290>
- Sweeney MD, Sagare AP, Zlokovic BV (2018) Blood–brain barrier breakdown in Alzheimer’s disease and other neurodegenerative disorders. *Nat Rev Neurol* 14:133–150. <https://doi.org/10.1038/nrneurol.2017.188>
- Takada T, Yamamoto T, Matsuo H, et al (2018) Identification of ABCG2 as an Exporter of Uremic Toxin Indoxyl Sulfate in Mice and as a Crucial Factor Influencing CKD Progression. *Sci Rep* 8:11147. <https://doi.org/10.1038/s41598-018-29208-w>
- Tang W-H, Wang C-P, Yu T-H, et al (2018) Protein-bounded uremic toxin p-cresylsulfate induces vascular permeability alternations. *Histochem Cell Biol* 149:607–617. <https://doi.org/10.1007/s00418-018-1662-0>
- Tang WHW, Wang Z, Fan Y, et al (2014) Prognostic value of elevated levels of intestinal microbe-generated metabolite trimethylamine-N-oxide in patients with heart failure: refining the gut hypothesis. *J Am Coll Cardiol* 64:1908–1914. <https://doi.org/10.1016/j.jacc.2014.02.617>
- Tap J, Furet J-P, Bensaada M, et al (2015) Gut microbiota richness promotes its stability upon increased dietary fibre intake in healthy adults. *Environ Microbiol* 17:4954–4964. <https://doi.org/10.1111/1462-2920.13006>
- Tavassol ZH, Ejtahed H-S, Atlasi R, et al (2023) Alteration in Gut Microbiota Composition of Older Adults Is Associated with Obesity and Its Indices: A Systematic Review. *The Journal of nutrition, health and aging* 27:817–823. <https://doi.org/10.1007/s12603-023-1988-8>
- Tayab MA, Islam MN, Chowdhury KAA, Tasnim FM (2022) Targeting neuroinflammation by polyphenols: A promising therapeutic approach against inflammation-associated depression. *Biomedicine & Pharmacotherapy* 147:112668. <https://doi.org/10.1016/j.biopha.2022.112668>
- Terry N, Margolis KG (2017) Serotonergic Mechanisms Regulating the GI Tract: Experimental Evidence and Therapeutic Relevance. *Handb Exp Pharmacol* 239:319–342. https://doi.org/10.1007/164_2016_103

- The Gene Ontology Consortium, Aleksander SA, Balhoff J, et al (2023) The Gene Ontology knowledgebase in 2023. *Genetics* 224:iyad031. <https://doi.org/10.1093/genetics/iyad031>
- Theofilopoulos S, Wang Y, Kitambi SS, et al (2013) Brain endogenous liver X receptor ligands selectively promote midbrain neurogenesis. *Nat Chem Biol* 9:126–133. <https://doi.org/10.1038/nchembio.1156>
- Thomas DR (2006) Vitamins in Aging, Health, and Longevity. *Clin Interv Aging* 1:81–91
- Thompson PM, Hayashi KM, De Zubicaray GI, et al (2004) Mapping hippocampal and ventricular change in Alzheimer disease. *Neuroimage* 22:1754–1766. <https://doi.org/10.1016/j.neuroimage.2004.03.040>
- Tian P, Chen Y, Qian X, et al (2021) *Pediococcus acidilactici* CCFM6432 mitigates chronic stress-induced anxiety and gut microbial abnormalities. *Food Funct* 12:11241–11249. <https://doi.org/10.1039/d1fo01608c>
- Tian Y, Wang W, Xu L, et al (2019) Activation of Nrf2/ARE pathway alleviates the cognitive deficits in PS1V97L-Tg mouse model of Alzheimer's disease through modulation of oxidative stress. *J Neurosci Res* 97:492–505. <https://doi.org/10.1002/jnr.24357>
- Ticinesi A, Tana C, Nouvenne A, et al (2018) Gut microbiota, cognitive frailty and dementia in older individuals: a systematic review. *Clin Interv Aging* 13:1497–1511. <https://doi.org/10.2147/CIA.S139163>
- Ting KK, Brew BJ, Guillemain GJ (2009) Effect of quinolinic acid on human astrocytes morphology and functions: implications in Alzheimer's disease. *J Neuroinflammation* 6:36. <https://doi.org/10.1186/1742-2094-6-36>
- Tiwari S, Atluri V, Kaushik A, et al (2019) Alzheimer's disease: pathogenesis, diagnostics, and therapeutics. *Int J Nanomedicine* 14:5541–5554. <https://doi.org/10.2147/IJN.S200490>
- Toda N, Ayajiki K, Okamura T (2009) Cerebral blood flow regulation by nitric oxide: recent advances. *Pharmacol Rev* 61:62–97. <https://doi.org/10.1124/pr.108.000547>
- Tong T, Gray K, Gao Q, et al (2017) Multi-modal classification of Alzheimer's disease using nonlinear graph fusion. *Pattern Recognition* 63:171–181. <https://doi.org/10.1016/j.patcog.2016.10.009>
- Torres-Velázquez M, Sawin EA, Anderson JM, Yu J-PJ (2019) Refractory diet-dependent changes in neural microstructure: Implications for microstructural endophenotypes of neurologic and psychiatric disease. *Magn Reson Imaging* 58:148–155. <https://doi.org/10.1016/j.mri.2019.02.006>
- Tran CD, Grice DM, Wade B, et al (2015) Gut permeability, its interaction with gut microflora and effects on metabolic health are mediated by the lymphatics system, liver and bile acid. *Future Microbiol* 10:1339–1353. <https://doi.org/10.2217/FMB.15.54>
- Tran TTT, Corsini S, Kellingray L, et al (2019) APOE genotype influences the gut microbiome structure and function in humans and mice: relevance for Alzheimer's disease pathophysiology. *FASEB J* 33:8221–8231. <https://doi.org/10.1096/fj.201900071R>

- Travier L, Alonso M, Andronico A, et al (2021) Neonatal susceptibility to meningitis results from the immaturity of epithelial barriers and gut microbiota. *Cell Reports* 35:.
<https://doi.org/10.1016/j.celrep.2021.109319>
- Trichopoulou A, Costacou T, Bamia C, Trichopoulos D (2003) Adherence to a Mediterranean diet and survival in a Greek population. *N Engl J Med* 348:2599–2608.
<https://doi.org/10.1056/NEJMoa025039>
- Troppmann L, Gray-Donald K, Johns T (2002) Supplement use: is there any nutritional benefit? *J Am Diet Assoc* 102:818–825. [https://doi.org/10.1016/s0002-8223\(02\)90183-5](https://doi.org/10.1016/s0002-8223(02)90183-5)
- Tseng H-C, Graves DJ (1998) Natural Methylamine Osmolytes, Trimethylamine N-Oxide and Betaine, Increase Tau-Induced Polymerization of Microtubules. *Biochemical and Biophysical Research Communications* 250:726–730. <https://doi.org/10.1006/bbrc.1998.9382>
- Tseng HC, Lu Q, Henderson E, Graves DJ (1999) Phosphorylated tau can promote tubulin assembly. *Proc Natl Acad Sci U S A* 96:9503–9508. <https://doi.org/10.1073/pnas.96.17.9503>
- Tsivgoulis G, Judd S, Letter AJ, et al (2013) Adherence to a Mediterranean diet and risk of incident cognitive impairment. *Neurology* 80:1684–1692.
<https://doi.org/10.1212/WNL.0b013e3182904f69>
- Tucker LB, McCabe JT (2021) Measuring Anxiety-Like Behaviors in Rodent Models of Traumatic Brain Injury. *Front Behav Neurosci* 15:682935. <https://doi.org/10.3389/fnbeh.2021.682935>
- Tuttolomondo A, Simonetta I, Daidone M, et al (2019) Metabolic and Vascular Effect of the Mediterranean Diet. *Int J Mol Sci* 20:4716. <https://doi.org/10.3390/ijms20194716>
- Uddin O, Arakawa K, Raver C, et al (2021) Patterns of cognitive decline and somatosensory processing in a mouse model of amyloid accumulation. *Neurobiology of Pain* 10:100076.
<https://doi.org/10.1016/j.ynpai.2021.100076>
- Ufnal M, Zadlo A, Ostaszewski R (2015) TMAO: A small molecule of great expectations. *Nutrition* 31:1317–1323. <https://doi.org/10.1016/j.nut.2015.05.006>
- Vadukul DM, Gbajumo O, Marshall KE, Serpell LC (2017) Amyloidogenicity and toxicity of the reverse and scrambled variants of amyloid- β 1-42. *FEBS Lett* 591:822–830.
<https://doi.org/10.1002/1873-3468.12590>
- van Donkelaar EL, Blokland A, Ferrington L, et al (2011) Mechanism of acute tryptophan depletion: is it only serotonin? *Mol Psychiatry* 16:695–713. <https://doi.org/10.1038/mp.2011.9>
- Van Parys A, Brække MS, Karlsson T, et al (2022) Assessment of Dietary Choline Intake, Contributing Food Items, and Associations with One-Carbon and Lipid Metabolites in Middle-Aged and Elderly Adults: The Hordaland Health Study. *J Nutr* 152:513–524.
<https://doi.org/10.1093/jn/nxab367>
- Vanegas SM, Meydani M, Barnett JB, et al (2017) Substituting whole grains for refined grains in a 6-wk randomized trial has a modest effect on gut microbiota and immune and inflammatory markers of healthy adults. *Am J Clin Nutr* 105:635–650.
<https://doi.org/10.3945/ajcn.116.146928>

- Vangay P, Johnson AJ, Ward TL, et al (2018) US Immigration Westernizes the Human Gut Microbiome. *Cell* 175:962-972.e10. <https://doi.org/10.1016/j.cell.2018.10.029>
- Varesi A, Pierella E, Romeo M, et al (2022) The Potential Role of Gut Microbiota in Alzheimer's Disease: From Diagnosis to Treatment. *Nutrients* 14:668. <https://doi.org/10.3390/nu14030668>
- Vazquez-Medina A, Rodriguez-Trujillo N, Ayuso-Rodriguez K, et al (2024) Exploring the interplay between running exercises, microbial diversity, and tryptophan metabolism along the microbiota-gut-brain axis. *Front Microbiol* 15:. <https://doi.org/10.3389/fmicb.2024.1326584>
- Velasquez MT, Ramezani A, Manal A, Raj DS (2016) Trimethylamine N-Oxide: The Good, the Bad and the Unknown. *Toxins (Basel)* 8:. <https://doi.org/10.3390/toxins8110326>
- Verdu EF, Bercik P, Huang XX, et al (2008) The role of luminal factors in the recovery of gastric function and behavioral changes after chronic *Helicobacter pylori* infection. *American Journal of Physiology-Gastrointestinal and Liver Physiology* 295:G664–G670. <https://doi.org/10.1152/ajpgi.90316.2008>
- Verheggen ICM, de Jong JJA, van Boxtel MPJ, et al (2020) Increase in blood–brain barrier leakage in healthy, older adults. *GeroScience* 42:1183–1193. <https://doi.org/10.1007/s11357-020-00211-2>
- Verneti L, Gough A, Baetz N, et al (2017) Functional Coupling of Human Microphysiology Systems: Intestine, Liver, Kidney Proximal Tubule, Blood-Brain Barrier and Skeletal Muscle. *Scientific Reports* 7:42296. <https://doi.org/10.1038/srep42296>
- Visconti A, Le Roy CI, Rosa F, et al (2019) Interplay between the human gut microbiome and host metabolism. *Nat Commun* 10:4505. <https://doi.org/10.1038/s41467-019-12476-z>
- Vogt NM, Kerby RL, Dill-McFarland KA, et al (2017) Gut microbiome alterations in Alzheimer's disease. *Scientific Reports* 7:13537. <https://doi.org/10.1038/s41598-017-13601-y>
- Vogt NM, Romano KA, Darst BF, et al (2018) The gut microbiota-derived metabolite trimethylamine N-oxide is elevated in Alzheimer's disease. *Alzheimer's Research & Therapy* 10:124. <https://doi.org/10.1186/s13195-018-0451-2>
- Vorobyov V, Bakharev B, Medvinskaya N, et al (2019) Loss of Midbrain Dopamine Neurons and Altered Apomorphine EEG Effects in the 5xFAD Mouse Model of Alzheimer's Disease. *J Alzheimers Dis* 70:241–256. <https://doi.org/10.3233/JAD-181246>
- Vural Z, Avery A, Kalogiros DI, et al (2020) Trace Mineral Intake and Deficiencies in Older Adults Living in the Community and Institutions: A Systematic Review. *Nutrients* 12:1072. <https://doi.org/10.3390/nu12041072>
- Walker AW, Ince J, Duncan SH, et al (2011) Dominant and diet-responsive groups of bacteria within the human colonic microbiota. *ISME J* 5:220–230. <https://doi.org/10.1038/ismej.2010.118>
- Walsh DM, Selkoe DJ (2004) Deciphering the molecular basis of memory failure in Alzheimer's disease. *Neuron* 44:181–193. <https://doi.org/10.1016/j.neuron.2004.09.010>

- Wang F, Zhao C, Yang M, et al (2021) Four Citrus Flavanones Exert Atherosclerosis Alleviation Effects in ApoE^{-/-} Mice via Different Metabolic and Signaling Pathways. *J Agric Food Chem* 69:5226–5237. <https://doi.org/10.1021/acs.jafc.1c01463>
- Wang K, Guo J, Chang X, Gui S (2022) Painong-San extract alleviates dextran sulfate sodium-induced colitis in mice by modulating gut microbiota, restoring intestinal barrier function and attenuating TLR4/NF- κ B signaling cascades. *J Pharm Biomed Anal* 209:114529. <https://doi.org/10.1016/j.jpba.2021.114529>
- Wang Q, Garrity GM, Tiedje JM, Cole JR (2007) Naive Bayesian classifier for rapid assignment of rRNA sequences into the new bacterial taxonomy. *Appl Environ Microbiol* 73:5261–5267. <https://doi.org/10.1128/AEM.00062-07>
- Wang Q-J, Shen Y-E, Wang X, et al (2020a) Concomitant memantine and *Lactobacillus plantarum* treatment attenuates cognitive impairments in APP/PS1 mice. *Aging (Albany NY)* 12:628–649. <https://doi.org/10.18632/aging.102645>
- Wang R (2012) AdaBoost for Feature Selection, Classification and Its Relation with SVM, A Review. *Physics Procedia* 25:800–807. <https://doi.org/10.1016/j.phpro.2012.03.160>
- Wang X, Zhu B, Hua Y, et al (2024) *Astragalus mongholicus* Bunge and *Curcuma aromatica* Salisb. modulate gut microbiome and bile acid metabolism to inhibit colon cancer progression. *Front Microbiol* 15:. <https://doi.org/10.3389/fmicb.2024.1395634>
- Wang Y, An Y, Ma W, et al (2020b) 27-Hydroxycholesterol contributes to cognitive deficits in APP/PS1 transgenic mice through microbiota dysbiosis and intestinal barrier dysfunction. *J Neuroinflammation* 17:199. <https://doi.org/10.1186/s12974-020-01873-7>
- Wang Z, Levison BS, Hazen JE, et al (2014) Measurement of trimethylamine-N-oxide by stable isotope dilution liquid chromatography tandem mass spectrometry. *Anal Biochem* 455:35–40. <https://doi.org/10.1016/j.ab.2014.03.016>
- Waterland RA (2006) Assessing the Effects of High Methionine Intake on DNA Methylation. *The Journal of Nutrition* 136:1706S-1710S. <https://doi.org/10.1093/jn/136.6.1706S>
- Weaver D, Gupta M, Meek A, et al (2020) Alzheimer's Disease as a Disorder of Tryptophan Metabolism (2745). *Neurology* 94:
- Wei GZ, Martin KA, Xing PY, et al (2021) Tryptophan-metabolizing gut microbes regulate adult neurogenesis via the aryl hydrocarbon receptor. *Proceedings of the National Academy of Sciences* 118:e2021091118. <https://doi.org/10.1073/pnas.2021091118>
- Weng N (2006) Aging of the Immune System: How Much Can the Adaptive Immune System Adapt? *Immunity* 24:495–499. <https://doi.org/10.1016/j.immuni.2006.05.001>
- Whiley L, Chappell KE, D'Hondt E, et al (2021) Metabolic phenotyping reveals a reduction in the bioavailability of serotonin and kynurenine pathway metabolites in both the urine and serum of individuals living with Alzheimer's disease. *Alzheimer's Research & Therapy* 13:20. <https://doi.org/10.1186/s13195-020-00741-z>
- Więckowska-Gacek A, Mietelska-Porowska A, Wydrych M, Wojda U (2021) Western diet as a trigger of Alzheimer's disease: From metabolic syndrome and systemic inflammation to

- neuroinflammation and neurodegeneration. *Ageing Res Rev* 70:101397. <https://doi.org/10.1016/j.arr.2021.101397>
- Wikoff WR, Anfora AT, Liu J, et al (2009) Metabolomics analysis reveals large effects of gut microflora on mammalian blood metabolites. *PNAS* 106:3698–3703
- Willette AA, Pappas C, Hoth N, et al (2021) Inflammation, Negative Affect, and Amyloid Burden in Alzheimer's Disease: Insights from the Kynurenine Pathway. *Brain Behav Immun* 95:216–225. <https://doi.org/10.1016/j.bbi.2021.03.019>
- Williams AL, Hoofnagle JH (1988) Ratio of serum aspartate to alanine aminotransferase in chronic hepatitis. Relationship to cirrhosis. *Gastroenterology* 95:734–739. [https://doi.org/10.1016/s0016-5085\(88\)80022-2](https://doi.org/10.1016/s0016-5085(88)80022-2)
- Williams ZAP, Lang L, Nicolas S, et al (2024) Do microbes play a role in Alzheimer's disease? *Microb Biotechnol* 17:e14462. <https://doi.org/10.1111/1751-7915.14462>
- Wilmanski T, Diener C, Rappaport N, et al (2021) Gut microbiome pattern reflects healthy ageing and predicts survival in humans. *Nat Metab* 3:274–286. <https://doi.org/10.1038/s42255-021-00348-0>
- Winkler F, Koedel U, Kastenbauer S, Pfister HW (2001) Differential expression of nitric oxide synthases in bacterial meningitis: role of the inducible isoform for blood-brain barrier breakdown. *J Infect Dis* 183:1749–1759. <https://doi.org/10.1086/320730>
- Wlodarska M, Luo C, Kolde R, et al (2017) Indoleacrylic Acid Produced by Commensal *Peptostreptococcus* Species Suppresses Inflammation. *Cell Host Microbe* 22:25-37.e6. <https://doi.org/10.1016/j.chom.2017.06.007>
- World Health Organisation (2022) Ageing and health
- World Health Organization (2021) Global status report on the public health response to dementia. Security Research Hub Reports
- Wu L, Sun D (2017) Adherence to Mediterranean diet and risk of developing cognitive disorders: An updated systematic review and meta-analysis of prospective cohort studies. *Sci Rep* 7:41317. <https://doi.org/10.1038/srep41317>
- Wu M-L, Yang X-Q, Xue L, et al (2021) Age-related cognitive decline is associated with microbiota-gut-brain axis disorders and neuroinflammation in mice. *Behav Brain Res* 402:113125. <https://doi.org/10.1016/j.bbr.2021.113125>
- Wu Y-T, Shen S-J, Liao K-F, Huang C-Y (2022) Dietary Plant and Animal Protein Sources Oppositely Modulate Fecal *Bifidobacteria* and *Lachnospirillum* in Vegetarians and Omnivores. *Microbiology Spectrum* 10:e02047-21. <https://doi.org/10.1128/spectrum.02047-21>
- Wurtman RJ, Cansev M, Ulus IH (2009) Choline and Its Products Acetylcholine and Phosphatidylcholine. In: Lajtha A, Tettamanti G, Goracci G (eds) *Handbook of Neurochemistry and Molecular Neurobiology: Neural Lipids*. Springer US, Boston, MA, pp 443–501

- Xiao L, Huang L, Zhou X, et al (2022) Experimental Periodontitis Deteriorated Atherosclerosis Associated With Trimethylamine N-Oxide Metabolism in Mice. *Front Cell Infect Microbiol* 11:. <https://doi.org/10.3389/fcimb.2021.820535>
- Xie J, Song W, Liang X, et al (2020) Protective effect of quercetin on streptozotocin-induced diabetic peripheral neuropathy rats through modulating gut microbiota and reactive oxygen species level. *Biomedicine & Pharmacotherapy* 127:110147. <https://doi.org/10.1016/j.biopha.2020.110147>
- Xu F, Chong B-Q, Cai T, et al (2021) Associations between major dietary patterns and anxiety in middle-aged adults in eastern China. *Public Health Nutr* 24:1716–1724. <https://doi.org/10.1017/S1368980020000221>
- Xu R, Wang Q (2016) Towards understanding brain-gut-microbiome connections in Alzheimer's disease. *BMC Systems Biology* 10:63. <https://doi.org/10.1186/s12918-016-0307-y>
- Yamada A, Akimoto H, Kagawa S, et al (2009) Proinflammatory cytokine interferon- γ increases induction of indoleamine 2,3-dioxygenase in monocytic cells primed with amyloid β peptide 1–42: implications for the pathogenesis of Alzheimer's disease. *Journal of Neurochemistry* 110:791–800. <https://doi.org/10.1111/j.1471-4159.2009.06175.x>
- Yan Y, Wang C (2006) A β 42 is More Rigid than A β 40 at the C Terminus: Implications for A β Aggregation and Toxicity. *Journal of Molecular Biology* 364:853–862. <https://doi.org/10.1016/j.jmb.2006.09.046>
- Yang T, Wang H, Xiong Y, et al (2020) Vitamin D Supplementation Improves Cognitive Function Through Reducing Oxidative Stress Regulated by Telomere Length in Older Adults with Mild Cognitive Impairment: A 12-Month Randomized Controlled Trial. *J Alzheimers Dis* 78:1509–1518. <https://doi.org/10.3233/JAD-200926>
- Yanguas-Casás N, Barreda-Manso MA, Nieto-Sampedro M, Romero-Ramírez L (2017) TUDCA: An Agonist of the Bile Acid Receptor GPBAR1/TGR5 With Anti-Inflammatory Effects in Microglial Cells. *J Cell Physiol* 232:2231–2245. <https://doi.org/10.1002/jcp.25742>
- Yu D, Tao B-B, Yang Y-Y, et al (2015) The IDO Inhibitor Coptisine Ameliorates Cognitive Impairment in a Mouse Model of Alzheimer's Disease. *Journal of Alzheimer's Disease* 43:291–302. <https://doi.org/10.3233/JAD-140414>
- Yu F, Wang Z, Tchantchou F, et al (2012) Lithium ameliorates neurodegeneration, suppresses neuroinflammation, and improves behavioral performance in a mouse model of traumatic brain injury. *J Neurotrauma* 29:362–374. <https://doi.org/10.1089/neu.2011.1942>
- Yu M, Wang Q, Ma Y, et al (2018) Aryl Hydrocarbon Receptor Activation Modulates Intestinal Epithelial Barrier Function by Maintaining Tight Junction Integrity. *Int J Biol Sci* 14:69–77. <https://doi.org/10.7150/ijbs.22259>
- Yu Z, Chen W, Zhang L, et al (2023) Gut-derived bacterial LPS attenuates incubation of methamphetamine craving via modulating microglia. *Brain Behav Immun* 111:101–115. <https://doi.org/10.1016/j.bbi.2023.03.027>
- Zbeida M, Goldsmith R, Shimony T, et al (2014) Mediterranean diet and functional indicators among older adults in non-Mediterranean and Mediterranean countries. *J Nutr Health Aging* 18:411–418. <https://doi.org/10.1007/s12603-014-0003-9>

- Zehendner CM, Librizzi L, de Curtis M, et al (2011) Caspase-3 contributes to ZO-1 and Cl-5 tight-junction disruption in rapid anoxic neurovascular unit damage. *PLoS One* 6:e16760. <https://doi.org/10.1371/journal.pone.0016760>
- Zeisel SH, da Costa K-A (2009) Choline: An Essential Nutrient for Public Health. *Nutr Rev* 67:615–623. <https://doi.org/10.1111/j.1753-4887.2009.00246.x>
- Zelante T, Iannitti RG, Cunha C, et al (2013) Tryptophan catabolites from microbiota engage aryl hydrocarbon receptor and balance mucosal reactivity via interleukin-22. *Immunity* 39:372–385. <https://doi.org/10.1016/j.immuni.2013.08.003>
- Zeng H, Umar S, Rust B, et al (2019) Secondary Bile Acids and Short Chain Fatty Acids in the Colon: A Focus on Colonic Microbiome, Cell Proliferation, Inflammation, and Cancer. *International Journal of Molecular Sciences* 20:1214. <https://doi.org/10.3390/ijms20051214>
- Zhang J, Cashman JR (2006) Quantitative analysis of FMO gene mRNA levels in human tissues. *Drug Metab Dispos* 34:19–26. <https://doi.org/10.1124/dmd.105.006171>
- Zhang J, Li P, Wang Y, et al (2013) Ameliorative Effects of a Combination of Baicalin, Jasminoidin and Cholic Acid on Ibotenic Acid-Induced Dementia Model in Rats. *PLoS One* 8:. <https://doi.org/10.1371/journal.pone.0056658>
- Zhang X, Wang Y, Liu W, et al (2021a) Diet quality, gut microbiota, and microRNAs associated with mild cognitive impairment in middle-aged and elderly Chinese population. *The American Journal of Clinical Nutrition* 114:429–440. <https://doi.org/10.1093/ajcn/nqab078>
- Zhang X, Zhong H, Li Y, et al (2021b) Sex- and age-related trajectories of the adult human gut microbiota shared across populations of different ethnicities. *Nat Aging* 1:87–100. <https://doi.org/10.1038/s43587-020-00014-2>
- Zhang Y, Pan J, Liu Y, et al (2023) Effects of *Ficus pandurata* Hance var. *angustifolia* Cheng Flavonoids on Intestinal Barrier and Cognitive Function by Regulating Intestinal Microbiota. *Foods* 12:1682. <https://doi.org/10.3390/foods12081682>
- Zhao L, Zhang C, Cao G, et al (2019) Higher Circulating Trimethylamine N-oxide Sensitizes Sevoflurane-Induced Cognitive Dysfunction in Aged Rats Probably by Downregulating Hippocampal Methionine Sulfoxide Reductase A. *Neurochem Res* 44:2506–2516. <https://doi.org/10.1007/s11064-019-02868-4>
- Zheng D, Ge K, Qu C, et al (2024) Comparative profiling of serum, urine, and feces bile acids in humans, rats, and mice. *Commun Biol* 7:1–13. <https://doi.org/10.1038/s42003-024-06321-3>
- Zheng LJ, Lin L, Zhong J, et al (2020) Gut dysbiosis-influence on amygdala-based functional activity in patients with end stage renal disease: a preliminary study. *Brain Imaging Behav* 14:2731–2744. <https://doi.org/10.1007/s11682-019-00223-3>
- Zheng S, Zhang H, Liu R, et al (2021) Do short chain fatty acids and phenolic metabolites of the gut have synergistic anti-inflammatory effects? – New insights from a TNF- α -induced Caco-2 cell model. *Food Research International* 139:109833. <https://doi.org/10.1016/j.foodres.2020.109833>

- Zheng X, Huang F, Zhao A, et al (2017) Bile acid is a significant host factor shaping the gut microbiome of diet-induced obese mice. *BMC Biology* 15:120. <https://doi.org/10.1186/s12915-017-0462-7>
- Zheng Y, He J-Q (2022) Pathogenic Mechanisms of Trimethylamine N-Oxide-induced Atherosclerosis and Cardiomyopathy. *Current vascular pharmacology* 20:29. <https://doi.org/10.2174/1570161119666210812152802>
- Zhou G, Ewald J, Xia J (2021) OmicsAnalyst: a comprehensive web-based platform for visual analytics of multi-omics data. *Nucleic Acids Research* 49:W476–W482. <https://doi.org/10.1093/nar/gkab394>
- Zhou L, Wang W, Huang J, et al (2016) In vitro extraction and fermentation of polyphenols from grape seeds (*Vitis vinifera*) by human intestinal microbiota. *Food Funct* 7:1959–1967. <https://doi.org/10.1039/C6FO00032K>
- Zhu C, Li G, Lv Z, et al (2020) Association of plasma trimethylamine-N-oxide levels with post-stroke cognitive impairment: a 1-year longitudinal study. *Neurol Sci* 41:57–63. <https://doi.org/10.1007/s10072-019-04040-w>
- Zhu W, Gregory JC, Org E, et al (2016) Gut Microbial Metabolite TMAO Enhances Platelet Hyperreactivity and Thrombosis Risk. *Cell* 165:111–124. <https://doi.org/10.1016/j.cell.2016.02.011>
- Zhuang Z, Gao M, Yang R, et al (2020) Causal relationships between gut metabolites and Alzheimer’s disease: a bidirectional Mendelian randomization study. *Neurobiology of Aging*. <https://doi.org/10.1016/j.neurobiolaging.2020.10.022>
- Zhuang Z, Gao M, Yang R, et al (2021) Causal relationships between gut metabolites and Alzheimer’s disease: a bidirectional Mendelian randomization study. *Neurobiology of Aging* 100:119.e15–119.e18. <https://doi.org/10.1016/j.neurobiolaging.2020.10.022>
- Zhuang Z-Q, Shen L-L, Li W-W, et al (2018) Gut Microbiota is Altered in Patients with Alzheimer’s Disease. *Journal of Alzheimer’s Disease* 63:1337–1346. <https://doi.org/10.3233/JAD-180176>
- Zilberter Y, Zilberter M (2017) The vicious circle of hypometabolism in neurodegenerative diseases: Ways and mechanisms of metabolic correction. *J Neurosci Res* 95:2217–2235. <https://doi.org/10.1002/jnr.24064>
- Zubrikhina MO, Abramova OV, Yarkin VE, et al (2023) Machine learning approaches to mild cognitive impairment detection based on structural MRI data and morphometric features. *Cognitive Systems Research* 78:87–95. <https://doi.org/10.1016/j.cogsys.2022.12.005>
- Zwilling D, Huang S-Y, Sathyaikumar KV, et al (2011) Kynurenine 3-monooxygenase inhibition in blood ameliorates neurodegeneration. *Cell* 145:863–874. <https://doi.org/10.1016/j.cell.2011.05.020>
- Çiçek S (2020) Structure-Dependent Activity of Natural GABA(A) Receptor Modulators. *Molecules (Basel, Switzerland)* 23:. <https://doi.org/10.3390/molecules23071512>

Appendix

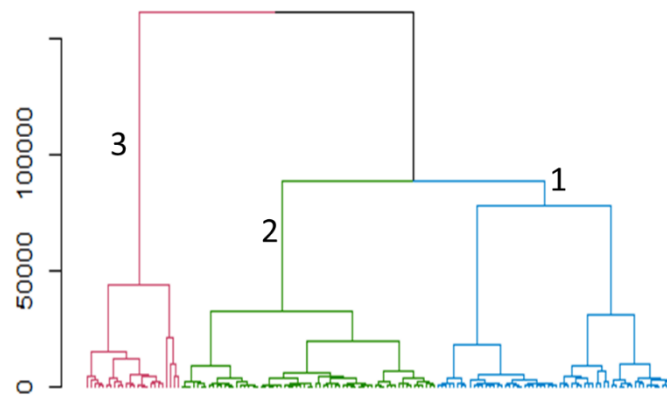


Figure S2.1: Hierarchical clustering of participant food frequency questionnaires. Food frequency questionnaires were analysed using the hierarchical clustering ‘Ward’ method to cluster participants with similar dietary patterns. This grouped participants into low intake of macronutrients (1), moderate intake of macronutrients (2) and high intake of macronutrients (3).

Supplementary Table S2.1: Gut microbiome abundance in control, MCI and SCI at the phylum level. P-value generated by one-way ANOVA, with false discovery rate (FDR) correction for multiple testing.

Phylum	Control (n=50)		SCI (n=50)		MCI (n=50)		F Value	P- value	FDR
	Mean	SD	Mean	SD	Mean	SD			
Unidentified Bacteria	922.44	594.05	650.33	501.09	935.52	937.25	2.543	0.082	0.572
Actinobacteria	6256.20	9912.81	3364.15	3993.76	4297.44	5447.30	2.202	0.114	0.572
Bacteroidota	15959.58	9704.01	18935.69	10742.37	18767.63	10264.87	1.315	0.272	0.637
Desulfobacterota	225.88	282.13	150.90	201.20	233.40	330.38	1.313	0.272	0.637
Euryarchaeota	2614.94	5094.50	1686.13	3064.45	2911.29	4357.00	1.079	0.343	0.637
Proteobacteria	2370.36	6826.07	1382.56	2843.53	3258.67	8728.70	0.968	0.382	0.637
Not Assigned	341.88	217.19	321.08	122.14	325.19	134.15	0.222	0.802	0.989
Actinobacteriota	2437.84	2206.50	2297.54	2171.70	2610.83	2937.17	0.195	0.823	0.989
Firmicutes	70229.50	17138.75	69177.04	20340.41	69458.27	15828.92	0.046	0.955	0.989
Verrucomicrobiota	1360.96	2029.93	1324.35	2433.39	1398.48	2787.95	0.011	0.989	0.989

SD= standard deviation

Supplementary Table S2.2: Gut microbiome abundance in control, MCI and SCI at the genus level. P-value generated by one-way ANOVA, with false discovery rate (FDR) correction for multiple testing.

Genus	Control (n=50)		SCI (n=50)		MCI (n=50)		F value	P-value	FDR
	Mean	SD	Mean	SD	Mean	SD			
<i>Holdemania</i>	1.12	1.14	3.58	3.24	1.10	1.14	20.140	<0.001	0.007
<i>UCG_009</i>	1.13	1.41	1.04	1.23	0.27	0.51	11.400	<0.001	0.007
<i>Lachnoclostridium</i>	23.83	16.15	43.29	30.72	29.44	17.06	9.446	0.001	0.044
<i>Turicibacter</i>	60.27	79.99	24.07	35.95	29.93	40.03	5.130	0.007	0.189
<i>Lachnospiraceae_ND3007_group</i>	116.70	92.88	132.60	96.04	78.22	73.04	4.597	0.012	0.255
<i>Lactonifactor</i>	0.14	0.40	0.58	1.13	0.31	0.55	4.253	0.016	0.300
<i>Ruminococcus_gnavus_group</i>	0.11	0.31	0.83	2.08	0.43	0.90	3.755	0.026	0.307
<i>Bacteroides</i>	1145.70	831.52	1678.54	1153.60	1471.77	969.21	3.606	0.030	0.324
<i>Romboutsia</i>	421.18	369.06	246.42	312.89	290.79	355.15	3.377	0.037	0.372
<i>Intestinibacter</i>	308.84	398.92	149.71	172.09	219.98	338.39	3.062	0.049	0.448
<i>Fusicatenibacter</i>	235.68	161.93	329.79	262.31	247.10	186.98	2.966	0.055	0.448
<i>Lachnospiraceae_UCG_004</i>	2.96	4.10	5.00	6.94	2.81	3.20	2.890	0.059	0.453
<i>DTU089</i>	2.78	3.86	1.40	1.94	1.79	2.78	2.816	0.063	0.460
<i>Parasutterella</i>	5.92	15.65	13.54	33.01	4.06	9.10	2.588	0.079	0.500
<i>unidentified_Ruminococcaceae</i>	5.06	11.68	10.06	22.47	3.48	5.01	2.571	0.080	0.500
<i>Parabacteroides</i>	124.64	115.60	222.08	331.41	161.08	128.52	2.566	0.080	0.500
<i>Bifidobacterium</i>	819.82	1362.41	416.54	483.27	527.65	645.06	2.514	0.085	0.500
<i>Shuttleworthia</i>	5.38	11.37	2.88	3.81	2.38	3.22	2.435	0.091	0.500
<i>Coprobacter</i>	6.24	11.97	10.00	14.11	5.00	7.73	2.432	0.092	0.500
<i>Defluviitaleaceae_UCG_011</i>	3.02	3.74	1.77	2.89	1.85	2.90	2.334	0.101	0.513
<i>Oscillospira</i>	0.82	1.62	0.40	0.71	0.42	0.71	2.284	0.106	0.513
<i>Monoglobus</i>	39.80	37.65	57.69	68.53	38.54	34.68	2.283	0.106	0.513
<i>Family_XIII_UCG_001</i>	7.94	6.94	5.60	4.49	6.35	5.00	2.231	0.111	0.520
<i>Erysipelatoclostridium</i>	11.36	21.75	22.79	44.76	12.13	15.61	2.194	0.115	0.520

<i>Butyricimonas</i>	6.58	10.63	7.13	12.82	14.29	31.71	2.118	0.124	0.541
<i>Roseburia</i>	105.44	104.08	162.33	178.58	132.94	136.81	1.948	0.146	0.578
<i>Negativibacillus</i>	6.14	9.62	8.90	14.42	12.02	19.69	1.862	0.159	0.578
<i>Butyricococcus</i>	50.02	45.21	65.42	62.85	47.90	33.85	1.856	0.160	0.578
<i>Dorea</i>	246.36	143.07	235.52	115.79	290.96	183.05	1.853	0.161	0.578
<i>Ruminococcus_torques_group</i>	65.32	86.53	79.60	69.12	100.90	115.25	1.842	0.162	0.578
<i>Desulfovibrio</i>	20.96	35.43	8.81	23.60	19.42	40.57	1.836	0.163	0.578
<i>Streptococcus</i>	51.30	85.73	123.77	320.59	156.48	365.15	1.779	0.173	0.578
<i>Eubacterium_ventriosum_group</i>	65.46	151.98	32.52	25.73	38.17	38.58	1.774	0.173	0.578
<i>Hungatella</i>	0.80	1.62	2.81	7.15	7.23	29.21	1.768	0.174	0.578
<i>Catenibacillus</i>	0.74	1.50	0.46	1.38	0.27	0.71	1.756	0.176	0.578
<i>Lacticaseibacillus</i>	0.90	3.85	0.58	1.65	3.10	11.98	1.709	0.185	0.590
<i>unidentified_Gastranaerophilales</i>	0.54	1.68	0.69	1.85	1.48	4.13	1.610	0.203	0.620
<i>Lachnospira</i>	47.66	56.85	63.13	109.70	36.17	34.73	1.609	0.204	0.620
<i>Faecalibacterium</i>	704.26	513.26	895.96	581.74	785.65	539.99	1.522	0.222	0.648
<i>Faecalitalea</i>	4.08	10.48	9.33	22.59	4.31	15.14	1.518	0.223	0.648
<i>UBA1819</i>	4.00	5.35	3.10	3.92	5.90	12.52	1.470	0.233	0.664
<i>Escherichia_Shigella</i>	277.36	852.95	104.96	306.82	369.40	1018.23	1.394	0.251	0.681
<i>Gordonibacter</i>	1.82	2.63	0.98	1.72	1.52	3.05	1.386	0.253	0.681
<i>Phoceea</i>	0.30	0.74	0.48	1.03	0.21	0.62	1.381	0.255	0.681
<i>Adlercreutzia</i>	9.76	10.62	11.10	12.54	14.70	21.16	1.328	0.268	0.691
<i>Eubacterium_eligens_group</i>	27.82	32.88	42.21	43.61	31.94	55.84	1.323	0.270	0.691
<i>unidentified_Erysipelotrichaceae</i>	9.76	17.12	8.46	37.92	2.38	6.08	1.289	0.279	0.691
<i>Lachnospiraceae_FCS020_group</i>	36.82	22.63	30.40	22.23	31.35	19.69	1.272	0.283	0.691
<i>Sutterella</i>	11.82	18.64	21.44	50.48	12.75	19.18	1.265	0.285	0.691
<i>Odoribacter</i>	12.12	12.45	14.94	15.44	11.04	9.08	1.227	0.296	0.691
<i>Blautia</i>	1175.92	587.50	1407.38	755.54	1260.94	865.82	1.211	0.301	0.691
<i>Frisingicoccus</i>	0.98	3.99	3.29	8.85	5.54	23.41	1.206	0.302	0.691
<i>GCA_900066575</i>	4.06	4.14	5.31	5.40	4.00	4.53	1.194	0.306	0.691
<i>UC5_1_2E3</i>	0.20	0.45	0.50	1.34	0.42	1.03	1.175	0.312	0.692

<i>Veillonella</i>	5.22	17.90	9.65	31.08	3.50	6.94	1.091	0.339	0.700
<i>Prevotella_9</i>	396.22	924.21	195.83	526.81	450.58	1122.81	1.085	0.341	0.700
<i>Tyzzerella</i>	7.16	19.74	4.71	13.10	11.04	28.67	1.064	0.348	0.700
<i>Methanobrevibacter</i>	336.18	669.38	211.06	374.14	361.23	537.90	1.058	0.350	0.700
<i>UCG_003</i>	16.74	28.81	15.29	21.65	10.40	15.59	1.036	0.357	0.700
<i>Marvinbryantia</i>	24.22	20.89	18.29	15.80	23.15	26.92	1.031	0.359	0.700
<i>Haemophilus</i>	4.36	12.82	32.75	201.64	2.56	9.50	1.029	0.360	0.700
<i>Bilophila</i>	8.08	9.68	10.90	10.10	10.50	11.94	1.018	0.364	0.700
<i>GCA_900066755</i>	0.32	0.71	0.17	0.43	0.31	0.62	0.997	0.372	0.700
<i>UCG_008</i>	0.32	0.89	0.15	0.50	0.40	1.16	0.988	0.375	0.700
<i>Parvibacter</i>	0.62	2.63	1.17	3.03	1.42	3.00	0.978	0.379	0.700
<i>Corynebacterium</i>	0.20	0.53	0.13	0.39	0.29	0.77	0.973	0.381	0.700
<i>UCG_005</i>	94.14	83.08	80.00	81.08	72.69	68.88	0.961	0.385	0.700
<i>Eggerthella</i>	3.46	14.11	7.81	21.48	5.31	10.27	0.916	0.402	0.722
<i>Ruminococcus</i>	628.98	491.31	613.60	545.71	506.04	474.47	0.854	0.428	0.753
<i>Christensenella</i>	0.26	0.75	0.52	1.40	0.38	0.70	0.837	0.435	0.753
<i>Lachnospiraceae_NK4A136_group</i>	76.24	92.21	106.42	95.02	97.50	161.80	0.816	0.444	0.753
<i>unidentified_Lachnospiraceae</i>	0.78	1.27	1.10	2.30	1.29	2.32	0.811	0.447	0.753
<i>Actinomyces</i>	2.56	2.82	3.63	5.63	2.98	3.62	0.806	0.448	0.753
<i>Holdemanella</i>	126.22	224.72	214.31	560.79	208.42	368.27	0.724	0.487	0.807
<i>Anaerofustis</i>	0.38	0.75	0.29	0.62	0.23	0.52	0.693	0.502	0.810
<i>Merdibacter</i>	0.94	1.80	1.04	4.28	0.42	1.46	0.693	0.502	0.810
<i>Enterobacter</i>	49.44	345.85	89.06	419.64	13.52	68.22	0.683	0.507	0.810

SD= standard deviation

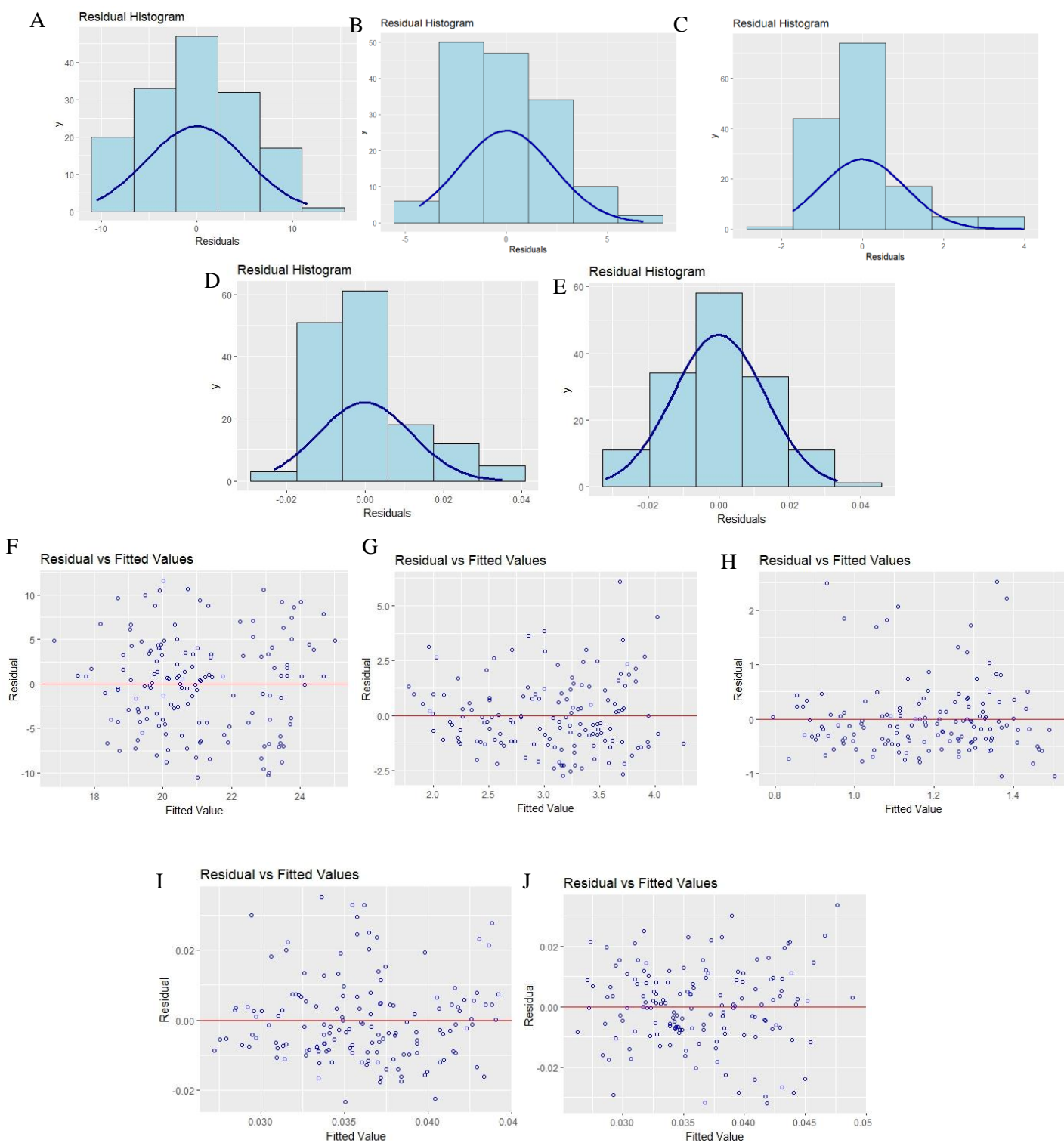


Figure S2.2: Assumptions of the multiple linear regression analysis. Histogram displaying normality of the residuals for (A) choline, (B) indoxyl sulfate, (C) indole propionic acid, (D) kynurenic acid, (E) 5-hydroxyindole acetic acid. Residuals versus fitted plot confirming homoscedasticity of (F) choline, (G) indoxyl sulfate, (H) indole propionic acid, (I) kynurenic acid, (J) 5-hydroxyindole acetic acid.

Table S2.3: Serum metabolite concentrations in control, subjective cognitive impairment (SCI) and mild cognitive impairment (MCI) by LC-MS/MS. Mean \pm SD. P-value generated from one-way ANOVA. <LOD= below the limit of detection.

Pathway	Metabolite	Control (μ M)	SCI (μ M)	MCI (μ M)	P-value
TMAO Pathway	Trimethylamine	0.94 \pm 0.31	0.96 \pm 0.78	1.03 \pm 1.15	0.86
	Trimethylamine N-oxide	4.49 \pm 2.96	5.81 \pm 8.46	7.04 \pm 9.63	0.25
	Choline	23.25 \pm 6.20	19.79 \pm 4.93	20.09 \pm 4.81	<0.01
Tryptophan Pathway	Tryptophan	36.09 \pm 4.78	36.62 \pm 4.44	36.08 \pm 6.96	0.79
	Kynurenine	1.07 \pm 0.27	1.16 \pm 0.29	1.16 \pm 0.27	0.19
	Serotonin	0.35 \pm 0.16	0.31 \pm 0.17	0.35 \pm 0.14	0.32
	5-hydroxyindole acetic acid	0.05 \pm 0.02	0.04 \pm 0.01	0.03 \pm 0.01	<0.01
	Kynurenic acid	0.03 \pm 0.01	0.04 \pm 0.01	0.04 \pm 0.01	0.18
	Xanthurenic acid	0.01 \pm 0.01	0.02 \pm 0.01	0.02 \pm 0.01	0.88
	3-hydroxyanthranilic acid	<LOD	<LOD	<LOD	-
	Anthranilic acid	0.07 \pm 0.06	0.09 \pm 0.07	0.06 \pm 0.06	0.11
	Indole	<LOD	<LOD	<LOD	-
	Indole-3 -acetic acid	1.33 \pm 0.48	1.4 \pm 0.48	1.36 \pm 0.68	0.84
	Indole-3- lactic acid	0.54 \pm 0.23	0.49 \pm 0.14	0.50 \pm 0.13	0.42
	Indole-3- carboxaldehyde	0.03 \pm 0.01	0.03 \pm 0.01	0.03 \pm 0.01	0.50
	Indole-3 -propionic acid	1.34 \pm 0.67	1.19 \pm 0.62	0.96 \pm 0.68	0.02
	Methyl indole 3- acetate	0.03 \pm 0.02	0.03 \pm 0.02	0.03 \pm 0.02	0.41
	Indoxyl sulfate	2.41 \pm 1.24	3.54 \pm 2.03	3.18 \pm 1.55	<0.01
<i>P</i> -Cresol Pathway	<i>P</i> -cresol sulfate	19.93 \pm 10.87	22.79 \pm 13.22	23.45 \pm 12.21	0.31
	<i>P</i> -cresol glucuronide	0.13 \pm 0.14	0.13 \pm 0.20	0.12 \pm 0.12	0.87
	CA	0.23 \pm 0.35	0.26 \pm 0.48	0.24 \pm 0.40	0.95
	CDCA	0.01 \pm 0.01	0.01 \pm 0.02	0.01 \pm 0.02	0.71
	HDCA	0.02 \pm 0.02	0.02 \pm 0.02	0.03 \pm 0.06	0.17
	GCDCA	0.39 \pm 0.26	0.49 \pm 0.90	0.41 \pm 0.33	0.64
	GDCA	0.16 \pm 0.15	0.20 \pm 0.33	0.23 \pm 0.24	0.46

Bile Acid Pathway	GCA	0.10 ± 0.08	0.23 ± 0.84	0.14 ± 0.19	0.43
	DCA	0.26 ± 0.26	0.27 ± 0.31	0.31 ± 0.45	0.75
	TCDC	0.05 ± 0.05	0.10 ± 0.35	0.06 ± 0.07	0.43
	TDCA	0.02 ± 0.02	0.04 ± 0.10	0.05 ± 0.07	0.21
	GUCDA	0.06 ± 0.08	0.05 ± 0.07	0.05 ± 0.06	0.75
	TUDCA	<LOD	<LOD	<LOD	-
	TLCA	<LOD	<LOD	<LOD	-
	THCA	<LOD	<LOD	<LOD	-
	GLCA	0.02 ± 0.02	0.01 ± 0.01	0.03 ± 0.06	0.19
	GHCA	<LOD	<LOD	<LOD	-
	GHDCA	<LOD	<LOD	<LOD	-
	UDCA	0.03 ± 0.05	0.04 ± 0.07	0.03 ± 0.06	0.83
	TCA	0.03 ± 0.03	0.09 ± 0.40	0.04 ± 0.06	0.41
	HCA	0.01 ± 0.01	0.01 ± 0.01	0.01 ± 0.1	0.39
	LCA	0.03 ± 0.03	0.04 ± 0.03	0.05 ± 0.07	0.13

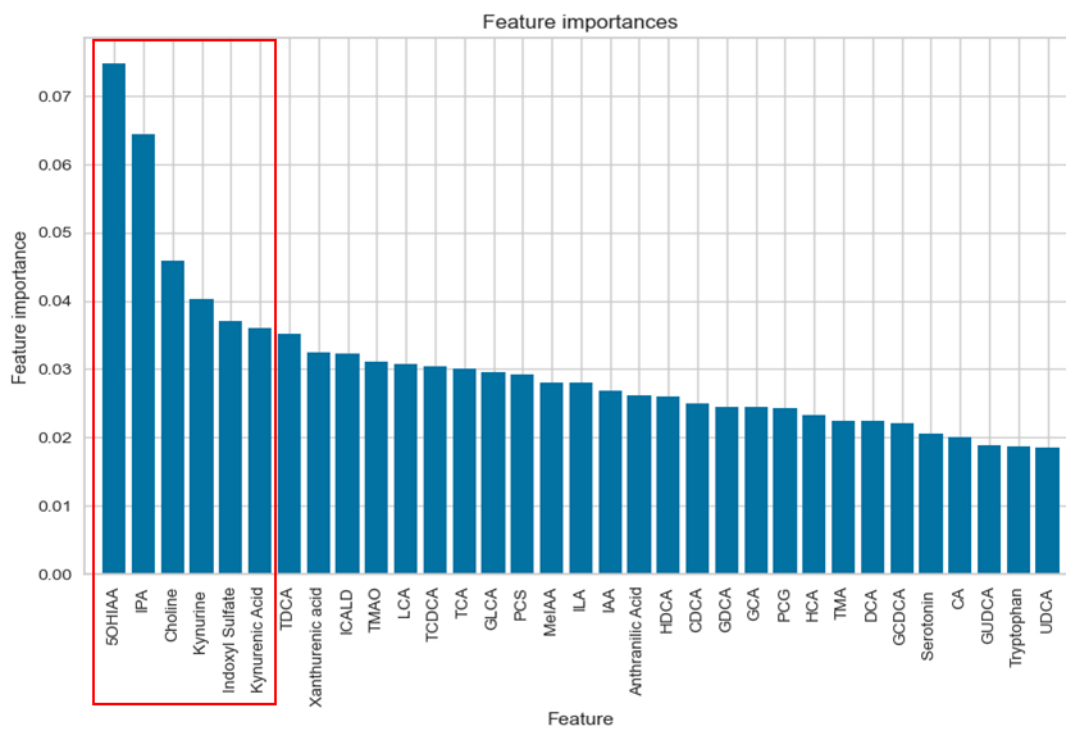


Figure S2.3: Identification of the top metabolites predictive of early cognitive decline. Mean decrease Gini values highlighting the importance of each metabolite in our model. Red box indicates the top six metabolites that gave the highest AUC scores.

Supplementary Table S3.1: Summary of the dietary composition of chow and refined diet (rLFD).

	Chow Diet SDS RM3	rLFD D17060802
KJ/g	15.21	16.21
Protein (%)	26.9	20
Carbohydrate (%)	61.2	70
Fat (%)	11.5	10
Starch (g/Kg)	338.8	452.2 Corn Starch
Maltodextrin 10 (g/Kg)	0	75
Sucrose (g/Kg)	43.7	173
Fibre (g/Kg)	161.5	50
Fibre Content	Soluble and insoluble	Cellulose

Supplementary Table S3.2: Primer Sequences

GenBank Accession	Gene	Description	Forward primer sequence (5' -> 3')	Reverse primer sequence (5' -> 3')
NM_013842	<i>Xbp1</i>	Xbox binding protein 1	AGCAGCAAGTGGTGG ATTTG	GAGTTTTCTCCCGTAA AAGCTGA
NM_017406	<i>Atf6b</i>	Activating transcription factor 6 beta	TCGCCTTTTAGTCCGG TTCTT	GGCTCCATAGGTCTGA CTCC
NM_133819	<i>Ppp1r15b</i>	Protein phosphatase 1, regulatory (inhibitor) subunit 15b; Gadd34	CGCCTGCTCTTCGGAG TTC	TCTAGCCATCTGGTAG GAATCAG
NM_007527	<i>Bax</i>	BCL2-associated X protein	AGGATGCGTCCACCAAG AAGCT	TCCGTGTCCACGTCAGCA ATCA
NM_008745	<i>Ntrk2</i>	Neurotrophic tyrosine kinase, receptor, type 2; TrkB	CCACGGATGTTGCTGAC CAAAG	GCCAAACTTGGAATGTC TCGCC
NM_010548	<i>Il10</i>	Interleukin 10	CGGGAAGACAATAACTG CACCC	CGGTTAGCAGTATGTTGT CCAGC
NM_008689	<i>Nfkb1</i>	Nuclear factor of kappa light polypeptide gene enhancer in B-cells 1, p105	ATGGCAGACGATGATCC CTAC	TGTTGACAGTGGTATTC TGGTG
NM_011905	<i>Tlr2</i>	Toll-like receptor 2	ACAGCAAGGTCTTCCTG GTTCC	GCTCCCTTACAGGCTGA GTTCT
NM_009788	<i>Calb1</i>	Calbindin 1	GGCTTCATTTGACGCTG AC	ACGTGAGCCAACCTCTAC AATTC
NM_011330	<i>Ccl11</i>	Chemokine (C-C motif) ligand 11	TCCATCCCAACTTCCTGC TGCT	CTCTTTGCCCAACCTGGT CTTG
NM_013492	<i>Clu</i>	Clusterin	AGCAGGAGGTCTCTGAC AATG	GGCTTCCTCTAAACTGTT GAGC
NM_009883	<i>Cebp</i>	CCAAT/enhancer binding protein (C/EBP), beta	CAACCTGGAGACGCAGC ACAAG	GCTTGAACAAGTCCGC AGGGT
NM_008337	<i>Ifng</i>	Interferon gamma	GCCACGGCACAGTCATT GA	TGCTGATGGCCTGATTGT CTT
NM_008361	<i>Il1b</i>	Interleukin 1 beta	GAAATGCCACCTTTTGA CAGTG	TGGATGCTCTCATCAGG ACAG
NM_001313921	<i>Nos2</i>	Nitric oxide synthase 2, inducible	GAGACAGGGAAGTCTGA AGCAC	CCAGCAGTAGTTGCTCCT CTTC
NM_021297	<i>Tlr4</i>	Toll-like receptor 4	AAATGCACTGAGCTTTA GTGGT	TGGCACTCATAATGATG GCAC
NM_013693	<i>Tnf</i>	Tumor necrosis factor	CAGGCGGTGCCTATGTC TC	CGATCACCCCGAAGTTC AGTAG
NM_009652	<i>Akt1</i>	Thymoma viral proto-oncogene 1	CCTTTATTGGCTACAAG GAACGG	GAAGGTGCGCTCAATGA CTG
NM_018790	<i>Arc</i>	Activity regulated cytoskeletal-associated protein	GCTGGAAGAAGTCCATC AAGGC	ACCTCTCCAGACGGTAG AAGAC
NM_007540	<i>Bdnf</i>	Brain derived neurotrophic factor	GGCTGACACTTTTGAGC ACGTC	CTCCAAAGGCACTTGAC TGCTG

NM_010234	<i>Fos</i>	FBJ osteosarcoma oncogene	CGGGTTTCAACGCCGAC TA	TTGGCACTAGAGACGGA CAGA
NM_133828	<i>Creb1</i>	CAMP responsive element binding protein 1	ACCCAGGGAGGAGCAAT ACAG	TGGGGAGGACGCCATAA CA
NM_177407	<i>Camk2a</i>	Calcium/calmodulin-dependent protein kinase II alpha	AGCCATCCTCACCCTA TGCTG	GTGTCTTCGTCCTCAATG GTGG
NM_008171	<i>Grin2b</i>	Glutamate receptor, ionotropic, NMDA2B (epsilon 2)	CTGGTGACCAATGGCAA GCATG	GGCACAGAGAAGTCAAC CACCT
NM_008170	<i>Grin2a</i>	Glutamate receptor, ionotropic, NMDA2A (epsilon 1)	ACGTGACAGAACGCGAA CTT	TCAGTGCGGTTTCATCAAT AACG
NM_176942	<i>Gabra5</i>	Gamma-aminobutyric acid (GABA) A receptor, subunit alpha 5	GCAGGTGCGAACAGACA TCTA	CCTTAAACCGCAGCCTTT CATC
NM_011101	<i>Pkca</i>	Protein kinase C, alpha	AGAGGTGCCATGAGTTC GTTA	GGCTTCCGTATGTGTGGA TTTT
NM_010875	<i>Ncam1</i>	Neural cell adhesion molecule 1	GGTTCCGAGATGGTCAG TTGCT	CAAGGACTCCTGTCCAA TACGG
NM_011949	<i>Mapk1</i>	Mitogen-activated protein kinase 1	GGTTGTTCCCAAATGCT GACT	CAACTTCAATCCTCTTGT GAGGG
NM_177340	<i>Synpo</i>	Synaptopodin	CCTGCCCGTAACCTCCGT G	GAGCGCGGGTAGGGAAA AG
NM_011739	<i>Ywhaq</i>	Tyrosine 3-monooxygenase/tryptophan 5-monooxygenase activation protein, theta polypeptide	ATTGAGCAGAAGACCGA CACC	TGTTTTTCGATCATCGCCA CAA
NM_008324	<i>Ido1</i>	Indoleamine 2,3-dioxygenase 1	GCAGACTGTGTCCTGGC AAACT	AGAGACGAGGAAGAAGC CCTTG
NM_007864	<i>Dlg4</i>	Discs, large homolog 4 (Drosophila); PSD95	TCAGACGGTCACGATCA TCGCT	GTTGCTTCGCAGAGATG CAGTC
NM_010142	<i>Ephb2</i>	Eph receptor B2	CAACGGTGTGATCCTGG ACTAC	CACCTGGAAGACATAGA TGGCG
NM_008712	<i>Nos1</i>	Nitric oxide synthase 1, neuronal	ACCAGCACCTTTGGCAA TGGAG	GAGACGCTGTTGAATCG GACCT
NM_001081304	<i>Atf6</i>	Activating transcription factor 6b	TCGCCTTTTAGTCCGG TTCTT	GGCTCCATAGGTCTGA CTCC
NM_016700	<i>Mapk8</i>	Mitogen activated protein kinase 8	AGCAGAAGCAAACGT GACAAC	GCTGCACACACTATTC CTTGAG
NM_009716	<i>Atf4</i>	Activating transcription factor 4	CTCTTGACCACGTTGG ATGAC	CAACTTCACTGCCTAG CTCTAAA

NM_001005509	<i>Eif2a</i>	Eukaryotic translation initiation factor 2a	CCACACTTCACAGAAA GCACGG	TCGAAGGAGTGCAGT AGTCCCT
NM_010121	<i>Eif2ak3</i>	Eukaryotic translation initiation factor 2 alpha kinase 3	AGTCCCTGCTCGAATCTT CCT	TCCAAGGCAGAACAGA TATACC
		Endoplasmic reticulum (ER) to nucleus signalling 1	ACACTGCCTGAGACCT TGTTG	GGAGCCCCTCCTCTTG CTA
NM_174985	<i>Tgr5</i>	G protein-coupled bile acid receptor 1; Gpbar1	CACTGCTCTTCTTGCT GTGTTGG	GAGCGATAACAGAGT TCCAGGC
NM_008003	<i>Fgf15</i>	Fibroblast growth factor 15	GTCGCTCTGAAGACGA TTGCCA	CAGTCTTCCTCCGAGT AGCGAA
NM_009108	<i>Fxr</i>	Nuclear receptor subfamily 1, group H, member 4; Nr1h4	GGGATGAGTGTGAAG CCAGCTA	GTGGCTGAACTTGAGG AAACGG
NM_022310	<i>Hspa5</i>	Heat shock protein 5	ACTTGGGGACCACCTA TTCCT	ATCGCCAATCAGACGC TCC
NM_007837	<i>Ddit3</i>	DNA damage inducible transcript 3	CTGGAAGCCTGGTATG AGGAT	CAGGGTCAAGAGTAG TGAAGGT
NM_008907	<i>Ppia</i>	Peptidylprolyl isomerase A	GAGCTGTTTGCAGACA AAGTTC	CCCTGGCACATGAATC CTGG
NM_007591	<i>Calr</i>	Calreticulin	AAAGGACCCTGATGCT GCCAAG	TCAGGGATGTGCTCTG GCTTGT
NM_138677	<i>Edem1</i>	ER degradation enhancer, mannosidase alpha-like 1	GGGGCATGTTTCGTCTT CGG	CGGCAGTAGATGGGG TTGAG
NM_009735	<i>B2m</i>	Beta-2 microglobulin	TTCTGGTGCTTGTCTCAC TGA	CAGTATGTTTCGGCTTCCC ATTC
NM_011146	<i>Pparg</i>	Peroxisome proliferator activated receptor gamma	GTA CTGTCGGTTTCAG AAGTGCC	ATCTCCGCCAACAGCT TCTCCT
NM_011787	<i>Amfr</i>	Autocrine motility factor receptor	CCTCGCTTGAACCAGC ACAATC	TTGCTTGCCTGCGTGA TGCCAA
NM_028769	<i>Syvn1</i>	Synovial apoptosis inhibitor 1, synoviolin	CCAACATCTCCTGGCT CTTCCA	CAGGATGCTGTGATAA GCGTGG
NM_007643	<i>Cd36</i>	CD36 molecule	GGACATTGAGATTCTTTT CCTCTG	GCAAAGGCATTGGCTGG AAGAAC
NM_008654	<i>Ppp1r15a</i>	Protein phosphatase 1, regulatory (inhibitor) subunit 15A; Gadd34	GGCGGCTCAGATTGTTC AAAGC	CCAGACAGCAAGGAAAT GGACTG
NM_010902	<i>Nfe2l2</i>	Nuclear factor, erythroid derived 2, like 2; Nrf2	CAGCATAGAGCAGGACA TGGAG	GAACAGCGGTAGTATCA GCCAG

Supplementary Table S3.3: Changes in gut microbiome Phyla between chow and refined diet (rLFD). P-value generated by Mann-Whitney.

	P-value	FDR	Statistics
Deferribacterota	0.000468	0.003745	-11.139
Desulfobacterota	0.002519	0.010075	-8.9805
Firmicutes	0.069563	0.15002	2.2074
Not_Assigned	0.075008	0.15002	-2.6806
Bacteroidota	0.23995	0.38392	1.3281
Actinobacteriota	0.29488	0.39317	-1.1339
Patescibacteria	0.67031	0.76607	0.44634
Proteobacteria	0.87823	0.87823	-0.15903

Table S3.4: ¹H NMR metabolomic concentrations. All concentrations are given in μmol/g.

	Chow		rLFD		p-value
	Mean	SD	Mean	SD	
3-Dihydroxyacetone	0.04	0.02	0.10	0.03	0.01
2-Oxoisocaproate	0.48	0.22	0.34	0.10	0.29
2-methylbutyric	0.15	0.06	0.46	0.34	0.08
3-Methyl-2-oxovalerate	0.55	0.23	0.47	0.15	0.60
3-Phenylpropionate	0.29	0.17	0.22	0.03	0.48
5-Aminopentanoic acid	0.28	0.06	0.26	0.10	0.73
AMP	0.10	0.09	0.04	0.01	0.19
Acetate	39.98	4.67	28.15	10.06	<0.01
Acetoin	0.04	0.09	0.00	0.00	0.41
Alanine	1.81	0.93	6.13	1.48	<0.01
Alpha-ketoisovaleric acid	0.28	0.11	0.36	0.12	0.34
Arabinose	2.20	1.16	1.00	0.13	0.08
Asparagine	1.19	0.66	3.15	1.11	0.01
Aspartate	0.46	0.18	0.89	0.32	0.04
Butyrate	22.47	3.09	5.17	2.68	<0.01
Choline	0.53	0.07	1.38	0.59	0.01
Creatine	0.61	0.15	1.36	0.72	0.05
Cytidine monophosphate	0.73	0.47	0.60	0.12	0.61
Dimethylamine	0.02	0.01	0.05	0.04	0.11
Ethanol	23.84	18.33	21.43	24.17	0.87
Ferulate	0.09	0.02	0.06	0.02	0.06
Formate	0.14	0.01	0.20	0.05	0.05
Fructose	1.68	0.94	1.22	1.59	0.60
Fumarate	0.04	0.01	0.05	0.02	0.24
GTP	0.33	0.12	0.12	0.03	0.02
Galactose	2.56	1.89	1.19	0.66	0.21
Glucose	15.27	6.15	13.52	1.91	0.60
Glutamate	8.09	2.15	10.56	3.37	0.22
Glutamine	2.00	0.66	3.83	1.11	0.02
Glycerol	4.53	2.73	9.39	5.89	0.14
Glycine	3.48	1.84	7.06	1.74	0.02
Histidine	0.94	0.27	1.27	0.52	0.25
Hypoxanthine	2.50	0.50	1.49	0.21	<0.01
Isobutyrate	0.32	0.13	0.63	0.42	0.16
Isoleucine	4.14	1.86	6.55	1.65	0.08
Lactaldehyde	0.22	0.04	0.15	0.05	0.04
Lactate	1.40	0.88	1.35	1.62	0.95
Leucine	6.19	2.71	10.41	4.37	0.12
Lysine	4.50	1.66	8.99	3.21	0.03
Malic	0.38	0.15	1.05	0.89	0.14
Methanol	0.38	0.09	0.23	0.14	0.08
Methionine	2.55	0.87	3.39	0.69	0.16
Methylamine	0.16	0.03	0.04	0.03	<0.01
Nicotinate	0.81	0.19	0.31	0.06	<0.01
Ornithine	0.03	0.07	0.10	0.13	0.35
Phenylalanine	2.95	1.15	3.78	1.09	0.31
Proline	2.13	1.23	1.84	0.63	0.68
Propionate	4.33	0.43	1.50	0.29	<0.01
Pyruvate	6.59	2.93	5.24	1.93	0.45
Ribose	1.70	0.06	4.36	0.77	<0.01
Sn-Glycero-3-phosphocholine	0.04	0.08	0.27	0.24	0.08
Succinate	0.67	0.05	0.16	0.23	<0.01
Taurine	3.31	1.18	8.19	2.48	<0.01
Threonine	3.21	0.86	5.11	1.70	0.06
Trimethylamine	0.45	0.30	0.61	0.19	0.39
Tryptophan	0.40	0.17	0.98	0.33	0.01

Tyrosine	3.61	1.30	4.45	1.87	0.45
Uracil	1.78	0.35	1.19	0.32	0.03
Urocanate	0.10	0.03	0.24	0.09	0.01
Valerate	1.16	0.36	1.29	0.49	0.66
Valine	4.09	1.32	8.36	2.38	0.01
Xanthine	1.32	0.40	1.44	1.17	0.84
Xylose	3.00	1.41	2.14	1.53	0.41

Supplementary Table S3.5: Bile acid concentrations in chow and refined diet (rLFD). All concentrations are given in $\mu\text{g/g} \pm \text{SD}$. <LOD= below the limit of detection.

	Colon			Brain		
	Chow ($\mu\text{g/g}$)	rLFD ($\mu\text{g/g}$)	p -value	Chow ($\mu\text{g/g}$)	rLFD ($\mu\text{g/g}$)	p-value
Primary Bile Acids	195 \pm 100	653 \pm 210	< 0.01	1.39 \pm 0.58	0.84 \pm 0.59	0.15
Secondary Bile Acids	129 \pm 47	219 \pm 61	0.10	0.60 \pm 0.64	0.28 \pm 0.15	0.42
Total Bile Acids	324 \pm 140	872 \pm 261	0.02	1.99 \pm 0.81	1.12 \pm 0.68	0.10
CDCA:CA	1.12 \pm 0.76	1 \pm 0.5	0.80	0.22 \pm 0.34	0.33 \pm 0.45	0.68
α-MCA	134 \pm 77	401 \pm 107	< 0.01	0.04 \pm 0.06	0.06 \pm 0.02	0.51
β-MCA	27 \pm 21	160 \pm 60	0.02	0.07 \pm 0.10	0.05 \pm 0.05	0.99
CA	8 \pm 5	30 \pm 48	0.35	0.15 \pm 0.07	0.09 \pm 0.02	0.03
CDCA	7 \pm 4	14 \pm 9	0.22	0.03 \pm 0.04	0.03 \pm 0.03	0.68
DCA	97 \pm 33	135 \pm 34	0.11	0.17 \pm 0.08	0.13 \pm 0.03	0.31
GCA	0.5 \pm 0.1	0.5 \pm 0.1	0.84	0.06 \pm 0.03	0.04 \pm 0.01	0.22
GDCA	0.1 \pm 0.1	0.8 \pm 1.5	0.31	0.02 \pm 0.03	<0.01 \pm 0.01	0.44
HDCA	16 \pm 11	46 \pm 20	0.02	0.05 \pm 0.10	0.01 \pm 0.03	0.99
LCA	13 \pm 4	24 \pm 10	0.06	0.20 \pm 0.17	0.11 \pm 0.08	0.31
HCA	1 \pm 1	7 \pm 5	< 0.01	0.11 \pm 0.24	<LOD	-
T-α-MCA	4 \pm 6	7 \pm 3	0.15	0.11 \pm 0.04	0.07 \pm 0.10	0.51
T-β-MCA	3 \pm 3	30 \pm 56	0.10	0.31 \pm 0.25	0.19 \pm 0.18	0.41
TCA	8 \pm 7	8 \pm 10	0.39	0.60 \pm 0.19	0.27 \pm 0.21	0.03
TCDCa	1 \pm 0	1 \pm 1	0.69	0.01 \pm 0.02	0.27 \pm 0.21	0.99
TDCA	1 \pm 0	1 \pm 1	0.22	0.03 \pm 0.01	0.02 \pm 0.02	0.25
UDCA	1 \pm 1	7 \pm 7	0.03	<LOD	<LOD	-
THCA	<LOD	<LOD	-	0.01 \pm 0.01	<LOD	-
THDCA	<LOD	<LOD	-	0.02 \pm 0.02	0.01 \pm 0.02	0.40
TLCA	<LOD	<LOD	-	0.01 \pm 0.02	<LOD	-
TUDCA	<LOD	<LOD	-	0.01 \pm 0.01	0.02 \pm 0.02	0.44

Supplementary Table S3.6: Mean gene expression changes in the cortex

Gene	Log ₂ fold change	SD	P-value
<i>Xbp1</i>	0.117904	0.220742	0.421
<i>Atf6b</i>	0.233409	0.140083	0.056
<i>Ppp1r15b</i>	0.079978	0.304882	0.421
<i>Bax</i>	0.044443	0.231752	0.69
<i>Ntrk2</i>	-0.00194	0.169467	>0.999
<i>IL10</i>	0.576834	0.404209	0.222
<i>Nfkb1</i>	0.335252	0.254242	0.222
<i>Tlr2</i>	0.218698	0.258916	0.69
<i>Calb1</i>	-0.16187	0.249433	0.421
<i>Ccl11</i>	-0.17397	0.213919	0.222
<i>Clu</i>	0.175136	0.145812	0.222
<i>Cebpb</i>	0.29525	0.231078	0.095
<i>Infg</i>	1.081934	1.411046	0.421
<i>Il1b</i>	0.040631	0.215669	0.548
<i>Nos2</i>	-0.21341	0.231326	0.548
<i>Tlr4</i>	0.32446	0.332804	0.548
<i>Tnf</i>	-1.12733	0.805701	0.095
<i>Akt1</i>	-0.12674	0.238261	0.421
<i>Arc</i>	0.524494	0.270549	0.032
<i>Bdnf</i>	0.214297	0.196109	0.151
<i>Fos</i>	-0.07488	0.281572	0.841
<i>Creb1</i>	0.118054	0.212447	0.548
<i>Camk2a</i>	-0.17155	0.252877	0.421
<i>Grin2b</i>	-0.23407	0.189714	0.056
<i>Grin2a</i>	0.140092	0.134217	0.222
<i>Gabra5</i>	-0.16585	0.171997	0.421
<i>Pkca</i>	-0.23312	0.171113	0.095
<i>Ncam1</i>	0.091753	0.20004	0.69
<i>Mapk1</i>	-0.09856	0.131331	0.151
<i>Synpo</i>	-0.03244	0.460685	0.69
<i>Ywhaq</i>	0.137488	0.17008	0.31
<i>Ido1</i>	-0.13467	0.560055	0.548
<i>Dlg4</i>	-0.27481	0.24059	0.056
<i>Ephb2</i>	0.161734	0.093298	0.151
<i>Nos1</i>	-0.06371	0.3398	0.841
<i>Atf6b</i>	-0.00683	0.121122	0.841
<i>Mapk8</i>	0.212154	0.176042	0.421
<i>Atf4</i>	0.047317	0.232509	>0.999
<i>Eif2a</i>	-0.20756	0.24417	0.222
<i>Eif2ak3</i>	0.212838	0.132352	0.151
<i>Ern1</i>	0.07803	0.167437	0.421
<i>Tgr5</i>	0.072078	0.306385	>0.999
<i>Fgf15</i>	-0.5188	2.701011	0.841
<i>Fxr</i>	-0.16402	0.503783	0.69
<i>Hspa5</i>	0.078503	0.416496	>0.999
<i>Ddit3</i>	0.292109	0.102124	0.008
<i>Ppia</i>	-0.33676	0.189853	0.016
<i>Calr</i>	0.052836	0.1504	0.841
<i>Edem1</i>	-0.02515	0.206688	0.69
<i>B2m</i>	-0.29783	0.185758	0.032

<i>Pparg</i>	-0.10865	0.11167	0.151
<i>Edem3</i>	-0.07809	0.161365	0.548
<i>Amfr</i>	-0.17729	0.279158	0.421
<i>Syvn1</i>	0.020999	0.198971	0.841
<i>Cd36</i>	-0.36926	0.245942	0.095
<i>Gadd34</i>	-0.22895	0.205482	0.151
<i>Nrf2</i>	-0.45581	0.295427	0.222

Supplementary Table S3.7: Mean gene expression changes in the hippocampus

Gene	Log ₂ Fold change	SD	P value
<i>Xbp1</i>	0.160361	0.325175	0.69
<i>Atf6</i>	0.172331	0.114132	0.151
<i>Atf6b</i>	-0.56453	0.854434	0.421
<i>Ppp1r15b</i>	-0.75754	0.989472	0.421
<i>Bax</i>	-0.24082	0.218589	0.421
<i>Ntrk2</i>	-0.26993	0.444226	0.421
<i>Il10</i>	1.423756	2.255259	0.286
<i>Nfkb1</i>	0.745194	0.556222	0.032
<i>Tlr2</i>	0.374688	0.281371	0.095
<i>Calb1</i>	0.256945	0.153532	0.222
<i>Ccl11</i>	-0.09421	2.068536	0.421
<i>Clu</i>	0.229062	0.289147	0.151
<i>Cebpb</i>	-0.26133	0.99178	0.841
<i>Infg</i>	-0.63927	0.673609	0.421
<i>Il1b</i>	0.825737	0.307975	0.056
<i>Nos2</i>	-1.11097	0.812072	0.032
<i>Tlr4</i>	0.566726	0.49631	0.151
<i>Tnf</i>	0.458924	1.217278	0.841
<i>Akt1</i>	-0.63517	1.253795	0.69
<i>Arc</i>	-0.918	1.249075	0.31
<i>Bdnf</i>	0.090411	0.442328	0.841
<i>Fos</i>	-0.61787	0.555103	0.151
<i>Creb1</i>	-0.0121	0.316744	>0.999
<i>Camk2a</i>	-0.40381	1.237311	>0.999
<i>Grin2b</i>	-0.48778	0.421435	0.095
<i>Grin2a</i>	-0.20743	0.88121	0.69
<i>Gabra5</i>	0.317001	0.633053	0.421
<i>Ncam1</i>	-0.63927	0.673609	0.421
<i>Mapk1</i>	0.295096	0.38809	0.421
<i>Synpo</i>	-0.40366	0.963626	0.31
<i>Ywhaq</i>	-0.53787	0.414626	0.032
<i>Ido1</i>	-0.06402	0.635909	0.841
<i>Dlg4</i>	-1.29497	1.337436	0.222
<i>Ephb2</i>	-1.35709	1.347946	0.222
<i>Nos1</i>	-0.28916	1.073662	>0.999
<i>Mapk8</i>	0.428808	0.138169	0.008
<i>Atf4</i>	0.065781	0.592775	0.841
<i>Eif2a</i>	0.032798	0.383453	>0.999
<i>Ern1</i>	-0.01424	0.624501	0.841
<i>Hspa5</i>	0.071186	0.554422	>0.999
<i>Ddit3</i>	0.480545	0.25445	0.008
<i>Calr</i>	-0.16029	0.452068	0.31
<i>Edem1</i>	-0.51765	0.549356	0.222
<i>Pparg</i>	-0.29818	0.348302	0.31
<i>Edem3</i>	-0.1429	0.340121	0.69
<i>Amfr</i>	-0.5239	0.571331	0.31
<i>Syvn1</i>	-0.69246	1.08655	0.421
<i>Gadd34</i>	-0.64907	0.696014	0.151
<i>Nrf2</i>	0.097466	0.191963	0.548

Supplementary Table S4.1: Composition of phenolic components of the polyphenol-rich grape and blueberry extract Memophenol™.

Compounds	Mean (%)
Total flavonoids (flavan-3-ols, flavonols and anthocyanins)	≥ 43
Flavan-3-ols monomers	≥ 20
Oligomers	≥ 22
Flavonols (quercetin, glycosylated derivatives)	≥ 0.15
Anthocyanins	≥ 0.1
Phenolic acids (chlorogenic acids, gallic acids)	≥ 0.5
Stilbenes (trans-resveratrol)	≥ 300 ppm

Supplementary Table S4.2: Dietary composition of the control (AIN-93M) and Memophenol™ (D21011502) diets

Diet	D10012M AIN-93M		D21011502 879 mg Memophenol/kg	
	gm %	Kcal %	gm %	Kcal %
Protein	14	15	14	15
Carbohydrate	73	76	73	76
Fat	4	9	4	9
Total		100		100
Kcal/gm	3.8		3.8	
Dietary Component	gm	Kcal	gm	Kcal
Casein	140	560	140	560
L-Cystine	1.8	7.2	1.8	7.2
Corn	495.692	1983	495.692	1983
Maltodextrin	125	500	125	500
Sucrose	100	400	100	400
Cellulose	50	0	50	0
Soybean	40	360	40	360
t-Butylhydroquinone	0.008	0	0.008	0
Mineral	35	0	35	0
Vitamin	10	40	10	40
Choline	2.5	0	2.5	0
Memophenol	0	0	0.88	0
FD&C	0	0	0.05	0
Total	1000	3850	1000.93	3850

Supplementary Table S4.3: Chapter 4 primer sequences

GenBank Accession	Gene	Description	Forward primer sequence (5' -> 3')	Reverse primer sequence (5' -> 3')
NM_009386	<i>Tjp1</i>	Tight Junction Protein 1 (ZO-1)	GTTGGTACGGTGCCCTGAA AGA	GCTGACAGGTAGGACAGACGA T
NM_030687	<i>Slco1a4</i>	Solute carrier organic anion transporter family member 1A4	GCCAAAGAGGAGAAGCAC AGAG	AAAGGCATTGACCTGGATCAC AC
NM_013556	<i>Hprt1</i>	Hypoxanthine phosphoribosyl transferase 1	CTGGTGAAAAGGACCTCT CGAAG	CCAGTTTCACTAATGACACAAA CG
NM_008084	<i>Gapdh</i>	Glyceraldehyde -3-phosphate dehydrogenase	CATCACTGCCACCCAGAA GACTG	ATGCCAGTGAGCTTCCC GTTCA G
NM_013684	<i>Tbp</i>	TATA-box binding protein	CTACCGTGAATCTTGGCTG TAAAC	AATCAACGCAGTTGTCCGTGGC

Supplementary Table S4.4: Gut microbiome abundances at the genus level significantly ($q < 0.05$) modulated between groups.

Genus	Control	LPS	LPS + Memo	P-value	FDR	Statistics
<i>Erysipelotrichaceae</i>	0.3 ± 1	2 ± 1	2 ± 1	0.0004	0.0161	13.96
<i>Muribaculum</i>	41 ± 23	7 ± 5	16 ± 15	0.0005	0.0161	13.40
<i>Rikenellaceae_RC9_group</i>	191 ± 96	51 ± 24	85 ± 104	0.0008	0.0170	12.03
<i>Butyricicoccus</i>	10 ± 7	28 ± 10	32 ± 14	0.0010	0.0170	11.41
<i>Alistipes</i>	218 ± 87	91 ± 38	170 ± 163	0.0019	0.0267	9.79
<i>Eubacterium_brachy_group</i>	20 ± 6	14 ± 3	28 ± 6	0.0020	0.0271	9.67
<i>Lachnospiraceae A2</i>	81 ± 101	325 ± 136	454 ± 219	0.0026	0.0300	9.11
<i>Desulfovibrio</i>	10 ± 7.27	44 ± 11	27 ± 15	0.0027	0.0313	9.08
<i>Muribaculaceae</i>	1525 ± 788	549 ± 253	753 ± 614	0.0032	0.0321	8.62
<i>Romboutsia</i>	164 ± 73	78 ± 47	385 ± 184	0.0039	0.0339	8.29

Supplementary Table S4.5: Circulatory concentrations of dietary and microbial-derived metabolites. All concentrations are given in μM . P-value generated by One-way ANOVA. SD= standard deviation. Bold values $p < 0.05$.

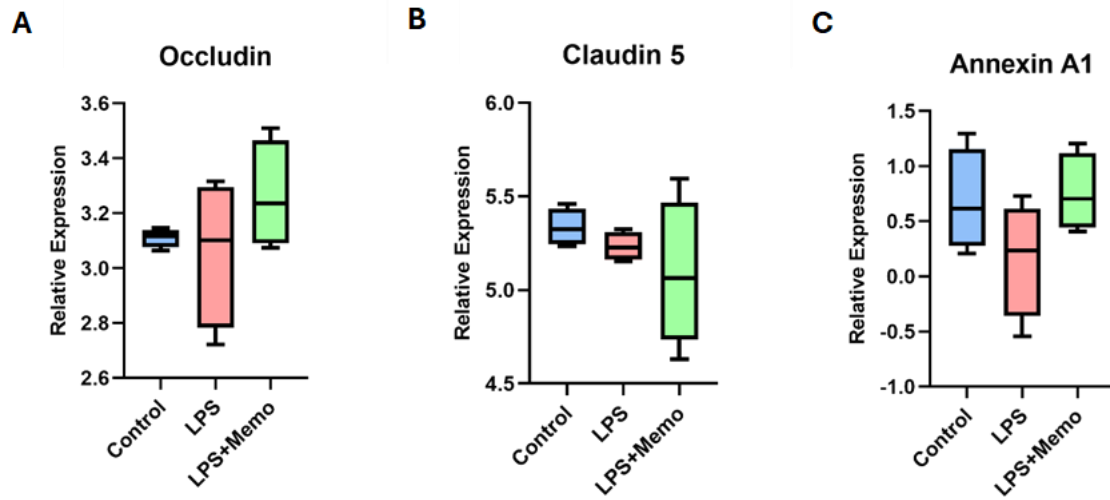
Metabolite	Control (μM)		LPS (μM)		LPS+ Memophenol™ (μM)		F stat	P-value	FDR
	Mean	SD	Mean	SD	Mean	SD			
TMAO	3.21	1.15	4.46	1.00	2.70	0.93	6.96	0.004	0.157
Choline	14.82	3.63	18.54	4.04	17.79	3.22	2.62	0.093	0.393
TMA	0.76	0.33	0.75	0.37	0.55	0.36	1.04	0.368	0.635
<i>p</i> -Cresol Glucuronide	0.91	0.88	0.79	0.66	0.01	0.03	5.36	0.012	0.191
<i>p</i> -Cresol Sulfate	3.79	3.29	4.10	3.94	0.25	0.13	4.68	0.019	0.191
Indole-3-Lactic Acid	0.73	0.14	0.68	0.24	0.52	0.11	5.41	0.056	0.359
Indole-3-Carboxaldehyde	0.13	0.07	0.13	0.04	0.08	0.04	2.27	0.125	0.384
Indole-3-Carboxylic acid	0.05	0.03	0.03	0.03	0.03	0.01	0.82	0.451	0.635
Tryptophan	58.29	5.62	51.41	6.57	52.55	7.19	2.90	0.074	0.369
Indole Acetic Acid	0.21	0.09	0.15	0.05	0.16	0.03	2.85	0.078	0.369
5-Hydroxyindole Acetic Acid	0.20	0.08	0.22	0.05	0.17	0.03	1.22	0.312	0.635
Xanthurenic Acid	0.48	0.06	0.45	0.06	0.47	0.05	0.87	0.433	0.635
Indoxyl Sulfate	3.98	2.29	6.37	2.18	3.70	1.17	5.12	0.014	0.191
Kynurenine	0.61	0.14	0.62	0.07	0.52	0.11	2.31	0.121	0.431
Anthranilic Acid	0.06	0.02	0.06	0.03	0.04	0.02	2.24	0.128	0.431
Serotonin	10.28	6.54	9.23	6.53	4.63	5.21	2.17	0.136	0.431
Indole-3-Propionic Acid	1.78	0.98	1.74	0.68	1.15	0.81	1.59	0.225	0.627
Kynurenic Acid	0.08	0.03	0.09	0.03	0.07	0.03	0.16	0.857	0.881
Picolinic Acid	1.31	0.63	1.05	0.51	1.01	0.67	0.65	0.531	0.651
Quinolinic Acid	0.21	0.19	0.15	0.19	0.13	0.06	0.67	0.521	0.651
UDCA	0.69	0.84	0.21	0.15	0.35	0.66	1.38	0.270	0.627
TLCA	0.88	0.04	0.85	0.03	0.93	0.18	1.35	0.277	0.627
TDCA	0.08	0.06	0.07	0.03	0.18	0.26	1.34	0.280	0.627
TCA	3.99	6.76	0.28	0.13	2.38	5.85	1.16	0.329	0.635
THDCA	0.18	0.28	0.06	0.06	0.20	0.28	1.01	0.378	0.635
α -MCA	0.95	1.38	0.53	0.73	0.69	0.79	0.39	0.681	0.739
β -MCA	17.50	33.20	0.95	0.97	9.69	28.30	0.97	0.393	0.635
CDCA	0.66	1.19	0.08	0.07	0.50	1.11	0.92	0.411	0.635

TCDCa	0.10	0.19	0.02	0.02	0.14	0.29	0.89	0.422	0.635
TUDCa	0.79	1.25	0.21	0.10	0.63	1.09	0.85	0.441	0.635
CA	13.33	22.71	10.43	0.73	10.77	29.74	0.76	0.480	0.651
T- β -MCA	73.52	171.59	2.56	3.06	195.39	582.85	0.70	0.509	0.651
T- α -MCA	13.01	23.74	2.27	2.14	18.85	53.07	0.56	0.576	0.674
HDCA	0.33	0.30	0.18	0.08	0.28	0.44	0.55	0.585	0.674
MCA	0.15	0.21	0.33	0.95	0.09	0.16	0.43	0.655	0.732
LCA	0.10	0.12	0.09	0.05	0.11	0.08	0.15	0.858	0.881
DCA	2.87	1.13	3.02	0.65	2.84	1.21	0.07	0.929	0.929

Supplementary Table S4.6: Correlation of circulatory metabolites with *Tjp1* expression. Bold values are significant at $p < 0.05$.

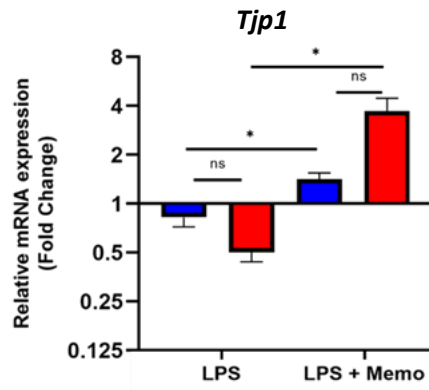
Metabolite	r	p-value
TMAO	-0.88	<0.01
Choline	0.03	0.91
TMA	0.07	0.79
<i>p</i> -Cresol Glucuronide	-0.37	0.15
<i>p</i> -Cresol Sulfate	-0.29	0.18
Indole-3-Lactic Acid	-0.31	0.21
Indole-3-Carboxaldehyde	-0.26	0.30
Indole-3-Carboxylic acid	0.03	0.89
Tryptophan	-0.26	0.30
Indole Acetic Acid	0.09	0.71
5-Hydroxyindole Acetic Acid	-0.34	0.17
Xanthurenic Acid	-0.09	0.72
Indoxyl Sulfate	-0.45	0.04
Kynurenine	-0.20	0.44
Anthranilic Acid	-0.21	0.40
Serotonin	-0.24	0.33
Indole-3-Propionic Acid	-0.42	0.08
Kynurenic Acid	-0.02	0.94
Picolinic Acid	-0.01	0.97
Quinolinic Acid	0.22	0.39
UDCA	-0.20	0.43
TLCA	0.27	0.27
TDCA	0.33	0.18
TCA	0.03	0.90
THDCA	0.43	0.07
α -MCA	0.15	0.56
β -MCA	-0.09	0.74
CDCA	-0.20	0.42
TCDCa	-0.33	0.19
TUDCA	0.24	0.34
CA	-0.29	0.24
T- β -MCA	-0.29	0.24
T- α -MCA	-0.17	0.49
HDCA	-0.27	0.29
MCA	-0.34	0.17

LCA	0.13	0.62
DCA	-0.05	0.84

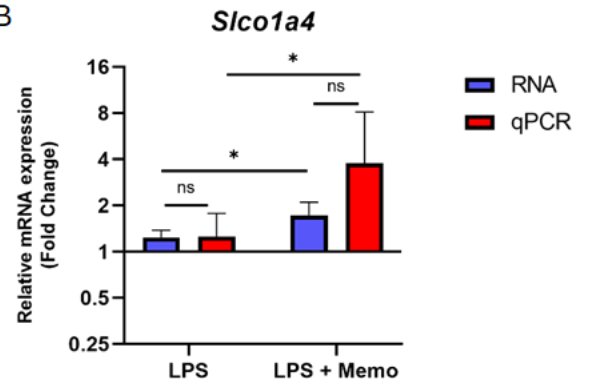


Supplementary Figure S4.1: Gene expression related to the blood-brain barrier. (A) Occludin, (B) Claudin-5, (C) Annexin A1

A



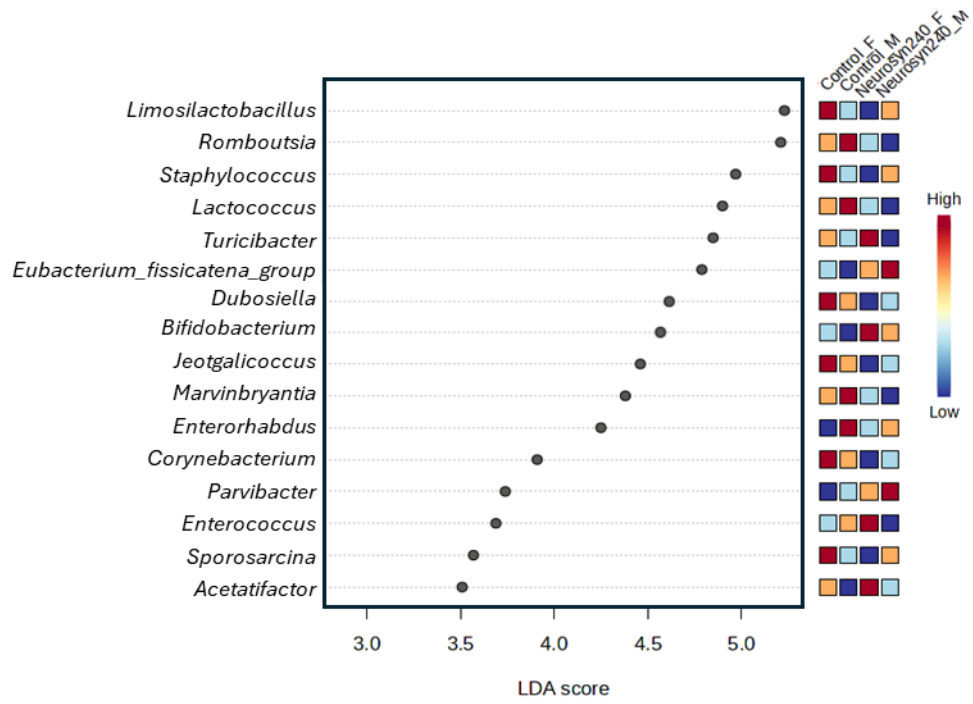
B



Supplementary Figure S4.2: Comparison of qPCR and RNA sequencing results in (A) *Tjp1* and (B) *Slco1a4*. Significant changes occurred between LPS and LPS+ Memophenol for both RNA and qPCR results. However, RNA and qPCR results did not differ significantly from each other. Ns= not significant at $p < 0.05$.

Supplementary Table S5.1: Beta diversity pairwise PERMANOVA analysis. FDR= Benjamini-Hochberg procedure

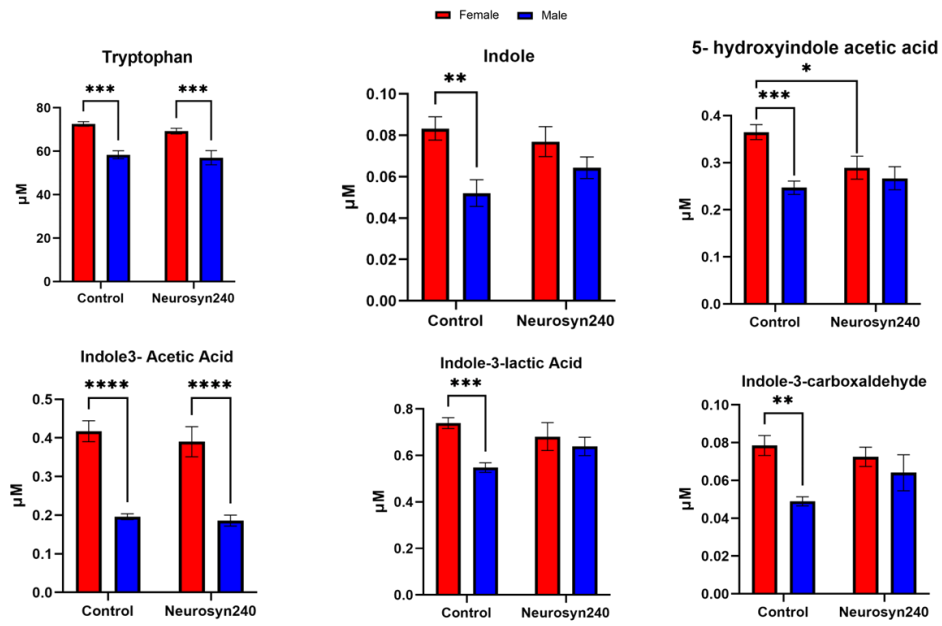
Pair	F-Value	R-Squared	P-value	FDR
Control_Female vs Control_Male	1.948	0.130	0.083	0.093
Control_Female vs Neurosyn240_Male	5.999	0.316	0.007	0.021
Control_Female vs Neurosyn240_Female	1.978	0.132	0.093	0.093
Control_Male vs Neurosyn240_Male	4.391	0.239	0.003	0.018
Control_Male vs Neurosyn240_Female	2.108	0.131	0.059	0.0885
Neurosyn240_Male vs Neurosyn240_Female	3.300	0.191	0.024	0.048



Supplementary Figure S5.1: Linear discrimination analysis (LDA) effect size (LEfSe) revealed significant differences in 16 genera between groups at the genus level.

Supplementary Table S5.2: Microbiome abundance counts. P-values generated by two-way ANOVA between sex (males and females) and diet (control and Neurosyn240) and interaction. Bold values= p<0.05.

Metabolite	Control Female		Control Male		Neurosyn240 Female		Neurosyn240 Male		Source of Variation					
	Mean	SD	Mean	SD	Mean	SD	Mean	SD	Diet		Sex		Interaction	
									F	p	F	p	F	p
<i>Lactococcus</i>	12263.71	7723.70	5811.00	4919.62	9370.50	11298.46	3017.83	3571.01	6.666	0.016	4.287	0.048	5.434	0.028
<i>Limosilactobacillus</i>	2453.29	2067.80	0.38	0.74	0.00	0.00	4.00	8.00	12.12	0.0017	12.11	0.0017	12.34	0.0016
<i>Marvinbryantia</i>	131.86	78.68	411.88	255.27	69.75	41.62	49.83	41.73	17.220	<0.001	7.407	0.011	8.424	0.007
<i>Parvibacter</i>	0.43	0.79	2.63	2.13	46.13	32.01	65.83	48.63	25.520	<0.001	1.778	0.194	1.312	0.262
<i>Romboutsia</i>	1476.43	1644.51	2591.63	1467.04	844.75	737.33	237.33	334.59	12.690	0.001	0.419	0.523	4.163	0.051
<i>Dubosiella</i>	3724.43	3705.44	2305.29	2088.94	11.50	13.53	369.00	352.86	13.140	0.001	0.832	0.370	1.947	0.174
<i>Sporosarcina</i>	56.43	46.81	0.88	1.81	0.00	0.00	3.17	5.00	10.880	0.003	10.170	0.004	13.940	0.001
<i>Turicibacter</i>	303.29	445.91	0.00	0.00	990.75	805.64	0.00	0.00	4.296	0.048	15.220	0.001	4.296	0.048
<i>Acetatifactor</i>	26.43	60.01	0.00	0.00	43.13	43.21	0.00	0.00	0.535	0.471	6.756	0.015	0.311	0.582
<i>Corynebacterium</i>	106.57	168.56	15.13	25.67	0.50	1.41	11.83	21.09	3.282	0.081	1.720	0.201	3.298	0.081
<i>Enterococcus</i>	29.86	27.58	30.50	28.06	76.00	66.04	2.33	1.51	0.434	0.516	6.766	0.015	7.008	0.013
<i>Enterorhabdus</i>	105.57	87.36	356.75	307.40	139.25	56.26	181.50	106.44	1.413	0.245	5.444	0.027	3.007	0.094
<i>Eubacterium_fissicatena_group</i>	180.29	333.22	0.25	0.71	578.88	351.07	773.83	1241.61	8.772	0.006	0.071	0.791	1.222	0.279
<i>Facklamia</i>	11.71	12.20	4.25	6.14	0.00	0.00	3.50	5.86	5.713	0.024	0.504	0.484	5.026	0.033
<i>Jeotgalicoccus</i>	412.57	738.38	47.50	85.51	0.63	1.77	28.00	34.98	2.753	0.109	1.660	0.209	2.560	0.121
<i>Staphylococcus</i>	1360.14	2229.76	139.00	244.89	15.50	27.23	143.00	169.76	2.382	0.134	1.500	0.231	3.709	0.065
<i>Bifidobacterium</i>	2004.43	2175.03	1863.13	2866.25	4536.25	3115.18	3131.17	3647.64	4.255	0.049	0.636	0.432	2.521	0.124

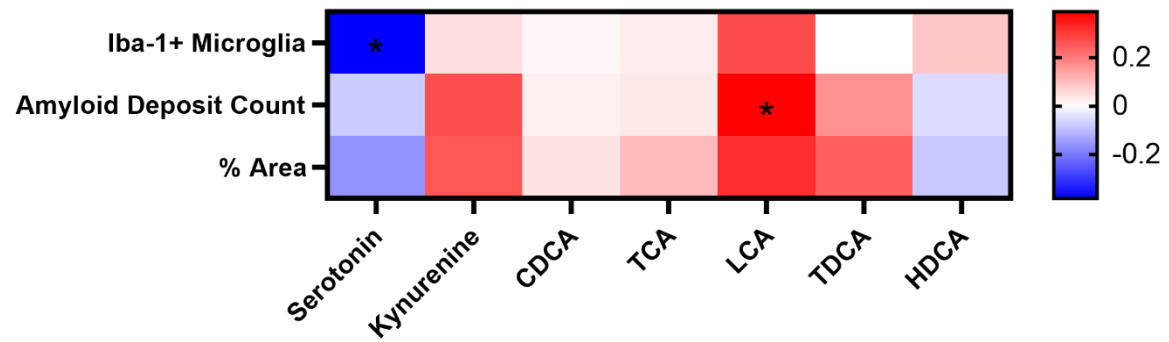


Supplementary Figure S5.2: Tryptophan and indole metabolites significantly modulated by sex.

Supplementary Table S5.3: Serum metabolite concentrations. P-values generated by two-way ANOVA between sex (males and females) and diet (control and Neurosyn240) and interaction. Bold values= p<0.05. All concentrations are given in μM .

Metabolite	Control Female (μM)		Control Male (μM)		Neurosyn240 Female (μM)		Neurosyn240 Male (μM)		Source of Variation					
	Mean	SD	Mean	SD	Mean	SD	Mean	SD	Diet		Sex		Interaction	
									F	p	F	p	F	p
Serotonin	0.37	0.18	0.37	0.30	3.99	4.65	2.07	2.29	13.140	0.001	2.860	0.104	2.927	0.100
Kynurenine	0.42	0.08	0.28	0.04	0.34	0.11	0.31	0.06	6.459	0.018	0.687	0.415	0.001	0.993
Tryptophan	72.59	2.83	58.65	5.59	69.25	3.16	57.02	9.27	1.111	0.302	35.070	<0.001	0.194	0.663
5-Hydroxyindole Acetic Acid	0.36	0.04	0.25	0.04	0.29	0.06	0.27	0.07	1.855	0.185	11.930	0.002	5.524	0.027
Anthranilic Acid	0.03	0.01	0.04	0.01	0.03	0.01	0.04	0.01	0.890	0.355	10.430	0.004	0.593	0.448
Kynurenic Acid	0.05	0.02	0.06	0.01	0.04	0.02	0.07	0.04	0.184	0.672	5.199	0.031	1.839	0.187
p-Cresol Sulfate	7.91	2.45	3.26	1.38	4.78	3.52	5.96	2.30	0.146	0.706	3.065	0.092	9.178	0.006
p-Cresol Glucuronide	1.37	0.33	0.55	0.21	0.71	0.74	1.66	0.40	1.390	0.249	0.299	0.589	26.310	<0.001
Indole Acetic Acid	0.42	0.07	0.19	0.02	0.39	0.10	0.19	0.04	0.681	0.417	89.410	<0.001	0.146	0.705
Indole-3-Propionic Acid	0.49	0.24	0.61	0.21	0.62	0.49	1.09	1.01	1.952	0.175	1.689	0.206	0.647	0.429
Xanthurenic Acid	0.03	0.02	0.03	0.01	0.03	0.02	0.07	0.08	1.483	0.235	1.202	0.283	1.546	0.225
Indole-3-Lactic Acid	0.74	0.06	0.56	0.06	0.68	0.15	0.64	0.11	0.201	0.658	10.120	0.004	4.133	0.053
Indole-3-carboxaldehyde	0.08	0.01	0.05	0.01	0.07	0.01	0.06	0.03	0.500	0.486	8.686	0.007	2.703	0.113
Indole	0.08	0.01	0.05	0.02	0.08	0.02	0.06	0.01	0.231	0.635	12.720	0.002	2.286	0.143
Indoxyl Sulfate	10.56	2.66	4.01	1.43	10.08	6.07	7.22	4.80	0.975	0.334	10.280	0.004	1.706	0.203
TMAO	33.55	16.35	6.46	3.26	38.22	28.55	9.94	2.45	0.550	0.465	23.920	<0.001	0.006	0.939
Choline	36.86	6.92	32.52	5.76	33.07	4.57	30.08	4.63	2.709	0.112	2.713	0.112	0.037	0.849
T-a-MCA	13.61	6.11	10.82	24.80	37.19	79.22	3.88	4.07	0.397	0.534	1.745	0.199	1.088	0.307
T-b-MCA	3.85	2.36	4.68	11.52	35.23	82.73	1.30	1.16	1.037	0.318	1.440	0.241	1.492	0.233
TUDCA	0.93	0.29	0.67	1.07	2.85	5.77	0.41	0.18	0.749	0.395	1.929	0.177	1.171	0.289
THDCA	0.37	0.13	0.09	0.12	0.43	0.71	0.06	0.02	0.019	0.893	7.140	0.013	0.128	0.724
TCDCa	0.10	0.05	0.07	0.12	0.52	1.02	0.04	0.01	1.237	0.277	2.178	0.153	1.653	0.210
a-MCA	2.69	0.36	1.05	0.74	1.46	0.57	2.16	2.51	0.003	0.956	0.910	0.349	5.141	0.032
b-MCA	0.84	0.28	0.36	0.24	0.52	0.25	0.85	0.94	0.200	0.659	0.168	0.685	4.206	0.051
CA	2.27	1.09	0.31	0.30	0.71	0.41	0.99	1.18	1.852	0.186	7.005	0.014	12.440	0.002
UDCA	0.45	0.18	0.20	0.13	0.26	0.16	0.42	0.38	0.044	0.836	0.284	0.599	5.412	0.028

HDCA	0.71	0.18	0.09	0.10	0.33	0.23	0.19	0.20	4.509	0.044	30.390	<0.001	12.570	0.002
CDCA	0.30	0.18	0.17	0.08	0.18	0.16	0.12	0.04	8.414	0.008	1.998	0.170	1.942	0.176
DCA	1.34	0.44	0.15	0.12	0.80	0.65	0.34	0.22	1.420	0.245	32.580	<0.001	6.470	0.018
LCA	0.87	0.14	0.92	0.17	0.70	0.18	0.63	0.21	11.110	0.003	0.108	0.745	0.681	0.417
TCA	2.75	1.42	0.10	0.05	0.07	0.06	0.17	0.10	11.440	0.002	21.340	<0.001	17.510	0.003
TDCA	0.31	0.33	0.02	0.01	0.01	0.00	0.03	0.02	5.654	0.025	4.738	0.039	6.521	0.017



Supplementary Figure S5.3: Heatmap displaying the correaltion between AD neuropathology and metabolites significantly modulated by the effect of diet (p<0.05).

Supplementary Table S5.4: A main of diet was observed with amyloid beta-related genes. Bold values are significant at $P_{FDR} < 0.1$

Gene	Description	Category	log2FoldChange	P-value	FDR P-value
Vcam1	vascular cell adhesion molecule 1	cellular response to amyloid-beta	-0.51	0.000	0.027
Lrp2	low density lipoprotein receptor-related protein 2	amyloid-beta clearance	-1.73	0.001	0.045
Clu	clusterin	amyloid-beta binding	-0.85	0.000	0.051
Ager	advanced glycosylation end product-specific receptor	amyloid-beta binding	1.32	0.000	0.077
Fcgr2b	Fc receptor, IgG, low affinity IIb	amyloid-beta binding	-0.69	0.003	0.192
Itga4	integrin alpha 4	cellular response to amyloid-beta	-0.66	0.005	0.235
Tlr2	toll-like receptor 2	amyloid-beta binding	-0.71	0.011	0.305
Efna1	ephrin A1	positive regulation of amyloid-beta formation (amyloid-beta formation)	-0.41	0.013	0.329
Rab11b	RAB11B, member RAS oncogene family	amyloid-beta clearance by transcytosis	0.13	0.013	0.334
Dlgap3	DLG associated protein 3	amyloid-beta binding	0.50	0.017	0.357
Itgb2	integrin beta 2	amyloid-beta binding	-0.41	0.017	0.366
Lrrtm3	leucine rich repeat transmembrane neuronal 3	positive regulation of amyloid-beta formation (amyloid-beta formation)	0.31	0.021	0.396
Ttr	transthyretin	amyloid-beta binding	-2.35	0.022	0.400
Fzd4	frizzled class receptor 4	amyloid-beta binding	-0.55	0.023	0.407
Pin1	peptidyl-prolyl cis/trans isomerase, NIMA-interacting 1	negative regulation of amyloid-beta formation (amyloid-beta formation)	0.22	0.023	0.409
Tgfb2	transforming growth factor, beta 2	amyloid-beta binding	-0.59	0.024	0.410
Igf1	insulin-like growth factor 1	negative regulation of amyloid-beta formation (amyloid-beta formation)	-0.46	0.025	0.415
Picalm	phosphatidylinositol binding clathrin assembly protein	amyloid-beta clearance by transcytosis	-0.16	0.028	0.438
Necab3	N-terminal EF-hand calcium binding protein 3	amyloid beta (A4) precursor protein-binding, family A, member 2 binding protein	0.47	0.028	0.438
Apoa1	apolipoprotein A-I	amyloid-beta binding	1.71	0.027	0.457

<i>Cacnb1</i>	calcium channel, voltage-dependent, beta 1 subunit	cellular response to amyloid-beta	0.34	0.042	0.501
<i>Gja1</i>	gap junction protein, alpha 1	cellular response to amyloid-beta	-0.25	0.043	0.502
<i>Tlr6</i>	toll-like receptor 6	cellular response to amyloid-beta	-0.86	0.043	0.502
<i>Grin1</i>	glutamate receptor, ionotropic, NMDA1 (zeta 1)	amyloid-beta binding	0.25	0.044	0.505
<i>Sp1</i>	trans-acting transcription factor 1	positive regulation of amyloid-beta formation (amyloid-beta formation)	-0.29	0.045	0.512
<i>Gga3</i>	golgi associated, gamma adaptin ear containing, ARF binding protein 3	negative regulation of amyloid-beta formation (amyloid-beta formation)	0.13	0.048	0.520
<i>Aph1a</i>	aph1 homolog A, gamma secretase subunit	amyloid-beta formation	0.16	0.051	0.533
<i>Ace</i>	angiotensin I converting enzyme	amyloid-beta metabolic process	-0.52	0.059	0.567
<i>Rtn1</i>	reticulum 1	negative regulation of amyloid-beta formation (amyloid-beta formation)	0.22	0.063	0.577
<i>Aplp1</i>	amyloid beta precursor like protein 1	amyloid beta precursor like protein 1	0.18	0.071	0.592
<i>Apha3</i>	amyloid beta precursor protein binding family A member 3	amyloid beta precursor protein binding family A member 3	0.24	0.074	0.600
<i>Psenen</i>	presenilin enhancer gamma secretase subunit	amyloid-beta formation	0.15	0.076	0.607
<i>Snx6</i>	sorting nexin 6	cellular response to amyloid-beta	-0.17	0.080	0.615
<i>Mme</i>	membrane metallo endopeptidase	amyloid-beta metabolic process	0.57	0.087	0.630
<i>Chrna7</i>	cholinergic receptor, nicotinic, alpha polypeptide 7	amyloid-beta binding	-0.53	0.092	0.634
<i>Nae1</i>	NEDD8 activating enzyme E1 subunit 1	amyloid beta precursor protein binding protein 1	-0.18	0.095	0.638
<i>Appbp2</i>	amyloid beta precursor protein binding protein 2	amyloid beta precursor protein binding protein 2	-0.13	0.096	0.640
<i>Trem2</i>	triggering receptor expressed on myeloid cells 2	amyloid-beta binding	-0.37	0.102	0.653
<i>Cacna1b</i>	calcium channel, voltage-dependent, N type, alpha 1B subunit	response to amyloid-beta	0.12	0.140	0.710
<i>Lrpap1</i>	low density lipoprotein receptor-related protein associated protein 1	amyloid-beta clearance by transcytosis	0.10	0.142	0.713
<i>Cdk5</i>	cyclin dependent kinase 5	cellular response to amyloid-beta	0.11	0.147	0.719

Lgmn	legumain	cellular response to amyloid-beta	-0.15	0.150	0.722
Ldlr	low density lipoprotein receptor	amyloid-beta binding	-0.14	0.153	0.724
Mmp9	matrix metalloproteinase 9	response to amyloid-beta	0.52	0.158	0.729
Becn1	beclin 1, autophagy related	amyloid-beta metabolic process	0.13	0.165	0.738
Pfdn6	prefoldin subunit 6	amyloid-beta binding	0.16	0.172	0.746
Gria1	glutamate receptor, ionotropic, AMPA1 (alpha 1)	amyloid-beta binding	-0.21	0.173	0.746
Rtn2	reticulin 2 (Z-band associated protein)	negative regulation of amyloid-beta formation (amyloid-beta formation)	0.11	0.178	0.753
Insr	insulin receptor	amyloid-beta binding	-0.12	0.186	0.761
Clstn1	calsynenin 1	amyloid-beta binding	0.20	0.188	0.763
Gsk3a	glycogen synthase kinase 3 alpha	positive regulation of amyloid-beta formation (amyloid-beta formation)	0.17	0.200	0.777
Gria3	glutamate receptor, ionotropic, AMPA3 (alpha 3)	amyloid-beta binding	0.19	0.221	0.793
Lrp8	low density lipoprotein receptor-related protein 8, apolipoprotein e receptor	amyloid-beta binding	-0.11	0.229	0.795
Unc13a	unc-13 homolog A	amyloid-beta metabolic process	0.18	0.229	0.795
Slc2a13	solute carrier family 2 (facilitated glucose transporter), member 13	positive regulation of amyloid-beta formation (amyloid-beta formation)	0.14	0.248	0.811
Tlr4	toll-like receptor 4	cellular response to amyloid-beta	-0.54	0.254	0.816
Pfdn5	prefoldin 5	amyloid-beta binding	0.11	0.255	0.818
Pfdn4	prefoldin 4	amyloid-beta binding	-0.19	0.258	0.820
Ephb2	Eph receptor B2	amyloid-beta binding	-0.24	0.264	0.824
Clstn2	calsynenin 2	amyloid-beta binding	-0.26	0.265	0.824
Ldlrap1	low density lipoprotein receptor adaptor protein 1	amyloid-beta binding	-0.41	0.268	0.826
Csnk1e	casein kinase 1, epsilon	positive regulation of amyloid-beta formation (amyloid-beta formation)	0.11	0.268	0.827
Pfdn1	prefoldin 1	amyloid-beta binding	0.14	0.278	0.833
Sort1	sortilin-related receptor, LDLR class A repeats-containing	amyloid-beta binding	-0.19	0.305	0.849
Itm2a	integral membrane protein 2A	amyloid-beta binding	-0.16	0.310	0.851

<i>Apbb1</i>	amyloid beta precursor protein binding family B member 1	amyloid beta precursor protein binding family B member 1	0.15	0.310	0.852
<i>Epha4</i>	Eph receptor A4	positive regulation of amyloid-beta formation (amyloid-beta formation)	-0.39	0.316	0.856
<i>Cd74</i>	CD74 antigen (invariant polypeptide of major histocompatibility complex, class II antigen-associated)	amyloid-beta binding	-0.61	0.324	0.859
<i>Aph1c</i>	aph1 homolog C, gamma secretase subunit	amyloid-beta formation	-0.15	0.329	0.863
<i>Itgam</i>	integrin alpha M	amyloid-beta clearance	-0.15	0.335	0.865
<i>C3</i>	complement component 3	amyloid-beta clearance	-0.60	0.340	0.866
<i>Cyp51</i>	cytochrome P450, family 51	negative regulation of amyloid-beta clearance (amyloid-beta clearance)	-0.09	0.350	0.870
<i>Ngfr</i>	nerve growth factor receptor (TNFR superfamily, member 16)	amyloid-beta binding	0.43	0.357	0.870
<i>Ntrk2</i>	neurotrophic tyrosine kinase, receptor, type 2	negative regulation of amyloid-beta formation (amyloid-beta formation)	-0.08	0.360	0.872
<i>Itm2c</i>	integral membrane protein 2C	amyloid-beta binding	0.09	0.373	0.877
<i>Bace2</i>	beta-site APP-cleaving enzyme 2	amyloid-beta metabolic process	-0.19	0.393	0.886
<i>Srf</i>	serum response factor	negative regulation of amyloid-beta clearance (amyloid-beta clearance)	0.16	0.400	0.890
<i>Itm2b</i>	integral membrane protein 2B	amyloid-beta binding	-0.05	0.409	0.891
<i>Tmed10</i>	transmembrane p24 trafficking protein 10	regulation of amyloid-beta formation (amyloid-beta formation)	-0.07	0.416	0.893
<i>Igf1r</i>	insulin-like growth factor I receptor	amyloid-beta clearance	-0.11	0.434	0.899
<i>Rela</i>	v-rel reticuloendotheliosis viral oncogene homolog A (avian)	positive regulation of amyloid-beta formation (amyloid-beta formation)	-0.08	0.436	0.900
<i>Ramp3</i>	receptor (calcitonin) activity modifying protein 3	response to amyloid-beta	-0.40	0.447	0.904
<i>Gsap</i>	gamma-secretase activating protein	amyloid-beta binding	-0.12	0.473	0.912
<i>Ifngr1</i>	interferon gamma receptor 1	negative regulation of amyloid-beta clearance (amyloid-beta clearance)	-0.09	0.482	0.913
<i>Apbb2</i>	amyloid beta precursor protein binding family B member 2	amyloid beta precursor protein binding family B member 2	-0.07	0.499	0.918

Hap1	huntingtin-associated protein 1	negative regulation of amyloid-beta formation (amyloid-beta formation)	0.19	0.504	0.920
Cltc	clathrin heavy chain	amyloid-beta clearance by transcytosis	-0.08	0.506	0.920
Apbb1ip	amyloid beta precursor protein binding family B member 1 interacting protein	amyloid beta precursor protein binding family B member 1 interacting protein	-0.12	0.516	0.925
Pfdn2	prefoldin 2	amyloid-beta binding	0.09	0.519	0.926
Abca2	ATP-binding cassette, sub-family A member 2	positive regulation of amyloid-beta formation (amyloid-beta formation)	-0.07	0.546	0.932
Ide	insulin degrading enzyme	amyloid-beta binding	-0.09	0.547	0.932
Hmgcr	3-hydroxy-3-methylglutaryl-Coenzyme A reductase	negative regulation of amyloid-beta clearance (amyloid-beta clearance)	-0.09	0.554	0.933
Aph1b	aph1 homolog B, gamma secretase subunit	amyloid-beta formation	-0.07	0.557	0.934
Icam1	intercellular adhesion molecule 1	cellular response to amyloid-beta	-0.15	0.564	0.936
Il4	interleukin 4	positive regulation of amyloid-beta clearance (amyloid-beta clearance)	-0.08	0.568	0.936
Bcl2l2	BCL2-like 2	cellular response to amyloid-beta	0.05	0.569	0.936
Clstn3	calsyntenin 3	amyloid-beta binding	0.04	0.572	0.936
Atp1a3	ATPase, Na ⁺ /K ⁺ transporting, alpha 3 polypeptide	amyloid-beta binding	0.05	0.577	0.936
Col25a1	collagen, type XXV, alpha 1	amyloid-beta binding	-0.10	0.574	0.936
Cst3	cystatin C	amyloid-beta binding	0.06	0.575	0.936
Bace1	beta-site APP cleaving enzyme 1	amyloid-beta binding	-0.09	0.581	0.937
Rtn3	reticulon 3	negative regulation of amyloid-beta formation (amyloid-beta formation)	-0.06	0.587	0.938
Cacna2d1	calcium channel, voltage-dependent, alpha2/delta subunit 1	cellular response to amyloid-beta	0.08	0.589	0.938
Cacna1a	calcium channel, voltage-dependent, P/Q type, alpha 1A subunit	response to amyloid-beta	0.07	0.622	0.944
Mgat3	mannoside acetylglucosaminyltransferase 3	amyloid-beta metabolic process	-0.07	0.628	0.945
Gria2	glutamate receptor, ionotropic, AMPA2 (alpha 2)	amyloid-beta binding	-0.07	0.632	0.946
Tm2d1	TM2 domain containing 1	amyloid-beta binding	0.06	0.635	0.946
Lrp1	low density lipoprotein receptor-related protein 1	amyloid-beta clearance by transcytosis	-0.04	0.636	0.946

Scarb1	scavenger receptor class B, member 1	amyloid-beta binding	0.06	0.647	0.948
Olfm1	olfactomedin 1	amyloid-beta binding	0.11	0.653	0.950
ApoE	apolipoprotein E	amyloid-beta binding	0.07	0.654	0.950
Abcc1	ATP-binding cassette, sub-family C member 1	cellular response to amyloid-beta	0.04	0.701	0.961
Foxo3	forkhead box O3	cellular response to amyloid-beta	0.08	0.703	0.961
Hsd17b10	hydroxysteroid (17-beta) dehydrogenase 10	amyloid-beta binding	-0.05	0.713	0.963
Ttpa	tocopherol (alpha) transfer protein	positive regulation of amyloid-beta clearance (amyloid-beta clearance)	0.09	0.716	0.963
Grm5	glutamate receptor, metabotropic 5	cellular response to amyloid-beta	-0.05	0.718	0.964
App	amyloid beta precursor protein	amyloid beta precursor protein	0.04	0.731	0.967
Parp1	poly (ADP-ribose) polymerase family, member 1	cellular response to amyloid-beta	-0.05	0.750	0.971
Aplp2	amyloid beta precursor-like protein 2	amyloid beta precursor-like protein 2	-0.03	0.761	0.972
Fpr2	formyl peptide receptor 2	amyloid-beta binding	-0.27	0.753	0.972
Calcr	calcitonin receptor	amyloid-beta binding	0.39	0.775	0.974
Rab11a	RAB11A, member RAS oncogene family	amyloid-beta clearance by transcytosis	0.02	0.777	0.974
Dyrk1a	dual-specificity tyrosine phosphorylation regulated kinase 1a	amyloid-beta formation	0.03	0.782	0.975
Adam10	a disintegrin and metallopeptidase domain 10	amyloid-beta formation	-0.04	0.784	0.975
Psen1	presenilin 1	amyloid-beta formation	-0.02	0.794	0.976
Apeh	acylpeptide hydrolase	amyloid-beta metabolic process	-0.06	0.794	0.976
Apba1	amyloid beta precursor protein binding family A member 1	amyloid beta precursor protein binding family A member 1	-0.03	0.797	0.977
Apba2	amyloid beta precursor protein binding family A member 2	amyloid beta precursor protein binding family A member 2	-0.04	0.800	0.978
Prnp	prion protein	amyloid-beta binding	0.03	0.807	0.979
Psen2	presenilin 2	amyloid-beta formation	0.03	0.806	0.979
Casp3	caspase 3	positive regulation of amyloid-beta formation (amyloid-beta formation)	-0.05	0.810	0.980
Abcg1	ATP binding cassette subfamily G member 1	positive regulation of amyloid-beta formation (amyloid-beta formation)	-0.03	0.811	0.981

Rock1	Rho-associated coiled-coil containing protein kinase 1	amyloid-beta complex	-0.03	0.811	0.981
Vbp1	von Hippel-Lindau binding protein 1	amyloid-beta binding	-0.03	0.815	0.982
Cryab	crystallin, alpha B	amyloid-beta binding	-0.04	0.821	0.982
Pla2g3	phospholipase A2, group III	negative regulation of amyloid-beta clearance (amyloid-beta clearance)	-0.06	0.851	0.986
Rtn4	reticulon 4	negative regulation of amyloid-beta formation (amyloid-beta formation)	0.02	0.854	0.986
Ldlrad3	low density lipoprotein receptor class A domain containing 3	amyloid-beta binding	-0.03	0.857	0.987
Hba-a1	hemoglobin alpha, adult chain 1	amyloid-beta binding	-0.15	0.874	0.989
Gprasp2	G protein-coupled receptor associated sorting protein 2	amyloid-beta binding	-0.04	0.876	0.989
Bin1	bridging integrator 1	negative regulation of amyloid-beta formation (amyloid-beta formation)	-0.01	0.877	0.990
Adrb2	adrenergic receptor, beta 2	amyloid-beta binding	-0.04	0.888	0.992
Nat8f1	N-acetyltransferase 8 (GCN5-related) family member 1	amyloid-beta metabolic process	0.02	0.903	0.992
Rock2	Rho-associated coiled-coil containing protein kinase 2	positive regulation of amyloid-beta formation (amyloid-beta formation)	-0.02	0.903	0.992
Fbxo2	F-box protein 2	amyloid-beta binding	0.01	0.920	0.992
Lrp4	low density lipoprotein receptor-related protein 4	amyloid-beta clearance by cellular catabolic process	0.02	0.922	0.993
Abca7	ATP-binding cassette, sub-family A member 7	amyloid-beta clearance by cellular catabolic process	0.01	0.937	0.994
Sirt1	sirtuin 1	cellular response to amyloid-beta	-0.01	0.938	0.994
Rab5a	RAB5A, member RAS oncogene family	amyloid-beta clearance by transcytosis	-0.01	0.944	0.995
Fzd5	frizzled class receptor 5	amyloid-beta binding	0.03	0.947	0.995
Spon1	spondin 1, (f-spondin) extracellular matrix protein	negative regulation of amyloid-beta formation (amyloid-beta formation)	0.00	0.961	0.997
Fyn	Fyn proto-oncogene	response to amyloid-beta	0.00	0.983	0.999

<i>Gsk3b</i>	glycogen synthase kinase 3 beta	cellular response to amyloid-beta	0.00	0.981	0.999
<i>Ncstn</i>	nicastrin	amyloid-beta formation	0.00	0.977	0.999

Supplementary Table S5.5: Amyloid beta-related genes are not significantly modulated by the main effect of sex.

Gene	Description	Category	log2FoldChange	P-value	FDR P-value
<i>Cryab</i>	crystallin, alpha B	amyloid-beta binding	-0.64	0.000	0.247
<i>Itgb2</i>	integrin beta 2	amyloid-beta binding	-0.58	0.001	0.373
<i>Vbp1</i>	von Hippel-Lindau binding protein 1	amyloid-beta binding	-0.32	0.003	0.607
<i>Trem2</i>	triggering receptor expressed on myeloid cells 2	amyloid-beta binding	-0.65	0.004	0.670
<i>Apbb1ip</i>	amyloid beta precursor protein binding family B member 1 interacting protein	amyloid beta precursor protein binding family B member 1 interacting protein	-0.55	0.005	0.692
<i>C3</i>	complement component 3	amyloid-beta clearance	-1.91	0.005	0.692
<i>Atp1a3</i>	ATPase, Na ⁺ /K ⁺ transporting, alpha 3 polypeptide	amyloid-beta binding	0.20	0.016	0.840
<i>Lgmn</i>	legumain	cellular response to amyloid-beta	-0.26	0.017	0.840
<i>Fcgr2b</i>	Fc receptor, IgG, low affinity IIb	amyloid-beta binding	-0.58	0.017	0.841
<i>Itgam</i>	integrin alpha M	amyloid-beta clearance	-0.38	0.022	0.888
<i>Scarb1</i>	scavenger receptor class B, member 1	amyloid-beta binding	0.27	0.043	0.905
<i>Rtn2</i>	reticulon 2 (Z-band associated protein)	negative regulation of amyloid-beta formation (amyloid-beta formation)	0.16	0.048	0.907
<i>Adrb2</i>	adrenergic receptor, beta 2	amyloid-beta binding	-0.54	0.067	0.909
<i>Pla2g3</i>	phospholipase A2, group III	negative regulation of amyloid-beta clearance (amyloid-beta clearance)	0.58	0.055	0.909
<i>Rab11a</i>	RAB11A, member RAS oncogene family	amyloid-beta clearance by transcytosis	-0.15	0.058	0.909
<i>Mgat3</i>	mannoside acetylglucosaminyltransferase 3	amyloid-beta metabolic process	0.26	0.075	0.921
<i>Psenen</i>	presenilin enhancer gamma secretase subunit	amyloid-beta formation	-0.15	0.079	0.923
<i>Chrna7</i>	cholinergic receptor, nicotinic, alpha polypeptide 7	amyloid-beta binding	0.54	0.091	0.938
<i>Abcg1</i>	ATP binding cassette subfamily G member 1	positive regulation of amyloid-beta formation (amyloid-beta formation)	0.17	0.150	0.946
<i>Apoe</i>	apolipoprotein E	amyloid-beta binding	-0.21	0.191	0.946
<i>Bace2</i>	beta-site APP-cleaving enzyme 2	amyloid-beta metabolic process	0.33	0.146	0.946
<i>Bin1</i>	bridging integrator 1	negative regulation of amyloid-beta formation (amyloid-beta formation)	-0.13	0.166	0.946

Calcr	calcitonin receptor	amyloid-beta binding	-1.84	0.176	0.946
Cdk5	cyclin dependent kinase 5	cellular response to amyloid-beta	-0.12	0.112	0.946
Cst3	cystatin C	amyloid-beta binding	-0.15	0.141	0.946
Gga3	golgi associated, gamma adaptin ear containing, ARF binding protein 3	negative regulation of amyloid-beta formation (amyloid-beta formation)	0.09	0.172	0.946
Gria1	glutamate receptor, ionotropic, AMPA1 (alpha 1)	amyloid-beta binding	0.21	0.169	0.946
Gria2	glutamate receptor, ionotropic, AMPA2 (alpha 2)	amyloid-beta binding	0.20	0.169	0.946
Grm5	glutamate receptor, metabotropic 5	cellular response to amyloid-beta	0.22	0.131	0.946
Gsap	gamma-secretase activating protein	amyloid-beta binding	0.22	0.167	0.946
Gsk3b	glycogen synthase kinase 3 beta	cellular response to amyloid-beta	0.16	0.145	0.946
Il4	interleukin 4	positive regulation of amyloid-beta clearance (amyloid-beta clearance)	-0.20	0.190	0.946
Mme	membrane metallo endopeptidase	amyloid-beta metabolic process	0.45	0.175	0.946
Parp1	poly (ADP-ribose) polymerase family, member 1	cellular response to amyloid-beta	0.26	0.115	0.946
Psen2	presenilin 2	amyloid-beta formation	-0.17	0.187	0.946
Tm2d1	TM2 domain containing 1	amyloid-beta binding	-0.16	0.188	0.946
Ttr	transthyretin	amyloid-beta binding	-1.40	0.173	0.946
Grin1	glutamate receptor, ionotropic, NMDA1 (zeta 1)	amyloid-beta binding	0.16	0.207	0.948
Fyn	Fyn proto-oncogene	response to amyloid-beta	0.12	0.216	0.953
Apbb2	amyloid beta precursor protein binding family B member 2	amyloid beta precursor protein binding family B member 2	-0.12	0.248	0.957
Cltc	clathrin heavy chain	amyloid-beta clearance by transcytosis	0.14	0.237	0.957
Itm2c	integral membrane protein 2C	amyloid-beta binding	0.11	0.253	0.957
Pfdn1	prefoldin 1	amyloid-beta binding	-0.15	0.268	0.957
Srf	serum response factor	negative regulation of amyloid-beta clearance (amyloid-beta clearance)	0.23	0.235	0.957
Tlr2	toll-like receptor 2	amyloid-beta binding	-0.33	0.264	0.957
Foxo3	forkhead box O3	cellular response to amyloid-beta	0.21	0.296	0.963
Gsk3a	glycogen synthase kinase 3 alpha	positive regulation of amyloid-beta formation (amyloid-beta formation)	0.14	0.297	0.963

<i>Cacnb1</i>	calcium channel, voltage-dependent, beta 1 subunit	cellular response to amyloid-beta	0.17	0.300	0.963
<i>Dyrk1a</i>	dual-specificity tyrosine phosphorylation regulated kinase 1a	amyloid-beta formation	0.10	0.305	0.963
<i>Itm2a</i>	integral membrane protein 2A	amyloid-beta binding	0.16	0.312	0.963
<i>Ldlrad3</i>	low density lipoprotein receptor class A domain containing 3	amyloid-beta binding	-0.18	0.309	0.963
<i>Slc2a13</i>	solute carrier family 2 (facilitated glucose transporter), member 13	positive regulation of amyloid-beta formation (amyloid-beta formation)	0.12	0.314	0.963
<i>Unc13a</i>	unc-13 homolog A	amyloid-beta metabolic process	0.15	0.311	0.963
<i>Pfdn5</i>	prefoldin 5	amyloid-beta binding	-0.10	0.323	0.966
<i>Gprasp2</i>	G protein-coupled receptor associated sorting protein 2	amyloid-beta binding	-0.26	0.325	0.967
<i>Dlgap3</i>	DLG associated protein 3	amyloid-beta binding	0.20	0.337	0.967
<i>Lrp8</i>	low density lipoprotein receptor-related protein 8, apolipoprotein e receptor	amyloid-beta binding	0.09	0.336	0.967
<i>Ramp3</i>	receptor (calcitonin) activity modifying protein 3	response to amyloid-beta	-0.51	0.343	0.969
<i>Snx6</i>	sorting nexin 6	cellular response to amyloid-beta	-0.09	0.348	0.969
<i>Sort1</i>	sortilin-related receptor, LDLR class A repeats-containing	amyloid-beta binding	0.17	0.341	0.969
<i>Tmed10</i>	transmembrane p24 trafficking protein 10	regulation of amyloid-beta formation (amyloid-beta formation)	-0.08	0.346	0.969
<i>Cacna1a</i>	calcium channel, voltage-dependent, P/Q type, alpha 1A subunit	response to amyloid-beta	0.12	0.363	0.969
<i>Insr</i>	insulin receptor	amyloid-beta binding	0.08	0.368	0.970
<i>Cacna1b</i>	calcium channel, voltage-dependent, N type, alpha 1B subunit	response to amyloid-beta	-0.07	0.374	0.971
<i>Ngfr</i>	nerve growth factor receptor (TNFR superfamily, member 16)	amyloid-beta binding	-0.42	0.372	0.971
<i>Tgfb2</i>	transforming growth factor, beta 2	amyloid-beta binding	0.23	0.371	0.971
<i>Prnp</i>	prion protein	amyloid-beta binding	-0.10	0.377	0.972

Abcc1	ATP-binding cassette, sub-family C member 1	cellular response to amyloid-beta	0.08	0.378	0.972
Sirt1	sirtuin 1	cellular response to amyloid-beta	0.13	0.384	0.973
Ifngr1	interferon gamma receptor 1	negative regulation of amyloid-beta clearance (amyloid-beta clearance)	-0.12	0.387	0.974
Hmgcr	3-hydroxy-3-methylglutaryl-Coenzyme A reductase	negative regulation of amyloid-beta clearance (amyloid-beta clearance)	0.13	0.402	0.974
Icam1	intercellular adhesion molecule 1	cellular response to amyloid-beta	-0.22	0.421	0.974
Lrp2	low density lipoprotein receptor-related protein 2	amyloid-beta clearance	-0.52	0.427	0.974
Lrp4	low density lipoprotein receptor-related protein 4	amyloid-beta clearance by cellular catabolic process	0.13	0.430	0.974
Pin1	peptidyl-prolyl cis/trans isomerase, NIMA-interacting 1	negative regulation of amyloid-beta formation (amyloid-beta formation)	0.08	0.398	0.974
Rela	v-rel reticuloendotheliosis viral oncogene homolog A (avian)	positive regulation of amyloid-beta formation (amyloid-beta formation)	0.08	0.429	0.974
Rtn4	reticulon 4	negative regulation of amyloid-beta formation (amyloid-beta formation)	0.11	0.417	0.974
Tlr4	toll-like receptor 4	cellular response to amyloid-beta	-0.40	0.425	0.974
Ide	insulin degrading enzyme	amyloid-beta binding	0.12	0.433	0.975
Cd74	CD74 antigen (invariant polypeptide of major histocompatibility complex, class II antigen-associated)	amyloid-beta binding	-0.48	0.440	0.975
Lrrtm3	leucine rich repeat transmembrane neuronal 3	positive regulation of amyloid-beta formation (amyloid-beta formation)	0.10	0.461	0.979
Ldlr	low density lipoprotein receptor	amyloid-beta binding	-0.07	0.466	0.980
Rab11b	RAB11B, member RAS oncogene family	amyloid-beta clearance by transcytosis	-0.04	0.469	0.980
Aph1c	aph1 homolog C, gamma secretase subunit	amyloid-beta formation	-0.11	0.475	0.981
Epha4	Eph receptor A4	positive regulation of amyloid-beta formation (amyloid-beta formation)	0.27	0.479	0.981
Apba1	amyloid beta precursor protein binding family A member 1	amyloid beta precursor protein binding family A member 1	0.07	0.521	0.983
Apba3	amyloid beta precursor protein binding family A member 3	amyloid beta precursor protein binding family A member 3	-0.09	0.516	0.983

Hap1	huntingtin-associated protein 1	negative regulation of amyloid-beta formation (amyloid-beta formation)	-0.19	0.515	0.983
Spon1	spondin 1, (f-spondin) extracellular matrix protein	negative regulation of amyloid-beta formation (amyloid-beta formation)	-0.06	0.529	0.983
Bcl2l2	BCL2-like 2	cellular response to amyloid-beta	0.06	0.542	0.983
Cyp51	cytochrome P450, family 51	negative regulation of amyloid-beta clearance (amyloid-beta clearance)	-0.06	0.546	0.984
Efna1	ephrin A1	positive regulation of amyloid-beta formation (amyloid-beta formation)	-0.10	0.569	0.987
Rtn1	reticulon 1	negative regulation of amyloid-beta formation (amyloid-beta formation)	-0.07	0.564	0.987
Clstn1	calsyntenin 1	amyloid-beta binding	0.08	0.584	0.987
Psen1	presenilin 1	amyloid-beta formation	0.05	0.582	0.987
Tlr6	toll-like receptor 6	cellular response to amyloid-beta	0.25	0.575	0.987
Fzd4	frizzled class receptor 4	amyloid-beta binding	0.13	0.589	0.990
Ntrk2	neurotrophic tyrosine kinase, receptor, type 2	negative regulation of amyloid-beta formation (amyloid-beta formation)	0.05	0.598	0.992
Picalm	phosphatidylinositol binding clathrin assembly protein	amyloid-beta clearance by transcytosis	-0.04	0.599	0.992
Ace	angiotensin I converting enzyme	amyloid-beta metabolic process	-0.14	0.612	0.994
Casp3	caspase 3	positive regulation of amyloid-beta formation (amyloid-beta formation)	0.09	0.647	0.994
Col25a1	collagen, type XXV, alpha 1	amyloid-beta binding	-0.08	0.643	0.994
Gja1	gap junction protein, alpha 1	cellular response to amyloid-beta	0.05	0.670	0.994
Gria3	glutamate receptor, ionotropic, AMPA3 (alpha 3)	amyloid-beta binding	0.08	0.619	0.994
Hba-a1	hemoglobin alpha, adult chain 1	amyloid-beta binding	-0.40	0.672	0.994
Lrp1	low density lipoprotein receptor-related protein 1	amyloid-beta clearance by transcytosis	0.03	0.672	0.994
Nae1	NEDD8 activating enzyme E1 subunit 1	amyloid beta precursor protein binding protein 1	0.05	0.627	0.994
Pfdn2	prefoldin 2	amyloid-beta binding	-0.07	0.630	0.994
Pfdn4	prefoldin 4	amyloid-beta binding	-0.08	0.651	0.994

Sp1	trans-acting transcription factor 1	positive regulation of amyloid-beta formation (amyloid-beta formation)	0.06	0.663	0.994
Vcam1	vascular cell adhesion molecule 1	cellular response to amyloid-beta	-0.06	0.661	0.994
App	amyloid beta precursor protein	amyloid beta precursor protein	0.05	0.685	0.995
Rock2	Rho-associated coiled-coil containing protein kinase 2	positive regulation of amyloid-beta formation (amyloid-beta formation)	0.06	0.691	0.996
Ttpa	tocopherol (alpha) transfer protein	positive regulation of amyloid-beta clearance (amyloid-beta clearance)	-0.10	0.696	0.996
Clu	clusterin	amyloid-beta binding	0.09	0.701	0.996
Hsd17b10	hydroxysteroid (17-beta) dehydrogenase 10	amyloid-beta binding	0.05	0.708	0.997
Itm2b	integral membrane protein 2B	amyloid-beta binding	-0.02	0.715	0.998
Nat8f1	N-acetyltransferase 8 (GCN5-related) family member 1	amyloid-beta metabolic process	-0.06	0.726	0.998
Aplp2	amyloid beta precursor-like protein 2	amyloid beta precursor-like protein 2	0.03	0.728	0.998
Aplp1	amyloid beta precursor like protein 1	amyloid beta precursor like protein 1	-0.03	0.732	0.999
Fbxo2	F-box protein 2	amyloid-beta binding	-0.04	0.732	0.999
Abca7	ATP-binding cassette, sub-family A member 7	amyloid-beta clearance by cellular catabolic process	-0.04	0.761	0.999
Appbp2	amyloid beta precursor protein binding protein 2	amyloid beta precursor protein binding protein 2	0.02	0.770	0.999
Bace1	beta-site APP cleaving enzyme 1	amyloid-beta binding	0.05	0.760	0.999
Ldlrap1	low density lipoprotein receptor adaptor protein 1	amyloid-beta binding	-0.12	0.755	0.999
Mmp9	matrix metalloproteinase 9	response to amyloid-beta	-0.12	0.739	0.999
Abca2	ATP-binding cassette, sub-family A member 2	positive regulation of amyloid-beta formation (amyloid-beta formation)	-0.03	0.789	0.999
Itga4	integrin alpha 4	cellular response to amyloid-beta	0.06	0.805	0.999
Igf1r	insulin-like growth factor I receptor	amyloid-beta clearance	0.03	0.809	1.000
Adam10	a disintegrin and metalloproteinase domain 10	amyloid-beta formation	-0.02	0.876	1.000
Ager	advanced glycosylation end product-specific receptor	amyloid-beta binding	-0.01	0.972	1.000

<i>Apba2</i>	amyloid beta precursor protein binding family A member 2	amyloid beta precursor protein binding family A member 2	0.03	0.841	1.000
<i>Apbb1</i>	amyloid beta precursor protein binding family B member 1	amyloid beta precursor protein binding family B member 1	0.01	0.967	1.000
<i>Apeh</i>	acylpeptide hydrolase	amyloid-beta metabolic process	-0.01	0.956	1.000
<i>Aph1a</i>	aph1 homolog A, gamma secretase subunit	amyloid-beta formation	-0.01	0.903	1.000
<i>Aph1b</i>	aph1 homolog B, gamma secretase subunit	amyloid-beta formation	0.03	0.839	1.000
<i>Apoa1</i>	apolipoprotein A-I	amyloid-beta binding	-0.05	0.936	1.000
<i>Becn1</i>	beclin 1, autophagy related	amyloid-beta metabolic process	0.01	0.901	1.000
<i>Cacna2d1</i>	calcium channel, voltage-dependent, alpha2/delta subunit 1	cellular response to amyloid-beta	-0.01	0.938	1.000
<i>Clstn2</i>	calsyntenin 2	amyloid-beta binding	0.02	0.914	1.000
<i>Clstn3</i>	calsyntenin 3	amyloid-beta binding	0.01	0.908	1.000
<i>Csnk1e</i>	casein kinase 1, epsilon	positive regulation of amyloid-beta formation (amyloid-beta formation)	-0.01	0.911	1.000
<i>Ephb2</i>	Eph receptor B2	amyloid-beta binding	0.05	0.827	1.000
<i>Fpr2</i>	formyl peptide receptor 2	amyloid-beta binding	-0.01	0.993	1.000
<i>Fzd5</i>	frizzled class receptor 5	amyloid-beta binding	0.06	0.892	1.000
<i>Igf1</i>	insulin-like growth factor 1	negative regulation of amyloid-beta formation (amyloid-beta formation)	-0.02	0.932	1.000
<i>Lrpap1</i>	low density lipoprotein receptor-related protein associated protein 1	amyloid-beta clearance by transcytosis	-0.01	0.910	1.000
<i>Ncstn</i>	nicastrin	amyloid-beta formation	0.01	0.905	1.000
<i>Necab3</i>	N-terminal EF-hand calcium binding protein 3	amyloid beta (A4) precursor protein-binding, family A, member 2 binding protein	0.00	0.986	1.000
<i>Olfm1</i>	olfactomedin 1	amyloid-beta binding	-0.04	0.888	1.000
<i>Pfdn6</i>	prefoldin subunit 6	amyloid-beta binding	0.00	0.995	1.000
<i>Rab5a</i>	RAB5A, member RAS oncogene family	amyloid-beta clearance by transcytosis	-0.01	0.888	1.000
<i>Rock1</i>	Rho-associated coiled-coil containing protein kinase 1	amyloid-beta complex	0.01	0.913	1.000

<i>Rtn3</i>	reticulon 3	negative regulation of amyloid-beta formation (amyloid-beta formation)	0.00	0.996	1.000
--------------------	-------------	--	------	-------	-------